

NMR STUDIES OF REACTIONS  
OF  $\beta$ -DIKETONATE COMPLEXES

NUCLEAR MAGNETIC RESONANCE STUDIES  
OF REACTIONS OF  $\beta$ -DIKETONATE COMPLEXES

By

ALAN JOHN CHAMBERLAIN NIXON, B.Sc.

A Thesis

Submitted to the School of Graduate Studies

in Partial Fulfilment of the Requirements

for the degree

Doctor of Philosophy

McMaster University

1976

DOCTOR OF PHILOSOPHY (1976)  
(Chemistry)

McMASTER UNIVERSITY  
Hamilton, Ontario

TITLE: Nuclear Magnetic Resonance Studies of Reactions  
of  $\beta$ -diketonate Complexes

AUTHOR: Alan John Chamberlain Nixon, B.Sc. (Aberdeen University)

SUPERVISOR: Dr. D.R. Eaton

NUMBER OF PAGES: xii, 225

## ABSTRACT

Metal derivatives of  $\beta$ -diketones form a very extensive class of coordination compounds. This thesis deals with three related aspects of the chemistry of these compounds; the effect of acid on a number of acetylacetonate complexes; the kinetics of ligand exchange reactions of  $V(acac)_3$  with Hacac and Hhfac and the rearrangement reactions of some vanadium  $\beta$ -diketonate complexes. These topics have been investigated primarily by means of nuclear magnetic resonance techniques.

Kinetic evidence of protonation of a number of acetylacetonate complexes on the  $\gamma$ -carbon has been obtained. No evidence was found to support the hypothesis of species containing a 'dangling' monodentate ligand protonated on oxygen.

The ligand exchange reaction of  $V(acac)_3$  with Hacac and Hhfac has been found to occur through two independent pathways, one of which is acid catalysed and another by the reaction of the neutral ligand with a species which probably contains the 'dangling' monodentate ligand. The 'dangling ligand' hypothesis is also supported by the observation that the ligand exchange reaction of  $V(acac)_3$  with Hacac is also catalysed by water.

The rearrangement of tris  $\beta$ -diketonato V(III) complexes has been found to proceed via an intramolecular mechanism. Total lineshape analysis of the temperature dependent NMR spectra of  $V(tfac)_3$  indicate that the trigonal twist ( $RC_3(p)$ ) and mechanisms involving only trigonal

bipyramidal states can be ruled out as the sole reaction pathways.  $V(\text{dibm})_3$  has been synthesized and confirmation of enantiomerization of this complex has been inferred from the lineshape analysis of the NMR spectra of the diastereotopically non-equivalent methyl groups.

In an attempt to establish the existence of a bond rupture process, an attempt was made to synthesize  $V(\text{triac})_3$ . Because of partial decomposition of the ligand, the product was a mixture of  $V(\text{triac})_3$  and  $V(\text{triac})_2(\text{acac})$ . Although coalescence of the resonances of the methyl groups bonded to the ring carbons of the triac<sup>-</sup> ligand of  $V(\text{triac})_2(\text{acac})$  was observed at about 76°C, no evidence of site exchange of the acetyl methyl group and the ring methyl groups (linkage isomerization) was obtained up to 200°C. for either compound. This evidence does not support a bond rupture mechanism.

The effect of solvent on the rates of rearrangement of  $V(\text{tfac})_3$  and  $V(\text{hfac})_2(\text{acac})$  has been determined. For  $V(\text{tfac})_3$ , the effects are small. However, for  $V(\text{hfac})_2(\text{acac})$ , the solvent effects are pronounced. The large solvent effect is most readily interpreted in terms of a bond rupture mechanism.

The enthalpies and entropies of the rearrangement processes of a number of  $\beta$ -diketonato V(III) complexes have been estimated and found to exhibit a linear relationship suggesting that the rearrangement processes may occur via a common mechanism.

### Acknowledgements

The author wishes to express his sincere appreciation to Dr. D.R. Eaton for his patient and helpful guidance during the completion of this project. He also wishes to thank the Department of Chemistry at McMaster University for financial support.

Finally, he wishes to thank his wife, Martha, who proofread and typed this thesis.

## Table of Contents

Chapter		Page
1	Metal $\beta$ -diketonate Complexes	1
2	Magnetic Resonance	18
3	Experimental	37
4	Reactions of $\beta$ -diketonate Complexes with Acid	49
5	Ligand Exchange of $V(acac)_3$ with Hhfac and Hacac $d_8$	80
6	Rearrangement of Vanadium $\beta$ -diketonates	117
7	Conclusion	209
Appendix	Arrhenius plots of Rearrangement Reactions of Vanadium $\beta$ -diketonate Complexes	215
References		218

## List of Tables

Number	Description	Page
4-1	Chemical Shifts of Acetylacetone and Aluminium Acetylacetonates in Various Solvents with and without Trifluoroacetic Acid	60
6-1	Temperature Dependence of Chemical Shifts of Methyl and Trifluoromethyl Groups of Vanadium $\beta$ -diketonate Complexes	141
6-2	Activation Parameters of Rearrangement Processes of Vanadium $\beta$ -diketonate Complexes	151
6-3	Permutational Analysis of $M(AB)_3$ and $M(AA)_2AB$ Complexes	158
6-4	Permutations of Octahedral Tris chelate Complex Obtained via a SP Primary Mechanism	166
6-5	Correlation of Octahedral Isomers and TBP Intermediates	171
6-6	Comparison of Rates and Activation Energies of Rearrangement of Some Tris $\beta$ -diketonate Complexes	208



### List of Figures

Number	Description	Page
3-1	Arrhenius Plots Demonstrating the Effect of Deliberately Choosing Incorrect Line-width Parameters	45
4-1	NMR Spectrum of $\text{Al}(\text{acac})_3$ with $\text{CF}_3\text{COOH}$ in DMF and DMSO	52
4-2	NMR Spectrum of $\text{Al}(\text{acac})_3$ with $\text{CF}_3\text{COOH}$ in $\text{CDCl}_3$ and $\text{CD}_2\text{Cl}_2$	53
4-3	NMR Spectrum of $\text{Al}(\text{acac})_3$ with $\text{CF}_3\text{COOH}$ showing Resolution of Resonance Assigned to $\text{Al}(\text{acac})_2^+$	55
4-4	Conductivity of Trifluoroacetic Acid in Acetone	56
4-5	NMR Spectrum of $\text{Al}(\text{acac})_3$ with $\text{CF}_3\text{COOH}$ in Benzene showing the Effect of Acid on the Methine Proton Signal	58
4-6	NMR Spectrum of a Mixture of $\text{Al}(\text{acac})_3$ and $\text{Al}(\text{CF}_3\text{COO})_3$ in Acetone	61
4-7	NMR Spectrum of $\text{Rh}(\text{acac})_3$ in $\text{CDCl}_3$ showing the Effect of $\text{CF}_3\text{COOH}$ on the Methine Proton Signal	64

Number	Description	Page
4-8	Possible Mechanism of Acid Catalysis of Ligand Exchange of a $\beta$ -diketonate Complex	69
5-1	NMR Spectrum of the Methyl Region of a Mixture of $V(acac)_3$ and Hhfac	89
5-2	Intensity of $^1H$ Methyl Resonances of $V(acac)_3$ , $V(acac)_2(hfac)$ and $V(hfac)_2(acac)$ during a Typical Ligand Exchange Reaction of $V(acac)_3$ with Hhfac	90
5-3	Variation of Concentrations of Vanadium $\beta$ -diketonates during a Typical Ligand Exchange Reaction	92
5-4	Intensity of $^1H$ Resonances of $V(acac)_3$ during a Ligand Exchange Reaction of $V(acac)_3$ with $Hacac-d_8$	94
5-5	Initial Rate of Exchange of $V(acac)_3$ with Hhfac as a Function of Hhfac Concentration	96
5-6	Initial Rate of Exchange of $V(acac)_3$ with Hhfac as a Function of Trifluoroacetic Acid Concentration	97
5-7	Initial Rate of Exchange of $V(acac)_3$ with Hhfac as a Function of Triethylamine Concentration	99

Number	Description	Page
5-8	R as a Function of Hhfac Concentration at $t_0$ , at Limiting Rate with the Addition of Triethylamine	100
5-9	Initial Rate of Exchange of $V(acac)_3$ with Hacac $d_8$ as a Function of Hacac $d_8$ Concentration	102
5-10	Initial Rate of Exchange of $V(acac)_3$ with Hacac $d_8$ as a Function of Water Concentration	103
5-11	Potentiometric Titration of Hhfac with n-butyl Ammonium Hydroxide	105
6-1	Trigonal Bipyramidal States, Axial and Equatorial	123
6-2	Square Pyramidal States, Apical and Basal	123
6-3	Formation of SP states by Primary and Secondary Mechanisms	123
6-4	Rearrangement of TBP State by Berry Pseudorotation	125
6-5	Rhombic Twist Mechanism (Ray and Dutt)	125
6-6	Trigonal Twist Mechanism (Bailar)	125
6-7	Trigonal Twist Mechanism (Springer and Sievers)	125

Number	Description	Page
6-8	Chemical Shifts of $\text{CF}_3$ Groups of $\text{V}(\text{tfac})_3$ versus Reciprocal Temperature	144
6-9	Variation of Linewidth of $\text{CF}_3$ Resonances of $\text{V}(\text{hfac})_2(\text{tfac})$ with Chemical Shift	146
6-10	Linewidth of $\text{CH}_3$ Groups of $\text{V}(\text{acac})_3$ versus Temperature	148
6-11	16 Possible Permutational Isomers of a Tris Chelate Complex	155
6-12	Comparison of Experimental and Simulated NMR Spectra of $\text{V}(\text{tfac})_3$ at Various Temperatures	156
6-13	Comparison of Experimental and Simulated NMR Spectra of $\text{V}(\text{tfac})_3$ for Different Mechanisms	163
6-14	16 Possible Isomers of a TBP Structure Derived from a Tris Chelate by Rupture of Bond 6	169
6-15	Correlation Diagram Connecting 16 Isomers of Figure 6-14 by a Berry Pseudorotation Mechanism	170
6-16	Comparison of Experimental and Simulated NMR Spectra of $\text{V}(\text{hfac})_2(\text{tfac})$ at Various Temperatures	174

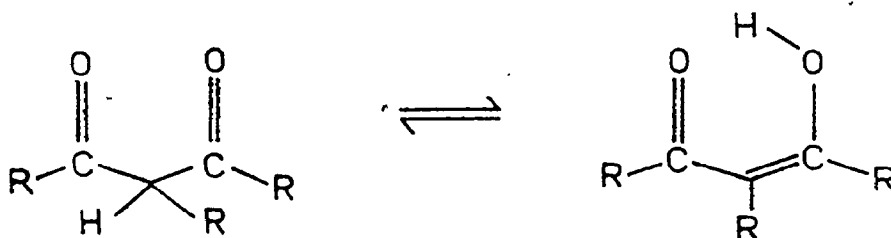
Number	Description	Page
6-17	Linear Relationship between $\Delta H$ and $\Delta S$ for Rearrangement of Vanadium $\beta$ -diketonate Complexes	180
6-18	NMR Spectra of $V(\text{hfac})_2(\text{acac})$ in Various Solvents at 29°C	182
6-19	NMR Spectrum of $V(\text{triac})_3/V(\text{triac})_2(\text{acac})$	188
6-20	Experimental and Simulated Spectra of Paramagnetic Region of $V(\text{triac})_3/V(\text{triac})_2(\text{acac})$ at Various Temperatures	190
6-21	NMR Spectrum of $V(\text{dibm})_3$	197
6-22	Chemical Shift of Methyl Groups of $V(\text{dibm})_3$ versus Reciprocal Temperature	198
6-23	Comparison of Experimental and Simulated NMR Spectra of Methyl Region of $V(\text{dibm})_3$ at Various Temperatures	200

1.

METAL  $\beta$ -DIKETONATE COMPLEXES

Introduction

$\beta$ -diketone compounds which have at least one hydrogen bonded to the carbon between the carbonyl groups often behave as both the dicarbonyl and as an unsaturated hydroxyketone. This behaviour is explained by the structural isomerism of these compounds.



This phenomenon is called tautomerism and is one of the best known properties of  $\beta$ -dicarbonyl compounds. Under appropriate conditions, the enol proton may be removed to form the  $\beta$ -diketonate anion. The  $\beta$ -diketonate anion exhibits a remarkable ability to form a large number of inorganic derivatives with almost all of the metallic elements.

Because the systematic names of many  $\beta$ -diketonate ligands are rather unwieldy, it has been general practice to adopt abbreviations for many of the ligands. Different authors have adopted different abbreviations for the same ligands; however, the abbreviations given below for the ligands used in the present work appear to be the most widely used.

<u>Systematic Name</u>	<u>Trivial Name</u>	<u>Abbreviation</u>
pentane-2,4-dionato	acetylacetonato	acac <sup>-</sup>
1,1,1,5,5,5-hexafluoro- pentane-2,4-dionato	hexafluoroacetyl- acetonato	hfac <sup>-</sup>
1,1,1-trifluoropentane- 2,4-dionato	trifluoroacetyl- acetonato	tfac <sup>-</sup>
3-acetylpentane- 2,4-dionato	triacetylmethanato	triac <sup>-</sup>
2,6-dimethylheptane- 3,5-dionato	diisobutyrylmethanato	dibm <sup>-</sup>

The first preparation of several metal derivatives of acetylacetonato was reported by Combes<sup>1</sup> in 1887. From an early date, metal  $\beta$ -diketonato derivatives have generated great interest among chemists, and many aspects of their properties have been investigated. Despite the very large amount of research done on metal  $\beta$ -diketonato derivatives since the turn of the century, much of the most interesting work is quite recent and it seems unlikely that the potential of metal  $\beta$ -diketonato derivatives to yield interesting information has yet been exhausted.

One area of investigation which has received a good deal of attention in the last decade has been the rearrangement process of some of these compounds and to a lesser extent, ligand exchange reactions. Despite the fact that a considerable amount of work has been carried out in this field, most of it has been restricted to complexes of aluminium and cobalt. The aluminium complexes are highly labile compared to the cobalt complexes and have been studied largely by dynamic nuclear magnetic resonance methods, whereas the cobalt complexes have been studied mostly by classical techniques. Virtually no work in this field

has dealt with the rearrangement reactions of labile transition metal  $\beta$ -diketonates. We have attempted, in this work, to study the behaviour of a set of vanadium  $\beta$ -diketonate complexes to learn something about the nature of the rearrangement mechanism and the factors which influence it. Ligand exchange reactions, which may have some steps in common with the rearrangement reactions, have also been studied with two aspects in mind: 1) to determine whether or not ligand exchange would be sufficiently rapid to account for the rearrangement of the  $\beta$ -diketonate complexes. 2) to determine what relationships, if any, the ligand exchange reactions and the rearrangement reactions have in common.

As a prelude to ligand exchange reactions which from reports in the literature on aluminium and palladium<sup>2,3,4</sup> are expected to be acid catalyzed, the behaviour of a number of simple acetylacetonate complexes with acid was studied to attempt to determine the nature of protonated intermediates in acid catalyzed ligand exchange. Much of this material deals with aluminium acetylacetonate, as this complex gave the most comprehensive and interpretable results. However, it is believed that the behaviour of this complex with acid will serve as a model for the interaction of other  $\beta$ -diketonate complexes with acid, and particularly, with the vanadium complexes with which it appears to have a good deal in common.

The reasons for the choice of vanadium  $\beta$ -diketonate complexes in this study are twofold: 1) extensive studies on the nuclear magnetic resonance spectra of some series of these compounds had already been



carried out in this laboratory to determine the nature of transmission of substituent effects<sup>5,6</sup>. The nuclear magnetic resonance spectra have been shown to be well-resolved in most cases and have been assigned.

2) Although a report by Holm et al.<sup>7</sup> stated that  $V(\text{tfac})_3$  did not isomerize in deuteriochloroform at temperatures below 100°C, preliminary experiments in this laboratory indicated that, in fact, temperature dependent effects due to rearrangement of the vanadium complexes could be observed in every case where they might be expected at temperatures between approximately -20°C and 80°C depending on the compound. This temperature range is quite convenient for the observation of temperature dependent exchange processes by nuclear magnetic resonance methods. The theoretical aspects of this topic are discussed briefly in the following chapter.

Before proceeding to the results and discussion, it is appropriate to review briefly some of the properties and chemistry of metal  $\beta$ -diketonate derivatives as a background to the material of this thesis. Because of the diversity of the subject, only a limited amount of material may be dealt with here. However, more extensive reviews are available elsewhere<sup>8,9,10</sup>.

### Review

The first account of the preparation of metal  $\beta$ -diketonate derivatives by Combes appeared in 1887<sup>1</sup>. In 1914, Morgan and Moss<sup>8</sup> reviewed the current standing of the known chemistry of metal  $\beta$ -diketonates which included some 39 compounds. The next survey of

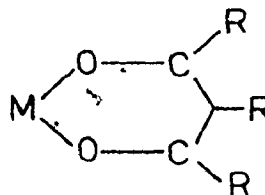
$\beta$ -diketonate chemistry was published by Fackler in 1967<sup>9</sup>. A comparison of these two reviews will reveal the dramatic growth of the field.

Thompson<sup>10</sup> has also reviewed some general features of  $\beta$ -diketonate chemistry fairly recently. A number of reviews, dealing with specific aspects of the properties of  $\beta$ -diketonates have also appeared in the literature.<sup>11,12,13,14,15</sup>

This section of the review will be somewhat arbitrarily divided into the following sections: 1) Molecular structure. 2) Electronic structure. 3) IR and NMR spectroscopy. 4) Chemistry. 5) Miscellaneous.

### Molecular Structure

There are a wide variety of types of bonding found in metal  $\beta$ -diketonates which are described by Thompson<sup>10</sup>. By far, the majority of metal  $\beta$ -diketonates, however, have the ligand bonded through both oxygens.



Crystallographic studies of numerous oxygen chelated acetylacetonate complexes<sup>16</sup> show that the two ring C-C bond lengths are the same at an average value of 1.390 Å as are the two C-O bond lengths at 1.274 Å. These distances are also insensitive, within experimental error, to changes in the central metal ion. In general, the acetylacetonate

anion has  $C_{2v}$  symmetry and the six electrons occupying the  $\pi$  system of the ligand may be regarded as occupying orbitals delocalized over the  $\pi$  system of the ligand.

Lingafelter and Braun<sup>16</sup> have carried out a simple Hückel calculation to estimate the bond orders in the  $acac^-$  ion. Using the equation of Berstein, they estimated the C-C bond distance at 1.395 Å and the C-O distance at 1.274 Å, in excellent agreement with the observed average values. With trivalent ions, the arrangement of the oxygens about the metal ion is expected to be close to octahedral, provided the ionic radius does not much exceed  $\sim 0.9$  Å. Fackler<sup>17</sup> has collected structural parameters for a variety of tris chelate complexes, among them some acetylacetonates. The parameter  $\phi$  is of particular interest. It gives the projection of the angle between the two oxygen atoms on the same ligand, and the metal, on a plane normal to the  $C_3$  axis. For a regular octahedron, this angle is  $60^\circ$ . For all of the complexes, except that of scandium, the value of  $\phi$  is within  $8^\circ$  of the octahedral value.  $V(acac)_3$  shows only a very slight distortion towards trigonal prismatic coordination at  $\phi = 56^\circ$ .

Bivalent ions with ligands coordinated in this fashion often exhibit oligomerisation. Apparently, greater stability is obtained by octahedral coordination. Examples of this behaviour are found for Ni(II), Co(II) and Zn(II)<sup>18, 19, 20</sup>.

Some interesting data on bond lengths of acetylacetonate com-

plexes are presented by Lingafelter and Braun<sup>16</sup>. The metal-oxygen bond lengths of complexes of Be(II), Al(III), Zr(IV), Ce(IV) which contain ions having the noble gas electronic configuration, can be predicted quite accurately from the sums of the Pauling crystal radii, while for all the other metals, the metal-oxygen distances are less than the sum of the Pauling crystal radii. The authors felt that this result indicated a greater covalency in the acetylacetonates compared to the compounds used to estimate the ionic radii.

It has been suggested that electron withdrawing groups such as trifluoromethyl groups on the carbonyl carbons should cause weakening of the M-O bonds<sup>21</sup>. It would, therefore, be of interest to compare M-O bond lengths of acetylacetonate complexes with those of trifluoroacetylacetonate and hexafluoroacetylacetonate complexes. Unfortunately, no X-ray crystallographic studies of complexes containing bidentate trifluoroacetylacetonate or hexafluoroacetonate ligands have yet yielded information concerning the M-O bond lengths.

Another type of oxygen-bonded metal derivative of  $\beta$ -diketones is the Lewis acid-base adduct<sup>22</sup>. In these complexes, the  $\beta$ -diketone is coordinated to the metal as the neutral molecule rather than the anion. In the majority of cases, the ligand is bonded through both oxygens in the keto form, although complexes containing the neutral enol are also known. Although the number of complexes of this type known is very limited, they may well be important as intermediates in the formation of normally coordinated  $\beta$ -diketonate complexes and possibly

in the acid catalyzed ligand exchange reactions of  $\beta$ -diketonate complexes.

### The Electronic Structure of $\beta$ -diketonate Complexes

The electronic structure of  $\beta$ -diketonate complexes has received considerable attention.

On the basis of a non-linear relationship between the  $pK_D$ 's of a variety of  $\beta$ -diketones and the stabilities of the Cu(II) chelates, Calvin and Wilson<sup>23</sup> suggested that "a benzenoid resonance effect involving copper plays a very important role in determining the stabilities of these compounds". Crystallographic data are consistent with a benzenoid structure for the complex. The  $C_{2v}$  symmetry of the ligand, however, may be explained by resonance stabilization of the ligand alone.

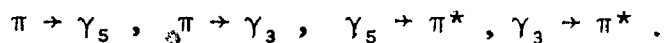
The enol form of acetylacetonate exhibits an intense absorption band at about 272  $m\mu$ . In basic solution, the band shifts to lower energy to about 292  $m\mu$ . From Hückel-LCAO-MO calculations, this band is assigned to the  $\pi_3 \rightarrow \pi_4$  transition<sup>24</sup>. Barnum<sup>24</sup> has investigated the visible - UV spectra of some tris(acetylacetonate) complexes and has attempted to assign the spectral bands. The band which corresponds to the  $\pi_3 \rightarrow \pi_4$  transition in the free anionic ligand may shift to longer or shorter wavelengths on chelation with a metal.

Belford et al.<sup>26</sup> predicted from a Hückel LCAO-MO calculation, that an increase of one positive unit of charge on the central metal ion should cause the  $\pi \rightarrow \pi^*$  transition to shift about  $3,200 \text{ cm}^{-1}$  to

lower energy. The interaction of metal orbitals with ligand orbitals was not taken into account. Holm and Cotton<sup>27</sup> have shown that such an effect is seldom observed even in cases where the metal ligand bonding is ionic. Holm and Cotton concluded that the position of the band was determined by a number of factors which are not readily separated. Barnum<sup>24</sup> suggests that the effect of metal-ligand  $\pi$  interaction is the major factor in determining the position of this band. Barnum<sup>24</sup> assigns the band which occurs between 300 and 400 m $\mu$  to the  $d_{\epsilon} \rightarrow \pi_4$  transition. The band is characteristic of neither the ligand nor the metal, and is therefore likely to be a charge transfer band. The band shifts to higher energy on going from Ti to Co which parallels the increasing difficulty of oxidizing the central metal ion. The band is therefore assigned to a metal to ligand charge transfer band, rather than vice versa. The assignment of the band to the  $d_{\epsilon} \rightarrow \pi_4$  transition rather than the  $d_{\epsilon} \rightarrow \pi_5$  transition was made on the basis of the calculated energy differences. Hückel LCAO-MO calculations by Barnum<sup>25</sup> indicate that the  $d_{\epsilon} \rightarrow \pi_4$  transition is split into three bands by bonding. A less intense band is shifted to lower energy with increasing metal  $\pi$  bonding interaction, while the other two overlap and are almost independent of  $\pi$  bonding. Metal-ligand  $\pi$  bonding is also expected to split the  $\pi_3 \rightarrow \pi_4$  transition into four bands, one of which is less intense and is independent of  $\pi$  bonding, whereas the other three are shifted to higher energy. The calculations allowed a rough estimate of the energy of metal-oxygen  $\pi$  bonding. These values are estimated at close to zero for Ti(acac)<sub>3</sub> to about 40 kcals. per mole per bond in Co(acac)<sub>3</sub>.

Barnum points out that the metal-oxygen  $\pi$  bonding occurs mainly through overlap of the metal  $d_{\epsilon}$  - orbitals with the  $\pi$  system of the ligand. The orthogonality of the  $d_{\epsilon}$  orbitals of the metal does not permit the electrons to move freely in a circular path around the ring and that the chelate ring cannot therefore be considered to be analogous to benzene.

Jørgensen<sup>28</sup>, while admitting that Barnum's treatment of the absorption spectra of tris(acetylacetonates) 'presents a large part of the truth', nevertheless expresses reservations about Barnum's assignments of the bands. Jørgensen suggests that the absorption spectra in the near UV are caused by the simultaneous presence of four types of electron transfer spectra



Although some features of the electronic spectra of transition metal acetylacetonates do not appear to have been unambiguously explained, it seems reasonable to suppose that there is a significant interaction between the d orbitals of the metal and the  $\pi$  orbitals of the ligand.

#### Infrared Spectra of $\beta$ -diketonate Complexes

This field has been reviewed some time ago by Cotton<sup>29</sup> and by Nakamoto<sup>30</sup>.

From the inorganic chemists point of view, the bands due to the metal-oxygen stretching frequencies are of the greatest interest and

occur in the IR region of the spectrum from approximately  $700\text{ cm}^{-1}$  to  $300\text{ cm}^{-1}$ . For molecules as complicated as  $\beta$ -diketonate complexes, pure metal-ligand stretching modes cannot be expected due to extensive coupling of modes.

Three metal ligand stretching modes are expected to be IR active in  $D_3$  symmetry,  $A_2$  and  $2E$ . They may be described as  $\Gamma$  symmetric (correlating to  $E_g$  in  $O_h$ ) and  $A_2$  and  $E$  asymmetric (correlating to  $T_{1u}$  in  $O_h$ ). Mikami<sup>31</sup> has carried out a comprehensive normal-coordinate analysis of  $\text{Fe}(\text{acac})_3$  and has been able to identify the M-O stretching bands. The assignments are in good agreement with results obtained by Nakamoto et al.<sup>32</sup>, who used metal isotope shift techniques to identify the metal ligand stretching bands in  $\text{Fe}(\text{III})$ ,  $\text{Cr}(\text{III})$ ,  $\text{Pd}(\text{II})$ ,  $\text{Cu}(\text{II})$ , and  $\text{Ni}(\text{II})$  acetylacetonates. Avdeef and Fackler<sup>17</sup> have noted the linear relationship between the frequencies of three band series in the far IR spectrum of a number of acetylacetonate complexes and the metal oxygen bond distances. The band series which has the steepest slope also has the largest isotope shifts as found by Nakamoto<sup>32</sup>. Avdeef and Fackler<sup>17</sup> also note the 'double hump' characteristic of the graph of the metal-oxygen bond distances plotted against atomic number, which correlates to the crystal field stabilization energies of the central metal ion. The effect of placing electron withdrawing groups on the ligand has been confirmed for  $\text{Cu}(\text{II})$  and  $\text{Ni}(\text{II})$  by Nakamoto and co-workers<sup>33</sup>, who found a substantial decrease in the metal-oxygen force constants on going from the acetylacetonate complexes to the hexa-fluoroacetylacetonate complexes.



### NMR of $\beta$ -diketonate Complexes

A considerable amount of work has been carried out in the field of NMR spectroscopy of metal  $\beta$ -diketonate complexes. Recently, much of this work has centered on the rearrangements of  $\beta$ -diketonate complexes. As this topic will be covered extensively in a later part of this thesis, it will be omitted here.

NMR of  $\beta$ -diketonate complexes has been used to investigate two closely related aspects of metal  $\beta$ -diketonate chelates: the existence of ring currents and  $d\pi - p\pi$  interactions of metal and ligand. The NMR spectrum of the enol form of acetylacetonate closely resembles that of many diamagnetic acetylacetonate complexes. The six equivalent protons of the methyl groups of the ligand give rise to a resonance at approximately 2 ppm downfield of TMS, while the single proton bonded to the  $\gamma$ -carbon has a shift of approximately 5.5 ppm downfield of TMS, typical of a vinylic proton. The enolic proton is found quite far downfield at about 13.4 ppm downfield of TMS. The single resonance observed for the methyl groups of Hacac indicate that either the molecule has a symmetric structure or that the enolic proton is being rapidly transferred from one oxygen to the other.

The keto tautomer of acetylacetonate gives rise to a quite different NMR spectrum. The protons of the methylene group have a shift of 3.5 ppm downfield of TMS, and the methyl protons a shift of  $\sim 2.1$  ppm downfield of TMS. In this case, the intensity ratio of the peaks is 1:3.

Holm and Cotton<sup>27</sup> have carried out a fairly extensive study of the NMR spectra of a number of diamagnetic acetylacetonate complexes. They concluded that the shifts of the methine proton afforded little evidence in support of a benzenoid resonance of the chelate ring. Furthermore, there was no apparent correlation between the methine proton shifts and the  $\pi$  bonding ability of the metal.

The NMR signal of the methine proton of  $\text{Si}(\text{acac})_3^+$  was found by Hester<sup>34</sup> to be significantly shifted to downfield of the normal position for diamagnetic acetylacetonates (6.35 versus 5.5 ppm). Hester inferred from this evidence, the existence of  $d\pi - p\pi$  bonding between silicon and the ligand, and also the existence of considerable benzenoid resonance. Hester's interpretation has been criticized<sup>9,25,35</sup>, principally on the basis that he did not take into account the inductive effect of the positive charge on the complex. Fay and Serpone<sup>36</sup> have effectively settled the question by preparing several cationic  $\text{B}(\text{acac})_2^+$  complexes, all of which exhibit shifts of the methine proton downfield of  $\text{Si}(\text{acac})_3^+$ . In the case of the boron complexes, it is unlikely that significant  $d\pi - p\pi$  bonding could exist, because of the lack of energetically suitable d orbitals on boron. Link and Sievers<sup>37</sup> have pointed out that the absence of ring currents does not necessarily imply the lack of  $d\pi - p\pi$  bonding.

That  $d\pi - p\pi$  interactions do occur between the metal and the ligand has been demonstrated by Forman et al.<sup>38</sup> for  $\text{V}(\text{acac})_3$ . The methine protons of this complex exhibited large contact shifts, indicative of unpaired spin density delocalized through the ligand  $\pi$  system. Eaton

and Chua<sup>5,6</sup> have examined the NMR spectra of a number of vanadium  $\beta$ -diketonate complexes, and have quite successfully accounted for the observed shifts on the basis of a model, in which the contact shifts of the substituents on the ring carbons can be interpreted by assuming delocalization of unpaired electron spin density through the  $\pi$  system of the ligand.

### Chemistry of Metal $\beta$ -diketonates

#### Synthesis

A number of synthetic routes to the preparation of  $\beta$ -diketonate complexes are available. A summary of the procedures used before 1957 is given by Fernelius and Bryant<sup>39</sup>, while a brief account of more recent approaches is given by Fackler<sup>9</sup>.

The direct reaction of a salt of the metal with the appropriate  $\beta$ -diketonate ligand is perhaps the most widely used method. In aqueous solution, acetates are often used, as the acetate has the effect of buffering the reaction medium while in non-aqueous solution, a halide may be used, as the hydrogen halide evolved is insoluble. A  $\beta$ -diketonate complex may also be prepared from the reaction of a metal salt and a salt of the  $\beta$ -diketone. A very useful variation of this method is the use of salts which will produce a soluble product and insoluble by-product, such as the reaction of a metal halide with a Tl(I)  $\beta$ -diketonate. Solvent extraction of a neutral chelate from an

aqueous solution can often provide a method of forcing the reaction and removing unwanted by-products. The reaction of a  $\beta$ -diketone with a metal oxide, hydroxide or carbonate, offers a route which has the advantage of introducing minimal impurities. The  $\beta$ -diketone may also be reacted directly with the metal itself. This method is often useful in the case of alkali metals and alkali earths. The complexes are obtained in the anhydrous state. More recently,  $\beta$ -diketonate complexes have been prepared from the reactions of zero valent compounds, particularly carbonyls, with  $\beta$ -diketones.

#### Organic Reactions of $\beta$ -diketonate Complexes

The essentially organic reactions of the coordinated  $\beta$ -diketonate ligand have been extensively investigated by Collman and his students<sup>12</sup>. Much of this work is presented in a review in 'Reactions of Coordinated Ligands'<sup>12</sup>. Most of the reactions were carried out on the relatively stable tris(acetylacetonate) complexes of chromium, cobalt, and rhodium. The central carbon of the chelate ring was found to undergo electrophilic substitution reactions, such as halogenation, nitration, thiocyanation, acylation, formylation, chloromethylation and aminomethylation. Reactions performed on partially resolved substrates tended to indicate that, as optical activity was not greatly changed in most cases, substitution at the central ring carbon probably occurred without cision of the metal-chelate ring. Since the optical purity and molar rotations of the pure enantiomers were unknown, it was not possible to determine whether partial racemization occurred. These results were

taken to indicate that the reactions could be regarded as an electrophilic substitution with the metal chelate ring as a 'quasiaromatic system'.

#### Miscellaneous

Martell and Calvin<sup>40</sup> have presented a table of formation constants of  $\beta$ -diketonate complexes of bivalent ions. It is interesting to note the values of the formation constants for monoacetylacetonato Cu(II) and monohexafluoroacetylacetonato Cu(II),  $\text{Log } K = 9.73$  and  $2.70$  respectively. The large decrease in  $K$ , on going from the acetylacetonate complex to the hexafluoroacetylacetonate complex bears out the prediction that the metal-oxygen bond strengths will be decreased, when the methyl groups are substituted by the electron withdrawing trifluoromethyl groups.

$\beta$ -diketones may be used to separate metal ions by solvent extraction from an aqueous phase into an organic phase. A detailed account of the theory is given by Martell and Calvin<sup>40</sup>. Even the chemically very similar metals zirconium and hafnium may be separated quite readily by this technique using theonyltrifluoroacetone.

The high vapour pressure of many metal  $\beta$ -diketonate complexes may be used to advantage to separate metals by gas-liquid chromatography. A review monograph on this topic has been written by Moshier and Sievers<sup>11</sup>. This technique may provide a valuable method for the quantitative and qualitative analysis of metals. The derivatives of hexafluoro-

acetylacetone appear to be particularly promising in this regard.

Another interesting use of  $\beta$ -diketonate derivatives is as the so-called 'shift reagents'. These are paramagnetic complexes of some of the rare earth compounds. The dipolar interaction between the anisotropic magnetic dipole moment of the chelate, and in the nuclei of the diamagnetic molecule, result in a spreading of the resonances of the diamagnetic molecule. Overlapping peaks may be resolved by this technique and geometric information may be obtained from the magnitudes of the shifts. One of the most useful complexes of this type is  $\text{Eu}(\text{fod})_3$  (where  $\text{Hfod}$  is 1,1,1,2,2,3,3-heptafluoro-7,7-dimethyloctane-4,6-dione).

### Introduction

The nuclear magnetic resonance (NMR) effect was first detected in bulk matter in 1945 by Purcell, Torrey and Pound<sup>41</sup> and by Bloch, Hansen and Packard<sup>42</sup>. The first 'high resolution' NMR spectra in which different resonances were observed for chemically different nuclei in the same molecule were obtained for simple alcohols by Arnold, Dharmatti and Packard<sup>43</sup> in 1951. Since then, NMR has rapidly expanded to become one of the most ubiquitous spectroscopic techniques of modern chemistry.

The application of NMR to problems of chemical structure is sufficiently familiar to require no introduction. In the present thesis, extensive reference is made to two rather specialized areas of NMR spectroscopy. In chapter 6, the NMR spectra of a series of paramagnetic complexes are discussed. Also, in chapter 6, NMR lineshape measurements are used to derive kinetic information. It is appropriate, therefore, to briefly review the application of NMR to paramagnetic molecules and the effect of chemical exchange on the NMR lineshape.

### Nuclear Magnetic Resonance in Paramagnetic Species

The interaction of the nuclear spins with unpaired electron spin introduces additional complexities in the interpretation of the NMR spectra

of paramagnetic molecules. However, the nature of the interaction may provide information on the electronic structure and geometry of the molecule which is often inaccessible by other means. This approach has found important applications to a variety of fields in chemistry in recent years: first, in the chemistry of transition metal complexes; in biochemistry, as paramagnetic ions were used as structural probes; and more recently, in organic chemistry with the advent of 'shift' and 'relaxation' reagents for structural studies.

Proton-electron hyperfine interaction in solution ESR spectra was first observed for various types of organic free radicals<sup>44,45,46</sup>. Equations<sup>47,48,49</sup> were derived relating the isotropic hyperfine splittings to 'dipolar' and 'contact' interactions and to the spin density distribution in the  $\pi$  orbitals of these ions. These equations are applicable with some modifications to the NMR of transition metal complexes. The first observations<sup>50,51</sup> in this area were carried out by McConnell and Holm on various paramagnetic bis( $\pi$ -cyclopentadienyl)-metal complexes. However, the full potential of this approach was only begun to be realized when Eaton, Phillips<sup>53 to 59</sup> and co-workers presented a detailed analysis of  $^1\text{H}$  and  $^{19}\text{F}$  spectra of a variety of substituted Ni(II) aminotroponeiminate complexes. Their studies demonstrated that the chemical shifts observed could be related to spin density distribution in the  $\pi$  orbitals of the ligand yielding information concerning the nature of the metal-ligand bonds.



It is probably fair to say that although theoretical understanding of NMR in paramagnetic complexes has become considerably more sophisticated in recent years, the complexity of the phenomenon precludes a quantitative analysis of the results in all but the most favourable cases.

### Theory

In principle, a paramagnetic species may be studied by either ESR or NMR. The observation of an NMR line is critically dependent on the relaxation time of the nucleus, which is dominated in a paramagnetic species by fluctuating magnetic fields at the nucleus caused by changes in orientation of the electron spin. Only fluctuations about the Larmor frequency are effective in producing nuclear relaxation. When electronic relaxation is very fast, i.e., when  $T_{1e}^{-1} \gg A/h$  (where  $A$  is the hyperfine coupling constant in ergs), the components of frequencies at and below the Larmor frequency are minimal, and relatively sharp NMR lines may be observed. The condition for a well-resolved ESR hyperfine structure to be observed is  $T_{1e}^{-1} \ll A/h$ . The condition for the ESR experiment and NMR experiment are, therefore, almost mutually exclusive. Since electronic relaxation is dependent upon temperature, it is possible in some cases to observe an NMR spectrum of a species in solution at high temperature, and an ESR spectrum of the same species at low temperature in the solid. Under the condition of a very fast electronic relaxation, the nucleus does not experience a field due to an  $\alpha$  spin or to a  $\beta$  spin, but to an average field proportional to  $\langle S_z \rangle$ . The mean value of  $S_z$  is non-zero, due to

different thermal populations of the spin states.

### The Spin Hamiltonian

The spin Hamiltonian for an electron-nuclear spin system may be given by

$$\mathcal{H}_S = -\mu_e \cdot H - \mu_N \cdot H + A_H \cdot I$$

The Zeeman terms, one and two, represent the interaction of the electron and nuclear magnetic moments with the external field  $H$ . The electronic Zeeman term may be written

$$\mathcal{H}_{ze} = -\mu_e \cdot H = \beta(L + gS) \cdot H = \beta \hat{S} \cdot g \cdot H,$$

where  $L$  and  $S$  are the true angular momentum operators. It is sometimes expressed as  $\beta \hat{S} \cdot g \cdot H$ , an effective spin Hamiltonian, where  $\hat{S}$  is a fictitious effective spin and  $g$  is an anisotropic  $g$  tensor which contains all the information concerning the values of the operators  $L$  and  $S$ . The nuclear Zeeman term  $\mathcal{H}_{ZN} = -\mu_N \cdot H$  can also be expressed as  $-\hbar \gamma_N H \cdot I = -g_N \beta_N H \cdot I$ . By convention, the magnetic field is usually chosen to be coincident with the  $Z$  axis, so that the nuclear Zeeman term becomes  $\mathcal{H}_{ZN} = -\hbar \gamma_N H I_Z = -g_N \beta_N H I_Z$ .

The hyperfine term  $A_H \cdot I$  represents the interaction between the electron spin and orbital magnetic moments and the nuclear magnetic moment. The large chemical shifts observed in the NMR spectra of many paramagnetic complexes occur as a result of this interaction. The hyperfine term can be subdivided into three parts,

$$\mathcal{H}_H = \mathcal{H}_F + \mathcal{H}_D + \mathcal{H}_L = (A_F + A_D + A_L) \cdot I = A_H \cdot I$$

$\mathcal{H}_F$  represents the Fermi contact term,  $\mathcal{H}_D$  represents the dipolar term and  $\mathcal{H}_L$  represents the orbital term. The Fermi contact term was first proposed by Fermi<sup>60</sup> to account for fine structure in the spectra of sodium and cesium atoms.

The contact term describes the interaction of the nuclear magnetic moment with electric currents arising from electron density at the nucleus and takes the form

$$\mathcal{H}_F = aS \cdot I$$

where  $a = \frac{8\pi}{3} \hbar \gamma_N g \beta |\psi(0)|^2$ .  $|\psi(0)|$  is the amplitude of the electronic wave function at the nucleus. For the Fermi contact term to be non-zero, the electron must occupy an orbital with s character. The Fermi contact term can also be expressed as

$$\mathcal{H}_F = \frac{8\pi}{3} \hbar \gamma_N g \beta \delta(r) S \cdot I,$$

where  $\delta(r)$  is the Dirac delta function which has a value of 1 for  $r = 0$  and 0 for  $r \neq 0$ .

The dipolar term describes the classical interaction between the magnetic moments of the electron and the nucleus. Provided that the distance between the electron and the nucleus is sufficiently large, the interaction between their magnetic moments is given by the classical expression for the coupling of two point dipoles and takes the form

$$\mathcal{H}_D = \hbar \gamma_N g \beta \left\{ \frac{3(\mathbf{r} \cdot \mathbf{S})(\mathbf{r} \cdot \mathbf{I})}{r^5} - \frac{(\mathbf{S} \cdot \mathbf{I})}{r^3} \right\}$$

The electron is located from the nucleus by the vector  $r$ . The expression is averaged over the probability distribution of the electron  $|\psi(r)|^2$ . For the hydrogen atom which is the simplest paramagnetic system, the electron distribution is spherical and averages to zero.

The orbital term,  $\mathcal{H}_L = \hbar\gamma_N g \beta \frac{\mathbf{l} \cdot \mathbf{I}}{r^3}$ , represents the interaction between the nuclear magnetic moment, and the magnetic moment due to the orbital motion of the electrons. It is non-zero only for electronic states with net angular momentum.

For systems of interest, the hyperfine term is usually small compared to the Zeeman terms. The nuclear spins are still effectively quantized along the direction of the applied magnetic field.

### Paramagnetic Shifts in Solution

In solution, rapid tumbling of the complex averages some of the hyperfine terms to zero. The remaining terms give rise to the isotropic shift. Two factors contribute to the isotropic shift: the 'Fermi contact shift' and the 'dipolar shift'.

#### The 'Fermi Contact Shift'

The Fermi contact shift occurs as a result of unpaired electron spin density at the nucleus, and is therefore dependent upon the electronic structure of the complex. For a simple system with no orbital angular momentum contribution, the expression for the Fermi contact shift is quite simple and is given by  $\frac{\Delta H}{H}^{iso} = \frac{-g\beta S(S+1)A}{\hbar\gamma_N 3kT} = \frac{A}{\hbar\gamma_N H} \langle S_z \rangle$ .

( $\Delta H$  is defined by  $(H_0 - H_0^0)$  where  $H_0^0$  is the resonance field for the same nuclear species in a diamagnetic reference compound). This result was first obtained by McConnell and Chesnut<sup>48</sup>. For a transition metal complex, however, the situation is usually more complicated due to the possibility of an anisotropic  $g$  tensor, unquenched orbital angular momentum in the ground state, thermal population of more than one electronic state, and mixing of these states by the applied magnetic field. Furthermore, the exact form of the time-independent Hamiltonian for a complex tumbling in solution is dependent upon the relative values of the parameters,  $\tau$ , the rotational correlation time of the tumbling molecule,  $T_{1e}$ , the spin lattice relaxation time of the electron, and the anisotropy of the  $g$  tensor. A detailed and general derivation of both the contact and pseudo-contact contributions to the isotropic shift has been given by Kurland and McGarvey<sup>61</sup>.

#### The Dipolar Shift

Most of the contribution to the dipolar part of the Hamiltonian is anisotropic and averages to zero for a complex tumbling in solution.

For a complex with only one thermally populated spin multiplet, with an effective spin  $\hat{S}$ , axial symmetry and averaging conditions most generally appropriate for a paramagnetic complex in solution<sup>62</sup>, the dipolar contribution to the isotropic shift is given by

$$\frac{\Delta H}{H} = \frac{\beta^2 S(S+1)}{9kT\tau^3} (g_{\parallel} + g_{\perp}) (g_{\parallel} - g_{\perp}) (1 - 3 \cos^2 \theta)$$

In general, this equation is not always applicable for reasons already given. The geometric dependence of the dipolar shift, however, is independent of the complexity of the model employed. This equation will still predict the ratios of the dipolar shifts, although it may fail to predict their absolute magnitude accurately. (For a species with an isotropic g tensor, the dipolar contribution to the isotropic shift will vanish. The components of the g tensor can sometimes be determined by ESR studies on single oriented crystals.

#### Line Broadening in Paramagnetic Complexes

While large chemical shifts may arise as a result of the interaction of the nucleus with unpaired electron spin in a paramagnetic complex, line broadening which is also a result of the same interactions almost invariably occurs. The degree of line broadening at any particular nucleus reflects the extent and duration of the interaction between the unpaired electrons and the nucleus.

Line broadening is capable of yielding information on structure and bonding, and in some cases, kinetic information.

In the Bloch description of the NMR phenomenon, the decay of magnetisation of a collection of nuclear spins to its equilibrium value in an applied magnetic field is characterized by two first order rates:

$$\frac{dM_z}{dt} = -\frac{(M_z - M_0)}{T_1} \quad \frac{dM_{x,y}}{dt} = -\frac{M_{x,y}}{T_2}$$

where  $\frac{1}{T_1}$  and  $\frac{1}{T_2}$  are the first order rate constants.  $T_1$  is termed the spin-lattice or longitudinal relaxation time and  $T_2$  is termed the spin-spin or transverse relaxation time.  $M$  is the vector sum of all the magnetic moments and is determined by the Boltzmann distribution function among the  $2I + 1$  energy states.  $M_0$  is the equilibrium value of  $M_z$  and the equilibrium value of  $M_{x,y}$  is zero, because of the random phase distribution in the  $xy$  plane at equilibrium. The decay of  $M_z$  to its equilibrium value involves the transfer of energy between the nuclear spin system and the lattice. It is basically a resonance phenomenon, and only fluctuations of magnetic field at or near the nuclear Larmor frequency are effective in producing  $T_1$  relaxation.  $T_2$  relaxation represents the dephasing of the nuclear magnetic moments in the  $xy$  plane and does not involve energy transfer.  $T_2$  relaxation is also sensitive to modulations of the magnetic field at less than the Larmor frequency.  $T_1$  and  $T_2$  are not totally independent, as the factors which affect spin-lattice relaxation also affect spin-spin relaxation, while the converse does not hold. Consequently, the transverse relaxation  $T_2$  is always less than or equal to the spin-lattice relaxation time  $T_1$ . For a single unsaturated resonance, the absorption signal has the familiar

$$\text{Lorentz lineshape } g(\omega) = \frac{T_2}{\pi} \frac{1}{(1 + T_2^2 (\omega - \omega_0)^2)}$$

The width of the resonance at half height is determined by  $T_2$ , and is given by  $\frac{1}{\pi T_2}$  in frequency units.

Nuclear relaxation arises from the same types of interactions which are responsible for the large shifts observed in paramagnetic systems. Relaxation is due to time-dependent variations in the interactions, while the shifts are due to the average value of the interactions. Nuclear relaxation is induced by rapid modulation of the magnetic field experienced by the nucleus. The time-dependent factors may arise from electronic relaxation, molecular motion, or chemical exchange, either of the electrons or the nuclei. Relaxation may occur via the dipolar or contact mechanisms. In practice, relaxation caused by the contact interaction is insignificant compared to relaxation caused by the dipolar interaction, unless delocalization of the unpaired electron spin is extensive and the nucleus is well-separated from the central metal ion. The largest value expected for  $T_{2N}^{-1}$  for a contact relaxation mechanism is of the order of  $10 \text{ sec.}^{-1}$  <sup>63</sup>.

The random fluctuations of the magnetic field may be described as an infinite sum of periodic variations over all frequencies and phases. Not only frequencies at the nuclear Larmor frequency,  $\omega_N$ , are effective at producing nuclear relaxation, but also frequencies at  $(\omega_e - \omega_N)$  and  $(\omega_e + \omega_N)$  due to electron-nuclear coupling.

For many systems for which well-resolved NMR spectra are observed,  $T_{1e}$  is sufficiently short that  $T_{2e} = T_{1e} = \tau_{c2} = \tau_{c1}$  and  $\omega_e^2 \tau_c^2 \ll 1$ .

This is known as the fast motion limit and the relaxation equations



simplify to

$$T_{1N}^{-1} = T_{2N}^{-1} = \frac{4S(S+1)}{3r^6} \gamma_N^2 g^2 \beta^2 T_{1e}$$

The linewidth may be of considerable help in determining the geometry of a complex because of its dependence on the parameter  $r$ . It should be used with caution, since the expressions are based on the assumption that the spin density is localized on the central metal ion. Because of the dependence on the sixth power of the distance, a very small amount of electron density delocalized onto a ligand may be more effective at producing relaxation than larger amounts of spin density, located at a greater distance on the central metal ion.

#### The Effect of Chemical Exchange on the NMR Lineshape

The shape and width of a NMR resonance is sensitive to a number of time-dependent processes including chemical exchange. This property has proved particularly valuable for studying the rates and mechanisms of a wide variety of chemical reactions.

The reactions which may be studied by this method have rates of the order of  $\Delta\omega \text{ sec}^{-1}$ , where  $\Delta\omega$  represents the difference in chemical shift between the resonances of the exchanging nuclei. Since  $\Delta\omega$  is of the order of  $10^0$  to  $10^4 \text{ sec}^{-1}$ , the processes which may be studied are often too fast to be studied by classical techniques. NMR spectroscopy permits the detection and study of rate processes which

are not readily detected by other conventional spectroscopic techniques.

The description of time-dependent effects caused by chemical exchange may be straightforwardly approached by suitable modifications to the Bloch equations.

A quantitative theory of the effects of chemical exchange on the NMR lineshape was first developed by Gutowsky, McCall and Slichter<sup>64</sup>. A simplified and more general treatment was later presented by McConnell<sup>65</sup>.

### The Bloch Equations

For a set of nuclei with a single chemical environment, the Bloch equations are

$$\frac{dM_x}{dt} = \omega_0 M_y - \frac{M_x}{T_2}$$

$$\frac{dM_y}{dt} = -\omega_0 M_x - \frac{M_y}{T_2}$$

$$\frac{dM_z}{dt} = -\frac{(M_z - M_0)}{T_1}$$

$M_x$ ,  $M_y$ , and  $M_z$  are the components of the magnetization vectors;  $\omega_0$  is the nuclear Larmor frequency in the steady applied field  $H_0$ , ( $\omega_0 = \gamma_N H_0$ ); and  $T_1$  and  $T_2$  are the longitudinal and transverse relaxation times respectively.

Transferring the coordinate system from the laboratory frame

of reference to a coordinate system rotating in phase with a rotating field  $H_1$  with an angular velocity  $\omega_1$ , the Bloch equations become

$$\begin{aligned}\frac{du}{dt} &= (\omega_0 - \omega)v - \frac{u}{T_2} \\ \frac{dv}{dt} &= -(\omega_0 - \omega)u + \gamma_N H_1 M_Z - \frac{v}{T_2} \\ \frac{dM_Z}{dt} &= -\gamma_N H_1 v - \frac{(M_Z - M_0)}{T_1}\end{aligned}$$

A steady state solution to these equations corresponding to slow passage conditions can readily be found by setting the time derivatives of the magnetization to zero. The solutions are

$$\begin{aligned}u &= M_0 \frac{\gamma_N H_1 T_2^2 (\omega_0 - \omega)}{1 + T_2^2 (\omega_0 - \omega)^2 + \gamma_N^2 H_1^2 T_1 T_2} \\ v &= M_0 \frac{\gamma_N H_1 T_2}{1 + T_2^2 (\omega_0 - \omega)^2 + \gamma_N^2 H_1^2 T_1 T_2} \\ M_Z &= M_0 \frac{1 + T_2^2 (\omega_0 - \omega)^2}{1 + T_2^2 (\omega_0 - \omega)^2 + \gamma_N^2 H_1^2 T_1 T_2}\end{aligned}$$

The quantities  $u, v$ , and  $M_Z$  denote the components of magnetization in phase with the rotating R.F. field, out of phase with the field and parallel to the stationary field respectively.

#### The Two-Site Case

The simplest case of chemical exchange involves the jumping of a nuclear spin between two sites A and B with different chemical shifts. The lifetimes of the nuclei at sites A and B are  $\tau_A$  and  $\tau_B$  respectively. The components of the magnetization vector are

$$u = u_A + u_B$$

$$v = v_A + v_B$$

$$M_Z = M_Z^A + M_Z^B$$

The modified Bloch equations become

$$\frac{du_A}{dt} = + (\omega_0^A - \omega)v_A - \frac{u_A}{T_{2A}} - \frac{u_A}{\tau_A} + \frac{u_B}{\tau_B}$$

$$\frac{dv_A}{dt} = - (\omega_0^A - \omega)u_A + \gamma_N H_1 M_Z^A - \frac{v_A}{T_{2A}} - \frac{v_A}{\tau_A} + \frac{v_B}{\tau_B}$$

$$\frac{dM_Z^A}{dt} = - \gamma_N H_1 v_A - \frac{(M_Z^A - M_0^A)}{T_{1A}} - \frac{M_Z^A}{\tau_A} + \frac{M_Z^B}{\tau_B}$$

There is an analogous set of equations to describe the magnetization of the nuclei at the B site. These equations differ from the usual Bloch equations by the addition of two terms in each case. For  $\frac{du_A}{dt}$ , these terms are  $-\frac{u_A}{\tau_A}$  and  $\frac{u_B}{\tau_B}$ . They represent the rate at which  $u$  decreases due to transfer of magnetization out of the A system and the rate at which  $u$  increases, due to transfer of magnetization into the A system from the B system respectively. Similar considerations apply to  $u_A$ ,  $M_Z^A$ ,  $u_B$ ,  $v_B$ , and  $M_Z^B$ . It is assumed that the time taken for a spin to jump from one site to the other is short compared to the lifetime at the site and the relaxation times, so that the nuclear precession during the jump may be neglected. The equations given cannot account for systems in which there is coherent spin-spin coupling of the nuclei

at the A and B sites. The extension of the modified Bloch equations, to multisite exchange is quite straightforward, but their solution is tedious and is usually carried out by a computer. The simplest problem to treat is the application to slow passage conditions where all time derivatives of the magnetization are set to zero. In this case, the set of coupled differential equations reduce to a set of simultaneous linear equations.

The general case for two site exchange can be solved fairly simply for low RF field, i.e., for the condition that  $\gamma_N^2 H_1^2 T_1 T_2 \ll 1$ . In this case,  $M_z \approx M_0$ ; this corresponds to no saturation of the NMR signals. The Bloch equations can be rewritten in terms of complex moments.

$$G = u + iv$$

The Bloch equations including chemical exchange become

$$\frac{dG_A}{dt} + \alpha_A G_A = -i\gamma_N H_1 M_0^A + \tau_B^{-1} G_B - \tau_A^{-1} G_A$$

$$\frac{dG_B}{dt} + \alpha_B G_B = -i\gamma_N H_1 M_0^B + \tau_A^{-1} G_A - \tau_B^{-1} G_B$$

where  $\alpha_A$  and  $\alpha_B$  are complex quantities defined by

$$\alpha_A = T_{2A}^{-1} - i(\omega_A - \omega)$$

$$\alpha_B = T_{2B}^{-1} - i(\omega_B - \omega)$$

$M_0^A = p_A M_0$  and  $M_0^B = p_B M_0$ , where  $p_A$  and  $p_B$  are the fractional populations at sites A and B. The solution is obtained by putting  $\frac{dG_A}{dt} = \frac{dG_B}{dt} = 0$ .

The total complex moment is given by

$$G = -i\gamma_N H_1 M_0 \frac{\tau_A + \tau_B + \tau_A \tau_B (\alpha_A p_B + \alpha_B p_A)}{(1 + \alpha_A \tau_A) (1 + \alpha_B \tau_B) - 1}$$

The intensity of absorption at frequency  $\omega$  is proportional to the imaginary part of  $G$ .

#### Slow Exchange

If  $\tau_A$  and  $\tau_B$  are sufficiently large relative to  $(\omega_A - \omega_B)^{-1}$ , the spectrum will consist of two distinct signals in the vicinity of  $\omega_A$  and  $\omega_B$ . If the RF frequency  $\omega$  is close to  $\omega_A$ , then  $G_B \approx 0$  and

$$G \approx G_A \approx -i\gamma_N H_1 M_0 \frac{p_A \tau_A}{1 + \alpha_A \tau_A}, \text{ the imaginary part is } \nu_A = \frac{\gamma_N H_1 M_0 p_A \tau_{2A}}{1 + (\tau_{2A})^2 (\omega_A - \omega)^2}$$

where  $\frac{1}{\tau_{2A}} = \frac{1}{T_{2A}} + \frac{1}{\tau_A}$ . There is, of course, a corresponding signal in the vicinity of  $\omega_B$ . If  $T_{2A}$  is known, the measurement of the linewidth provides a means of estimating  $\tau_A$ . This procedure is valid, provided the broadening is insufficiently rapid to cause appreciable overlap of the signals.

#### Rapid Exchange

In the limit of rapid exchange,  $\tau_A$  and  $\tau_B$  are very short. The nucleus experiences a field which is the average of the A and B environments, and a single resonance is obtained at the mean frequency of  $\omega_A$  and  $\omega_B$ , weighted by the fractional populations. The magnetization

is given by

$$G = -i\gamma_{N1} H_1 M_0 \frac{\tau_A + \tau_B}{\alpha_A \tau_A + \alpha_B \tau_B} = \frac{-i\gamma_{N1} H_1 M_0}{p_A \alpha_A + p_B \alpha_B}$$

The imaginary part is

$$v = -\gamma_{N1} H_1 M_0 \frac{T_2'}{(1 + T_2')^2 (p_A \omega_A + p_B \omega_B - \omega)^2}$$

This represents a line centered on the mean frequency

$$\omega_m = p_A \omega_A + p_B \omega_B$$

with a linewidth  $\frac{1}{T_2'} = \frac{p_A}{T_{2A}'} + \frac{p_B}{T_{2B}'}$

If the exchange is not sufficiently rapid to cause complete collapse, the width of the signal centered on  $\omega_m$  will be greater than the weighted average of  $T_{2A}^{-1}$  and  $T_{2B}^{-1}$ . In this case, the effective linewidth is

given by  $\frac{1}{T_2'} = \frac{p_A}{T_{2A}'} + \frac{p_B}{T_{2B}'} + p_A^2 p_B^2 (\omega_A - \omega_B)^2 (\tau_A + \tau_B)$

The transverse relaxation time in this case is appreciably shorter than the longitudinal relaxation time.

### Intermediate Rate of Exchange

The expression for the linewidth in the region of intermediate exchange rate is rather complicated even for a two-site exchange, unless some simplifying assumptions are made. If the A and B sites

have equal populations, equal lifetimes and large relaxation times, such that  $p_A = p_B = \frac{1}{2}$ ,  $\tau_A = \tau_B = 2\tau$  and  $T_{2A}^{-1} = T_{2B}^{-1} \approx 0$ , i.e., the linewidths are small compared to their separation, then the intensity of the absorption is proportional to

$$v = -\frac{1}{4} \gamma_N H_1 M_0 \frac{\tau(\omega_A - \omega_B)^2}{[\frac{1}{2}(\omega_A - \omega_B) - \omega]^2 + \tau^2(\omega_A - \omega)^2(\omega_B - \omega)^2}$$

A useful result derived from this equation is the rate at coalescence, i.e., when the lineshape exhibits neither a maximum or minimum at the mean frequency. For this case, the rate is given by

$$\tau^{-1} = \frac{2\pi(\nu_A - \nu_B)}{\sqrt{2}}$$

in frequency units. It should be noted that this equation applies only when the natural linewidth in the absence of exchange is very small compared to the separation of the lines.

#### General Case

When the number of sites involved in exchange exceeds two, it is not normal to calculate a lineshape function, as even when simplifying assumptions are made, the equations are extremely complex. The usual procedure is to set up a set of differential equation corresponding to the modified Bloch equations described above, expanded to the required number of sites with the inclusion of the appropriate terms required to describe the transfer of magnetization from each site to every other site. For the steady state solution of these equations, the values



of the derivatives of the magnetization are set to zero and the magnitudes of the magnetization are computed numerically at each value of  $\omega$ . The intervals of  $\omega$  must be chosen to provide sufficient resolution to allow comparison of the calculated spectra with experimental spectra. In favourable cases, it is possible to distinguish between different values for the relative rates of transfer of magnetization from one site to another on the basis of the agreement between the calculated and experimental spectra. In this fashion, it is possible to determine which of a variety of mechanisms of exchange is compatible with an experimentally determined lineshape. This procedure was used in the present work to obtain some of the results presented in chapter six. The programme used in the present work was originally written by Saunders<sup>66</sup>. The mathematics is described in greater detail by Sack<sup>67</sup>. Although the equations used are, in fact, derived from a quantum mechanical description of the NMR phenomenon, it is pointed out by Sack that the description is identical to that obtained by expansion of the Bloch equations in the manner of Gutowsky, McCall and Slichter<sup>64</sup>.

3.

## EXPERIMENTAL

### Sources of Compounds

The ligands acetylacetone, hexafluoroacetylacetone and trifluoroacetylacetone were obtained from Eastman Kodak Company. Diisobutyrylmethane was obtained from Fisher Scientific Company. Triacetylmethane was obtained from Aldrich Chemical Company. Vanadium (III) trichloride and all acetylacetonate complexes were purchased from the Research Organic/Inorganic Chemical Company. Deuterated solvents, acetone- $d_6$ , nitromethane- $d_3$  and acetonitrile- $d_3$  were purchased from Merck, Sharp and Dohme Canada Limited. Deuteriochloroform and benzene- $d_6$  were obtained from Stohler Isotope Chemicals.

### Preparation of Compounds

$V(acac)_3$ ,  $V(tfac)_3$ , and  $V(hfac)_3$  were prepared by a method similar to that reported by Morris et al.<sup>68</sup>

Carbon tetrachloride was flushed with dry nitrogen for a few minutes prior to the addition of anhydrous vanadium trichloride, and the stoichiometric quantity of the appropriate  $\beta$ -diketone. The mixture was refluxed with stirring for about 3 hours, during which time a small flow of nitrogen was maintained to prevent oxidation of the compound. The reaction was judged to be complete when a damp piece of blue litmus

held at the open end of the condenser no longer changed colour. The dark brown solution was filtered hot and allowed to cool in a nitrogen atmosphere. Crystallization of the complex was encouraged by cooling the carbon tetrachloride solution on ice. The precipitate was filtered and allowed to dry under nitrogen. The complexes were purified by repeated crystallization from carbon tetrachloride.

Preparation of tris(2,6-dimethylheptane-3,5-dionato)vanadium(III)

A very similar procedure to that described above was adopted. The reaction period had to be extended to twenty-four hours and a small amount of zinc dust was found to effectively retard oxidation.<sup>69</sup> The resulting solution was filtered and evaporated almost to dryness. A dark brown oil was obtained which was dissolved in methanol. The complex was precipitated out of solution by the gradual addition of water. The precipitate was washed with dilute aqueous sodium carbonate solution to remove excess ligand, washed with water and dried in vacuo over phosphorus pentoxide. The dried complex,  $V(\text{dibm})_3$ , was recrystallized from methanol. The compound was found to be very soluble in a wide variety of organic solvents and was found to be very difficult to recrystallize if a small amount of excess ligand remained. Because of the high susceptibility of this compound to oxidation, a sample suitable for analysis was not prepared. The composition of the compound was fully consistent with its NMR spectrum.

The method used in the above syntheses was found to be unsuccessful for  $V(\text{triac})_3$ . Under the conditions employed, the triacetylmethane decomposed to form acetylacetone and the product

obtained from the synthesis was almost pure  $V(\text{acac})_3$ . For this reason, a number of synthetic methods were attempted. The following was found to be the most successful. Although pure  $V(\text{triac})_3$  was not prepared, the material was quite adequate for the intended experiments.

#### Preparation of tris(3-acetylpentane-2,4-dionato)vanadium(III)

Triacetyl methane, 1.1 g. (0.0077 mol) was added to a solution of 0.4 g. of vanadium trichloride (0.0026 mol) in a 1:1 acetone-water mixture which had been previously flushed with dry nitrogen. Triethylamine 0.79 g. was added dropwise under nitrogen and the reaction mixture was left for about 16 hours. The resulting mixture was extracted with methylene chloride, dried with anhydrous magnesium sulphate, and the solution evaporated almost to dryness under nitrogen. Cold petroleum ether (30-60°) was added and the dark brown oil which separated was induced to crystallize by scratching the inside of the vessel with a glass rod. The product was recrystallized from carbon tetrachloride under nitrogen. From the NMR spectrum it was apparent that some of the ligand had partially decomposed and that the product was a mixture of  $V(\text{triac})_3$  and  $V(\text{triac})_2(\text{acac})$ . Chromatography on an alumina column failed to separate the complexes.

#### Preparation of Deuterated pentane-2,4-dione

A mixture of 20 ml. of acetylacetone (0.194 mol), 100 g. of deuterium oxide (5 mol) and a small amount of sodium carbonate was refluxed for 24 hours, cooled and extracted with anhydrous ethyl ether.

The ether layer was dried with anhydrous sodium sulphate for 24 hours and distilled. The distillate was further dried with potassium carbonate and again distilled. The fraction coming over at  $129^{\circ} \pm 1^{\circ}$  was collected. The degree of deuteration was estimated by comparison of the integrals of the  $^1\text{H}$  methyl resonances of sample containing 0.4 ml. of  $\text{CDCl}_3$  and 25  $\mu\text{l}$  of the deuterated acetylacetone and a sample containing 0.4 ml. of  $\text{CDCl}_3$ , 25  $\mu\text{l}$  of deuterated acetylacetone and a further 25  $\mu\text{l}$  of normal acetylacetone. The degree of deuteration was found to be 83.8% (estimated maximum degree of deuteration 86.6%). The procedure was not repeated, as complete deuteration was not required.

#### Preparation of Samples for Equilibrium and Experiments

Samples of the appropriate complex were recrystallized, and stored overnight in an evacuated dessicator containing phosphorus pentoxide. Solutions were prepared in a glove bag under a dry nitrogen atmosphere and transferred to NMR sample tubes. The sample tubes were then removed from the glove bag to a vacuum line. The solutions were degassed and the sample tubes evacuated and sealed. Samples prepared in this way appeared to be stable indefinitely. Samples for the ligand exchange experiments were prepared in a similar fashion, immediately before a set of runs. However, in this case, they were sealed with serum caps to allow the introduction of ligand. Evidence of decomposition of samples made up in this manner was usually visible after

several days, but was negligible in the time period required to complete the kinetic run. Deuterated solvents for these experiments were used as received, while other solvents were flushed with dry nitrogen and dried with 4A molecular sieves. Samples for lineshape analysis were allowed to equilibrate thermally, in the probe of NMR spectrometer for at least 10 minutes before the spectrum was scanned. The time required for a sample to equilibrate depends on the difference between the starting temperature of the sample and the temperature of the probe. The half time for the sample, i.e., the time required to reduce the temperature difference between the sample and the probe by half was estimated at approximately 20 seconds. This time period would allow a sample to become thermally equilibrated with the probe, to within experimental error, at any temperature in the range used in the present work. The temperature of the probe was measured before and after the running of a spectrum with a copper-constantin thermocouple placed in an NMR tube at the height of the transmitter and receiver coils of the spectrometer. The thermocouple was attached to a Leeds Northrup temperature potentiometer. The instrument was checked at 0°C and 100°C in an ice-water mixture and condensing steam respectively. It was found to be accurate to within 0.1° at 0°C and 0.25° at 100°C. In any case, where the initial and final temperatures differed by more than one degree, the spectrum was discarded. Spectra were also checked to ensure that saturation was not occurring. This was done by running a spectrum of the same sample with all settings on the spectrometer identical, except for the scan rate which was reduced to one fifth of the normal

value. If the spectra matched to within the noise level, saturation was considered to be insignificant.

### Errors in the Calculation of Activation Parameters

The precision of the activation parameters evaluated from the data presented in the Arrhenius plots may be readily evaluated by normal statistical methods<sup>70</sup>. The values of the errors in table 6-2 are given at the one  $\sigma$  level, i.e., at the 68% confidence level. In many of the calculations, as few as five points have been used and therefore, the values of  $\sigma$  cannot be regarded as highly reliable. Nevertheless, it is believed that they give a reasonable indication of the internal consistency of the data. If only random errors were to make a contribution to the errors in the activation parameters, the data could be regarded as rather satisfactory. There are, however, two major sources of error which will not affect the appearance of the Arrhenius plots within some limitations, and their magnitude cannot be estimated from the scatter of points around the Arrhenius plot. These are errors caused by an incorrect choice of the linewidth parameters, and errors caused by an incorrect choice of the temperature dependence of the lines.

For the cases of  $V(\text{tfac})_3$ ,  $V(\text{tfac})(\text{hfac})_2$  and for  $V(\text{triac})_2(\text{acac})$ , these errors are minimal, as most of the lines are well-resolved. At the highest temperatures employed, the linewidth in the absence of

exchange makes a relatively small contribution (~30%) to the total linewidth. An error in the estimation of the position of a line makes a relatively small error in the separation of one or more lines when that separation is large. From the Curie plots of temperature dependence, it is possible to estimate minimum and maximum separation of the lines at the highest experimental temperature. The maximum error in the separation of the upfield and downfield lines is about  $\pm 2.5\%$ . This leads to an error of approximately 0.12 kcals./mole in the activation energy. The contribution of linewidth to these errors is also expected to be relatively small, as the contribution of the natural linewidth to the total linewidth is only about 30%. An error of  $\pm 10\%$  in the estimated values of the linewidth will result in an error of approximately  $\pm 0.25$  kcals./mole. As shown below, a 10% error in the value of the linewidth parameter is probably quite reasonable. Taken together, these sources of error contribute about 0.3 kcals./mole. Taken with the random errors estimated at about 1.5 kcals./mole at the  $3\sigma$  level, the absolute value of the activation energy for the rearrangement of  $V(\text{tfac})_3$  is probably within 2 kcals. of the calculated value.

The situation is rather different for  $V(\text{hfac})_2(\text{acac})$ , and  $V(\text{dibm})_3$ . For these complexes, the linewidth in the absence of exchange makes a major contribution to the overall linewidth. Furthermore, because the separation of the lines is small, the relative error in the separation of the lines is larger than in the previous case. To estimate the magnitude of the error caused by an inaccurate choice of the linewidth parameter, Arrhenius plots were constructed using values of the rate constant obtained by calculating the total linewidth using an



erroneous value of the linewidth in the absence of exchange, and adjusting the rate parameter such that the overall linewidth matched that of the overall linewidth using the correct value. The parameters used in this calculation are approximately those of  $V(dibm)_3$ . Fig. 3-1 illustrates Arrhenius plots constructed, using values of the linewidth 10% and 30% different from the 'correct' value. The points on the central straight line are calculated and not experimental. When the value of the linewidth in the absence of exchange were altered by only 10%, the Arrhenius plot shows a distinct non-linearity. Whether or not a non-linearity can be observed in practice will depend upon how closely the overall linewidth approaches the line narrowing limit, (on the graphs in Fig. 3-1, the linewidth in the absence of exchange contributes about 80% to the total linewidth at the fastest rate calculated), and also on the scatter of the experimental points. From Fig. 3-1, it is possible to estimate that an error of 10% in the choice of linewidth will result in an error of approximately 15% in the activation energy. Errors due to an incorrect estimation of the separation of the resonances are not as readily estimated. The accuracy of the Curie plots to determine the temperature dependence is limited by the errors in the temperature measurements, the relatively large linewidths and the presence of noise in the spectra. Using the data for the  $V(dibm)_3$  measurements, the error in the separation of the linewidth at the highest temperature at the 3 $\sigma$  level is approximately  $\pm 3$  Hz. At this temperature, the separation of the two lines is about 30 Hz. Using the usual formula for the linewidth under fast exchange conditions, i.e.,

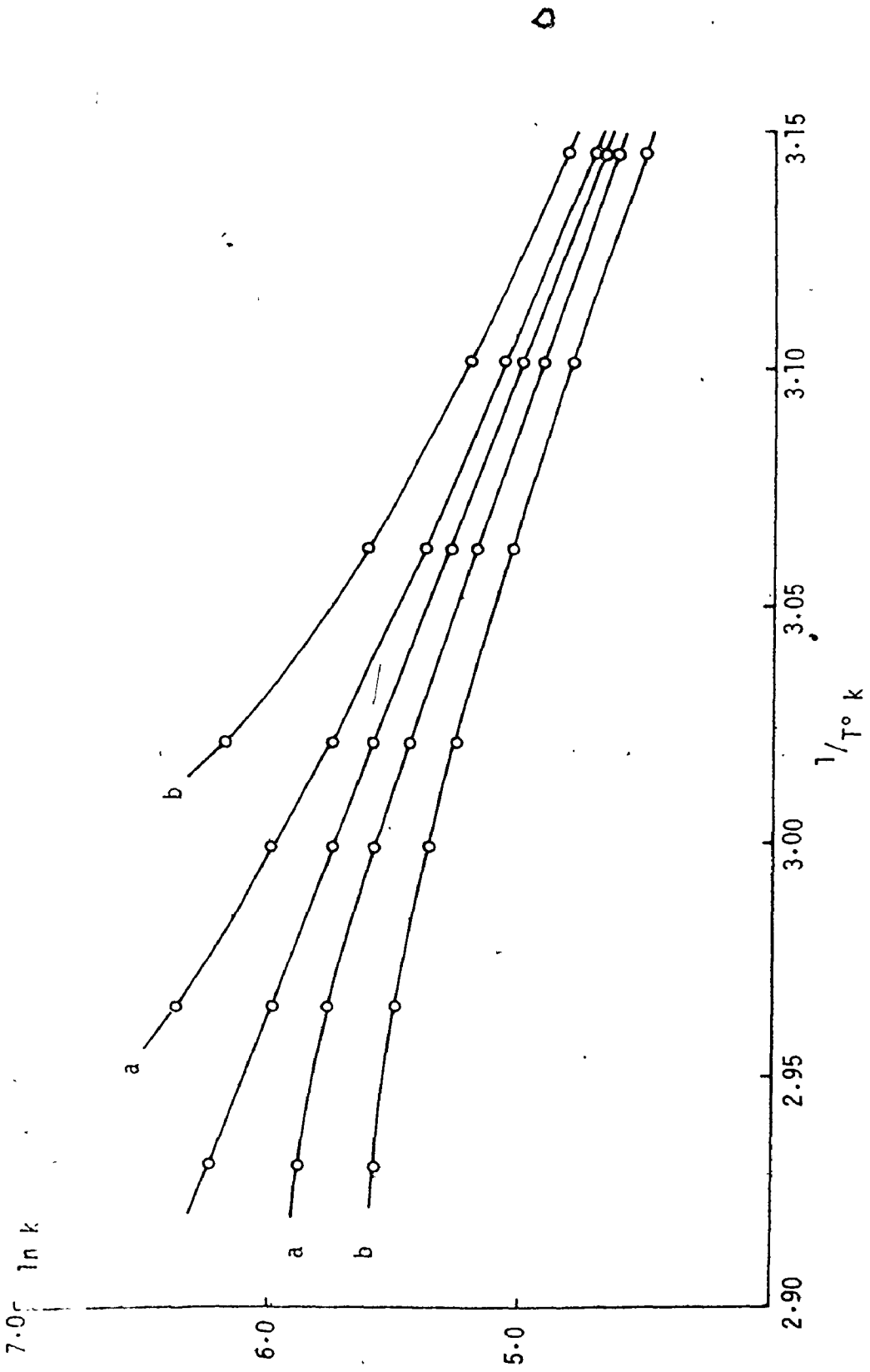


Figure 3-1. Arrhenius plots demonstrating the effect of deliberately choosing incorrect linewidth parameter; a  $\pm 10\%$ ; b  $\pm 30\%$ . Linewidth and line separation parameters are approximately those of  $V(dibm)_3$ .

$$k = \frac{(\nu_a - \nu_b)^2 \pi}{2\Delta\nu}$$

where  $k$  is the rate,  $\nu_a - \nu_b$  is the chemical shift difference in Hz., between the two sites, and  $\Delta\nu$  is the difference between the total linewidth and the average linewidth of the two sites in the absence of exchange. It is possible to calculate that this factor will contribute about 0.7 kcal/mole to the error in the activation energy. Summing the errors due to the various sources, i.e., random errors, the error due to a choice of linewidth parameter, and the error due to the estimated separation of the lines, a total error can be estimated at  $\sqrt{(1.5)^2 + (2)^2 + (0.7)^2} = 2.6$  kcal/mole. The errors in the calculation of the activation energies of the rearrangement of  $V(\text{hfac})_2(\text{acac})$  should be slightly greater than this as the lines are less well-resolved.

The activation energy for the site exchange of  $V(\text{acac})_2(\text{hfac})$  has not been included in table 6-2. When an attempt to make an Arrhenius plot of the rates for this compound was made, a reasonable activation energy of about 11 kcal/mole was obtained; however, the graph was distinctly non-linear. When the estimated linewidths in the absence of exchange were altered to give a linear plot, the value of the activation energy was estimated to be an anomalously high 26 kcal/mole. This discrepancy is probably due to the presence of a resonance of a methine proton which is almost coincident with one of the two methyl resonances. As this peak is unsymmetrically placed with respect to the methyl resonances, it is certain to have some effect on the apparent

linewidth of the coalesced peak. Because it is not observed independently and therefore its temperature dependence is undetermined, it is difficult to include the effect of this resonance in the lineshape calculation.

Some experiments carried out by Mr. I.A. Thompson, McMaster University, have indicated that there may be a rather serious systematic error in the measurement of temperature in these experiments. The temperature of the sample was measured by replacing the sample tube with another containing a thermocouple, placed at the height of the transmitting and receiving coils and packed with glass wool. This instrument performed remarkably well under static conditions; the error at  $0^{\circ}\text{C}$  was less than  $0.10^{\circ}$  and less than  $0.250^{\circ}$  at  $100^{\circ}\text{C}$ . A second thermocouple measuring the temperature of the gas flow immediately under the sample tube indicated a temperature different from that in the sample tube. This fact is, in itself, not particularly alarming; however, another thermocouple placed in the sample tube packed with methanol registered a different temperature from the original thermocouple packed in glass wool, even though the temperature measured at the thermocouple in the gas flow remained the same. The apparent difference between the temperature registered by the thermocouple packed in glass wool and the thermocouple packed in methanol is not explicable with certainty, but is probably related to the thermal conductivity of the materials. The difference in temperature between the thermocouple in methanol and in glass wool is not constant, but varies approximately linearly with temperature. The results indicate that the temperature intervals measured by the

thermocouple in methanol are smaller by a factor of about 0.88; thus, absolute activation energies may be about 15% greater than the calculated values, assuming that the measurements of temperature by the thermocouple placed in methanol more closely approximates the actual temperatures of the liquid samples than that of the dummy sample packed with glass wool.

Although the absolute values of the activation parameters for the rearrangement of the vanadium  $\beta$ -diketonate complexes may be in some doubt, internal comparisons of data should be reasonably valid within the limits imposed by other experimental errors discussed above, since as much care as was reasonably possible was taken to ensure that all spectra for kinetic measurements were obtained under the same experimental conditions. These limitations, due primarily to the difficulty of the measurement of temperature of the sample, are common to almost all high resolution NMR measurements of rate processes. It should be borne in mind that these results could probably not be obtained in any other way. Furthermore, the difficulties in estimating the activation parameters in no way affect the mechanistic conclusions based on lineshape analysis discussed in chapter six.

Introduction

The exchange of acetylacetonate with both palladium and aluminium acetylacetonates has been found by Saito et al.<sup>3,2</sup> to be accelerated by the presence of acids. This has been interpreted by the authors in terms of a protonated intermediate, in which the proton has attacked the free carbonyl group of the dangling ligand to retard its recombination to the metal and thus increase the reaction rate. Breaking of the second M-O bond was identified by Saito et al. as the rate determining step. If, as they suggest, the unidentate ligand has a 'considerably long lifetime', and breaking of the second M-O bond is relatively slow, it may be possible to obtain evidence for the existence of such a protonated intermediate directly by NMR.

The mechanism suggested by Saito et al. is by no means the only plausible mechanism for acid catalysed ligand exchange. Protonation may also occur on an oxygen coordinated to the metal, assisting in the rupture of the first chelate M-O bond, followed by rapid dissociation of the neutral ligand from the complex. Protonation of the  $\gamma$ -carbon of the acetylacetonate ligand is also possible. The first and second mechanisms would give rise to the enol form of the neutral ligand, while the third would give rise to the keto form. We have, therefore, investigated the behaviour of a number of simple metal acetylacetonate complexes with strong acid in non-aqueous solvents to obtain evidence for, if possible, the

existence of such protonated intermediates and to further the investigation of the mechanism(s) of acid catalyzed ligand exchange in  $\beta$ -diketonate complexes.

The technique of NMR spectroscopy has provided most of the data in this investigation. Preliminary experiments indicated the presence of more than one acetylacetonate species in some cases, which are in relatively rapid equilibrium. The IR spectra of acetylacetonates, although sensitive to changes in the complex are often complicated and difficult to interpret. With several species in solution, this problem is compounded. The UV spectra of acetylacetonate ligands are characterised by broad bands which do not offer much hope for resolution in a solution containing more than one species. NMR offers the distinct advantages that it is sensitive to changes in coordination of the ligand, while at the same time being relatively easy to interpret.

Trifluoroacetic acid ( $\text{CF}_3\text{COOH}$ ) has been used in most of these studies for several practical reasons: it is a relatively strong acid ( $\text{pK}_a$  0.25<sup>71</sup>); it is miscible with a wide variety of organic solvents; the conjugate base of the acid, the trifluoroacetate anion is generally a poor ligand; and undesirable side reactions such as dehydration or oxidation are unlikely with this acid. 100% sulphuric acid was used with  $\text{Al}(\text{acac})_3$  in some experiments and the results obtained were very similar to those obtained with trifluoroacetic acid. However, charring of the solutions containing sulphuric acid was usually evident at temperatures greater than 0° C.

## Results

Figure 4-1 (a and b) shows the  $^1\text{H}$  NMR spectrum of  $\text{Al}(\text{acac})_3$  in DMF and DMSO, containing approximately 0.5M trifluoroacetic acid. As well as the resonances of  $\text{Al}(\text{acac})_3$  itself, a number of new resonances are present. Three pairs of resonances with characteristic 'enolate' appearance are observed with chemical shifts of approximately 2.0 and 5.5 ppm and integral ratios of 6:1. The remaining pair has a 'keto' appearance with chemical shifts of approximately 2.2 and 3.6 ppm and an integral ratio of 3:1. The exact values of the shifts are dependent on the solvent and are reported in table 3-1.

It can be readily shown by the addition of acetylacetone to a solution containing  $\text{Al}(\text{acac})_3$  and  $\text{CF}_3\text{COOH}$  that one enol pair and the keto pair of resonances are due to free acetylacetone. One enolate pair of resonances is due to  $\text{Al}(\text{acac})_3$  itself, leaving another 'enolate' pair of resonances to be assigned. Since the acid appears to have displaced acetylacetone from the  $\text{Al}(\text{acac})_3$ , it seems most likely that the remaining pair of resonances is due to a species such as  $\text{Al}(\text{acac})_2^+$ . Both the methyl and methine signals assigned to this species are relatively broad, while the signals due to  $\text{Al}(\text{acac})_3$  and acetylacetone are sharp, suggesting that this species may be undergoing some exchange process which does not involve the other species.

In  $\text{CD}_2\text{Cl}_2$  and  $\text{CDCl}_3$ , the proton signals of the methine region are not well-resolved and do not integrate 1:6 with the methyl region (Fig. 4-2). This is not due to exchange of the methine protons with the deuterons



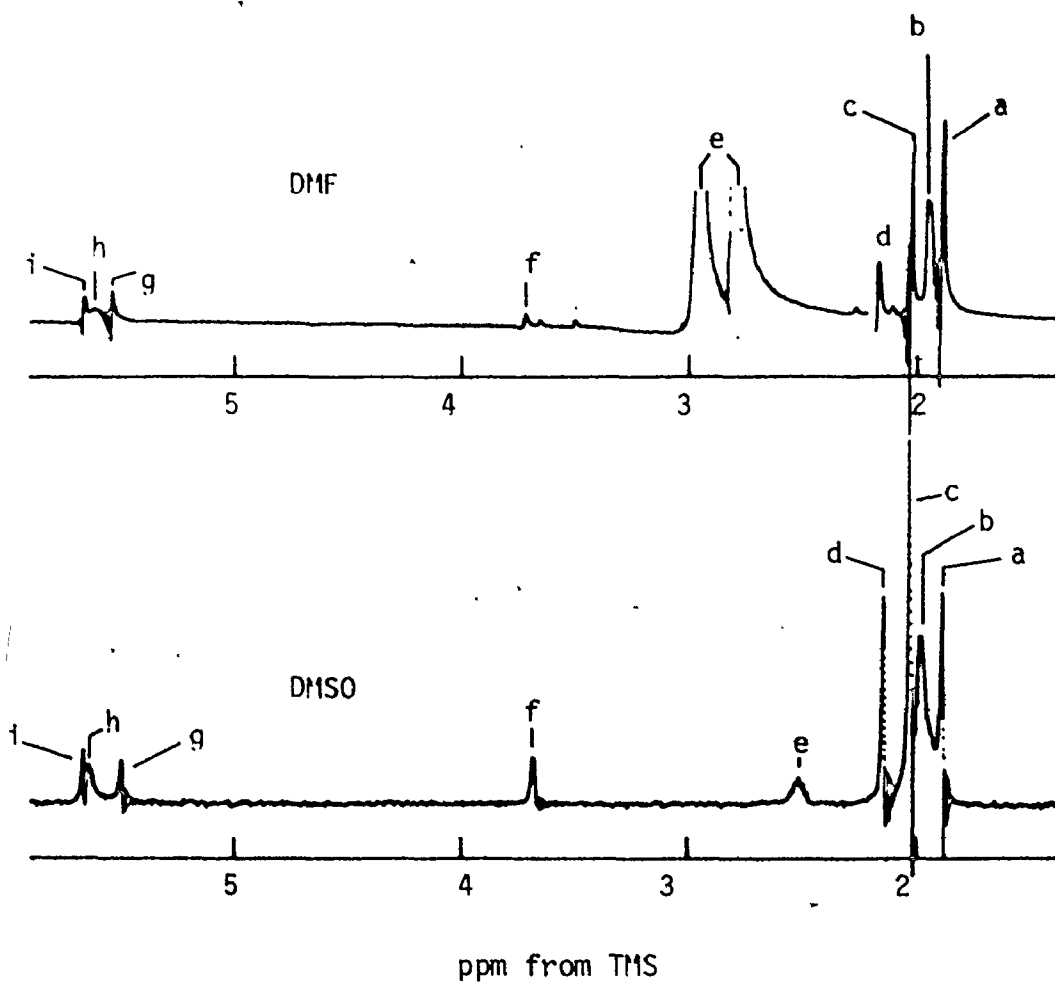


Figure 4-1.  $^1\text{H}$  100 MHz. NMR spectrum of  $\text{Al}(\text{acac})_3$  with  $\text{CF}_3\text{COOH}$  in DMF and DMSO.

a	$\text{Al}(\text{acac})_3$	}	methyl resonances
b	$\text{Al}(\text{acac})_2^+$		
c	Hacac (enol)		
d	acHac (keto)		
e	solvent		
f	acHac (keto)		methylene resonance
g	$\text{Al}(\text{acac})_3$	}	methine resonances
h	$\text{Al}(\text{acac})_2^+$		
i	Hacac		

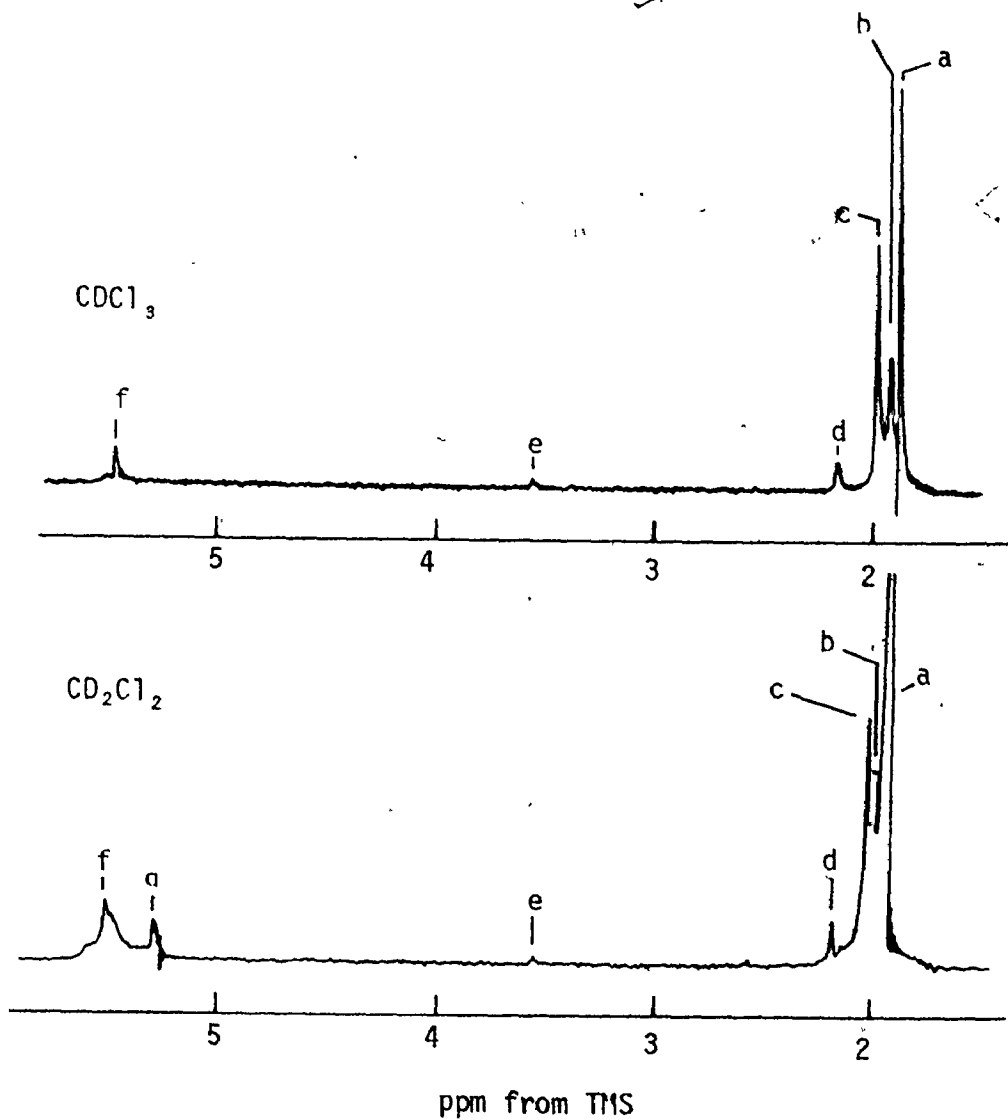


Figure 4-2.  $^1\text{H}$  100 MHz NMR spectrum of  $\text{Al}(\text{acac})_3$  with  $\text{CF}_3\text{COOH}$  in  $\text{CDCl}_3$  and  $\text{CD}_2\text{Cl}_2$

- |   |                              |   |                      |
|---|------------------------------|---|----------------------|
| a | $\text{Al}(\text{acac})_3$   | } | methyl resonances    |
| b | $\text{Al}(\text{acac})_2^+$ |   |                      |
| c | $\text{Hacac}$ (enol)        |   |                      |
| d | $\text{acHac}$ (keto)        | } | methylene resonances |
| e | $\text{acHac}$ (keto)        |   |                      |
| f | $\text{Hacac}$               |   | methine resonances   |
| g | solvent                      |   |                      |

of the solvent. No increase in the intensity of the residual protons in deuteriochloroform could be detected over a 24 hour period. The methyl region shows four peaks which can be assigned to the same species  $\text{Al}(\text{acac})_3$ , acetylacetonone in the enol and keto forms, and  $\text{Al}(\text{acac})_2^+$ .

At 220 M.Hz., the resonance assigned to  $\text{Al}(\text{acac})_2^+$  appears as two peaks which are considerably overlapped. Although the peaks are poorly resolved, they apparently have different line widths and have a similar dependence on the concentration of the acid. (Fig. 4-3) It is possible that the two peaks could be due to  $\text{Al}(\text{acac})_2^+$  and  $\text{Al}(\text{acac})_2^{2+}$ , or to  $\text{Al}(\text{acac})_2^+ \text{S}$ , cis and trans, where S is a solvent molecule, or to  $\text{Al}(\text{acac})_2^+ \text{S}_2$  cis alone, since a lack of sufficient symmetry in this complex would cause the methyl groups to occupy two chemically and magnetically different environments. The first possibility is unlikely, since the two species would have different dependences on the concentration of acid. The third possibility does not agree well either, since the two resonances would arise from the same complex and might be expected to have very similar line widths. The two peaks can, therefore, probably be assigned to  $\text{Al}(\text{acac})_2^+ \text{S}_2$  trans and cis. The broader peak can probably be assigned to the cis complex on the basis that it is composed of two closely overlapping peaks.

If charged species are formed, an increase in conductivity would be anticipated. The conductivity of a range of concentrations of trifluoroacetic acid in acetone was measured both in the presence and absence of  $\text{Al}(\text{acac})_3$  (Fig. 4-4). The conductivity of the solutions containing both  $\text{Al}(\text{acac})_3$  and  $\text{CF}_3\text{COOH}$  is indeed considerably greater than that of a solution containing  $\text{CF}_3\text{COOH}$  alone. This result supports the

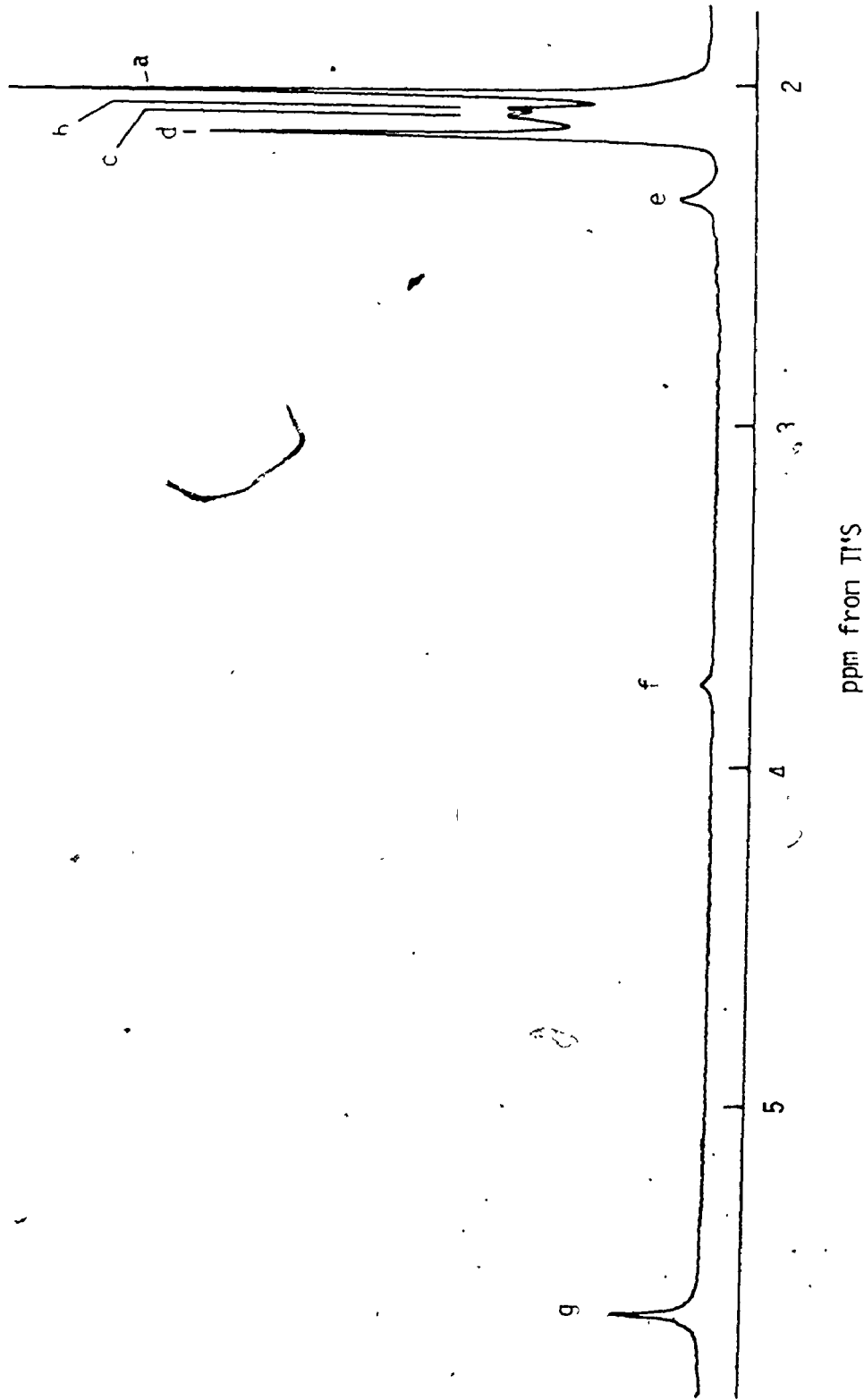


Figure 4-3.  $^1\text{H}$  220 MHz NMR spectrum of  $\text{Al}(\text{acac})_3$  with  $\text{CF}_3\text{COOH}$  in  $\text{CDCl}_3$  showing resolution of resonance assigned to  $\text{Al}(\text{acac})_2^+$

a	$\text{Al}(\text{acac})_3$		f	acHac	(keto)	methylene resonance
b	$\text{Al}(\text{acac})_2^+$	$\text{S}_2$ trans	g	Hacac	(enol)	methine resonance
c	$\text{Al}(\text{acac})_2^+$	$\text{S}_2$ cis	methyl resonances			
d	Hacac	(enol)				
e	acHac	(keto)				

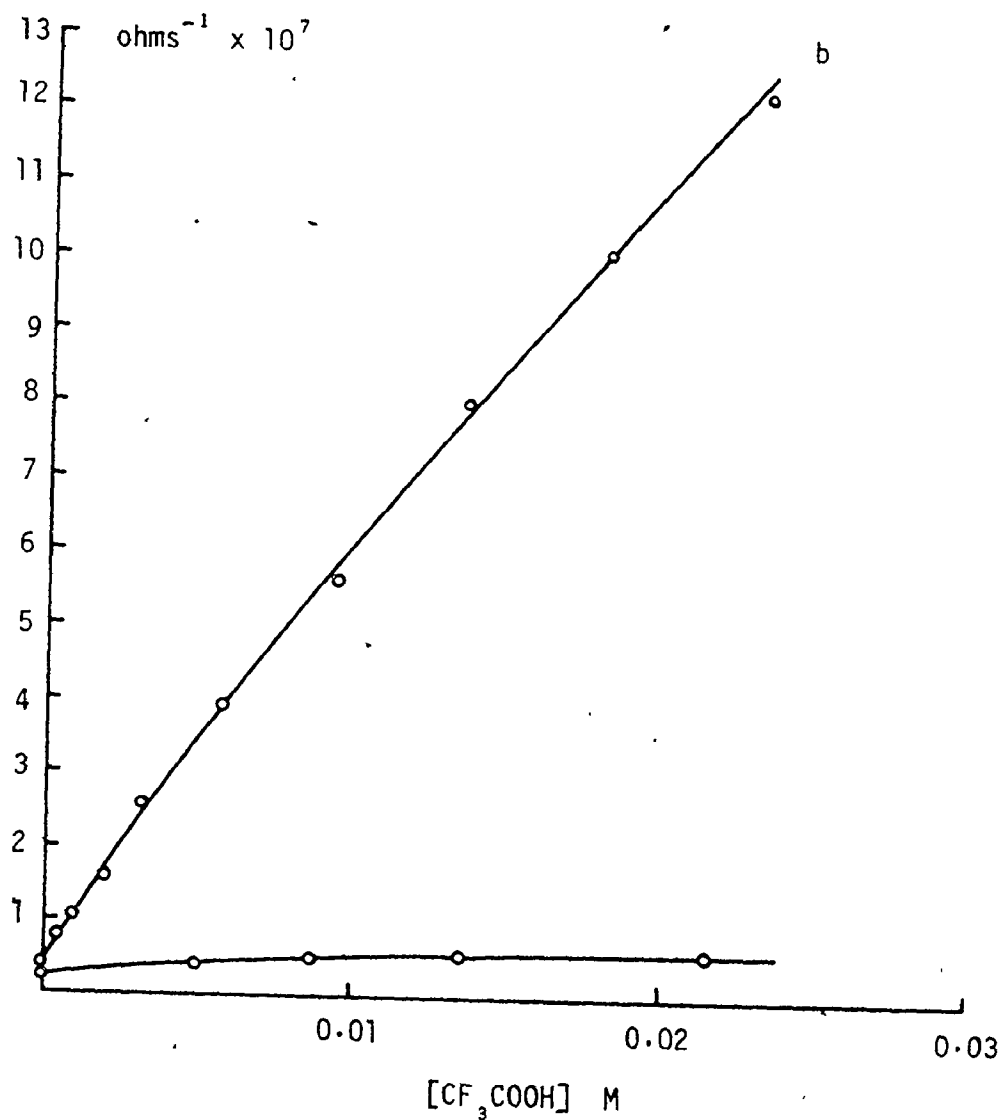


Figure 4-4. Conductivity of trifluoroacetic acid in acetone  
a, alone; b, in the presence of Al(acac)<sub>3</sub>  
(7.02 × 10<sup>-3</sup> M)

hypothesis that charged species are products of the reaction of  $\text{Al}(\text{acac})_3$  with  $\text{CF}_3\text{COOH}$ .

The behaviour of  $\text{Al}(\text{acac})_3$  with  $\text{CF}_3\text{COOH}$  in benzene solution is markedly different to that in DMF, DMSO, or acetone. The resonance of the methine proton of  $\text{Al}(\text{acac})_3$  is broadened by the addition of acid, (Fig. 4-5). The resonance of a small amount of free enol can be detected to high field of the  $\text{Al}(\text{acac})_3$  methyl resonance.  $\text{Al}(\text{acac})_3$  with  $\text{CF}_3\text{COOH}$  in nitromethane gives results very similar to those in benzene. The methine resonance is broadened by the addition of acid, and the methyl region consists of at least two broad, poorly resolved peaks. At high acid concentration (1M) in benzene, the methyl resonance of the free enol begins to broaden. The methine proton of the free acetylacetone also appears to be broadened to a similar extent.

If  $\text{CF}_3\text{COOH}$  is added to a solution of both  $\text{Al}(\text{acac})_3$  and acetylacetone in either benzene or nitromethane, the methine proton of the  $\text{Al}(\text{acac})_3$  is broadened, while the other resonances remain relatively sharp. This demonstrates that the ligand coordinated to the aluminium is not in fast exchange with free keto acetylacetone.

An attempt to 'freeze out' the exchange process involving the broad signal assigned to  $\text{Al}(\text{acac})_2^+$  was unsuccessful, as this signal decreased in intensity with decreasing temperature. In  $\text{CDCl}_3$  solution, solid material precipitated out of solution, making high resolution NMR impractical.

No exchange of the methyl groups in a  $\text{Al}(\text{acac})_3/\text{CF}_3\text{COOH}$  solution

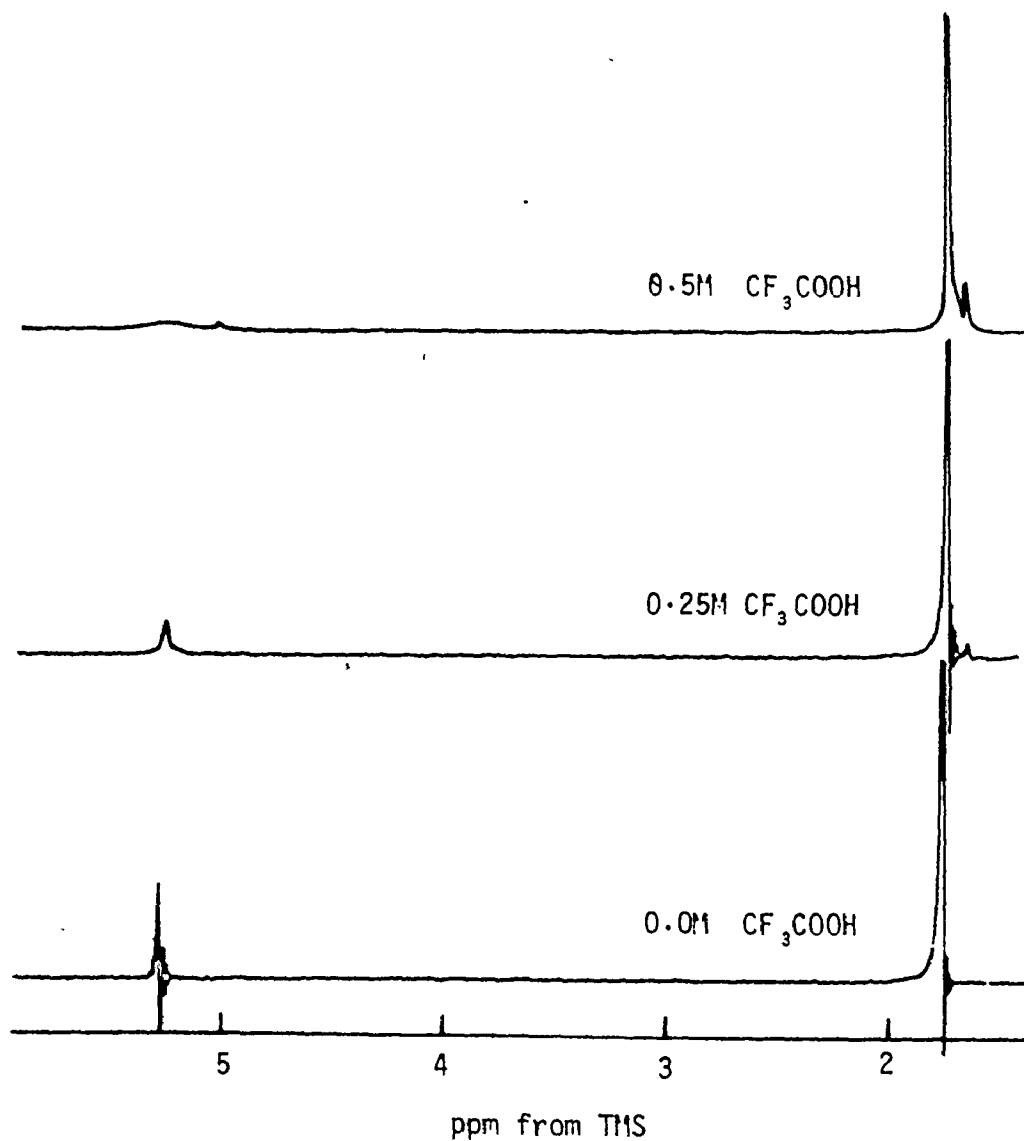
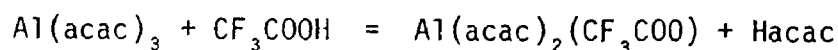


Figure 4-5.  $^1\text{H}$  100 MHz NMR spectrum of  $\text{Al}(\text{acac})_3$  with  $\text{CF}_3\text{COOH}$  in benzene showing the effect of acid on the methine proton signal. The signals appearing to high field of the  $\text{Al}(\text{acac})_3$  methyl and methine proton signals are those of free Hacac.

in acetone could be detected at 90°C, either by line broadening or by 'spin saturation transfer' (SST) techniques. Refluxing of the solvent prevented the use of higher temperatures.

There exists the possibility of species other than the proposed cationic  $\text{Al}(\text{acac})_2^+$  as products of the reaction of  $\text{Al}(\text{acac})_3$  and  $\text{CF}_3\text{COOH}$ . For example, the reaction



might be considered. Although such a reaction is not supported by conductivity measurements, it is helpful to have further confirmation of this. The  $^{19}\text{F}$  NMR of the  $\text{CF}_3$  group in  $\text{CF}_3\text{COOH}$  and in a trifluoroacetate anion coordinated to aluminium, might be expected to have different chemical shifts. Provided that the lifetime of a coordinated trifluoroacetate anion is sufficiently long, it should be possible to observe the NMR of a trifluoroacetate group coordinated to aluminium.

A  $^{19}\text{F}$  NMR spectrum of a chloroform solution of  $\text{Al}(\text{acac})_3$  and  $\text{CF}_3\text{COOH}$  showed only one resonance with the same chemical shift as  $\text{CF}_3\text{COOH}$ . Thus, there is no evidence for the formation of a non-labile complex containing trifluoroacetate as a ligand.

In chloroform, the methyl groups of both the enol and keto forms of the neutral ligand show small, but significant downfield shifts in the presence of  $\text{Al}(\text{acac})_3$  and  $\text{CF}_3\text{COOH}$ . These shifts cannot be accounted for by the presence of  $\text{CF}_3\text{COOH}$  alone (Table 4-1). In DMSO and DMF, however, no significant downfield shifts are observed. This result might



Table 4-1 Chemical shifts of acetylacetone and aluminium acetylacetonates in various solvents with and without trifluoroacetic acid

Species Solution	Hacac		acHac		Al(acac) <sub>3</sub>		Al(acac) <sub>2</sub> <sup>+</sup>	
	CH <sub>3</sub>	CH	CH <sub>3</sub>	CH <sub>2</sub>	CH <sub>3</sub>	CH	CH <sub>3</sub>	CH
CDCl <sub>3</sub> /Hacac	2.03	5.50	2.22	3.58	—	—	—	—
CDCl <sub>3</sub> /Al(acac) <sub>3</sub>	—	—	—	—	1.99	5.47	—	—
CDCl <sub>3</sub> /Hacac CF <sub>3</sub> COOH 0.5M	2.07	5.55	2.25	3.64	—	—	—	—
CDCl <sub>3</sub> /Al(acac) <sub>3</sub> CF <sub>3</sub> COOH 0.5M	2.12	5.57	2.70	3.66	2.03	5.6~	2.05	2.62
CD <sub>3</sub> NO <sub>2</sub> /Hacac	2.00	5.59	2.14	3.60	—	—	—	—
CD <sub>3</sub> NO <sub>2</sub> /Al(acac) <sub>3</sub>	—	—	—	—	1.91	5.54	—	—
CD <sub>3</sub> NO <sub>2</sub> /Al(acac) <sub>3</sub> CF <sub>3</sub> COOH 0.25M	—	some unresolved methyl signals	—	—	1.97	5.63 broad	—	—
benzene/Hacac	1.69	5.12	1.78	3.06	—	—	—	—
benzene/Al(acac) <sub>3</sub>	—	—	—	—	1.76	5.30	—	—
benzene/Al(acac) <sub>3</sub> CF <sub>3</sub> COOH 0.25M	1.66	4.98	—	—	1.76	5.30	—	—
DMF/Hacac	2.03	5.68	2.16	3.74	—	—	—	—
DMF/Al(acac) <sub>3</sub>	—	—	—	—	1.88	5.56	—	—
DMF/Al(acac) <sub>3</sub> CF <sub>3</sub> COOH 0.5M	2.03	5.68	2.16	3.74	1.88	5.56	1.92	5.64
DMSO/Hacac	2.02	5.68	2.14	3.69	—	—	—	—
DMSO/Al(acac) <sub>3</sub>	—	—	—	—	1.88	5.50	—	—
DMSO/Al(acac) <sub>3</sub> CF <sub>3</sub> COOH 0.25M	2.02	5.68	2.14	3.69	1.88	5.50	1.97	5.64

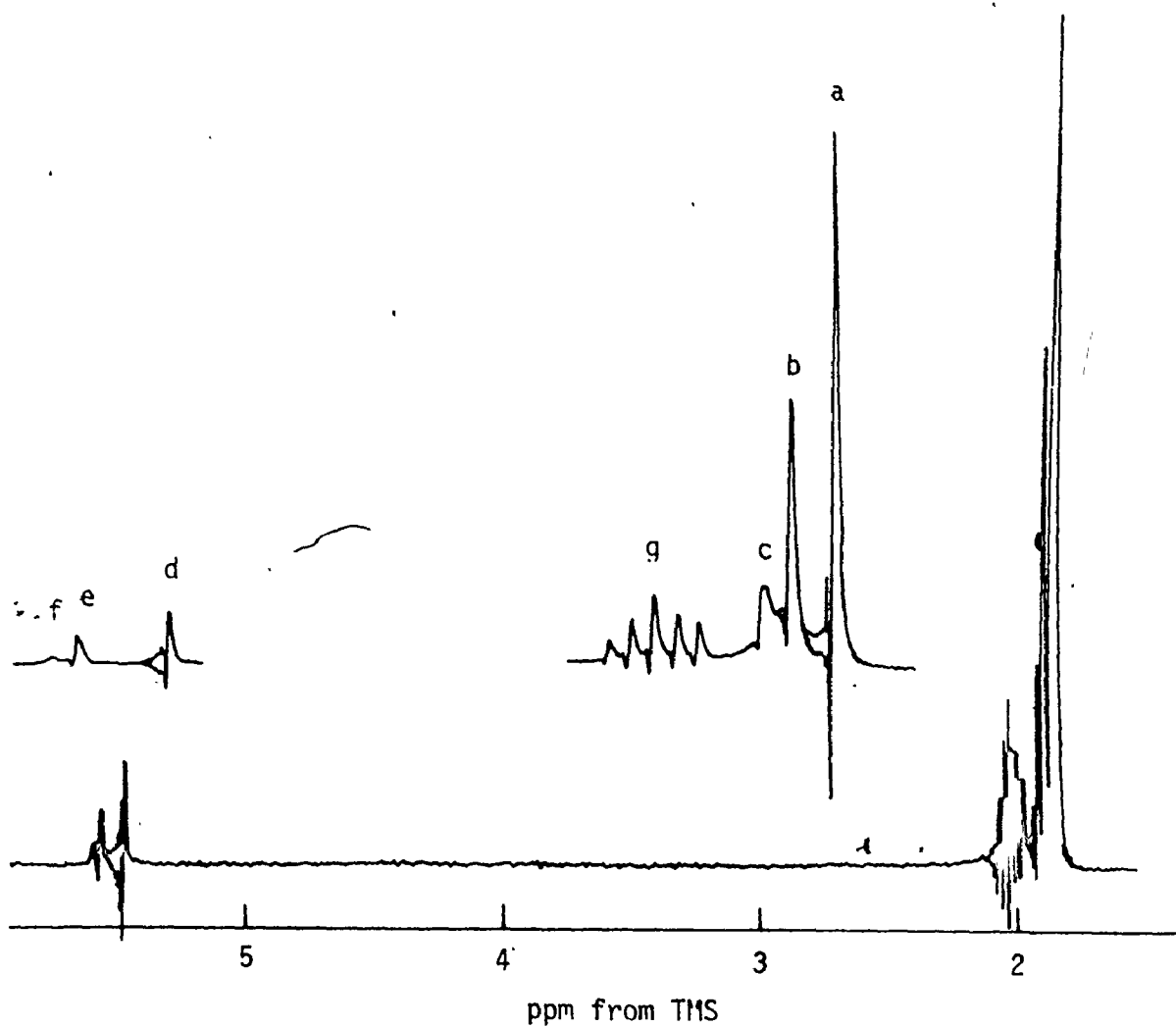


Figure 4-6. <sup>1</sup>H 100 MHz NMR spectrum of a mixture of Al(acac)<sub>3</sub> and Al(CF<sub>3</sub>COO)<sub>3</sub> in acetone. Insets show methyl and methine regions of the spectrum with the sweepwidth increased by a factor of four.

- |   |                                    |                     |
|---|------------------------------------|---------------------|
| a | Al(acac) <sub>3</sub>              | } methyl resonance  |
| b | Al(acac) <sub>2</sub> <sup>+</sup> |                     |
| c | Al(acac) <sub>2</sub> <sup>+</sup> |                     |
| d | Al(acac) <sub>3</sub>              | } methine resonance |
| e | Al(acac) <sub>2</sub> <sup>+</sup> |                     |
| f | Al(acac) <sub>2</sub> <sup>+</sup> |                     |
| g | solvent                            |                     |

be explained by some interaction of the neutral forms of acetylacetone with the tentatively proposed  $\text{Al}(\text{acac})_2^+$  complex.

If one of the products of the reaction of  $\text{CF}_3\text{COOH}$  is in fact  $\text{Al}(\text{acac})_2^+$ , it should be possible to generate this species in the absence of acid by the reaction of  $\text{Al}(\text{acac})_3$  with  $\text{Al}(\text{CF}_3\text{COO})_3$ .

A mixture of  $\text{Al}(\text{acac})_3$  and  $\text{Al}(\text{CF}_3\text{COO})_3$  in acetone gives rise to two new pairs of resonances other than those of  $\text{Al}(\text{acac})_3$ , both of which have a typical 'enolate' appearance, and have chemical shifts downfield of the corresponding  $\text{Al}(\text{acac})_3$  resonances (Fig. 4-6). The chemical shifts of the more intense pair is almost the same as that of the species tentatively identified as  $\text{Al}(\text{acac})_2^+$  in the presence of  $\text{CF}_3\text{COOH}$  in acetone. It is possible that the other pair of resonances are due to  $\text{Al}(\text{acac})_2^{2+}$ .

An intermediate involving a protonated dangling ligand has also been proposed in ligand substitution and ligand exchange reactions of  $\text{Pd}(\text{acac})_2^{2,4}$ . The behaviour of  $\text{Pd}(\text{acac})_2$  in solution with  $\text{CF}_3\text{COOH}$  was therefore also investigated in the same manner as that of  $\text{Al}(\text{acac})_3$ .

The action of  $\text{CF}_3\text{COOH}$  on  $\text{Pd}(\text{acac})_2$  gives rise to a number of new resonances in the  $^1\text{H}$  NMR spectrum. Some of the resonances are due to free acetylacetone in both keto and enol forms. The  $^{19}\text{F}$  spectrum of a solution of  $\text{Pd}(\text{acac})_2$  with  $\text{CF}_3\text{COOH}$  in  $\text{CDCl}_3$  has two new resonances, as well as that of  $\text{CF}_3\text{COOH}$  itself at 0.71 and 1.44 ppm downfield of  $\text{CF}_3\text{COOH}$ . These resonances occur, presumably, as a result of substitution of the trifluoroacetate anion on palladium in place of the acetylacetonate ligand, which has been protonated by the acid.

It is of interest to note that in a chloroform solution containing  $\text{Pd}(\text{acac})_2$ ,  $\text{CF}_3\text{COOH}$  and tetramethylsilane (TMS), a reaction occurs, in which loss of intensity of the TMS signal and the appearance of a new signal 0.21 ppm downfield from TMS is observed. At the same time, metallic palladium is plated out as a mirror on the wall of the NMR tube. These observations suggest a reaction similar to that which occurs between lead tetra-acetate and TMS in trifluoroacetic acid, in which oxidation of the TMS to trimethylsilylacetate occurs<sup>72</sup>. In this case, the product would have to be trimethylsilyltrifluoroacetate.

Even at 220 MHz., it was not possible to resolve all the signals in the  $^1\text{H}$  NMR spectra of chloroform solutions of  $\text{Pd}(\text{acac})_2$  and  $\text{CF}_3\text{COOH}$ . Since the palladium complexes having trifluoroacetate anion coordinated were not of immediate interest, this part of the investigation was not pursued further.

The broadening and subsequent loss of the methine proton signal which was observed when  $\text{Al}(\text{acac})_3$  was treated with  $\text{CF}_3\text{COOH}$  in benzene and nitromethane, was also observed when  $\text{Co}(\text{acac})_3$ ,  $\text{Rh}(\text{acac})_3$ , and to a lesser extent  $\text{Pt}(\text{acac})_2$  were treated with  $\text{CF}_3\text{COOH}$  in  $\text{CDCl}_3$ . However, the loss of neutral ligand and formation of cationic species was not observed. For example, the  $^1\text{H}$  NMR spectrum of the rhodium complex with  $\text{CF}_3\text{COOH}$  is illustrated in Fig. 4-7.

The  $^1\text{H}$  NMR spectrum of  $\text{V}(\text{acac})_3$  treated with  $\text{CF}_3\text{COOH}$  showed a decrease in intensity of the methyl and methine proton signals and the occurrence of free ligand resonances. There also appeared to be at least

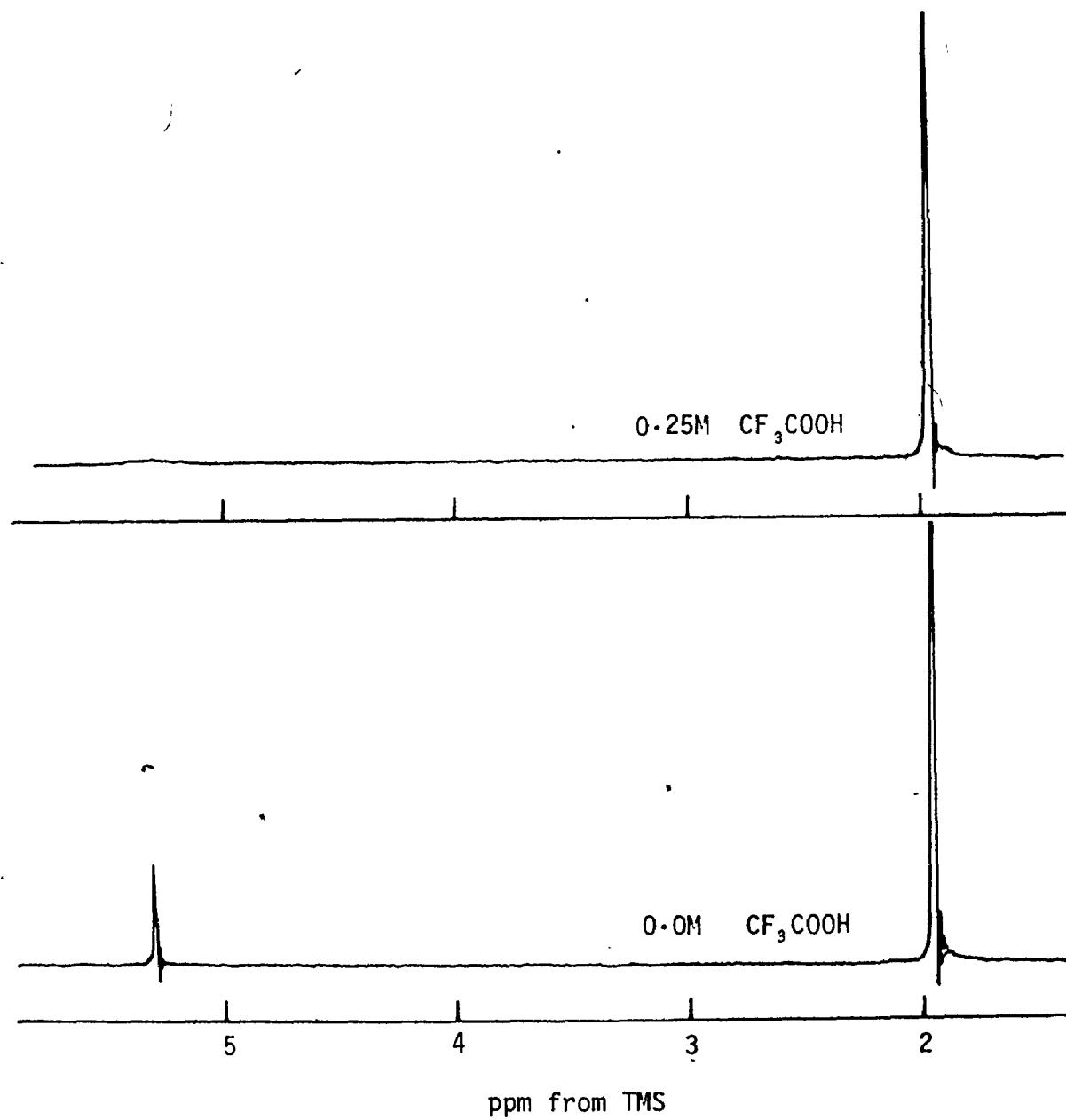


Figure 4-7.  $^1\text{H}$  100 MHz NMR spectrum of  $\text{Rh}(\text{acac})_3$  in  $\text{CDCl}_3$  showing the effect of  $\text{CF}_3\text{COOH}$  on the methine proton signal.

one extremely broad signal somewhat downfield of the  $V(acac)_3$  methyl signal. Superficially at least, the behaviour of  $V(acac)_3$  appears similar to that of  $Al(acac)_3$ .

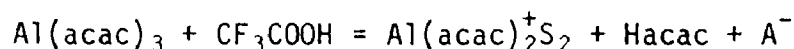
From the  $^1H$  NMR spectra and conductivity measurements, it seems reasonable to suppose that cationic aluminium  $\beta$ -diketonate complexes are formed when  $CF_3COOH$  reacts with  $Al(acac)_3$ . The exact nature of the observations are quite dependent on solvent.  $V(acac)_3$  appears to behave in a similar manner to  $Al(acac)_3$ .  $Pd(acac)_2$  behaves differently, losing acetylacetone and substituting trifluoroacetate. The remaining complexes examined, exhibited only one type of behaviour, i.e., the broadening and loss of the methine proton signal, similar to the behaviour observed for  $Al(acac)_3$  in benzene and nitromethane.

### Discussion

Cationic complexes of aluminium with acetylacetonate ligands have previously been reported by Movius and Matwiyoff<sup>73</sup>. They were prepared by the reaction of  $Al(acac)_3$  with  $Al(DMF)_6^{3+}(ClO_4^-)_3$  in DMF. The  $^1H$  chemical shifts of the complex  $Al(acac)_2(DMF)_2^+$  are quite similar to the shifts observed in the present work and are, as expected, downfield of the corresponding resonances in  $Al(acac)_3$ . Below  $5^\circ$ , separate signals for the cis and trans complex of  $Al(acac)_2^+(DMF)_2$  were observed, and the rate of isomerisation was found to be related to the rate of exchange of DMF between the first coordination sphere of the aluminium and the bulk solvent. In the present work, only a single broad peak attributed to  $Al(acac)_2^+$  was observed in DMF, DMSO, or acetone solutions, and it seems

likely that it is due to both the cis and trans complexes in fast exchange on the NMR time scale.

The above results are interpreted to indicate that the position of the equilibrium



is determined by the coordinating ability of the solvent. In coordinating solvents such as DMF, DMSO and acetone, the equilibrium is sufficiently far to the right to permit the observation of the cationic species which are presumably stabilized by the solvent molecules. The appearance of the cationic species does not appear to be so much dependent on the dielectric constant of the solvent, as in both nitromethane and benzene, the equilibrium tends to the left hand side of the equation. The trifluoroacetate anion is apparently not able to stabilize the cationic species confirming its poor ability as a ligand.

The ability of the acid to protonate the complex is also dependent on the solvent. Only in solvents of poor coordinating ability does exchange of the methine proton occur. The effective decrease in the strength of the acid in the coordinating solvents may occur directly as a result of hydrogen bonding with the solvent, or alternatively, as a result of a buffering action caused by the presence of trifluoroacetate anions.

The behaviour of  $\text{Al}(\text{acac})_3$  with  $\text{CF}_3\text{COOH}$  in  $\text{CDCl}_3$  and  $\text{CD}_2\text{Cl}_2$  represents a situation which is intermediate between the strongly coordinating solvents and the poorly coordinating solvents. Both

broadening of the methine proton of the complex and displacement of the ligand are observed.

In chloroform, small downfield shifts of the neutral ligand are observed with increasing acid concentration. Although the shifts are small, they cannot be accounted for solely by the presence of acid (Table 4-1). The remainder of the shift may be explained by coordination of both the enol and keto forms of the ligand to the cationic complex. No downfield shifts of the neutral ligands are observed in DMF or DMSO, presumably because the neutral ligands cannot displace the solvent molecules from the cationic complex.

The cationic  $\text{Al}(\text{acac})_2^+$  complex has been suggested by Saito and Masuda as an intermediate in the ligand exchange of  $\text{Al}(\text{acac})_3$  with  $\text{Hacac}$ . They have proposed that this intermediate occurs both as a result of the loss of the anionic acetylacetonate ligand, and also via acid catalysis as the result of the loss of a protonated ligand. The present discussion is concerned with the ways in which acid catalysis might promote ligand exchange.

#### Mechanisms of Acid Catalyzed Ligand Exchange

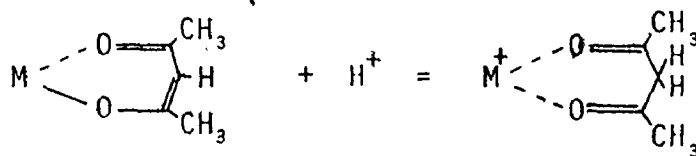
Three steps must occur in the acid-catalyzed dissociation of a neutral ligand of acetylacetone from the central metal ion, i.e., the breaking of each of the metal-oxygen bonds and protonation. Protonation may potentially occur on oxygen, leading ultimately to the dissociation of the ligand in the enol form, or on carbon, leading to dissociation of the ligand in the keto form. Protonation may occur before the breaking of



the first M-O bond, or between the breaking of the first and second bonds. Protonation of the ligand after rupture of the second M-O bond is not considered, as it would not affect acid catalysis. These various pathways are illustrated schematically in figure 4-8.

#### Protonation on Carbon

Protonation on the methine carbon is by no means implausible as a possible mechanism for acid catalysis of ligand exchange. Protonation at the methine carbon would result in a neutral molecule of acetylacetonone bonded in the keto form.



A number of complexes of this type containing a neutral molecule of acetylacetonone have been reported<sup>74 to 80</sup>

Adams and Larsen have reported that, while ligand exchange between zirconium, hafnium and thorium acetylacetonates and the free enol form of the ligand is observed to be fast on the NMR time scale<sup>81</sup>, the exchange of the keto isomer is very slow. This, they attribute to the difficulty of exchanging a proton which is bonded to carbon. This may be true when the proton must be transferred from one acetylacetonone molecule to another. The broadening and loss of the methine proton resonance of  $\text{Al}(\text{acac})_3$ ,  $\text{Co}(\text{acac})_3$ ,  $\text{Rh}(\text{acac})_3$ , and  $\text{Pt}(\text{acac})_2$ , when the  $\beta$ -diketonate complexes are treated with strong acid in non-coordinating solvents, demonstrates clearly that this is not necessarily the case.

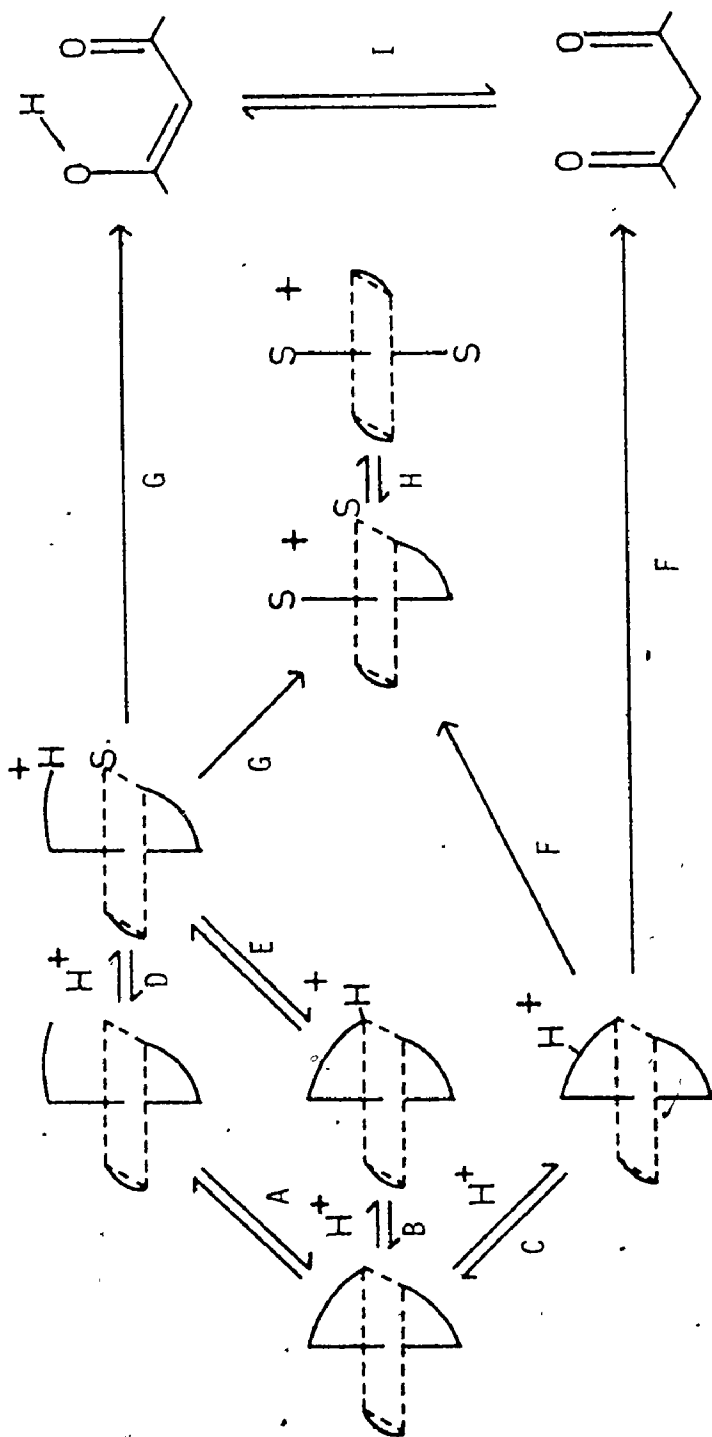


Figure 4-8. Possible mechanisms of acid catalysis of ligand exchange of a  $\beta$ -diketonate complex.

A, bond rupture; B, protonation on oxygen; C, protonation on carbon; D, protonation of free carbonyl group of dangling ligand; E, proton assisted bond rupture; F, loss of neutral 'keto' ligand; G, loss of neutral 'enol' ligand; H, rearrangement of cationic bis complex; I, tautomerism of ligand.

In a solution containing the complex, acid and acetylacetone, separate sharp resonances are observed for the methyl groups of the keto isomer and the complex. The broadened methine signal of the complex demonstrates clearly that protonation proceeds much faster than exchange and that dissociation of the neutral ligand rather than protonation is the rate limiting step. In contrast to this, however, Cramer<sup>75</sup> has found that separate keto and enol methyl peaks of acetylacetone coordinated to  $Zn^{2+}$  are observed in the NMR spectrum of  $Zn(acHac)_2(ClO_4)$  in nitromethane solution containing a small amount of water. The loss of a proton from the methylene group to water was identified as the rate determining step in the conversion of the keto form into the enol form of the coordinated ligand.

Exchange of the keto isomer between free and complexed sites has been observed to be fast on the NMR time scale for complexes of 3,3-dimethylacetylacetone with group IV halides<sup>72</sup> and for the keto isomer of acetylacetone with  $Mg^{2+}$ .<sup>74</sup> This indicates a rate which is probably in excess of  $10^2 \text{ sec}^{-1}$ . The loss of the methine proton resonance in the present work suggests a rate of ionisation of the coordinated keto form of acetylacetone, which is greatly in excess of the normal rate of ionisation, which is about  $1.5 \times 10^{-2} \text{ sec}^{-1}$ .<sup>82</sup> The metal ion presumably acts as a Lewis acid to assist in the deprotonation of the keto isomer. The catalysis of the deprotonation of the keto isomer of acetylacetone by  $Cu^{2+}$  ions in aqueous solution has previously been observed by Pearson and Anderson in the formation of  $Cu(acac)^+$ .<sup>83</sup>

It is interesting to note that the methine proton of the enol form of acetylacetone does not appear to exchange with trifluoroacetic acid on the NMR time scale. In accordance with this, acetylacetone is found to be protonated on oxygen rather than on carbon in HF,  $\text{HFSO}_3$  or  $\text{H}_2\text{SO}_4$ <sup>64</sup>. It is not immediately obvious why replacement of the enolic proton by a metal ion should increase the basicity of the methine carbon. An argument based on the relative size would predict that, as the C-C-C bond angle would be expected to decrease on protonation as the carbon is going from a  $\text{sp}_2$  to a  $\text{sp}_3$  configuration, the methine carbon should be more basic in the hydrogen chelate, rather than in the metal chelate.

Pearson has reported that he could find no evidence based on visible-UV spectra for the protonation of  $\text{Pt}(\text{acac})_2$  in aqueous perchloric acid solution. Our results show that exchange of the methine proton with  $\text{CF}_3\text{COOH}$  does occur, and that protonation must occur on the methine carbon. This does not contradict Pearson's result in any way, as the evidence for protonation in the present work is kinetic. The equilibrium concentration of the protonated intermediate is dependent upon the rate of loss of the proton which is presumably fast.

#### Protonation on Oxygen

The 'dangling ligand' has been postulated as an intermediate in both isomerization of octahedral chelate complexes and ligand exchange reaction. Saito and Masuda have interpreted the effect of acid catalysis of ligand exchange of  $\text{Al}(\text{acac})_3$  with Hacac and  $\text{Pd}(\text{acac})_2$  with Hacac, by

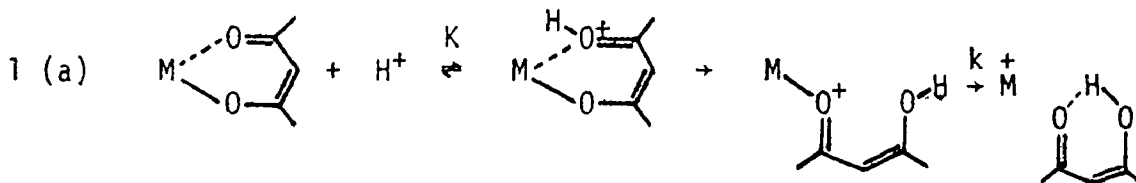
postulating that the acid protonates the free carbonyl group of the dangling ligand to prevent recombination to the metal. This, they suggest, merely serves to increase the effective concentration of the dangling ligand intermediate, and has no direct effect on the breaking of the second M-O bond.

Pearson and Johnson have interpreted the kinetics of some substitution reaction of  $\text{Pd}(\text{acac})_2$  complexes in a very similar way.

While the results of Pearson and Johnson are clearly consistent with this hypothesis, the results of Saito and Masuda are somewhat less definitive.

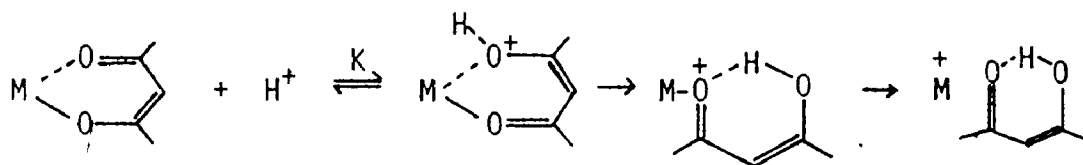
Two kinds of mechanism of acid catalysis may be considered.

1. The breaking of the first M-O chelate bond is the rate determining step, and the other end of the chelate breaks rapidly. Acid catalysis could operate by attacking the coordinated oxygen, effectively weakening the M-O bond to accelerate its rupture.



A plausible variation of this mechanism is that rather than undergo an initial bond rupture to form a dangling ligand, the protonated chelate might undergo a rearrangement such that the proton becomes coordinated to both oxygens and the metal becomes coordinated to a single oxygen.

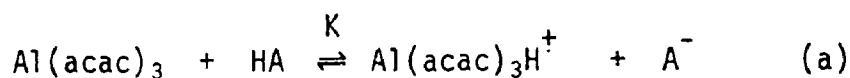
1 (b)



This could be considered analogous to the rearrangement undergone by the monocation of acetylacetonate<sup>84</sup> in strong acid systems. It is interesting to note that the x-ray structure of  $\text{MnBr}_2(\text{acacH})_2$ <sup>85</sup> shows acetylacetonate in the enol form bonded through a single oxygen to manganese. Presumably, in this mechanism, the rearrangement would be the rate determining step.

2. Breaking of the first M-O bond is rapid and reversible. Protonation of the free carbonyl occurs, resulting in a monodentate neutral enol ligand. The rate determining step will normally be the breaking of the second M-O bond.

Assuming that for mechanism 1 (a), the protonated intermediate is present in low concentration, i.e.,



the equilibrium concentration of  $\text{Al}(\text{acac})_3\text{H}^+$  is given by

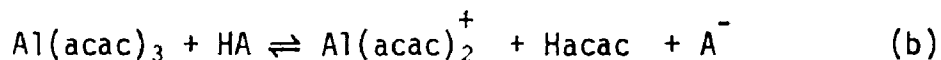
$$[\text{Al}(\text{acac})_3\text{H}^+] = \sqrt{K [\text{Al}(\text{acac})_3][\text{HA}]}$$

and the rate of loss of a neutral ligand is given by

$$k [\text{Al}(\text{acac})_3\text{H}^+] = k \sqrt{K [\text{Al}(\text{acac})_3][\text{HA}]}$$

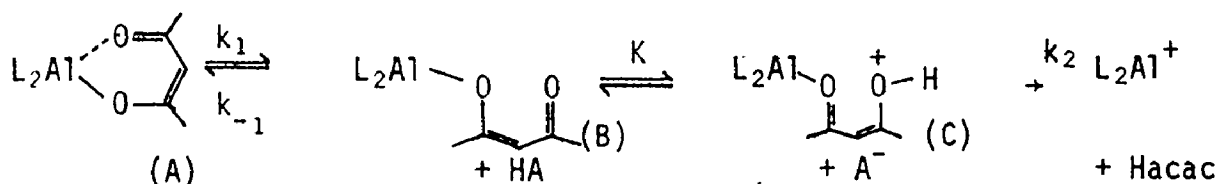
The rate of ligand exchange, therefore, would be proportional to the square root of the concentration of acid. This is true only if the concentration

of  $A^-$  is determined by the equilibrium above. However, our results indicate that in the presence of acid, the reaction



takes place. If the concentration of  $A^-$  is determined by this reaction, the rate would have a complex dependence on the acid concentration, but would not reach a limiting value until the  $Al(acac)_3$  were completely protonated.

If the reaction mechanism were



assuming that as in mechanism 1, the concentration of  $A^-$  is determined by the equilibrium (b), and that the concentration of intermediates (B) and (C) is small, application of the steady state approximation predicts that the rate of exchange is given by

$$R = \frac{k_1 [\text{complex}] [HA]}{\left( \frac{k_{-1}}{k_2 K} + \frac{[HA]}{[A^-]} \right) [A^-]}$$

This expression predicts that, at low acid concentration, i.e.,

$\frac{[HA]}{[A^-]} \ll \frac{k_{-1}}{k_2 K}$ , the rate of acid catalyzed exchange is dependent on acid concentration, and at sufficiently high acid concentration,  $\frac{[HA]}{[A^-]} \gg \frac{k_{-1}}{k_2 K}$ ,  $k_1$  is the rate determining step, and the rate of exchange is independent

of acid concentration. This expression is very similar to that derived by Pearson and Johnson<sup>4</sup> for the acid catalyzed substitution of  $\text{Pd}(\text{acac})_2$  in aqueous solution. The difference arises because the concentration of the conjugate base of the acid cannot be assumed to be constant. In aqueous solution it is, of course, the solvent itself.

Unfortunately, it was not possible to measure the rate of ligand exchange at high acid concentrations to determine whether a limiting rate of exchange could be observed. The rates of exchange were too fast to measure by classical techniques, and too slow to measure by line broadening or SST even at 95°C.

If  $k_2$  is in fact the slow step in the reaction, the protonated intermediate (C) should contribute to the chemical shift of  $\text{Al}(\text{acac})_3$  with which it must be averaged on the NMR time scale. Because of the inductive effect of both the central metal ion and the proton, the resonances of protonated ligand might be expected to have a substantial downfield shift. The enol form of acetylacetone has been observed to have a substantial downfield shift when coordinated to  $\text{Mg}^{2+}$ <sup>74</sup> and to  $\text{Zn}^{2+}$ <sup>75</sup> in nitromethane.

<sup>1</sup>H Chemical Shifts of Acetylacetone (enol) in Nitromethane Solution  
in ppm from TMS

	methyl	methine
Hacac	2.00	5.56
$\text{Al}(\text{acac})_3/\text{CF}_3\text{COOH}$	1.91	5.54
$\text{Mg}^{2+}(\text{Hacac})$	2.16	5.76 <sup>74</sup>
$\text{Zn}^{2+}(\text{Hacac})$	2.25	5.82 <sup>75</sup>



There is some doubt as to whether the values for the enol coordinated to  $Mg^{2+}$  represent the full extent of the shift of complexed enol, as the enol is in fast exchange between coordinated and uncoordinated sites.

The shifts of  $Al(acac)_3$  observed in coordinating solvents in the presence of acid are zero within experimental error, and are very small in the poorly coordinating solvents. (Table 4-1). The small shifts observed for  $Al(acac)_3$  could also be attributed to hydrogen bonding of the acid to the complex. This suggests that the existence of such a protonated intermediate is rather brief. Saito and Masuda claim that the activation energy of ligand exchange of  $Al(acac)_3$  is unaffected by acid catalysis. This is difficult to understand, as the enol form of acetylacetone is conjugated throughout, and the inductive effect of the proton on the free carbonyl might be expected to cause a weakening of the M-O bond. Their kinetic formula for the rate of exchange is expressed by

$$R = [\text{complex}] (k_1 + k_2 [H_2O] + k_1' [\text{acid}] + k_2' [\text{acid}] [H_2O])$$

Since their  $Hacac$   $^{14}C$  contained small amounts of water, the values of  $k_1$  and  $k_1'$  were not measured in the absence of water, but were estimated by extrapolation to zero concentration of  $H_2O$ , and as the authors themselves point out, their accuracy cannot be high enough. In Fig. 5 of reference 2, they identify  $k_2'$  as the slope of the graph. Since the graph plots  $k_0 = (k_1 + k_2[H_2O] + k_1'[\text{acid}] + k_2'[\text{acid}][H_2O])$  vs.  $H_2O$ , it appears that the slope of the graph is in fact  $k_2 + k_2'[\text{acid}]$  rather than  $k_2'$ . The major contribution to the slope is made by  $k_2$  in ethylacetate. It is therefore not surprising that Saito and Masuda estimate the same

activation energy for what they purport to be the  $k'_2$  path. Unfortunately, they do not report a value for  $k'_2$  in toluene where the contribution from  $k'_2$  [acid] appears to be rather greater than in ethylacetate. Thus, Saito and Masuda's claim that the activation energy of ligand exchange is unaffected by protonation does not appear to be unambiguously supported by their results.

The x-ray structure of the complex  $\text{MnBr}_2(\text{acacH})_2$  shows that the neutral enol ligand is coordinated to manganese through a single oxygen with a bond length of 2.20 Å. Comparison with M-O oxygen bond lengths found for normally coordinated acetylacetonate complexes of other transition metal ions ( $\text{Cu}(\text{acac})_2$ , 1.92 Å;  $\text{Zn}(\text{acac})_2 \cdot \text{H}_2\text{O}$ , 2.02;  $\text{Ni}(\text{acac})_2 \cdot 2\text{H}_2\text{O}$ , 2.01;  $\text{Co}(\text{acac})_2 \cdot 2\text{H}_2\text{O}$ , 2.06), suggests that the M-O bond of the neutral monodentate ligand is significantly longer.

The rapid exchange of enol between free and coordinated sites on  $\text{Mg}^{2+}$  in nitromethane observed by van Leeuwen and Praat<sup>74</sup>, indicates that breaking of the bond between the metal and the neutral enol is a relatively facile process.

The above arguments have been presented to imply that protonation on oxygen of coordinated  $\beta$ -diketonate ligand will result in a ligand which is weakly bonded to the central metal atom. A report by Fredette and Lock<sup>86</sup> of the crystal structure of bis ( $\mu$ -chlorotricarbonyl(1-phenyl-1-hydroxobut-1-ene-3-one) rhenium (I), indicates that this is not necessarily the case. A molecule of neutral Hbzac is bonded to rhenium through the keto group. The M-O distance is only 2.16 Å, which as the authors point out,

is identical to the M-O distances found for the  $\beta$ -diketonate ligand found in  $\text{Re}_2(\text{CO})_6(\text{dbm})_2$ , where the  $\beta$ -diketonate ligand is normally bonded<sup>87</sup>. Furthermore, the results of  $^1\text{H}$  NMR studies on this complex are in contrast to those for the enol complexes of  $\text{Mg}^{2+}$  and  $\text{Zn}^{2+}$  previously discussed, as a 0.05 ppm upfield shift relative to the free ligand was observed for the methine proton.

The coordinated neutral ligand was apparently not in rapid exchange with free ligand, as NMR spectra indicated free ligand as a decomposition product of the complex.

In chapter 6, evidence will be presented to suggest that intramolecular rearrangement of Vanadium  $\beta$ -diketonates proceeds via a bond rupture process. If the mechanism of acid catalyzed ligand exchange were 1a, then one might reasonably expect that as well as ligand exchange, intramolecular rearrangement would also be acid catalyzed. This is not the case for  $\text{V}(\text{tfac})_3$  or  $\text{V}(\text{hfac})_2(\text{acac})$ , suggesting that rupture of the first M-O bond is not assisted by protonation of these complexes.

These arguments are not intended to suggest that breaking of the second M-O bond is not the rate determining step in the acid catalyzed intermolecular ligand exchange. If breaking of the M-O bond is the rate determining step, deprotonation or dissociation of the neutral ligand is likely to be very rapid, resulting in a very low concentration of the protonated dangling ligand intermediate. This is quite consistent with the present results.

### Conclusion

To the extent that the cationic species  $\text{Al}(\text{acac})_2^+$  is observed, these results support the kinetic scheme of Saito and Masuda, although protonation on carbon would also be expected to give rise to the same intermediate. The observation that protonation occurs on the methine carbon of several acetylacetonate complexes indicates that a pathway involving a coordinated neutral keto ligand cannot be readily dismissed as a possible mode of acid catalyzed ligand exchange. However, no evidence to support a protonated dangling ligand with a 'considerably long lifetime' has been obtained.

## 5. LIGAND EXCHANGE OF $V(acac)_3$ with Hhfac and Hacac( $d_8$ )

### Introduction

Compared to molecular rearrangement processes of  $\beta$ -diketonate complexes, intermolecular ligand exchange reactions have received comparatively little attention. In recent years, a relatively small number of papers have appeared on the subject of ligand exchange of  $\beta$ -diketonate complexes. All of the studies reported have utilized either radio tracer techniques or line broadening and coalescence phenomena from magnetic resonance data. These two techniques are applicable to slow and fast exchange respectively. The former method suffers from the disadvantage that the product must be separated from the reaction mixture before measurement of the activity takes place. To collect a large amount of data is therefore a tedious and time consuming process. The latter technique is applicable to considerably faster reactions. It is limited to reactions where the lifetimes of the species involved are less than approximately 1 second. It is usually a relatively simple matter to adjust the temperature, at which the measurements are carried out to a range where the rate of the reaction is convenient. This technique also has the advantage that the system studied is at chemical equilibrium, and that a series of experiments may be carried out on a single sample.

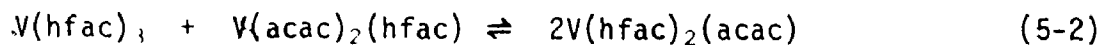
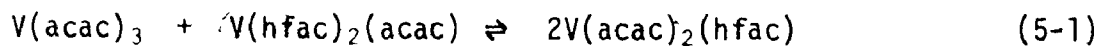
We have studied the exchange of hexafluoroacetylacetone and of deuterated acetylacetone with  $V(acac)_3$  by a simple NMR method. This

method is appropriate to exchange rates which are intermediate between those which can conveniently be studied by the techniques above. There have been no previous ligand exchange studies of (VII)  $\beta$ -diketonates. Preliminary experiments showed that the exchange rates were suitable for the NMR technique used. The information derived supplements the isomerization studies and will be compared with the conclusions of ligand exchange studies on other  $\beta$ -diketonates.

### Equilibria

Before proceeding to an analysis of the kinetics of the ligand exchange reaction, it is helpful to determine the position of the equilibria between the products:

The equilibrium constants for the reactions



may be determined by estimating the intensity of the resonances due to each complex in the  $^1H$  NMR spectrum. The relative concentration of each species can then be determined by dividing the intensity of the NMR signal by the number of protons which give rise to that signal. Although  $V(hfac)_3$  does not have any methyl protons, the concentration may still be determined by observation of the methine proton signal. Integration of the resonances was accomplished by tracing the signals from the original spectra and carefully cutting out the traced peaks and weighing them on an analytical balance.

The samples to be used for this experiment were prepared by intimately grinding together in a mortar and pestle, and under a dry nitrogen atmosphere, the appropriate ratios of  $V(\text{acac})_3$  and  $V(\text{hfac})_3$ . The concentrations of the solutions of the mixtures in  $\text{CDCl}_3$  were adjusted to approximately 0.1M. The NMR sample tubes were then removed from the dry nitrogen atmosphere to a vacuum line, degassed and sealed. Samples prepared in this way appeared to be stable indefinitely.

The equilibrium constant for equilibrium 5-1 is given by the expression

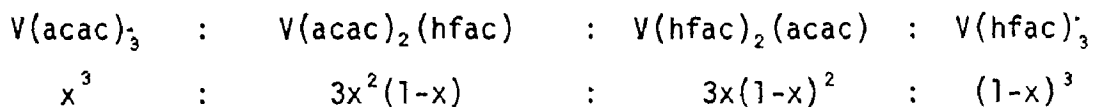
$$K_{V_1} = \frac{[V(\text{acac})_2(\text{hfac})]^2}{[V(\text{hfac})_3][V(\text{acac})_2(\text{hfac})]} \quad (5-3)$$

and for equilibrium 5-2 by the corresponding expression

$$K_{V_2} = \frac{[V(\text{hfac})_2(\text{acac})]^2}{[V(\text{hfac})_3][V(\text{acac})_2(\text{hfac})]} \quad (5-4)$$

The values of  $K_{V_1}$  and  $K_{V_2}$  are estimated at  $1.7 \pm .1 \times 10^2$  and  $2.8 \pm .2 \times 10^3$  respectively. The relatively large errors are due to the low intensity of the resonances of the species in the denominators of the equilibria expression in mixtures where the signals arising from both species can be observed.

A statistical value for the equilibrium constant is determined by the binomial expansion. The mole fraction of each complex is given by the expressions,



where  $x$  represents the mole fraction of  $\text{acac}^-$  of the total ligand present in all the complexes. The statistical values of the equilibrium constants are derived by substituting the statistically derived mole fractions of each complex into equations 5-3 and 5-4. For both  $K_{V_1}$  and  $K_{V_2}$ , the statistically expected value of the equilibrium constants is 3. Thus, the observed equilibrium constants are very much larger than the statistically expected values.

It is interesting to compare the equilibrium constants for the vanadium complexes to those for the analogous aluminium complexes<sup>21</sup>,  $K_{Al_1} = 46$  and  $K_{Al_2} = 725$ .

Although the deviation from the statistical value is considerably greater for the vanadium complexes, the ratios between the two sets of equilibrium constants for each case are quite similar.

$$\frac{K_{Al_2}}{K_{Al_1}} = 16 \qquad \frac{K_{V_2}}{K_{V_1}} = 17$$

Making the assumption that the difference between the statistical value of the equilibrium constant and the observed value for the vanadium is due only to enthalpy changes, values of  $\Delta H$  for equilibria 5-1 and 5-2 may be estimated from the expression

$$\Delta H = -RT \ln \frac{K_{\text{obs.}}}{K_{\text{stat.}}}$$



$\Delta H$  for equilibria 5-1 and 5-2 can be estimated at  $-2.4$  kcal/mole and  $-4.1$  kcal/mole respectively.

Pinnavaia and Fay<sup>88</sup> have shown from temperature dependence studies of  $Zr(acac)_4/Zr(tfac)$  mixtures, that the enthalpy of formation of mixed complexes from the parent complexes is within experimental error equal to zero. They suggest that the deviation from the statistical value of the equilibrium constant is due to differing entropies of solution. However, the deviation from statistical behaviour is small compared to that observed for either the aluminium  $(hfac)/(acac)$ ; or vanadium  $(hfac)/(acac)$  series.

Kida<sup>89</sup> has suggested a reason for deviation from statistical distribution based on an electrostatic model. He has shown that a reduction of the average ligand repulsion energy in mixed complexes, relative to the parent complexes, is to be expected whenever the charges on the ligands differ. This effect will lead to deviations from the statistical distribution in the sense observed.

This theory has been refined by Marcus and Eliezer<sup>90</sup> to include the effect of polarization on both the central ion and ligands. The effect of polarization can either enhance or reduce the stability of the mixed complexes. Application of this theory requires a knowledge of polarizabilities which are not readily available.

Using Kida's treatment, the energy of formation of a mixed six coordinate complex with cis configuration, is given by the expression

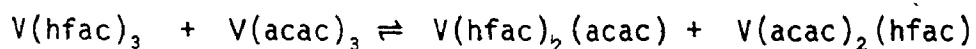
$$E(\text{cis})MX_4Y_2) - \frac{1}{6} (4E(MX_6) + 2E(MY_6)) =$$

$$\Delta e^2 (3\sqrt{2} + 1)/2r = 2.621 \Delta e^2/r$$

where E is the energy of the complex,  $\Delta e$  is the difference of the charge on the ligands and r is the M-X,Y bond length. For the formation of both mixed complexes, the expression is given by

$$E(\text{cis } MX_4Y_2 + MX_2Y_4) - E(MX_6) - E(MY_6) = 5.242 e^2/r$$

By summing  $\Delta H$  for equations 5-1 and 5-2,  $\Delta H$  for the reaction



is obtained and is equal to -6.5 kcal/mole. Assuming that the charges which determine the relative stability of the complexes reside mainly on the oxygen atoms, and that r has a value of 2.0 Å, it is possible to calculate that a difference of approximately 0.12 of an electronic charge on the hfac<sup>-</sup> and acac<sup>-</sup> oxygens would result in the observed deviations. This value appears reasonable; however, it should be pointed out that the model would also predict equal heats of reaction for reactions 5-1 and 5-2. The M-O bond lengths in the analogous aluminium complexes are shorter and therefore, this model would predict a greater deviation from the statistical equilibrium constants for aluminium. It is evident that these equilibria cannot be completely explained on purely electrostatic grounds.

#### Ligand Exchange Experimental Method

The concentration of the complex  $V(\text{acac})_3$  in the reaction mixture with Hhfac or Hacac  $d_8$  may conveniently be followed by repeatedly scanning through the area of interest while allowing the chart recorder to run

continuously. The samples containing the complex, solvent and other materials with the exception of the free ligand are prepared in NMR tubes prior to the experiment. The volumes are adjusted such that addition of the free ligand will bring the samples to a predetermined total volume. Sample tubes are allowed to thermally equilibrate in the probe of the NMR spectrometer before a run is begun. The sample is then removed, the appropriate volume of free ligand added, the sample tube vigorously shaken and replaced in the probe. The initial time ( $t_0$ ) is estimated from the time of mixing. The NMR tube must be removed from the probe for about thirty seconds to complete this process.

Because of the rather wide sweep range required to cover the methyl region of  $V(acac)_3$  and the subsequent products  $V(acac)_2(hfac)$  and  $V(acac)(hfac)_2$ , a field sweep mode is to be preferred to a frequency sweep mode as the exciting frequency is constant, and therefore the phase does not require adjustment. Because of the large scan width employed, any drift of the magnetic field during a kinetic run, typically 15 minutes, is usually insignificant. An unlocked mode is therefore quite acceptable. Another advantage of using paramagnetic samples is that the line widths are in this case, moderately large (50 Hz). Any small change in the homogeneity of the field will result in a change in the instrumental line width which is insignificant compared to the natural line width of the complex. It is therefore quite reasonable to estimate the intensity of a peak from the height alone, as one can be sure that the width will remain relatively constant. The rate at which the region of interest is scanned is limited by the requirement that slow passage conditions be

maintained. It is important also not to exceed the dynamic capabilities of the chart recorder, although this limitation could be easily circumvented if necessary.

In the present work, we have studied the reaction of Hhfac with  $V(acac)_3$  for the reason that the resonances of the methyl region of  $V(acac)_3$ ,  $V(acac)_2(hfac)$ , and  $V(acac)(hfac)_2$  are well resolved.  $V(hfac)_3$  has, of course, no methyl resonances and is not observed in this region.

It would also be of interest to study the reaction of  $V(hfac)_3$  with Hacac, but this is more difficult to accomplish, as it would be necessary to follow the course of the reaction using  $^{19}F$  NMR. Unfortunately, the trifluoromethyl resonances of  $V(hfac)_3$ ,  $V(hfac)_2(acac)$ , and  $V(hfac)(acac)_2$  are not well resolved, making analysis of the data difficult.

There are also difficulties in measuring the temperature dependence of the rates, as the experimental method requires that the sample tube be removed from the probe of the NMR spectrometer to introduce the free ligand. Because of the small mass of the sample and sample tube, the sample has a rather small heat capacity. The sample is expected, therefore, to change temperature quite rapidly, making the use of temperatures other than ambient impractical. The ambient temperature in these experiments is about 27°C.

$V(acac)_3$  is quite susceptible to oxidation, particularly in humid

conditions, and much more so in solution than in the crystalline state. Because of this, the  $V(acac)_3$  was recrystallized before use, and the solutions were prepared immediately prior to the experiment. Solvents were deoxygenated by flushing with dry nitrogen and stored over molecular sieves.

#### Analysis of Ligand Exchange Data

##### (i) $V(acac)_3$ with Hhfac

The H methyl resonances of  $V(acac)_3$ ,  $V(acac)_2(hfac)$  and  $V(hfac)_2(acac)$  have all been previously identified by Chua and Eaton<sup>6</sup>. The spectrum is illustrated in Fig. 5-1. Fig. 5-2 shows an example of a typical trace obtained during a kinetic run. The decay of the  $V(acac)_3$  peak, the appearance and subsequent decay of the  $V(acac)_2(hfac)$  peak and the appearance of the  $V(hfac)_2(acac)$  peak are readily apparent. The appearance of the complex  $V(hfac)_3$  cannot be observed in this manner, as the range swept covers only the methyl region. This, however, presents no real problem, since the value of the equilibrium constant  $K_{V_2} = 2.8 \times 10^3$  ensures that if there is an appreciable concentration of  $V(acac)_2(hfac)$  there will be a negligible concentration of  $V(hfac)_3$ . Under the conditions employed for the present experiment, a substantial concentration of  $V(acac)_2(hfac)$  remains, so that the total vanadium present is accounted for by the observed species.

Coefficients relating the height of the peaks to the actual concentration of the species can be obtained by solving a set of three simultaneous linear equations:

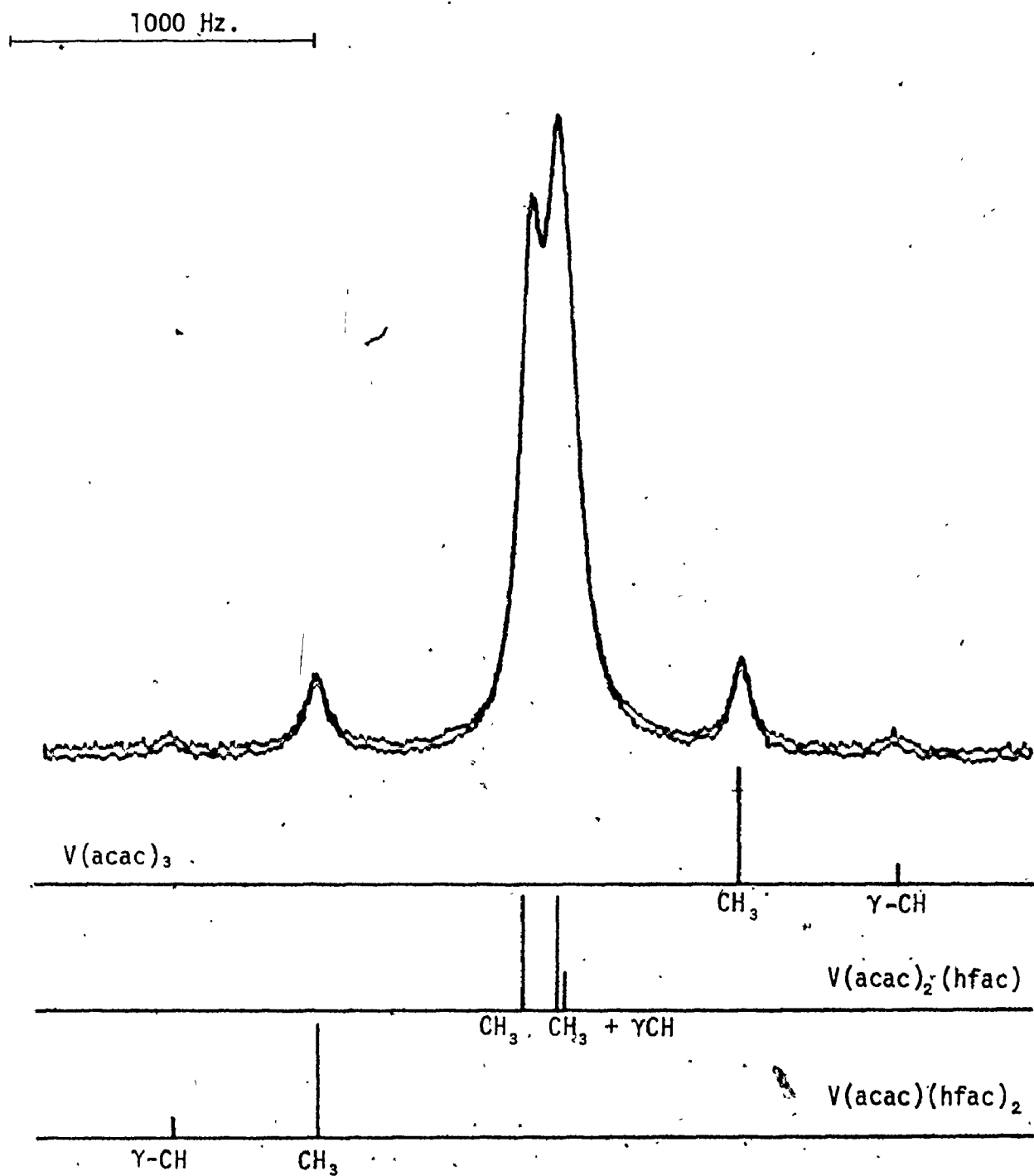


Figure 5-1.  $^1H$  spectrum of the methyl region of a mixture of  $V(acac)_3$  and  $Hhfac$  at 56.4 MHz. in  $CDCl_3$ .

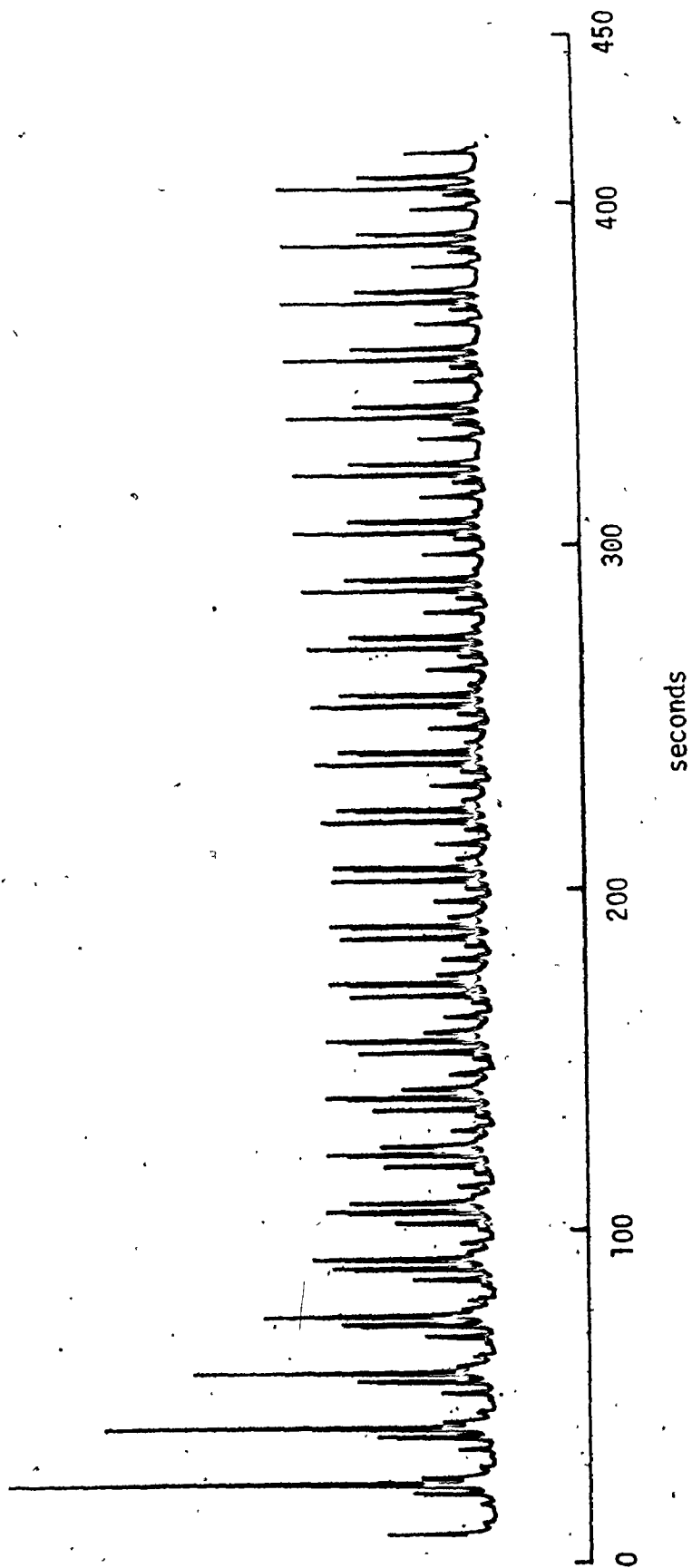


Figure 5-2. Intensity of  $^1\text{H}$  methyl resonances of  $\text{V}(\text{acac})_3$ ,  $\text{V}(\text{acac})_2(\text{hfac})$  and  $\text{V}(\text{hfac})_2(\text{acac})$  during a typical ligand exchange reaction of  $\text{V}(\text{acac})_3$  with  $\text{Hhfac}$ . Initial concentration of  $\text{V}(\text{acac})_3 = 0.178\text{M}$  and of  $\text{Hhfac} = 0.468\text{M}$ .

$$a A_1 + b B_1 + c C_1 = V$$

$$a A_2 + b B_2 + c C_2 = V$$

$$a A_3 + b B_3 + c C_3 = V$$

where  $a$  and  $b$  are the coefficients,  $A_1$ ,  $B_1$ , and  $C_1$  are the heights of the peaks due to  $V(\text{acac})_3$ ,  $V(\text{acac})_2(\text{hfac})$  and  $V(\text{hfac})_2(\text{acac})$  at  $t_1$  etc., and  $V$  is the total concentration of the vanadium  $\beta$ -diketonate complexes. From results such as those shown in Fig. 5-2, a plot of the variation of the concentration of each species with time may be obtained as in Fig. 5-3. The constancy of the total concentration of vanadium supports the validity of this method of analysis. Van Wazer<sup>91</sup> has pointed out that it is relatively easy to fit overall rate data to kinetics corresponding to an incorrect scheme where a number of adjustable rate constants are involved. For this reason, we have chosen to analyse the data by the method of initial rates, i.e., by estimating  $d[V(\text{acac})_3]/dt$  at  $t_0$  by extrapolation of the concentration back to  $t_0$  and estimating the slope of the line. In fact, it was found to be more convenient to plot  $\ln[V(\text{acac})_3]$  versus time, as during the initial stages of the reaction, the logarithmic plots were considerably more linear and therefore easier to extrapolate.

(ii)  $V(\text{acac})_3$  with  $(\text{Hacac})d_8$

The exchange of acetylacetone with  $V(\text{acac})_3$  was followed by observing the decay in intensity of the  $V(\text{acac})_3$  peaks in the  $^1\text{H}$  NMR spectrum as normal ligands were replaced by deuterated ligands:

The rates of exchange were obtained in this case, by treating the



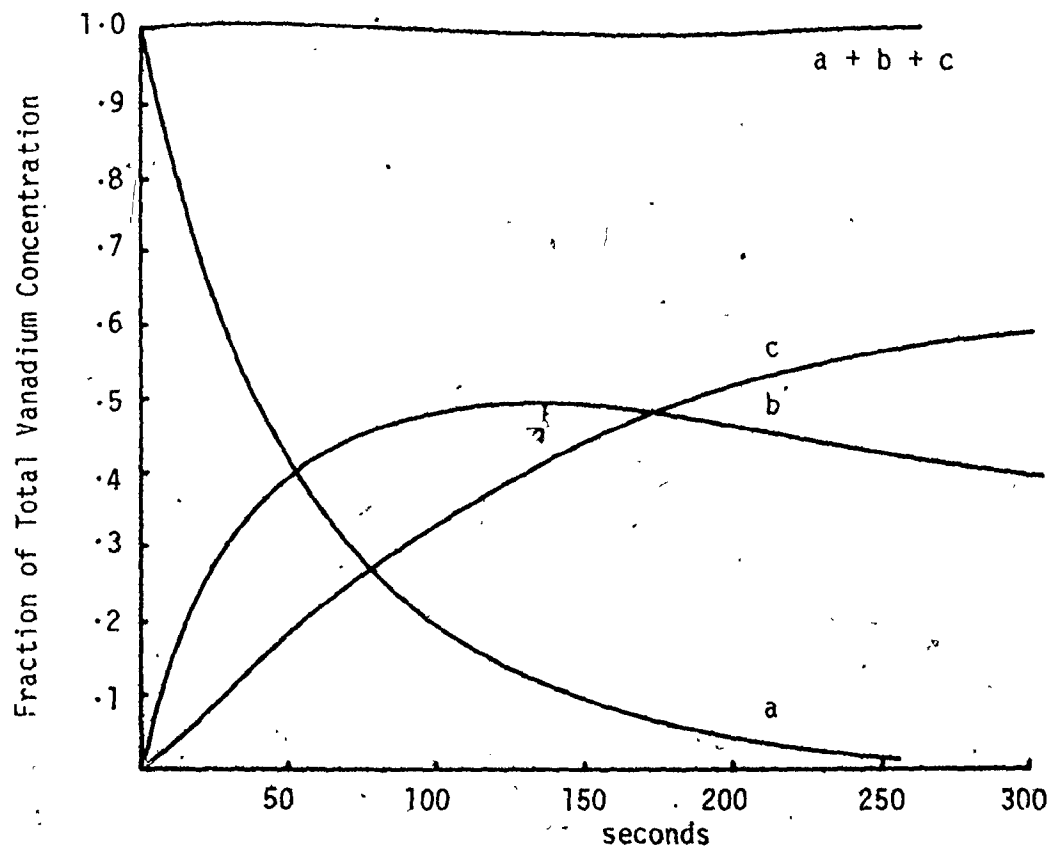


Figure 5-3. Variation of concentrations of vanadium  $\beta$ -diketonates as fractions of the total vanadium concentration during a typical run.

$[V]$  total = 0.178M  $[Hhfac]$  initial = 0.468M

a,  $V(acac)_3$ ; b,  $V(acac)_2(hfac)$ ; c,  $V(hfac)_2(acac)$

This diagram is based on data from figure 5-2.

Experimental points have been omitted for clarity.

observed rates of decay of the methyl peak of V(acac) with McKay's formula given below.

$$R = \frac{-3ab}{3a + b} \cdot \frac{\ln(1-F_t)}{t}$$

a and b denote the initial concentrations of a complex with three replaceable ligands and free ligand respectively.  $F_t$  is the fraction of the reaction which has occurred by time t.  $F_t$  may be estimated from some property of the system which varies with time, say P, such that  $P = P_0$  at time  $t_0$ ,  $P_t$  at time t and  $P_\infty$  at time  $t = \infty$ .

$$F_t \text{ is given by } (P_t - P_\infty) / (P_0 - P_\infty)$$

In this case, P corresponds to the intensity of the methyl signal of  $V(acac)_3$ . Because the rate is estimated from the fraction of reaction, it is not necessary for the ligand to be completely deuterated. In these experiments, the degree of deuteration of the ligand was about 85%. Total reaction, corresponding to  $P_\infty$ , was estimated from intensity of the methyl resonance of  $V(acac)_3$  after allowing the reaction mixture to reach equilibrium.

Fig. 5-4 is an example of a typical trace obtained for the reaction of  $V(acac)_3$  with deuterated acetylacetone. An important observation to make is that the intensity of the methine proton signal reaches its equilibrium value very much more rapidly than the methyl proton signal. Exchange of the methine proton evidently occurs by a different process from that which exchanges the methyl protons.

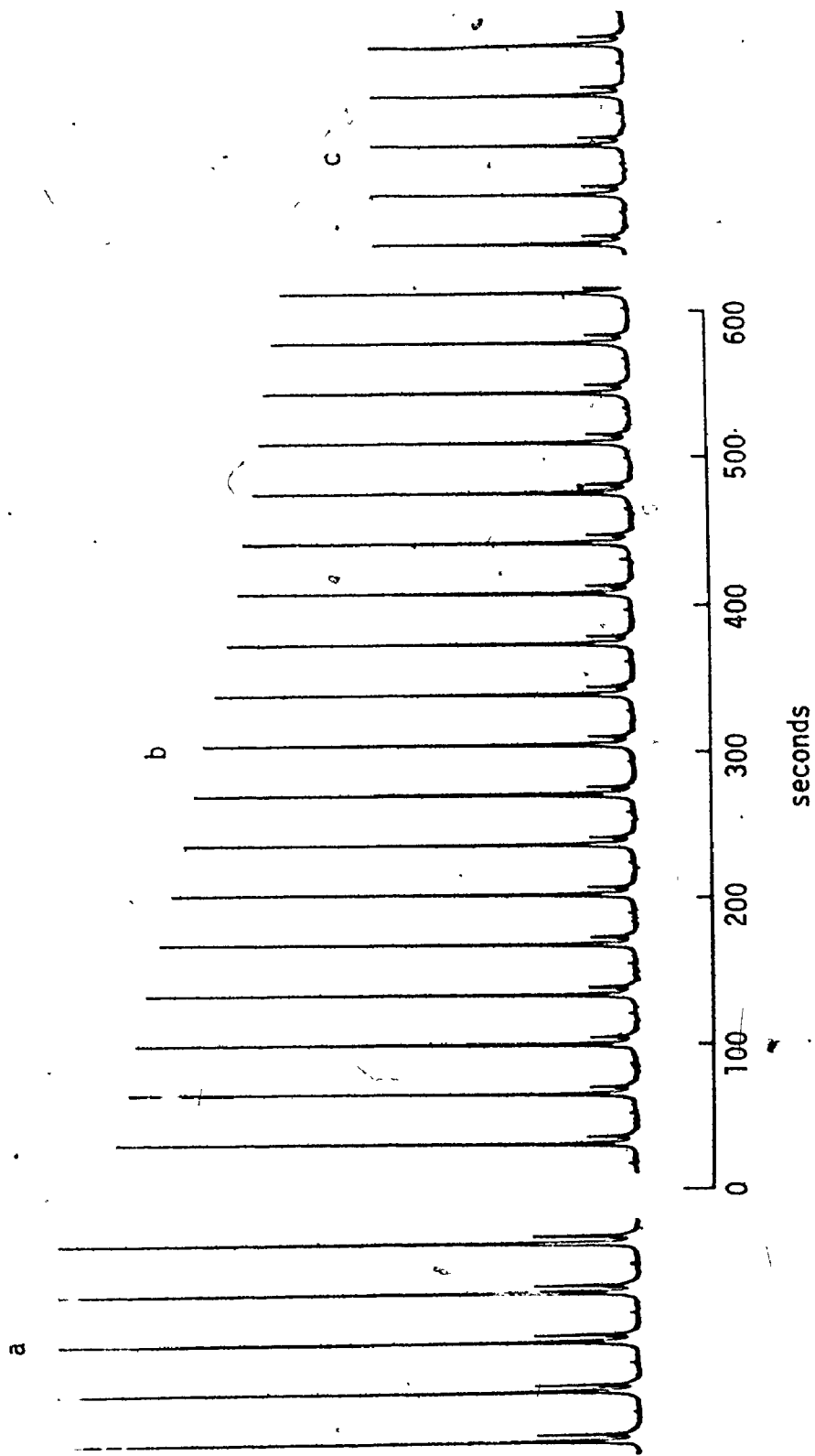


Figure 5-4. Intensity of  $^1\text{H}$  signals of  $\text{V}(\text{acac})_3$  during ligand exchange reaction of  $\text{V}(\text{acac})_3$  with  $\text{Hacac d}_8$ .

a, before addition of  $\text{Hacac d}_8$ ; b, during run; c, at equilibrium  
 Concentration of  $\text{V}(\text{acac})_3 = 0.143\text{M}$  and of  $\text{Hacac d}_8 = 0.572\text{M}$

## Results

### (i) Exchange of $V(acac)_3$ and Hhfac

In figure 5-5, a plot is shown of the initial rate of decay of the  $V(acac)_3$  peak as a function of Hhfac concentration. It is evident that the initial rate is not linearly dependent on the concentration of Hhfac. It depends upon a power of Hhfac concentration greater than one, but less than two.

Plots of rate versus  $[Hhfac]^{3/2}$  and of rate versus  $[Hhfac]^{4/3}$  both give approximately linear results. Alternatively, the data may also be fitted, with a reasonable degree of accuracy, to a rate expression of the form.

$$R/[complex] = k_1 [Hhfac] + k_2 [Hhfac]^2 \quad (5-5)$$

For the data presented in Fig. 5-5,  $k_1$  has the value of  $9.8 \times 10^{-3}$  liters moles<sup>-1</sup> sec.<sup>-1</sup>, and  $k_2$  the value of  $5.1 \times 10^{-2}$  liters<sup>2</sup> moles<sup>-2</sup> sec.<sup>-1</sup>. Various interpretations of these data will be discussed later.

The exchange of  $V(acac)_3$  with Hhfac is very sensitive to the presence of acid and the increased rate places the reaction at the limit of the present experimental method, but not, unfortunately, sufficiently rapidly to make use of line broadening or coalescence techniques. The addition of trifluoroacetic acid to the reaction mixture caused a dramatic increase in rate, illustrated in Fig. 5-6. Because the reaction in the presence of acid is very rapid, there are very few points with which to estimate the rates, especially at higher acid concentrations. The

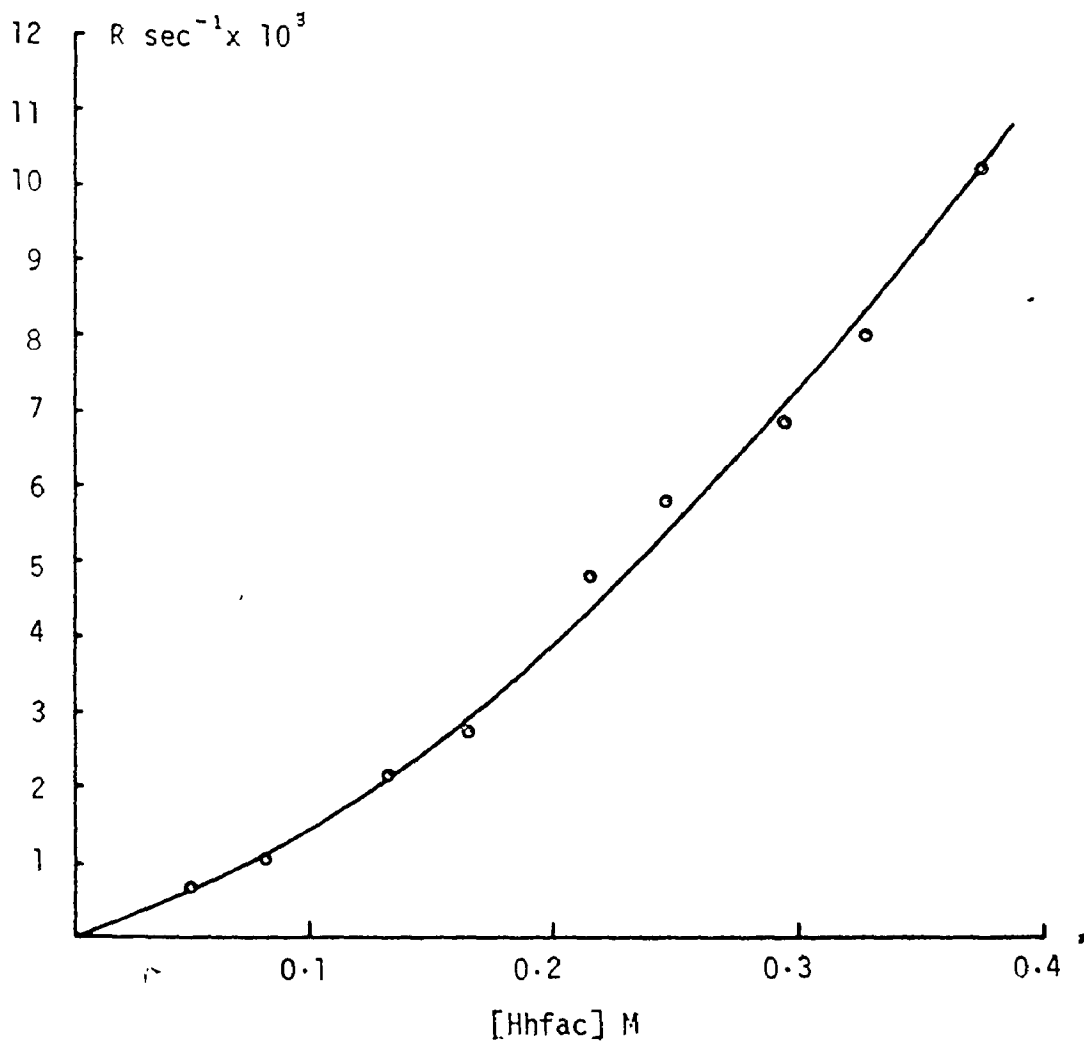


Figure 5-5. Initial rate of exchange of  $\text{V}(\text{acac})_3$  with Hhfac as a function of Hhfac concentration.

$$R = \frac{d \ln[\text{V}(\text{acac})_3]}{dt} \quad [\text{V}(\text{acac})_3] \text{ at } t_0 = 0.178\text{M}$$

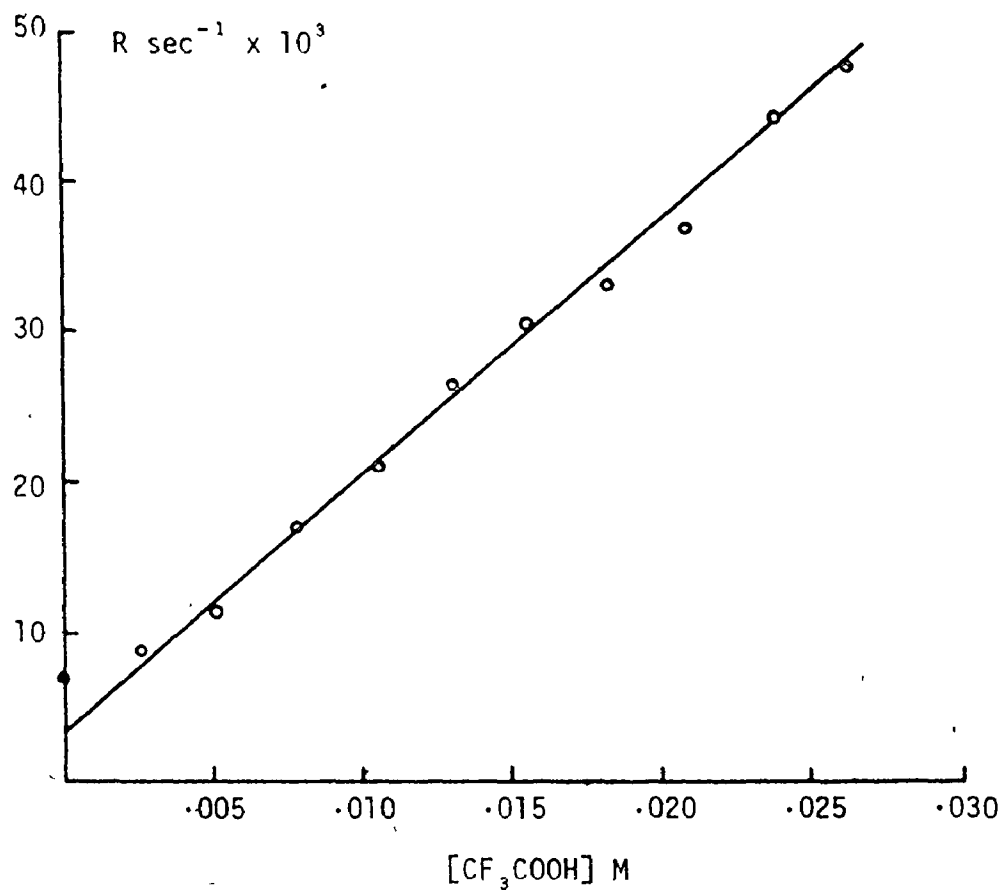


Figure 5-6. Initial rate of exchange of  $\text{V}(\text{acac})_3$  with Hhfac as a function of trifluoroacetic acid concentration.

$$R = \frac{d \ln[\text{V}(\text{acac})_3]}{dt} \quad [\text{V}(\text{acac})_3] \text{ at } t_0 = 0.178\text{M}$$

values of these rates, therefore, have limited accuracy. It is possible that the anion of the acid is responsible for the catalysis, but in view of the poor coordinating ability of the trifluoroacetate anion and the catalytic effect of acid on the ligand exchange of  $\text{Al}(\text{acac})_3$  and  $\text{Pd}(\text{acac})_2^{2,3}$ , this possibility seems rather unlikely.

The above results raise the possibility that acidic impurities may cause the rate of exchange to increase in the absence of deliberately added acid. There is also the possibility that ligand exchange may be base catalyzed. Saito and Masuda found that the presence of water accelerated the exchange of free and coordinated ligand with  $\text{Al}(\text{acac})_3$  and  $\text{Hacac}^2$ . The result was explained by coordination of the water as a Lewis base to stabilize the dangling ligand intermediate. Therefore, an experiment was carried out in which increasing amounts of triethylamine were added to the reaction mixture. If there were acid catalysis, the rate would decrease and if there were base catalysis, the rate would increase. Experimentally, it was found that the rate of exchange dropped to a limiting value, which was then virtually independent of further increases in the concentration of base (Fig. 5-7). The limiting value of the rate appeared, within experimental error, to be linearly dependent on the concentration of  $\text{Hhfac}$  with an intercept of close to zero (Fig. 5-8). The rate constant for this limiting rate has the value  $5.4 \times 10^{-3}$  liters moles<sup>-1</sup> sec.<sup>-1</sup>. Although this value is smaller than  $k_1$  in equation 5-5, this result suggested that equation 5-5 might reasonably be used as a basis for analysis of the rates in the absence of base.

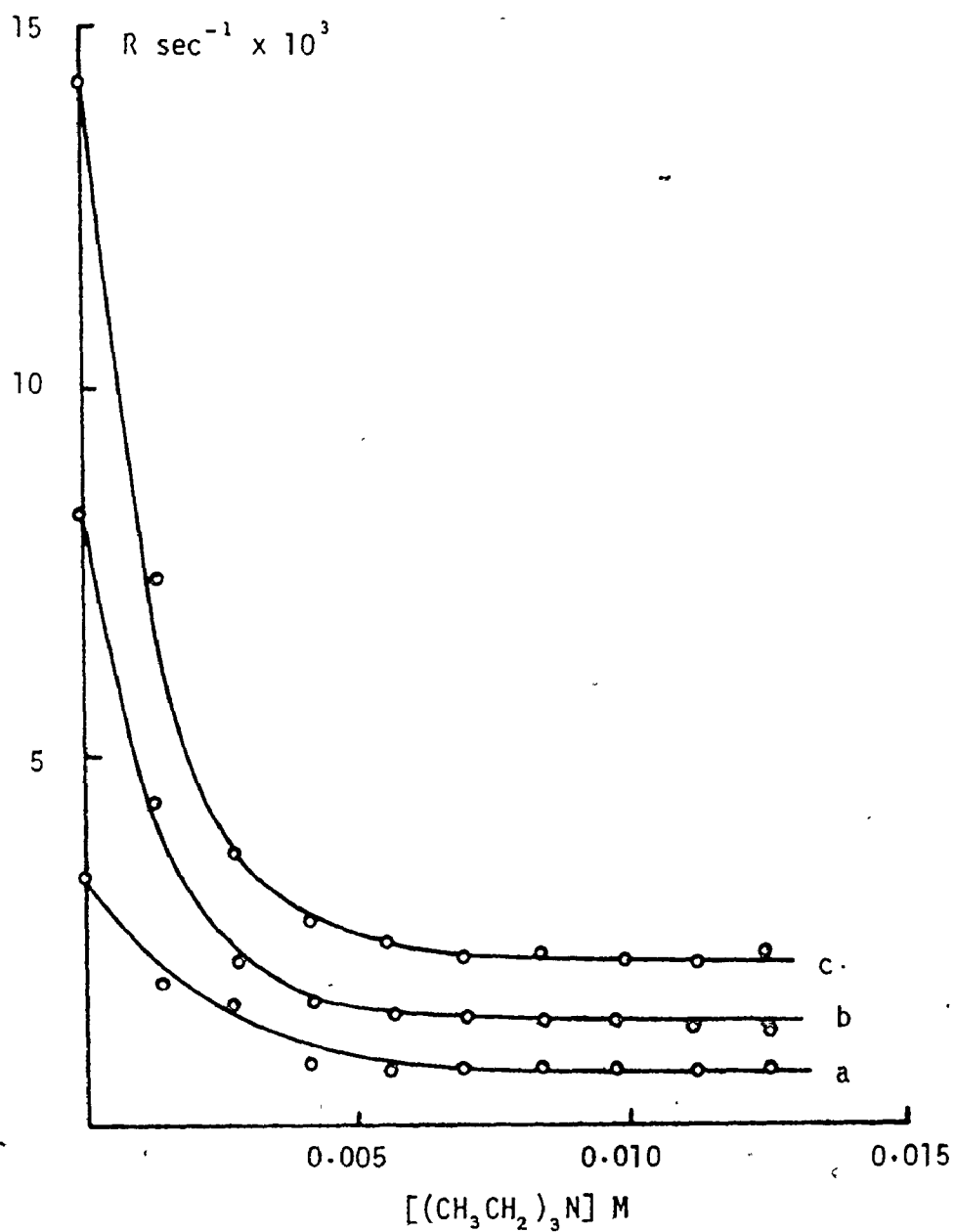


Figure 5-7. Initial rate of exchange of  $\text{V}(\text{acac})_3$  with Hhfac as a function of triethylamine concentration.

$$R = \frac{d \ln[\text{V}(\text{acac})_3]}{dt} \quad [\text{V}(\text{acac})_3] \text{ at } t_0 = 0.142\text{M}$$

$[\text{Hhfac}] =$  a, 0.131 M ; b, 0.261 M; c, 0.392 M



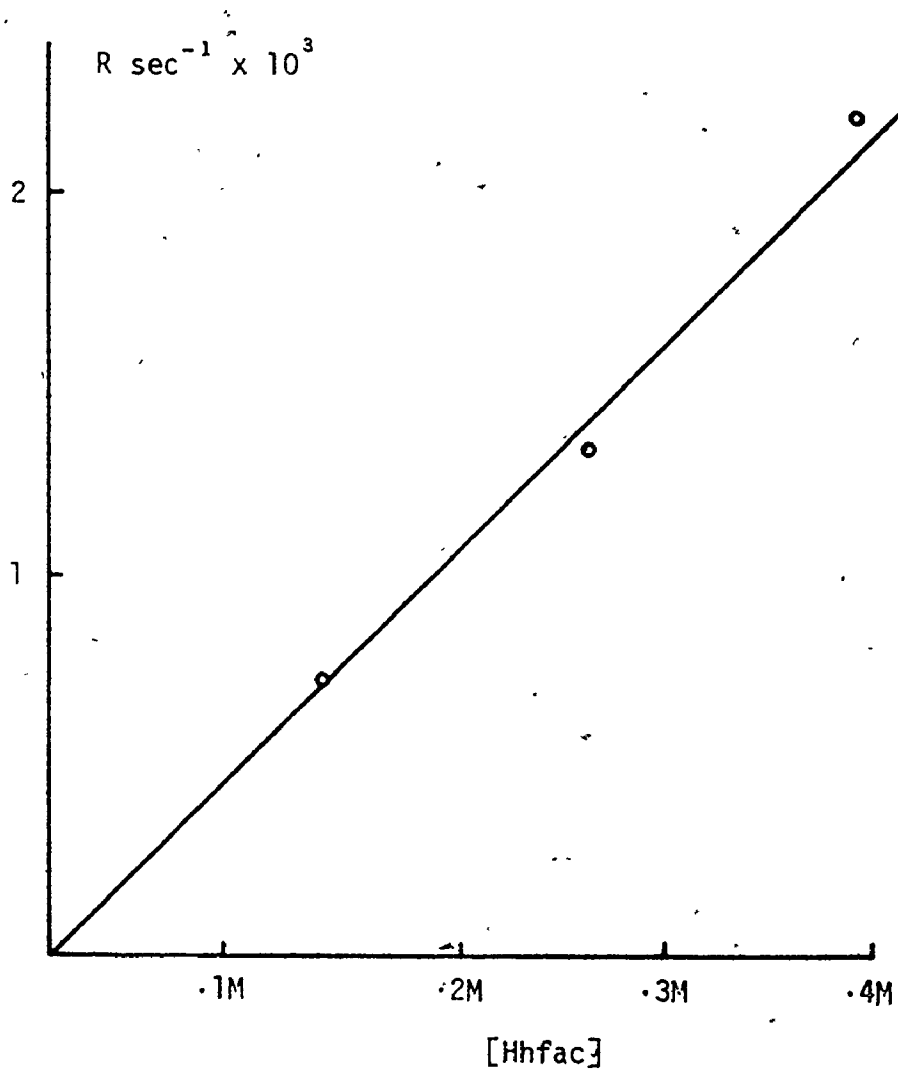


Figure 5-8.  $R$  as a function of  $\text{Hhfac}$  concentration at  $t_0$  at limiting rate with the addition of  $(\text{CH}_3\text{CH}_2)_3\text{N}$ . Average of last five points from Figure 5-7 at each concentration of  $\text{Hhfac}$ .

(ii) Exchange of  $V(acac)_3$  with  $Hacac d_8$

The relationship between the rate of exchange and the concentration of  $Hacac d_8$  is illustrated in Fig. 5-9. The dependence of rate on  $Hacac$  concentration appears to be linear with a relatively large non-zero intercept. This is to be contrasted with the results found for  $Hhfac$ .

Water appears to have a slight accelerating effect on the rate of exchange (Fig. 5-10). Since all the ligand exchange experiments had been carried out with chloroform as the solvent; chloroform was also used in this experiment. The experiment was carried out by combining varying proportions of a stock solution of water saturated chloroform with dry chloroform. A similar experiment was not performed with  $Hhfac$  because of its reactivity with water.

As in the reaction of  $Hhfac$  with  $V(acac)_3$ , triethylamine has an inhibiting effect on the rate of exchange of  $Hacac$  with  $V(acac)_3$ . At a very low concentration of triethylamine, a limiting rate is reached after which addition of further base causes no effect on the rate. A significant observation in this case is that the addition of base reduces the rate of exchange of the methine proton to a rate very close to that of the methyl protons. If it is assumed that this limiting rate is first order in ligand concentration as is the case with  $Hhfac$ , then  $k$  corresponds to a value of  $0.66 \times 10^{-3}$  liters mole<sup>-1</sup> sec.<sup>-1</sup>.

#### Mechanisms of Ligand Substitution

The effect of triethylamine on the rate of exchange of  $V(acac)_3$  with  $Hhfac$  and  $Hacac d_8$  suggests that the reaction occurs through two

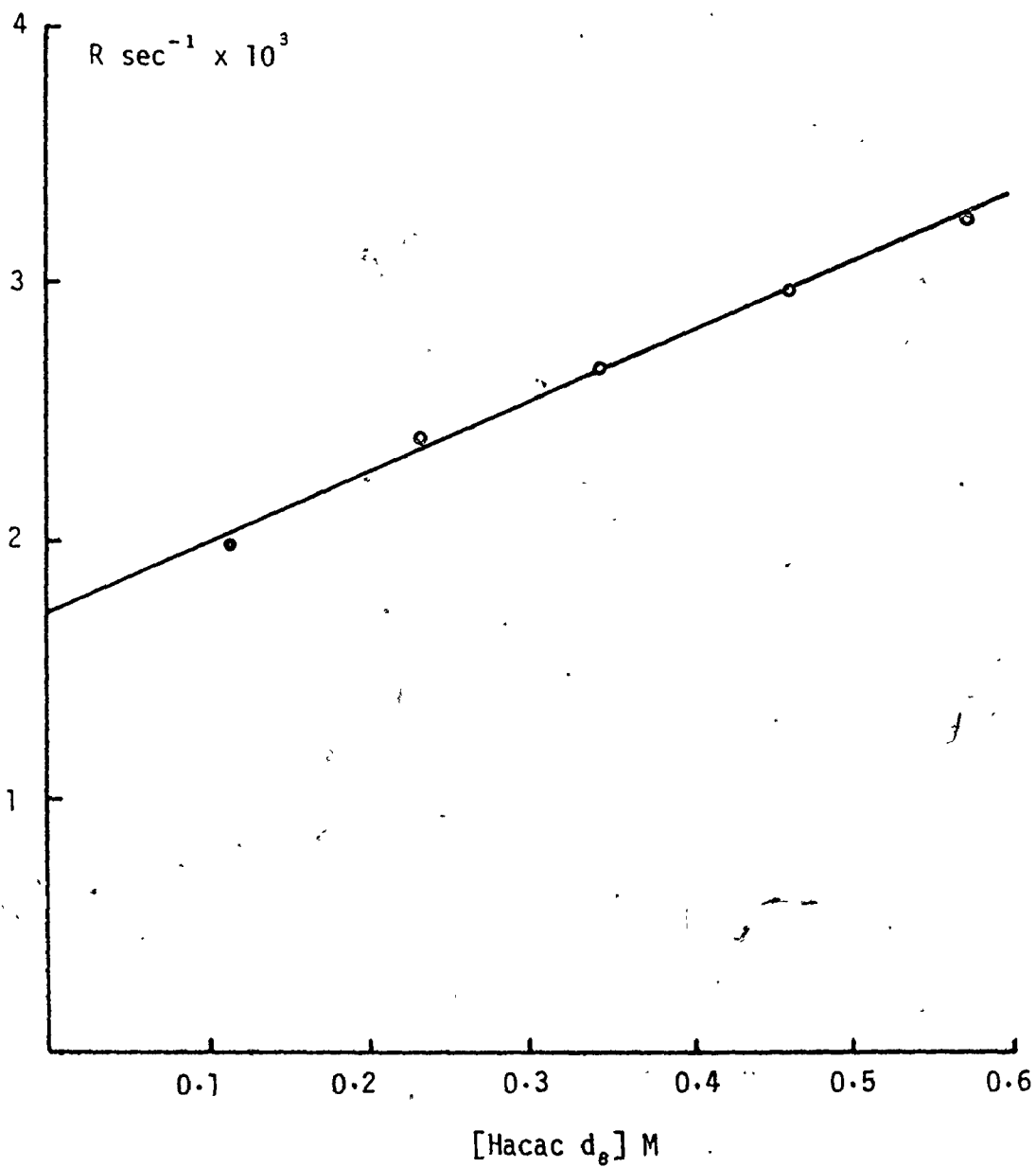
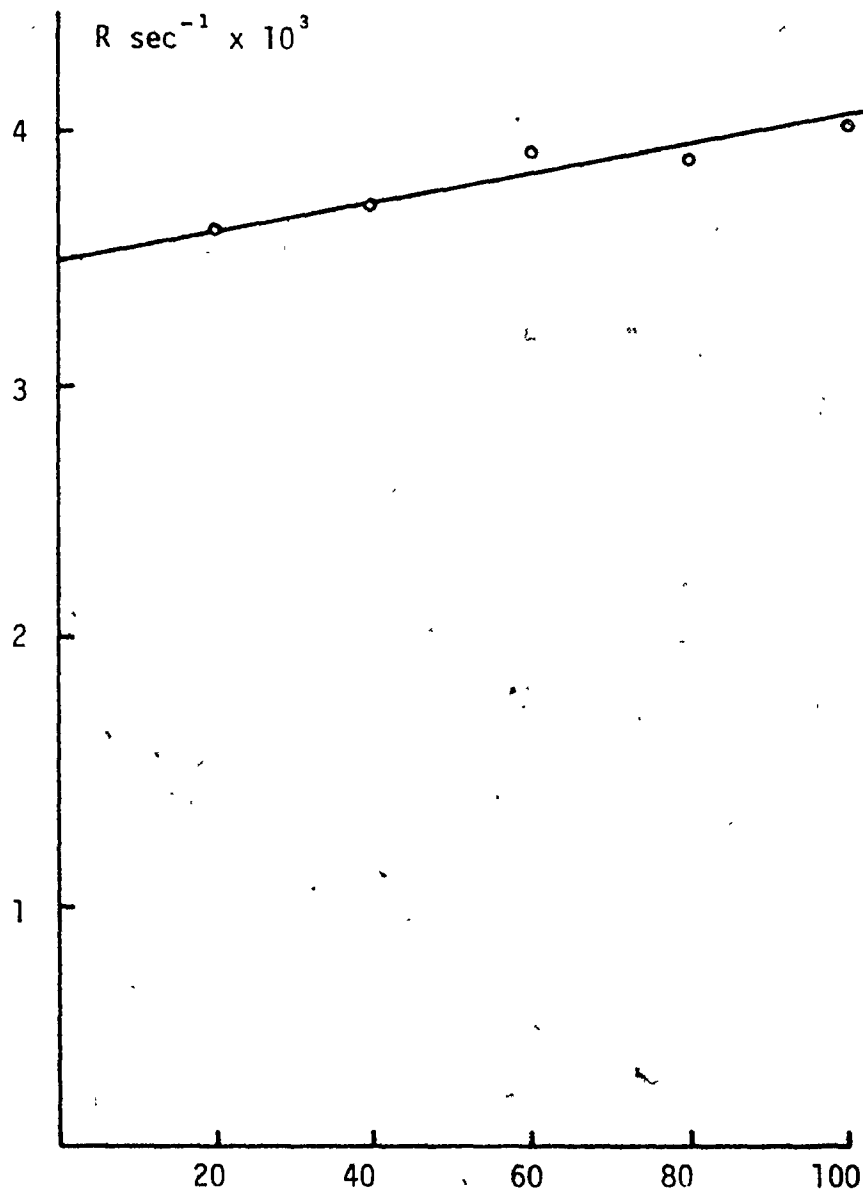


Figure 5-9. Initial rate of exchange of  $V(\text{acac})_3$  with  $\text{Hacac } d_8$  as a function of  $\text{Hacac } d_8$  concentration.

$$R = \frac{d \ln [V(\text{acac})_3]}{dt} \quad [V(\text{acac})_3] \text{ at } t_0 = 0.143\text{M}$$



μl of water saturated chloroform in sample with total volume of 425 μl.

Figure 5-10. Initial rate of exchange of  $V(acac)_3$  with  $Hacac d_8$  as a function of water concentration.

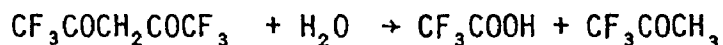
$$R = \frac{d \ln[V(acac)_3]}{dt} \quad [V(acac)_3] \text{ at } t_0 = 0.141M$$

$$[Hacac d_8] \text{ at } t_0 = 0.57M$$

independent pathways, one of which is acid catalyzed and the other which proceeds through direct reaction of the free ligand.

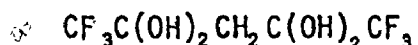
### The Acid Catalyzed Pathway

From Fig. 5-7, it can be seen that the limiting rate of exchange is reached at a concentration of triethylamine very much less than the concentration of free ligand. Thus, the effect of base may be to remove a trace of acid impurity present in the ligand and quench the acid catalyzed pathway. It is possible that some acid is present due to hydrolysis of the ligand.



Although trifluoroacetic acid seemed to be the most likely acid product, no peaks which could be attributed to  $\text{CF}_3\text{COOH}$  were observed in the  $^{19}\text{F}$  NMR spectrum of Hhfac which had been distilled. However, a small resonance with the same chemical shift was observed in the Hhfac before purification.

A sample of the ligand was titrated with tetrabutylammonium hydroxide in acetonitrile. The titration was followed potentiometrically. The titration curve, Fig. 5-11, has two points of inflection. The second occurs at the volume calculated for an equimolar mixture of Hhfac and base. The other point of inflection at a mole ratio of approximately 1:4 presumably occurs as a result of the reaction of Hhfac with water to form the dihydrate of Hhfac<sup>93</sup>.



The source of water is almost certainly the acid-base reaction

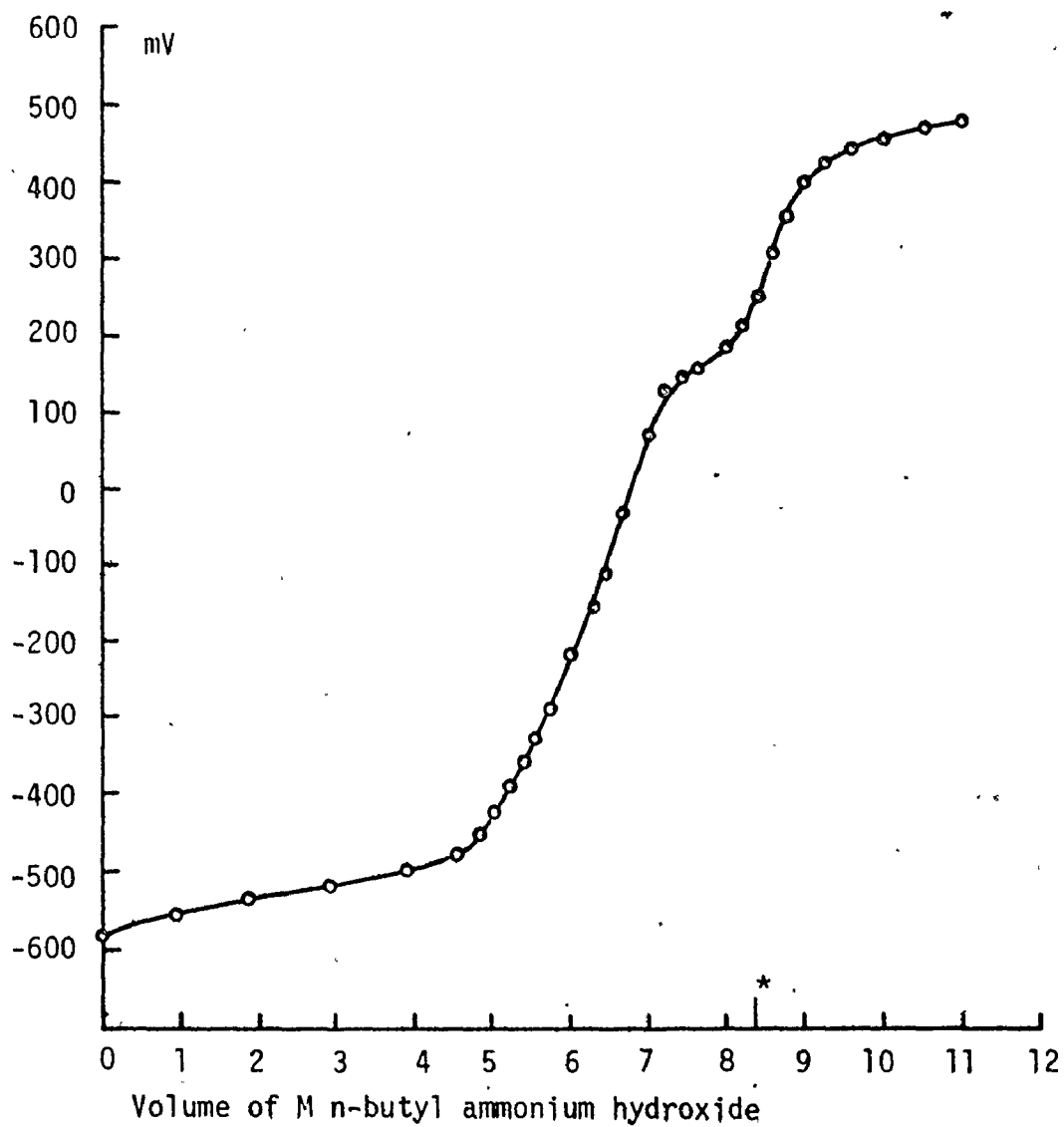
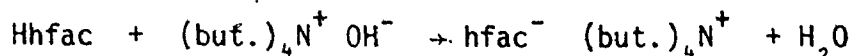


Figure 5-11. Potentiometric titration of 10  $\mu$ l. ( $6.92 \times 10^{-5}$  moles) of Hhfac with 0.0083 M n-butyl ammonium hydroxide.  
\*Volume calculated for total neutralization of Hhfac.



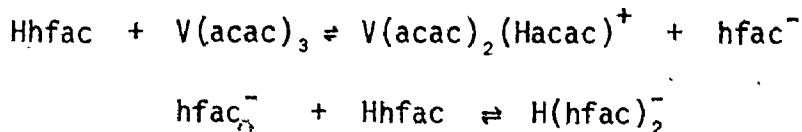
If the reaction of Hhfac with water were sufficiently rapid, the first point of inflection should occur at 2/3 of the volume of base required for total neutralization of the Hhfac. The reaction of Hhfac with water, although moderately rapid, is not instantaneous and the first point of inflection does not occur at the expected volume of base, presumably because the water and Hhfac have not had sufficient time to react.

No point of inflection which might have indicated the presence of a strongly acid impurity in the Hhfac was observed. A subsequent test in which  $\text{CF}_3\text{COOH}$  and Hhfac were titrated together with *n*-butyl ammonium hydroxide exhibited no point of inflection corresponding to  $\text{CF}_3\text{COOH}$ . This result demonstrated that it is unlikely that a small amount of acid impurity could be detected in Hhfac in this manner. It also suggests that Hhfac is an acid of comparable strength to  $\text{CF}_3\text{COOH}$ . The measurement of the  $\text{pK}_D$  of Hhfac accurately in aqueous solution is very difficult, owing to its reactivity with water. A report by Van Uitert et al. suggests that the  $\text{pK}_D$  in water is less than 2<sup>94</sup>. The  $\text{pK}_D$  of  $\text{CF}_3\text{COOH}$  is 0.25<sup>68</sup>.

Another possible explanation of the effect of base is that as Hhfac is a moderately strong acid, the ligand itself acts as the acid catalyst. If this is the case, protonation cannot be the rate determining step, as the amount of base required to quench the acid catalyzed pathway is much less than the amount of ligand present. The pathway must therefore involve the formation of a protonated intermediate prior to the rate determining step. The effect of base would simply be to reduce the

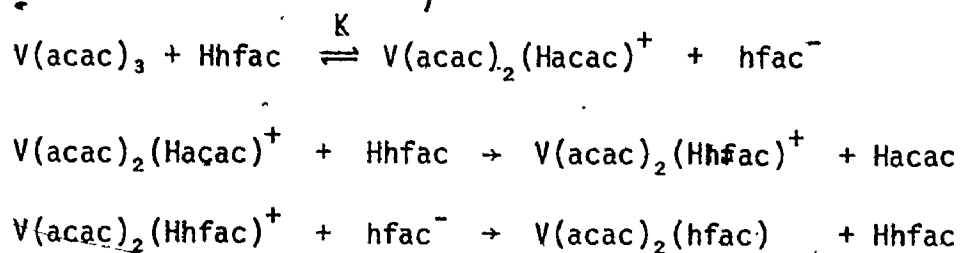
concentration of the protonated intermediate to a negligible value. This is consistent with the mechanisms of acid catalysis discussed in the previous chapter.

The reason for the second order dependence of the rate of the acid catalyzed pathway on Hhfac concentration is not immediately apparent. One plausible explanation is that a molecule of ligand protonates the complex in a pre-equilibrium step, and the anion of the ligand forms a hydrogen bonded complex with another molecule of the ligand. Two molecules of ligand would be required to protonate the complex leading to the second order dependence.



The  $^1\text{H}$  NMR resonance of the hydroxyl proton shows an upfield shift when  $\text{Na}(\text{hfac})$  is added to a solution of the ligand in acetone. This is consistent with formation of a dimer of this kind.

Another possibility to be considered is that protonation of the complex is followed by reaction of the protonated intermediate with a molecule of the neutral ligand



Such a scheme would be expected to have a dependence on ligand concentration of 3/2. However, the results presented in chapter 4 for  $\text{Al}(\text{acac})_3$ , suggest



that the lifetime of such a protonated intermediate is very brief and is thus likely to lose a neutral molecule of Hacac before reaction with a molecule of Hhfac. Saito and Masuda's<sup>2</sup> results for the acid catalyzed ligand exchange of  $\text{Al}(\text{acac})_3$  suggest that loss of the protonated ligand is the rate determining step. If the mechanism of acid catalyzed ligand exchange for  $\text{V}(\text{acac})_3$  is similar, then the reaction of a protonated intermediate with a neutral molecule of ligand seems an unlikely pathway.

The effect of triethylamine on the exchange of  $\text{V}(\text{acac})_3$  with Hacac  $d_8$  suggests the presence of acid in the reaction mixture. In this case, it is not possible that the ligand itself is the acid catalyst, as the  $\text{pK}_a$  of Hacac is 8.95<sup>68</sup>. The presence of acid is supported also by the observation of the rapid exchange of the methine proton. In chapter 4, it was shown that the presence of acid resulted in rapid exchange of the methine proton of a number of  $\beta$ -diketonate complexes. These observations are disturbing in view of the fact that the ligand was treated to remove acid impurities prior to distillation. It is not certain, therefore, whether the increase of the rate of ligand exchange with increasing ligand concentration is due to the ligand itself. This result, however, lends emphasis to the importance of considering protonation on carbon as a mechanism of acid catalyzed ligand exchange.

#### The First Order Ligand Pathway

When the acid catalyzed pathway has been quenched, ligand exchange of  $\text{V}(\text{acac})_3$  with both Hhfac and Hacac still proceeds, but at a much reduced rate. For the exchange of  $\text{V}(\text{acac})_3$  with Hhfac, the rate of exchange has been shown to be first order in the concentration of ligand. The fact that

increasing concentrations of base cause the reaction to slow to a limiting value which is independent of further increases in base concentration suggests that it is the neutral form of the ligand which is involved in this pathway.

Saito and Masuda<sup>2</sup> found that the rate of exchange of  $Al(acac)_3$  with  $Hacac$   $^{14}C$ , although apparently proportional to ligand concentration, was, in fact, proportional to a catalytic quantity of water present in the ligand. Catalysis by water is unlikely in the exchange of  $V(acac)_3$  with  $Hhfac$ , as  $Hhfac$  reacts strongly with water to form the dihydrate<sup>93</sup>. Because the intercept in Fig. 5-5 is zero within experimental error, it is unlikely that the presence of water in the solvent causes any substantial increase in the rate of exchange. Because measurement of the rate of exchange of  $Hacac$   $d_8$  in the presence of base was carried out at a single concentration of free ligand, it is not possible to be sure if there is a ligand exchange pathway which is first order in  $Hacac$ . Assuming that there is a first order pathway for  $Hacac$  exchange also, the rate of substitution of  $hfac^-$  is about ten times faster than the rate of  $acac^-$  exchange.

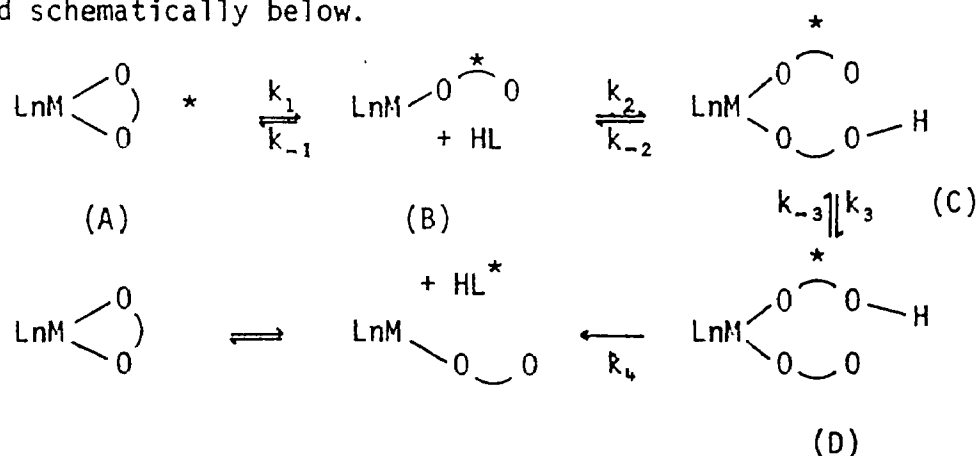
The first study of rates of ligand exchange of  $\beta$ -diketonate complexes was reported by Adams and Larsen<sup>81</sup>, who investigated the kinetics of ligand exchange between  $ML$  and free ligand where  $M = Zr, Hf, Th$ , and  $L = Htfac$  or  $Hacac$ . They found that the rate of exchange of  $Zr(tfac)_4$  and  $Hf(tfac)_4$  with  $Htfac$  in benzene and chlorobenzene and  $Zr(acac)_4$  and  $Hf(acac)_4$  with  $Hacac$  in chlorobenzene was first order in ligand concentration. The rates of exchange for these complexes was very much faster for these systems than for  $V(acac)_3$  with  $Hhfac$  or  $Hacac$ , allowing the use of NMR coalescence phenomena to determine the rates.

A term which is first order in the ligand concentration has also been found for the ligand exchange reactions of  $\text{Pd}(\text{acac})_3$  and  $\text{Be}(\text{acac})_2$ <sup>95</sup>. These reactions were relatively slow and the rates were determined by radio tracer techniques.

### The Mechanism of the First Order Pathway

The majority of subsequent workers who have reported on the kinetics of ligand exchange of  $\beta$ -diketonate complexes have interpreted their results on the basis of the mechanism postulated by Adams and Larsen<sup>81</sup>.

The initial step in their mechanism involves the rupture of the M-O bond to form the so called 'dangling ligand intermediate'. This is followed by coordination of a neutral ligand molecule to the vacant coordination site, transfer of a proton from the neutral ligand to the dangling anionic ligand, loss of the original dangling ligand and finally, coordination of the free end of the new dangling ligand. The mechanism is represented schematically below.



The rate determining step has been variously identified as 4 by Adams and Larsen for the exchange of free and coordinated ligands for

Zr and Hf acetylacetonates and 2 or 3 by the same authors for the corresponding trifluoroacetylacetonates.

Unfortunately, Glass and Tobias<sup>96</sup> who reported on the exchange rates of several organometallic acetylacetonate complexes of Sn(IV), Au(III), Ga(III) and Tl(III) did not conduct concentration studies.

Tanner et al.<sup>97</sup> identified the rate determining step in the exchange of some In(III)  $\beta$ -diketonate complexes as 3. However, they considered rotation of the ligand rather than the transfer of the proton as the rate determining step.

Serpone and Ishayek<sup>98</sup> have reported on the kinetics of intermolecular ligand exchange between  $(C_6H_5)_2Sn(acac)_2$  and  $(CH_3)_2Sn(acac)_2$ . They have proposed a mechanism of exchange which closely resembles that of Adams and Larsen. The rate determining step in this case is identified as M-O bond rupture in  $(C_6H_5)_2Sn(acac)_2$  to give a five coordinate species with a dangling ligand. This corresponds to step 1 in the Adams and Larsen scheme.

It is relatively straightforward to apply a steady state analysis to the kinetic scheme of Adams and Larsen. Since step 4 is irreversible, the overall rate of exchange can be predicted by finding the expression which gives the rate of this process. The expression for the rate of this process, R, is given below.

$$R = \frac{k_1 k_2 k_3 k_4 [A][HL]}{(k_{-3} + k_4) \left( \frac{k_{-2} + k_3 k_4}{(k_{-3} + k_4)} \right) \left( \frac{k_{-1} + k_2 [HL] k_3 k_4}{k_{-2} (k_{-3} + k_4) + k_3 k_4} \right)}$$

where  $[A]$ , and  $[HL]$  represent the concentrations of complex and ligand respectively. When the entering and leaving ligands are the same,  $k_4$  is identical to  $k_{-2}$  and  $k_3$  to  $k_{-3}$ . Substituting  $k_4$  for  $k_{-2}$  and  $k_3$  for  $k_{-3}$ , the expression simplifies to

$$R = \frac{k_1 k_2 k_3 [A] [HL]}{k_{-1} (k_4 + 2k_3) + k_3 k_2 [HL]}$$

If  $k_4$  is very small, i.e.,  $k_4 \ll 2k_3$ , the expression simplifies further to

$$R = \frac{k_1 k_2 [A] [HL]}{2k_{-1} + k_2 [HL]}$$

Thus, the rate of exchange is independent of the rate of loss of the neutral ligand from intermediate D; however, this is not necessarily true, if the entering and leaving ligands are different. If  $k_{-1}$  is large compared to  $k_2 [HL]$ , the rate expression becomes

$$R = \frac{k_2 k_1 [A] [HL]}{2k_{-1}}$$

The factor of 2 in the denominator of the expression arises from the assumption that the rate of proton transfer is rapid compared to the lifetime of intermediates C and D. There is therefore, an equal probability that either monodentate ligand will be lost. Only loss of the ligand originally coordinated to the metal will contribute to ligand exchange. In this case, the rate is proportional to the ligand concentration.

If, on the other hand, step 3 is assumed to be rate determining, i.e.,  $k_3 k_2 [HL] \ll k_{-1} k_{-2}$ , then

$$R = \frac{k_1 k_2 k_3 [A] [HL]}{k_{-1} k_{-2}}$$

and if step 2 is rate determining, then

$$R = \frac{k_1 k_2 [A] [HL]}{k_{-1}}$$

Finally, if step 1 is rate determining, the rate of exchange is given by

$$R = k_1 [A]$$

This is the only step in the scheme which, if rate determining, would cause the rate to be first order in complex and zero order in ligand. If any other step in the scheme were rate determining, the rate would be proportional to both complex and ligand concentration.

The observation that the rate of exchange is proportional to ligand concentration in the present work suggests that bond rupture to form the dangling ligand intermediate is not the rate determining step. Exchange of Hhfac with V(acac)<sub>3</sub> appears to be rather faster than exchange of Hacac, and therefore, it seems likely that step 3, proton transfer, is the rate determining step, as a proton is more likely to be transferred rapidly from Hhfac to acac<sup>-</sup> than from Hacac to acac<sup>-</sup>. If, on the other hand, step 2 were rate determining, it would be more difficult to explain why the reaction with Hhfac is more rapid than that with Hacac, as the latter might be expected to be a better nucleophile.

Despite the observation that the rate of ligand exchange of some

indium (III) trifluoro- $\beta$ -diketonates with free ligand is proportional to complex concentration and independent of ligand concentration, Tanner et al.<sup>97</sup> have identified the rate determining step in these reactions as rotation of part of the monodentate ligand around a partial double bond in the intermediate C. This corresponds to step 3 in Adams' and Larsen's scheme being rate determining. The identification of step 3 as the rate determining step was based on the fact that intramolecular rearrangement of  $\text{In}(\text{tfac})_3$  proceeds much more rapidly than ligand exchange and the assumption that intramolecular rearrangement proceeds via a bond rupture mechanism. A possible conclusion from these results is that the intramolecular rearrangement of indium  $\beta$ -diketonates proceeds via a twist mechanism.

#### Mechanism of Catalysis by Water

It is difficult to explain the catalytic effect of water observed for the ligand exchange of  $\text{V}(\text{acac})_3$  with  $\text{Hacac}$ , unless the dangling ligand intermediate hypothesis is accepted. Saito and Masuda<sup>2</sup>, who observed the catalysis of ligand exchange of  $\text{Al}(\text{acac})_3$  with free ligand, suggested that a molecule of water could coordinate at the site vacated by the dangling ligand, thereby preventing re-coordination of the free end of the dangling ligand and thereby increasing its concentration. This seems the most reasonable interpretation of these results.

Tanner et al.<sup>97</sup> found that water had no catalytic effect on the rate of ligand exchange of indium trifluoro- $\beta$ -diketonates. This is to be expected if step 1 is the rate determining step.

## Conclusion

The scheme of Adams and Larsen appears to be able to account for the present results. If this is correct, it would seem to imply that bond rupture is considerably faster than ligand exchange; otherwise, the dependence of rate upon ligand concentration would be zero. The rates of ligand exchange for  $V(acac)_3$  are about three orders of magnitude less than the rates of intramolecular rearrangement discussed in chapter six for vanadium  $\beta$ -diketonates. Thus, while it is possible to say that rearrangement of the vanadium  $\beta$ -diketonate complexes must proceed via an intramolecular mechanism, it is not possible to rule out the bond rupture mechanism for intramolecular rearrangement.

Because the ligand exchange studies which have been performed have been carried out under different experimental conditions, and because the mechanisms of exchange are not necessarily the same, it is impossible to make precise comparisons of the lability of  $\beta$ -diketonate complexes. On the other hand, it is possible to give a general indication of the dependence of the rate of ligand exchange on the central metal ion. This order is, Th(IV) [ $>650 M^{-1} sec^{-1}$  (25°)]  $>$  Zr(IV) [ $87 M^{-1} sec^{-1}$  (25°)]  $\approx$  Hf(IV) [ $78 M^{-1} sec^{-1}$  (25°)]<sup>81</sup>  $>$  V(III) [ $6.6 \times 10^{-4} M^{-1} sec^{-1}$  (27°)]  $>$  Pd(II) [ $4 \times 10^{-5} M^{-1} sec^{-1}$  (25°)]<sup>3</sup>  $>$  Be(II) [ $1.6 \times 10^{-5} M^{-1} sec^{-1}$  (30°)]<sup>95</sup>  $>$  Al(III) [ $1.0 \times 10^{-6} sec^{-1}$  (25°)]<sup>2</sup>  $>$  Cr(III)  $>$  Co(III)<sup>99</sup>. For all the metals except Al, Cr and Co, the order refers to the magnitude of the rate constant which is applicable to the first order ligand pathway. The first order ligand pathway apparently does not exist for aluminium and therefore, the rate constant for the zero order ligand pathway has



been used. The limiting value of the rate constant for Th is based on the assumption that the kinetics of exchange is similar to Zr and Hf. If the exchange is first order in complex and zero order in ligand, the lower limit of the rate constant would be  $325 \text{ sec}^{-1}$ . The kinetics of ligand exchange for Co and Cr acetylacetonates is, as yet, undetermined. It is interesting to note that the ratio of the rates of ligand exchange between  $\text{V}(\text{acac})_3$  and free ligand and  $\text{Al}(\text{acac})_3$  and free ligand is quite similar to the ratio of the rates of rearrangement of  $\text{V}(\text{tfac})_3$  and  $\text{Al}(\text{tfac})_3$  (at  $103^\circ\text{C}$ ). The rates for the vanadium complexes are between 2 and 3 orders of magnitude faster in both cases. The greater lability of vanadium  $\beta$ -diketonates compared to the aluminium analogues appears to be a general phenomenon which will be further illustrated in the following chapter.

Introduction

Inorganic chemists have long been interested in the rearrangement processes of octahedral chelate complexes. As early as 1912, Werner<sup>100</sup> proposed an intramolecular mechanism for the isomerization of bidentate chelate complexes. Prior to 1965, most work in this field had been carried out on the relatively inert complexes of Co(III) by classical methods. In 1965, Fay and Piper<sup>101</sup> demonstrated the value of NMR in their now classic paper on the isomerization of the trifluoroacetylacetonates of Al(III), Ga(III), In(III), Co(III), and Rh(III). Since then, a considerable number of papers concerning the study of the rearrangement of labile octahedral chelate complexes, involving both a variety of metals and ligands by NMR methods have been published. With NMR, it is possible to determine the rate of rearrangement and in favourable cases the probable mechanism.

In this chapter, we present the results of a NMR study of the rearrangement processes of some vanadium  $\beta$ -diketonate complexes. The only previous report dealing with rearrangements of vanadium  $\beta$ -diketonates is that of Gordon et al. who found no changes in the NMR spectrum of  $V(\text{tfac})_3$  attributable to exchange broadening below 100°C. This result is contrary to the present work. Most of the results obtained so far on the rearrangement of labile  $\beta$ -diketonate complexes have been confined to group IIIA metals, those of aluminium having been the most extensively

studied. No quantitative studies of  $\beta$ -diketonate complexes of labile transition metal ions have been carried out.  $\text{Mn}(\text{tfac})_3$  and  $\text{Mn}(\text{bzac})_3$  were reported, by Gordon et al.,<sup>7</sup> to isomerise on the NMR time scale above  $40^\circ$  and the absence of separate resonances due to the cis and trans forms of  $\text{Fe}(\text{tfac})_3$  and  $\text{Fe}(\text{bzac})_3$  at  $-70^\circ\text{C}$ <sup>7</sup> was tentatively taken to imply rapid isomerization. In the light of these results, the failure to observe isomerization in  $\text{V}(\text{tfac})_3$  appeared anomalous.

A study of the influence of substituent effects on the distribution of unpaired electron spin density in vanadium  $\beta$ -diketonates has already been carried out in this laboratory with some success<sup>5,6</sup>. It was hoped that, if non-random exchange patterns of exchange were observed for some vanadium  $\beta$ -diketonate complexes, it would be possible to identify either the axis around which a twist rearrangement occurred or the bond(s) which ruptured to lead to rearrangement. Furthermore, it was hoped that it might be possible to correlate the rate of rearrangement for different complexes with the magnitudes of the substituent effects.

The literature on the rearrangement of octahedral chelate complexes has recently been reviewed by Serpone and Bickley<sup>102</sup>. A review restricted to the rearrangement of  $\beta$ -diketonate complexes was presented at an earlier date by Fortman and Sievers. Brief accounts of this topic have also appeared in standard texts.<sup>103,104</sup> This introduction will therefore be restricted to a discussion of the mechanisms generally believed to be responsible for rearrangement in octahedral chelate complexes with some pertinent examples.

## Nomenclature

Before reviewing the mechanisms, it is advisable to define some of the terms which will be commonly used in this chapter.

Most tris chelate complexes have pseudo octahedral symmetry. Because of the chelate rings, however, the symmetry is reduced to  $D_3$  i.e., the molecule has no improper axis of rotation ( $S_n$ ). The lack of an improper axis of rotation implies the lack of a centre of symmetry and of planes of symmetry each of which correspond to an improper axis of rotation. The octahedral chelate complexes therefore exist in right and left-handed enantiomeric forms. An absolute assignment of configuration has been proposed by the IUPAC commission.<sup>105</sup> However, in the present work, the absolute configuration of the complexes is not known and is not necessary for the discussion. The process by which one enantiomer is converted into the other may be detected by NMR methods<sup>106</sup> and will be referred to as enantiomerization.

If the ligands are not symmetric, the complexes may exist as geometric isomers. For example, a tris  $\mu$ -chelate may exist in cis and trans forms. The cis form has  $C_3$  symmetry and therefore has two sets of equivalent groups. The trans form, on the other hand, is asymmetric and has no equivalent groups. When the complex contains different ligands which are not symmetric, a larger number of geometric isomers may exist. The process of conversion of one geometric isomer into another is referred to as isomerization. Finally, a nucleus at a site with a particular chemical environment may be transferred to a different site without the simultaneous isomerization or enantiomerization of the complex necessarily occurring. This is referred to as 'site exchange'. The term rearrangement

refers to all these processes and does not imply that all occur simultaneously.

### Mechanisms

The mechanisms by which rearrangement of octahedral tris chelate complexes may occur can conveniently be divided into two general categories: intermolecular and intramolecular.

#### Intermolecular

Intermolecular mechanisms can be further classified as associative or dissociative. The intermediate which results from the loss of a ligand from a tris chelate complex may rearrange to either square planar or tetrahedral geometry. If the complex has symmetric ligands, it is clear that the symmetry of the intermediate will result in a racemic product on recoordination of the ligand. Thomas<sup>107</sup> originally proposed such a mechanism to account for the behaviour of oxalato complexes. Although subsequently proved incorrect, this mechanism does appear to be operative in the case of  $\text{Ni}(\text{phen})_3^{2+}$ ,  $\text{Ni}(\text{bipy})_3^{2+}$ <sup>108</sup> and  $\text{Ni}(\text{phen})_2(\text{bipy})^{2+}$ <sup>109</sup>.

This mechanism has generally been thought unlikely as a mode of rearrangement for  $\beta$ -diketonate complexes, because of the high energy required to separate the anionic ligand from the positively charged metal ion in a medium of low dielectric constant. Piper and Fay<sup>101</sup> have estimated the activation energy required for this process for  $\text{Al}(\text{tfac})_3$  on the basis of a point charge model. Depending on the value of  $q$  chosen (where  $q$  = the fraction of an electronic charge on each of the six

oxygen atoms), the calculated values of the activation energy range from 250 to 60 kcal/mole. However, it is interesting to note that the activation energy estimated by Saito and Masuda<sup>2</sup> for the loss of an anionic acetylacetonate ligand from  $\text{Al}(\text{acac})_3$  in the ligand exchange reaction was only 21.4 kcal/mole. The free energy of activation estimated by Fay and Piper<sup>101</sup> for the isomerization of  $\text{Al}(\text{tfac})_3$  is only, approximately 3 kcal/mole less. It may, therefore, be premature to exclude the possibility of a dissociative rearrangement mechanism on the basis of a priori arguments.

Rearrangement might also occur through an associative process resulting in intermediates of increased coordination number. This mechanism is less likely for the elements of the first transition series owing to the relatively small size of the ions. The complexes of the heavier elements particularly of the lanthanide and actinide series are more likely to undergo associative exchange processes.

### Intramolecular

Strictly speaking, intramolecular mechanisms do not involve the participation of any species outside the primary coordination sphere with the possible exception of the solvent.

As with the intermolecular mechanisms, intramolecular mechanisms can be divided into two types: those which involve bond rupture to form an intermediate of reduced coordination number, and those which involve the rearrangement of the chelate rings without bond rupture.

### Bond Rupture Mechanisms

The bond rupture mechanism for the isomerization of bidentate chelate complexes was proposed by Werner in 1912<sup>100</sup>. The rupture of one of the bonds of a tris bidentate chelate would give rise to a structure of reduced coordination number. It is generally believed that the five coordinate structure derived from a tris chelate complex will have either trigonal bipyramidal (TBP) or square pyramidal (SP) geometry. They will be referred to here as 'intermediates', although some authors have preferred to refer to them as transition states<sup>110</sup>. There does not appear to be any good reason to prefer either term, as it is not known whether these idealized structures represent minima or maxima on the potential energy surface.

In the case of the TBP intermediate, the monodentate dangling ligand may occupy either an axial or an equatorial position (Fig. 6-1). The SP intermediate may have the dangling ligand coordinated at either an apical or a basal position (Fig. 6-2). Holm has argued that a SP basal intermediate is kinetically equivalent to a TBP axial intermediate and that, therefore, it need not be considered separately.<sup>101</sup> The reasoning is not obvious, as the formation of one of the products requires a greater degree of ligand motion than the other. Pignolet et al.<sup>111</sup> have suggested that a reaction which requires a lesser degree of ligand motion will be favoured. If this is the case, then it cannot be assumed that a SP basal intermediate is completely equivalent to a TBP axial intermediate.

Assuming that the TBP intermediate does not itself isomerize, rearrangement which proceeds via the axial intermediate will occur with



Figure 6-1 Trigonal bipyramidal states, axial and equatorial



Figure 6-2 Square pyramidal states, apical and basal.

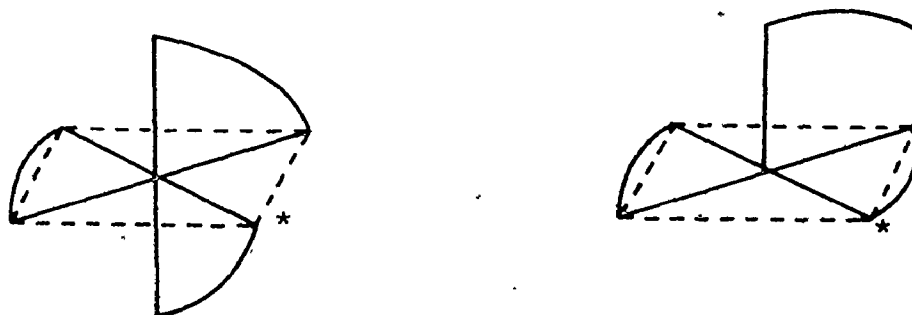


Figure 6-3a Formation of SP apical state by primary mechanism



Figure 6-3b Formation of SP apical state by secondary mechanism



inversion of configuration while rearrangement which proceeds via an equatorial intermediate will occur with retention of configuration. Both processes will result in geometric isomerization.

Rearrangement proceeding through the SP apical intermediate will result in geometrical isomerization and will occur with both inversion and retention of configuration. This process is further complicated by the possibility of two microscopically reversible pathways for the formation of the intermediate. The two pathways are designated by Holm<sup>110</sup> as primary (Fig. 6-3a) and secondary (Fig. 6-3b). The intermediate may be converted to products by attack of the free end of the dangling ligand at any one of the basal positions by both primary and secondary processes. Holm has argued that rearrangements involving SP apical intermediates are most likely to involve only the primary process or equal proportions of the primary and secondary process.<sup>110</sup> Pignolet et al. have suggested that the primary process is more probable, owing to the lesser degree of ligand motion involved.<sup>111</sup>

Since there appears to be no good a priori reason to favour a TBP or SP intermediate, it is quite reasonable to suppose that both may be involved in the rearrangement process. A TBP axial intermediate may be converted into a TBP equatorial intermediate via a SP basal intermediate (Fig. 6-4) and a TBP equatorial intermediate into another TBP equatorial intermediate via a SP apical intermediate by means of a Berry pseudorotation. The stereochemical lability of some pentacoordinate TBP structures is already well-established<sup>112</sup>. If the pentacoordinate intermediates are sufficiently long-lived, the formation of products may be controlled by the relative

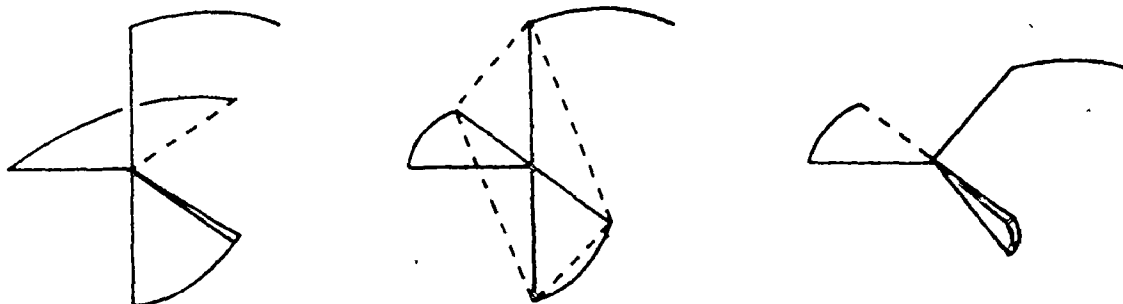


Figure 6-4 Rearrangement of TBP state by Berry pseudorotation

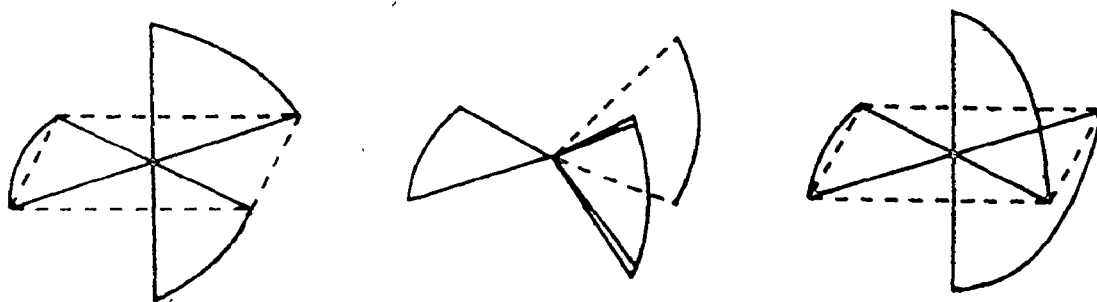


Figure 6-5 Rhombic twist mechanism (Ray and Dutt)

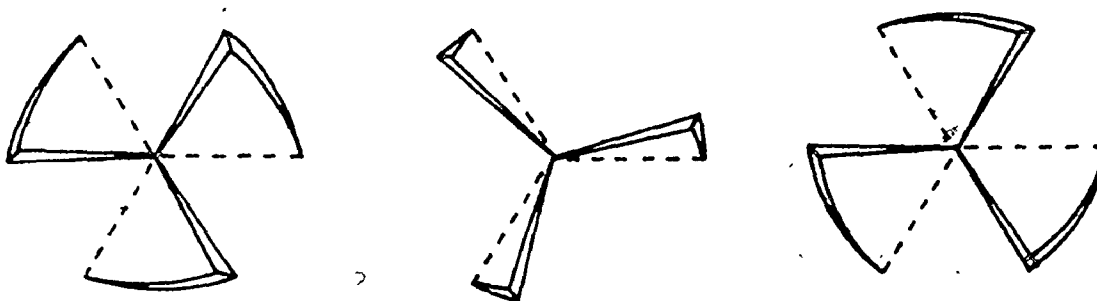


Figure 6-6 Trigonal twist mechanism (Bailar)

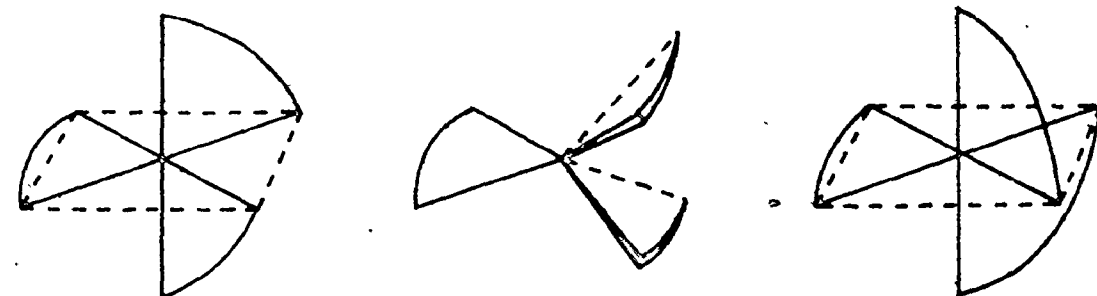


Figure 6-7 Trigonal twist mechanism (Springer and Sievers)

stability of the intermediates and their rate of conversion to products, rather than by kinetic control of formation of the intermediates. The relevance of a pseudorotation mechanism to NMR observations of the rearrangement process will be discussed in more detail below.

Examples of  $\beta$ -diketonate complexes which are believed to rearrange via a bond rupture mechanism include tris(5-methylhexane 2,4 dionato) Co(III),<sup>110</sup> and tris (1,1,1 trifluoro 2,4 pentamedionato) Al(III)<sup>101</sup>.

Calculations carried out by Fay and Piper<sup>101</sup> to estimate the energy of formation of TBP axial intermediate were unsuccessful, as the MO calculation to determine the loss of delocalization energy in the dangling ligand were sufficiently sensitive to the choice of resonance integrals to be indecisive.

### Twisting Mechanisms

Some mechanisms which may account for rearrangement which do not involve bond rupture have been proposed.

The first mechanism of this type was suggested by Ray and Dutt<sup>113</sup> to account for the anomalously low frequency factor determined for the racemization of tris (biguanidine) Co(III), (Co(bigH)<sub>3</sub><sup>3+</sup>). The mechanism is illustrated in Fig. 6<sup>12</sup>5. The formation of the transition state can be visualized in an idealized tris chelate molecule by imagining one of the chelate rings to be fixed, while allowing the other two to rotate in a contrary direction, in a plane defined by each chelate and the central metal ion, through an angle of 90°. For a molecule having three identical

symmetric ligands, the transition state or intermediate has  $C_{2v}$  symmetry and for this reason, this mechanism is commonly referred to as the "rhombic" twist. During the twisting process, the internal chelate D-M-D bond angles are assumed to remain constant and the dihedral angle between the planes of the rotating chelates is also assumed to remain constant at  $90^\circ$ .

Another mechanism which does not require metal ligand bond rupture is the "Bailar" twist<sup>114</sup>. This mechanism was proposed independently by Gehman and also by Seiden<sup>115,116</sup>.

A symmetric octahedral chelate complex has, in fact,  $D_{3h}$  symmetry. The twist mechanism may be visualized by viewing the complex along a  $C_3$  axis. One face of the octahedron defined by the upper three donor atoms is rotated through an angle of  $120^\circ$  (Fig. 6-6). When the angle of rotation is  $60^\circ$ , the lower donor atoms are eclipsed by the upper donor atoms. This state has  $D_{3h}$  symmetry and takes the form of a trigonal prism. The twisting process results in a decrease of an internal D-M-D angle, assuming that the donor atoms remain in the same plane. The contraction of the internal ligand D-M-D bond angles may be relaxed at the expense of external D-M-D bond angles. If all D-M-D bond angles are equal in the trigonal prismatic state, then the D-M-D bond angle would be  $81^\circ 47'$  compared to  $90^\circ$  in octahedral geometry.

A slightly different description of this mechanism has been proposed by Springer and Sievers<sup>117</sup>. In this, one ring may be regarded as being fixed, while the other two rotate past one another while changing planes. (Fig. 6-7)

The difference between the Springer and Bailar twists is in the angles maintained by the chelate donor atoms and the metal atom. In the Bailar description, the internal D-M-D angle is reduced, while in the Springer twist, the angle is maintained at  $90^\circ$ . The distinction between a Bailar and Springer and Sievers twist is artificial in that both result in a trigonal prismatic intermediate and give rise to the same rearrangement of the chelate. There appears to be, at present, no practical way of determining either the D-M-D<sup>118</sup> bond angles or the distance between counter rotating faces of donor atoms. Fay and Piper<sup>101</sup> have suggested that the Ray and Dutt transition state be referred to as "rhombic" and the Bailar and Springer and Sievers transition state be referred to as "trigonal". This terminology seems preferable, as it implies no artificially restricted description of the relative positions of the central metal and donor atoms.

Serpone and Bickley<sup>102</sup> have emphasized that basically, there is only one type of rearrangement relative to a regular octahedron. The octahedron has four  $C_3$  axes and the trigonal twist may be carried out with respect to any one of these four axes passing through a trigonal prismatic arrangement. When the donor atoms are connected through the chelate, the complex has  $D_3$  symmetry and therefore, only one real  $C_3$  axis. The remaining  $3C_3$  axes of the original octahedron are referred to as imaginary  $C_3$  axes. In a complex where the chelate groups are not symmetric, there may be no real  $C_3$  axis as in a  $\text{trans } M(\mu\text{-chel})_3$  complex. In this case, the axis which would be a real  $C_3$  axis if the chelate groups were symmetric is referred to as a pseudo  $C_3$  axis. This notation of the

axes was suggested by Springer and Sievers<sup>117</sup>.

When the axis, about which the twist takes place is the real or pseudo  $C_3$  axis, the rotation is referred to as an  $RC_3$  operation and corresponds to the Bailar twist. When the twist is carried out with respect to an imaginary  $C_3$  axis, the rotation is referred to as an  $RC_3(i)$  operation and corresponds to the Ray and Dutt twists; there are three  $C_3(i)$  axes, and rotation about each one corresponds to keeping one of each of the chelate rings fixed and allowing the plane of the other two to rotate.

It should be noted that all of these twist mechanisms occur with inversion of configuration. Another mechanism for rearrangement has been proposed<sup>119</sup> where the intermediate has a distorted hexagonal planar structure. This transition state cannot be regarded as being likely to occur in the case of  $\beta$ -diketonate complexes of metals of the first transition, as it would require a very considerable increase in the M-O bond lengths of all the ligating oxygen atoms (circa  $1 \text{ \AA}$ , normal bond length circa  $2 \text{ \AA}$ ).

#### Estimations of the Energies of Intermediates

Muetterties<sup>120</sup> has pointed out that there are no known examples of discrete  $ML_6$  complexes where the coordination is trigonal prismatic, although there is a class of chelates  $M(S_2C_2R_2)_3$  which have  $D_{3h}$  symmetry and where the sulphur atoms quite closely define the square faces of a trigonal prism.

He infers from the almost universal preference of discrete six coordinate structures to adopt octahedral geometry, that in general, the difference in energy between an octahedral and a trigonal prismatic arrangement must be quite large.

Fay and Piper<sup>101</sup> have carried out point charge calculations to attempt to estimate the contribution of the ligand-ligand repulsion terms to the intermediates of different geometries.

For the trigonal prismatic, 'Bailar' intermediate, they estimated an increase in ligand-ligand repulsion of  $0.194 q / r$  where  $q$  equals the fraction of an electronic charge on each oxygen and  $r$  equals the metal oxygen bond length. However, the contribution due to ring strain required to reduce the O-M-O angles to  $81^\circ$  was not included. If the original  $90^\circ$  O-M-O angle was preserved, the ligand-ligand repulsion energy was found to increase to  $0.242 q / r$ . For the rhombic 'Ray and Dutt' intermediate, the value of the ligand-ligand repulsion term was calculated to be  $0.286 q / r$ , although this value could be substantially reduced to  $0.114 q / r$ , if the dihedral angle between the two counter-rotating ligands were allowed to increase to  $115^\circ$ . Steric effects were not accounted for in the calculation. Piper and Fay conclude that for ions which do not have CFSE, the rhombic twist should be favoured over the trigonal twist. Fay and Piper point out that, on the other hand, CFSE may favour trigonal prismatic over octahedral geometry. Calculations by Piper and Carlin<sup>121</sup> suggest that the CFSE stabilization energy for Cr(III) in trigonal prismatic coordination relative to octahedral coordination may be as

much as 11 kcal/mole. Similar calculations by Fay and Piper for  $\text{Co(III)}$ <sup>101</sup> indicate CFSE stabilization energy may be as much as 21 to 30 kcal/mole. The CFSE energy is not readily calculated for the rhombic intermediate;<sup>101</sup> however, it is likely to be less than for the trigonal prismatic intermediate. CFSE would presumably be maximized in complexes with strong field ligands. Valence bond calculations by Hutgren<sup>122</sup> also suggest that the trigonal prism may achieve greater resonance energy per bond than the octahedron. A twist mechanism might therefore be expected in complexes in which the ligand-ligand repulsion terms are minimized and the CFSE is maximized. Ligand-ligand repulsion terms would presumably be minimized in ligands where the ligating atoms are neutral or where extensive delocalization of charge through an aromatic system can take place. Bonding between the ligating atoms may also serve to reduce the ligand-ligand repulsion terms. The dimension of the ligand relative to the metal-ligand bond distances may also influence favourability of the trigonal prism. Ideal radius to edge ratios for the trigonal prism (0.76) compared to the octahedron (0.71) suggest that a ligand with a relatively small 'bite' may favour the formation of a trigonal prism. On the other hand, a rigid bidentate ligand, while not decreasing the relative energy of the trigonal prism, might be expected to increase the necessary energy for a bond rupture process.

Complexes for which the twist mechanism have been established usually exhibit many of the features theoretically favouring the twist process. Thus, for example, the  $\text{Fe(phen)}_3^{2+}$  and  $\text{Fe(bipy)}_3^{2+}$  complexes for which the twist mechanism has been suggested by Basolo<sup>123</sup>



have neutral rigid ligands. Tris ( $\alpha$ -isopropenyltropolonato) and Tris ( $\alpha$ -isopropyltropolonato), Al(III) & Co(III), have been shown to rearrange via a trigonal twist mechanism.<sup>124</sup> Again, the tropolonato (T) ligand, although negatively charged, is capable of delocalizing the charge through the aromatic system. The bite distance of the ligand is also relatively short circa 2.5 Å compared to circa 2.7 to 2.9 Å in acetylacetonate. The radius to edge ratios of Co T<sub>3</sub> (0.74) and Al T<sub>3</sub> (0.76) approach the ideal for trigonal prismatic coordination; the acetylacetonates of Co and Al on the other hand have radius to edge ratios of 0.66 and 0.69 respectively, which is closer to the ideal for octahedral coordination.

It is also worthy of note that some of the complexes believed to rearrange via a trigonal twist mechanism show a distortion from octahedral geometry in the ground state. The angle  $\phi$ , which is defined by projection of metal ligand vectors on a plane normal to the C<sub>3</sub> (r or p) axis, has the value 60° in a regular octahedral complex and 0° in a trigonal prismatic complex. The twist angles for the complex Fe(MePh(dtc))<sub>2</sub>(tfd) for which the trigonal twist mechanism of rearrangement was established by Pignolet and co-workers,<sup>111</sup> are 33° for the dithiocarbamate ligands and 41° for the tfd ligand.

Tris(tropolonato) Al(III) has a twist angle of 48°;<sup>125</sup> however, the twist angle in tris(tropolonato)Co(III) is 55°, close to octahedral<sup>124</sup> Fe(phen)<sub>3</sub><sup>2+</sup><sup>124</sup> has a similar twist angle.

Tris (acetylacetonato) V(III),  $(V(acac)_3)$ , which has close to octahedral coordination of oxygen around vanadium, has a twist angle of  $56^\circ$  and an r/e value of  $0.71^{17}$  (ideal for octahedral coordination is 0.71). Crystal field stabilization energy for V(III) in TP coordination relative to octahedral coordination is moderate, probably less than the value for Cr(III) (11 kcal/mole).

Furthermore, the  $\beta$ -diketonate ligand, if monodentate, would not be expected to have much rigidity.

On the basis of these considerations, it might be expected that the rearrangement of tris  $\beta$ -diketonato V(III) complexes would proceed via a bond rupture rather than a twist mechanism, although this is by no means certain.

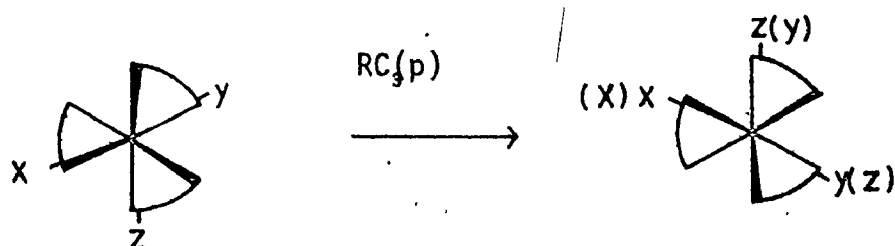
#### Methods of Obtaining Kinetic Data

Three methods have been used extensively for the study of rearrangement processes of chelate complexes; these are spectrophotometric, polarimetric and nuclear magnetic resonance (NMR) methods. The classical techniques of spectrophotometry and polarimetry have been applied to reactions of complexes whose rearrangement processes are 'slow'. The label 'slow' is applied to those complexes whose geometrical isomers can be separated and at least partially resolved, typically those of such non-labile metal ions such as Cr(III), Co(III), Rh(III), and Ru(II,III)<sup>124</sup>. Magnetic resonance may also be used to follow the reactions of the 'slow'

group, provided that the resonances due to the isomers of complexes are sufficiently resolved to allow accurate estimates of intensity of the signal. Separation of the isomers of a neutral  $\beta$ -diketonate complex is necessary to enable the spectrophotometric measurements to be made and is usually not particularly difficult. Resolution of the enantiomers of the complexes is difficult due to the electric neutrality of the complexes. Formation of a diastereoisomeric salt is not possible, but resolution of a number of tris  $\beta$ -diketonate complexes has been achieved by a variety of methods<sup>15</sup>.

Nuclear magnetic resonance methods are complementary to the classical techniques in that they are applicable to complexes of labile metals, complexes which rearrange at such a rate that their isomers and enantiomers cannot be separated, typically those of Al(III), Ga(III), In(III), V(III), high spin Mn(III), and Fe(III).

NMR also offers another important advantage; it is often possible to study a rearrangement process where the product is chemically indistinguishable to the reactant. The rearrangement of a trans tris ( $\mu$ -chelate) for example, has no element of symmetry and each of the sets of nuclei are magnetically non-equivalent.



If a twist occurs about the pseudo  $C_3$  axis, the product which results is also the trans isomer. The nuclei at sites  $y$  &  $z$ , however, have been exchanged. This particular rearrangement would also be detectable by polarimetry, as the reaction proceeds with inversion of configuration, but observation of this would require prior separation of the optical isomers.

There are two principal methods of determining the rate of exchange between magnetically non-equivalent sites as outlined in chapter II; lineshape analysis and 'spin saturation transfer' (SST). The observation of exchange between two sites by spin saturation transfer is optimized when  $\tau$ , the exchange lifetime, is equal to  $T_1$ , the spin lattice relaxation time of the site under observation. If  $T_1 = T_2$ , then  $\tau = T_2$ . At the optimum rate of exchange, the observed linewidth will be double the natural linewidth. This method is attractive when the natural linewidth is small, especially when compared to the instrumental linewidth, and therefore difficult to measure accurately. The SST technique requires that the peak in exchange with that under observation is saturated, i.e.

$$M_z = M_0 \frac{1 + T_2^2 (\omega_0 - \omega)^2}{1 + T_2^2 (\omega_0 - \omega)^2 + \gamma_N H_1^2 T_1 T_2} \approx 0$$

$$\therefore \gamma_N H_1^2 T_1 T_2 \gg 1 + T_2^2 (\omega_0 - \omega)^2$$

Assuming that  $T_1 = T_2$ , then  $H_1 \propto \frac{1}{T_2}$  for a constant degree of saturation.

The oscillating field required to saturate a line is therefore proportional to the width of the line. For this reason, SST is better applied to narrow lines as the requirement of saturation is much less demanding. Despite these limitations, we attempted to use the technique of SST with  $V(\text{tfac})_3$  and  $V(\text{tfac})(\text{hfac})_2$ . It was found that, although the saturating RF field was sufficiently strong to saturate a resonance, the intensity of the observed signal was decreased independently of chemical exchange. This is probably due to the fact that both the saturating field and the observing field are produced by AF modulation of the same constant frequency RF field.

The SST technique has the attraction that the data obtained by this method is particularly simple to interpret. A single measurement will give the rate of exchange between two sites. All the elements of the exchange matrix can be determined in turn. Lineshape analysis on the other hand, requires that the lineshape be calculated from a particular exchange matrix. The matrix is essentially determined by trial and error to produce the lineshape which best fits the experimental spectrum.

Lineshape analysis is the method most often used for determining rates of exchange from NMR data. Allerhand et al.<sup>126</sup> have pointed out that there are many potential hazards. Briefly, the hazards may be divided into two groups: a) use of a mathematical model which is not really applicable to the problem, e.g., the use of the 'exchange

narrowing' formula

$$\frac{1}{T_2} = \frac{f_A}{T_{2A}} + \frac{f_B}{T_{2B}} + \frac{f_A f_B (\omega_A - \omega_B)^2}{P_{AB} + P_{BA}}$$

to a range of linewidths from just above the coalescence temperature.

This formula is, in fact, strictly applicable only in the limit of exchange narrowing. b) Experimental errors: to calculate a lineshape, a number of parameters must be specified among them the position and width, in the absence of exchange, of each line. Since these parameters cannot be directly measured in the presence of exchange effects, it is necessary to measure them below the temperature at which exchange effects are observed and extrapolated to the fast exchange range.

For the vanadium  $\beta$ -diketonates, the extrapolation of chemical shifts is a simple matter, as the shifts obey a simple Curie-Weiss law<sup>5,127</sup>. The linewidths on the other hand do not appear to exhibit quite such a simple relationship with temperature.

The following discussion is presented in several parts: 1) the estimation of the parameters on which the lineshape calculations are based. 2) a brief account of permutational analysis and its application to the exchange spectra of the complexes to determine the most probable mechanisms: 3) the measurement of activation parameters and their relevance to the determination of mechanism. 4) the study of complexes containing the triacetylmethanato ligand which can, potentially, determine if bond rupture occurs. 5) the study of tris (diisobutyryl-

methanato V(III) to determine whether enantiomerization occurs.

6) a summary of conclusions.

### Results and Discussion

All the complexes which were examined,  $V(acac)_2(hfac)$ ,  $V(acac)(hfac)_2$ ,  $V(tfac)_3$ ,  $V(tfac)(hfac)_2$ ,  $V(tfac)(acac)_2$ ,  $V(triac)_2(acac)$ , and  $V(dibm)_3$ , showed distinct evidence of molecular rearrangement on the NMR time scale at temperatures in the range between  $-30^\circ$  and  $100^\circ$ .

The rearrangement of vanadium  $\beta$ -diketonates on the NMR time scale has not been previously reported. In fact, one group of workers has reported that the NMR spectrum of  $V(tfac)_3$  shows no changes attributable to exchange broadening up to  $100^\circ$ <sup>7</sup>. The origin of this discrepancy is not obvious. The  $^{19}F$  linewidths of  $V(tfac)_3$  reported by Everett and Johnson<sup>128</sup> are very much greater than the linewidths indicated as typical of Vanadium  $\beta$ -diketonate complexes by Eaton<sup>129</sup>. This may have been due to exchange broadening, but as the temperature at which the spectra were recorded was not stated, it is not possible to say whether their results are in agreement with the present work. The NMR spectrum of some optically active  $\beta$ -diketonates has been recorded<sup>130,131</sup>, but no indication of exchange phenomena was noted. The failure<sup>130</sup> to measure the temperature dependence of equilibria existing between the isomers of tris(hydroxymethylene camphor)V(III) was attributed to poor signal resolution at higher temperatures. It is possible this may have been due to exchange broadening.

In the present work, most of the spectra were obtained on a Varian DP 60 spectrometer operating at 58.3 MHz. for both  $^1\text{H}$  and  $^{19}\text{F}$ . Some  $^1\text{H}$  spectra were obtained on a Varian HA 100 spectrometer operating at 100 MHz. For most of the spectra, the instruments were operated in the HA field sweep mode, as the range of chemical shifts is rather large, e.g., around 19.3 ppm for  $\text{V}(\text{tfac})(\text{hfac})_2$  at  $-4^\circ$ . In the frequency sweep mode, a change of frequency results in a change of phase of the observed signal. As only the v or absorption mode signal, which has a Lorentzian lineshape is included in the lineshape calculations, it is important to avoid, as far as possible, the presence of any u or dispersion mode signal. The spectra were calibrated by the side band method using  $\text{CFCl}_3$  as a reference for the  $^{19}\text{F}$  spectra and TMS for the  $^1\text{H}$  spectra. Spectra of  $\text{V}(\text{hfac})_2(\text{acac})$  and  $\text{V}(\text{acac})_2(\text{hfac})$  were obtained, for the sake of convenience, on a frequency sweep mode. The difference in chemical shift of the two magnetically non-equivalent sites was small, circa one ppm, and therefore, the phase problem was minimal. Simulated spectra were calculated by total lineshape analysis using a Saunders many site lineshape programme<sup>66</sup>. The programme was modified slightly to give a punched card output which consisted of a list of frequencies with relative intensities. The input required by the NMR lineshape programme consists of the chemical shifts, line-widths at half-height, the relative intensity of each peak, the exchange matrix which consists of the probability of transfer of a nucleus or set of nuclei from each site to every other site, and an overall rate of exchange.



The input to the plotting routine was adjusted so that the simulated spectrum was plotted to conform to the same horizontal scale as the experimental spectrum, i.e., in Hz/inch, and the height of the plot was adjusted so that the maximum value of the simulated spectrum matched the height of the largest peak in the experimental spectrum. The overall rate parameter was adjusted to give the best visual match between the simulated and experimental spectrum. Allerhand<sup>126</sup> et al. have pointed out that this procedure is likely to incur larger errors than a programme which finds a best fit to the data by means of a non-linear regression. Since the data were obtained as a trace on chart paper rather than in digital form, the latter procedure would probably not have produced much superior results as the data would have had to have been converted into digital form manually. Besides being a very tedious and time-consuming process, the errors involved in estimating the intensity of a signal at a given frequency would be much the same as those involved in comparing the simulated and experimental spectra.

Both the chemical shifts and linewidths of vanadium  $\beta$ -diketonate complexes are dependent on solvent and temperature.

#### Solvent Dependence of Chemical Shifts

Table 6-1 compares the equations for the temperature dependence of the chemical shifts of the methyl and trifluoromethyl groups of the complexes under study. In the case of  $V(\text{tfac})_3$  where the dependence

Table 6-1 Temperature dependence of chemical shifts of methyl and trifluoromethyl groups of vanadium  $\beta$ -diketonate complexes.

The temperature dependences of the shifts are given in the form

$$\Delta\nu(\text{Hz.}) = a \times (1/T \text{ } ^\circ\text{K} \times 10^3) + b$$

The constants a and b are reported.

58.3  $^{19}\text{F}$   $\text{CF}_3$  shifts of  $\text{V}(\text{tfac})_3$  relative to central trans resonance.

		a	b
	1	downfield resonance	(trans)
	2	cis resonance	
	3	central resonance	(trans)
	4	upfield resonance	(trans)
Solvent		a	b
$\text{CDCl}_3$	1	-450	905
	2	-33.6	64.6
	3	0	0
	4	253	-489
acetone	1	-414	890.5
	2	-91	226
	3	0	0
	4	161	-268
$\text{CCl}_4$	1	-407	820
	2	-31	55
	3	0	0
	4	260	-503
chlorobenzene	1	-422	845
	2	-34	63
	3	0	0
	4	279	-554

58.3 MHz.  $^{19}\text{F}$   $\text{CF}_3$  shifts of  $\text{V}(\text{hfac})_2(\text{tfac})$  relative to  $\text{V}(\text{hfac})_3$ .

Solvent		a	b
$\text{CDCl}_3$	1	-458	1074
	2	-369	894
	3	0	0 ( $\text{CF}_3$ of $\text{V}(\text{hfac})_3$ )
	4	42	12.5
	5	342	-778

Separation of  $\text{CF}_3$  resonances of  $\text{V}(\text{hfac})_2(\text{acac})$  at 58.3 MHz.

Solvent	a	b
$\text{CDCl}_3$	17.8	34.3
chlorobenzene	16.1	19.9
$\text{CCl}_4$	16.9	18.5
acetone	18.7	18.1
acetonitrile	18.1	16.2

100 MHz.  $^1\text{H}$   $\text{CH}_3$  shifts of  $\text{V}(\text{triac})_3/\text{V}(\text{triac})_2(\text{acac})$  relative to  $\text{CH}_3$  resonance of  $\text{V}(\text{triac})_3$ .

Solvent		a	b
$\text{CDCl}_3$	1 $\text{V}(\text{triac})_2(\text{acac})^*$	-157	+252
	2 $\text{V}(\text{triac})_3$	0	0
	3 $\text{V}(\text{triac})_2^*(\text{acac})$	18.7	-1.6
	4 $\text{V}(\text{triac})_2^*(\text{acac})$	176	-279

100 MHz.  $^1\text{H}$  shifts of diastereotopically non-equivalent  $\text{CH}_3$  groups of  $\text{V}(\text{dibm})_3$  relative to TMS.

Solvent		a	b
$\text{CDCl}_3$	1	-56.9	-76.9
	2	36.3	-321.7

has been measured in different solvents, it is evident that the chemical shifts are solvent dependent. The origin of the solvent dependence is probably conformational changes in the complex due to Van der Waal's interaction with the solvent, which in turn, affect the overlap of the ligand  $\pi$  orbitals with the vanadium d orbitals, and hence influence spin distribution in the ligands.

### Temperature Dependence of the Chemical Shifts

It has been found that the shifts of the resonances vary linearly with  $1/T^\circ\text{K}$  within experimental error. The plots, however, do not pass through the origin. The shifts can, therefore, be described by a Curie-Weiss law, i.e.,  $\nu = a \times \frac{1}{T^\circ\text{K}} + b$ . A plot of shift versus  $1/T^\circ\text{K} \times 10^3$  is illustrated in Fig. 6-8 for  $\text{V}(\text{tfac})_3$  in  $\text{CDCl}_3$ . For all the resonances of  $\text{V}(\text{tfac})_3$ , the sign of the shift at  $1/T = 0$  is predicted to change. From the values of the constants a and b for each line, it is also predicted that each pair of resonances will become coincident at some temperature. Fortunately, the temperatures at which this would occur are well above the coalescence temperature. There are no marked differences of temperature dependence in different solvents. Although the simplest model of contact shifts predicts a simple Curie Law dependence of shifts on temperature, there are a number of sources which may give rise to non-zero intercepts which have been discussed by Perry and Drago<sup>132</sup>. The Curie Law dependence of the chemical shifts of vanadium  $\beta$ -diketonate complexes has also been observed by Eaton and Chua<sup>5</sup>. The temperature dependence of the iso-

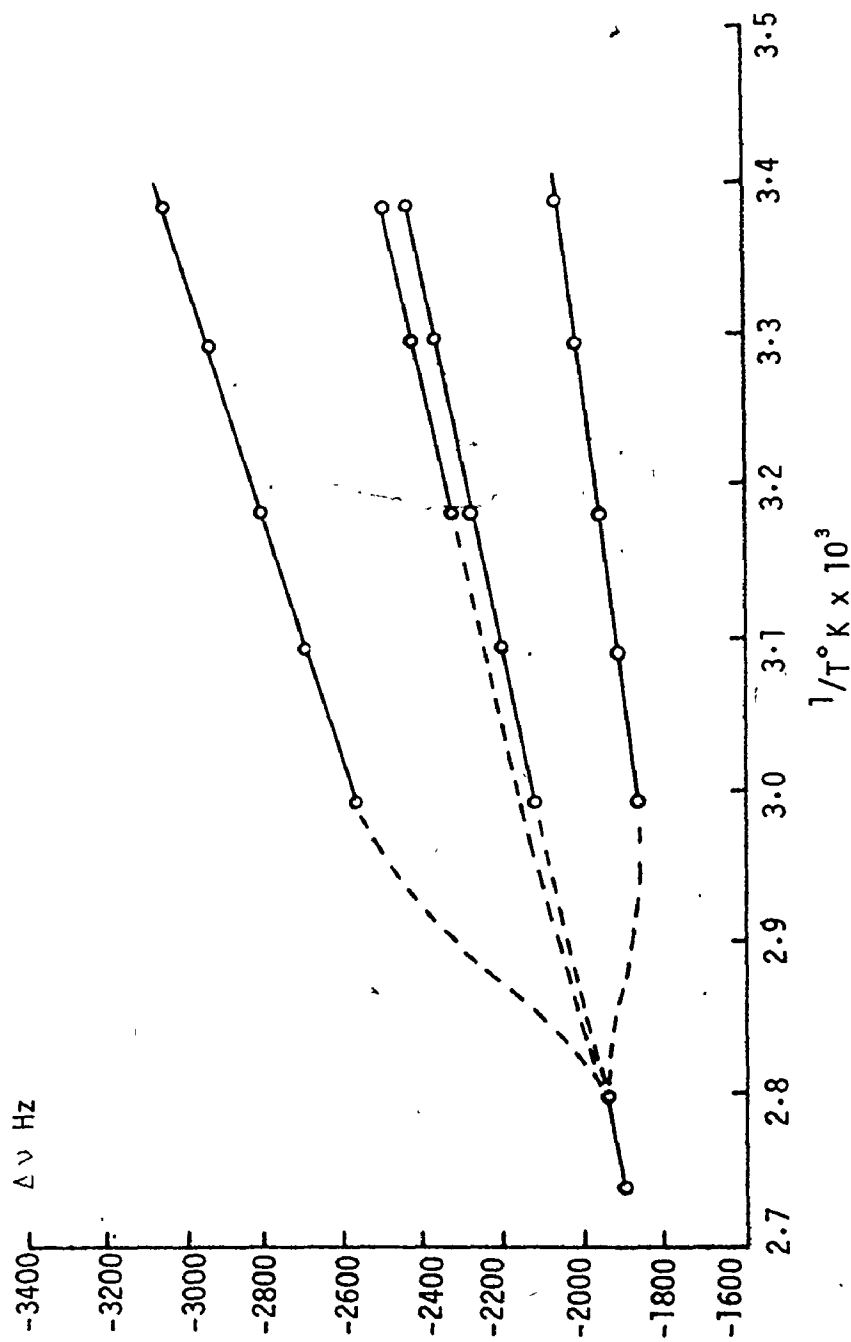


Figure 6-8 Chemical shift of  $\text{CF}_3$  groups of  $\text{V}(\text{tfac})_3$  versus reciprocal temperature.  $^{19}\text{F}$ , 58.3 MHz in  $\text{CDCl}_3$  (relative to  $\text{CF}_3$  resonance of free ligand).

tropic hyperfine shifts parallels the temperature dependence of the magnetic susceptibility which for  $V(acac)_3$  and  $V(tfac)_3$  has values of 2.80<sup>133</sup> and 2.78 BM<sup>127</sup> respectively, close to the spin only value of 2.83. These magnetic properties of octahedrally coordinated V(III) are consistent with a non-degenerate  $^3A_2$  (in  $D_3$  symmetry) ground state. Eaton and Chua<sup>5</sup> have argued that the isotropic shifts of the vanadium  $\beta$ -diketonates arise primarily from contact interactions, and that dramatic changes in the electronic ground state do not occur on formation of an unsymmetric chelate.

The precise origin of the isotropic shifts is not of great importance in the present work. What is important, is that the magnitudes of the shifts above the temperature at which exchange effects are observed, can be predicted with a reasonable degree of confidence.

### Linewidths

Both  $^1H$  and  $^{19}F$  linewidths are dependent upon a number of factors. Temperature, the composition of the complex, and the solvent, all appear to have some effect on the observed linewidth. For the resonances originating from a particular complex, the linewidths also appear to be correlated with chemical shift (Fig. 6-9). In general, the linewidth increases with increasing chemical shift, although not in direct proportion.

The dependence of linewidth on temperature is illustrated for

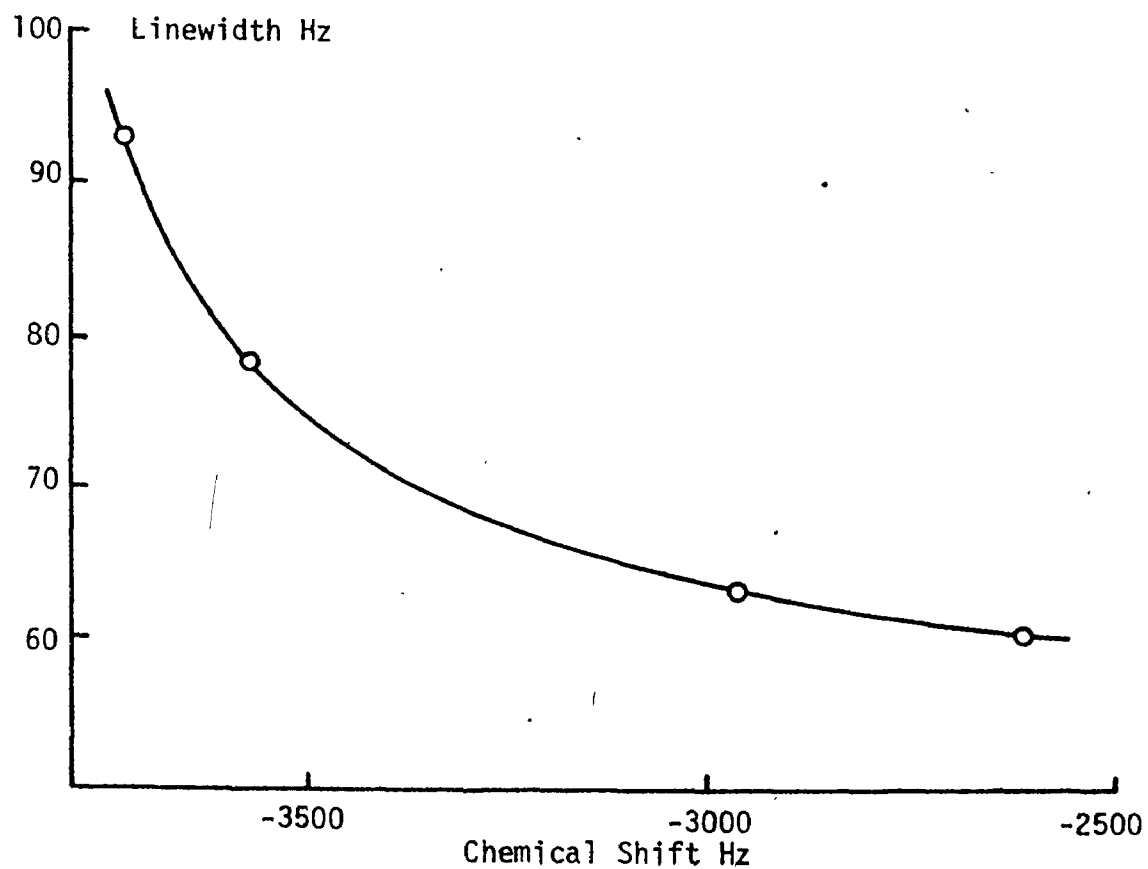


Figure 6-9 Variation of linewidth of  $\text{CF}_3$  resonances of  $\text{V}(\text{hfac})_2(\text{tfac})$  with chemical shift.  $^{19}\text{F}$  at 58.3 MHz in  $\text{CDCl}_3$  at  $-4^\circ\text{C}$ .

$V(acac)_3$  in Fig. 6-10. Over the temperature range in which most of the isomerization reactions are observed, the range of linewidth is, fortunately, relatively small. Even so, the estimation of linewidth is important for a reliable estimation of rates, particularly in the two site exchange cases,  $V(hfac)_2(acac)$  and  $V(acac)_2(hfac)$ , where the chemical shift between the exchanging sites is small (<100 Hz.) and the linewidth of the resonances is a major factor in determining the overall lineshape. A brief consideration of theoretical principles will show that it is not possible to make any a priori predictions about the behaviour of the linewidth with respect to temperature.

The NMR spectra of vanadium (III)  $\beta$ -diketonates are characterized by very narrow linewidths compared to most paramagnetic molecules. Almost certainly, the only process which is sufficiently rapid to account for such narrow lines is electronic relaxation. This case is known as the 'fast motion limit' and the relaxation times are given by

$$T_{1N}^{-1} = T_{2N}^{-1} = \frac{4 S(S+1)}{3r^6} \gamma^2 g^2 \beta^2 T_{1e} \quad (6-1)$$

The relationship between  $T_{2N}$  and temperature is therefore, dependent upon the relationship between  $T_{1e}$  and temperature. Eaton and Zaw<sup>136</sup> have pointed out that the relaxation situation for tetrahedral Co(II) complexes should be similar to that for octahedral V(III) complexes. In such a case, the electronic relaxation mechanism is dominated by coupling of the molecular motion with the zero field splitting. For tetrahedral Co(II),



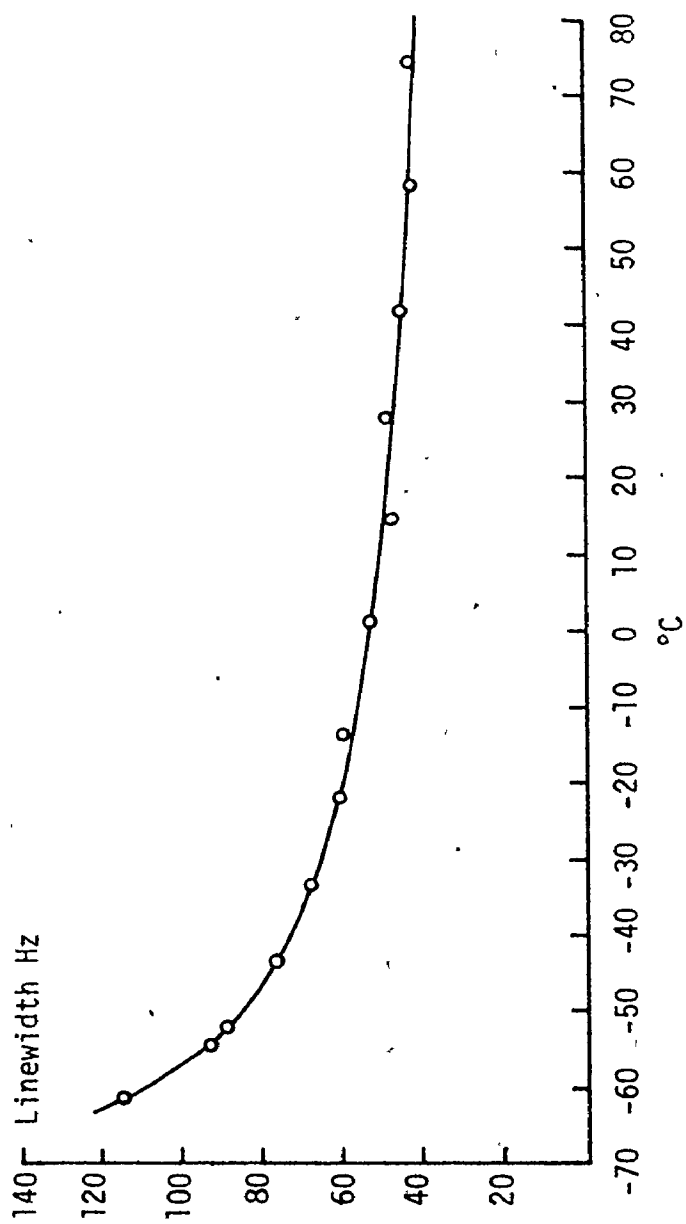


Figure 6-10 Linewidth of  $\text{CH}_3$  groups of  $\text{V}(\text{acac})_3$  versus temperature.  
 $^1\text{H}$  100 MHz in acetone.

LaMar<sup>135</sup> has shown that the electronic spin relaxation time is given by the equation

$$T_{1e}^{-1} = \frac{32\pi^2}{5} \left( \frac{D^2}{h^2} \right) \left[ \frac{\tau}{1+\omega_S^2\tau^2} + \frac{\tau}{1+4\omega_S^2\tau^2} \right] \quad (6-2)$$

In this equation,  $D$  is the Zero field, splitting parameter. The other terms have their usual meaning. If  $\omega_S^2\tau^2 \gg 1$ ,  $T_{1e}^{-1} \propto \tau^{-1}$  and if  $\omega_S^2\tau^2 \ll 1$ ,  $T_{1e}^{-1} \propto \tau$ . Since the NMR line becomes narrower as the electronic relaxation time decreases, in the former case the NMR line is predicted to become narrower with increasing temperature, and vice-versa in the latter case.

The correlation time can be estimated approximately from the expression

$$\tau_c = \frac{4\pi\eta r^3}{3kT}$$

where  $\eta$  is the viscosity of the medium in poises and  $r$  is the molecular radius in centimeters. For  $V(acac)_3$ , which has a molecular volume of  $433 \text{ \AA}^3$ <sup>136</sup>,  $\tau_c$  is calculated to have a value of approximately  $5.7 \times 10^{-11}$ . Considering the simplicity of the model, this value is remarkably close to the value of  $\tau_c$  obtained from  $^{13}C$  relaxation measurements on  $Co(acac)_3$  by Chan<sup>137</sup>, i.e.,  $\tau_c = 7.3 \times 10^{-11}$ . The values should be comparable as the dimensions of the cobalt complex are very similar to those of the vanadium complex. At 58.3 MHz,  $\omega_S$ , the electronic Larmor frequency has a value of approximately  $3.8 \times 10^{10} \text{ sec.}^{-1}$ ; therefore,  $\omega_S\tau_c$  has a value of 2.1 which is sufficiently close to unity, that a theoretical prediction of the variation of NMR linewidth with temperature

is somewhat dubious.

The small changes in linewidth due to solvent are most likely due to differences in the viscosity of the solvent. It is unlikely that the electronic configuration of a complex would be greatly affected by changes in solvation.

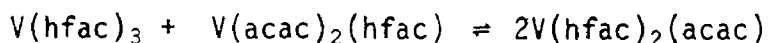
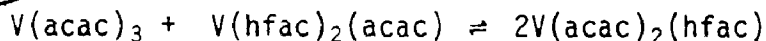
The correlation of linewidth with chemical shift is interesting. Significant line broadening due to a Fermi contact interaction is unlikely. If the dipolar interaction is responsible for relaxation, then the usual expression for dipolar relaxation above which involves the parameter  $r$ , the distance of relaxing nucleus from the paramagnetic metal ion, must vary up to 8%, equivalent to a distance of approximately 0.4 Å. There is an alternative explanation which would readily account for the correlation between chemical shift and linewidth. A significant degree of dipolar relaxation may be due to electron spin density, localised on the adjacent unsaturated carbon. Since the carbon-fluorine or carbon-proton distances are approximately constant, the linewidth would be proportional to the square of the spin density on the unsaturated carbon atom.

For the purpose of the lineshape calculations, we have assumed that for the complexes exhibiting relatively large chemical shifts, i.e.,  $V(\text{tfac})_3$ ,  $V(\text{tfac})(\text{hfac})_2$ ,  $V(\text{triac})_2(\text{acac})$ , the linewidths are constant. This approximation should not introduce an appreciable error until the limit of exchange narrowing is approached. For complexes such as

Table 6-2 Activation parameters of rearrangement processes of vanadium  $\beta$ -diketonate complexes in various solvents.

Complex	Solvent	$E_a$ ( $\sigma$ ) kcal/mol	$\ln A$ ( $\sigma$ )	$k_{25} \text{sec}^{-1}$	$\Delta H_{25}^\ddagger$ kcal/mol	$\Delta S_{25}^\ddagger$ eu.
V(tfac) <sub>3</sub>	CDCl <sub>3</sub>	18.6	33.6	8.9	18.0	6.3
	CH <sub>2</sub> Cl	17.1	31.1	9.2	16.5	1.3
	CCl <sub>4</sub>	17.0 (.5)	31.1 (.6)	10.9	16.4	1.3
	acetone	16.47	30.4	13.3	15.9	-0.1
V(hfac) <sub>2</sub> (tfac)	CDCl <sub>3</sub>	13.3 (.5)	27.1 <sup>+</sup> (.8)	103	12.7	-6.7
V(hfac) <sub>2</sub> (acac)	CDCl <sub>3</sub>	12.4 (.35)	25.4 (.6)	86	11.8	-10.0
	CH <sub>2</sub> Cl	12.4 (.3)	25.6 (.5)	105	11.8	-9.6
	CCl <sub>4</sub>	11.9 (.25)	24.8 (.5)	110	11.3	-11.2
	acetone	7.8 (.2)	19.9 (.4)	790	7.2	-21.0
	CH <sub>3</sub> CN	5.9 (.2)	16.3 (.4)	565	5.3	-28.1
	MeCl <sub>2</sub>	-	-	~30	-	-
	benzene	-	-	~40	-	-
V(acac) <sub>2</sub> (hfac)	CDCl <sub>3</sub>	-	-	40	-	-
	CH <sub>2</sub> Cl	-	-	23	-	-
V(triac) <sub>2</sub> (acac)	CDCl <sub>3</sub>	10.7	21.4	28	10.1	-18.0
V(dibm) <sub>3</sub>	CDCl <sub>3</sub>	15.5	29.1	19	14.9	-2.7

$V(hfac)_2(acac)$ ,  $V(acac)_2(hfac)$  and  $V(dibm)_3$ , the linewidth is a much more important factor in the overall lineshape. In this case, we have estimated the linewidths by linefitting at a temperature where exchange broadening is insignificant, and assumed that any changes in linewidth are proportional to the changes in linewidth of a line which is not involved in chemical exchange. This procedure should be valid, as theory predicts that changes in linewidth are due ultimately to changes in viscosity of the solvent, which is common to complexes in the same solution. Because of the equilibria which exist between the complexes,



there is always one and sometimes two non-exchanging lines which can be used for this purpose.

#### Mechanisms of Rearrangement of Vanadium $\beta$ -diketonates

The activation parameters derived from lineshape analysis are reported in table 6-2, along with the estimated values of the rate constants at 25°C. It is immediately evident that the rates of molecular rearrangement are considerably faster than the rate of ligand exchange previously determined for  $V(acac)_3$ ,  $H(acac)_4$  and  $Hhfac$ . It is, therefore, reasonable to suppose that rearrangement occurs via an intramolecular mechanism rather than an intermolecular mechanism. Confirmation is provided by the observation that free ligand resonances can be observed under conditions where the complex resonances have coalesced.

Distinguishing between twist mechanisms and bond breaking mechanisms is considerably more difficult. In some cases, attempts have been made to identify the mechanism of rearrangement by identifying the elements of the site exchange matrix and showing that the matrix is compatible only with a single mechanism. More often, it is possible only to eliminate some mechanisms which are definitely incompatible with the site exchange matrix.

In general, the mechanistic information provided by the NMR lineshape increases with the number of exchanging sites. The observation of a particular exchange pattern in the NMR spectrum of a rearranging complex does not, of course, 'prove' a mechanism as the lineshape depends only on the transfer of a set of nuclei at one set of sites to another set of sites, and not on how that transfer occurs. Eaton and Eaton<sup>138</sup> have carried out a permutational analysis for tris chelate complexes, treating the cases of complexes with three identical unsymmetrical ligands and two identical unsymmetric and one symmetric ligand in full detail.

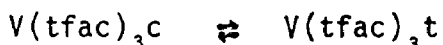
The analysis is based on the concept of molecular symmetry groups for non-rigid molecules introduced by Longuet-Higgins<sup>139</sup>. This procedure ensures that every feasible rearrangement is accounted for, whether or not a physically plausible mechanism has been postulated.

For an octahedral complex with six distinguishable ligands, there exist a total of  $6! = 720$  permutations. The set of permutations

may be factored into a set of 24 rigid body rotations and a set of 30 permutational isomers. If the restriction is imposed that the six ligands are paired in such a way that the members of a single pair may not span trans positions, the number of permutational isomers is reduced to sixteen. These sixteen permutational isomers are illustrated in Fig. 6-11.

V(tfac)<sub>3</sub>

Fig. 6-12 illustrates the comparison between the observed spectrum of V(tfac)<sub>3</sub> in carbon tetrachloride and the simulated spectrum calculated from the chemical shift, linewidth, exchange matrix and overall rate parameters. It is evident from inspection of the spectra that the nuclei at all four sites must be in exchange. The exchange matrix used in the calculation of the simulated spectra was initially set up such that the lifetime at all sites is equal, and the probability of transfer of a nucleus from any site in the trans complex to any other site in the trans complex is equal. The ratio of the probabilities of transfer of a nucleus from a trans site to a cis site and vice versa is determined by the equilibrium constant for the reaction



and the signal multiplicities. These constraints lead to a unique exchange matrix.

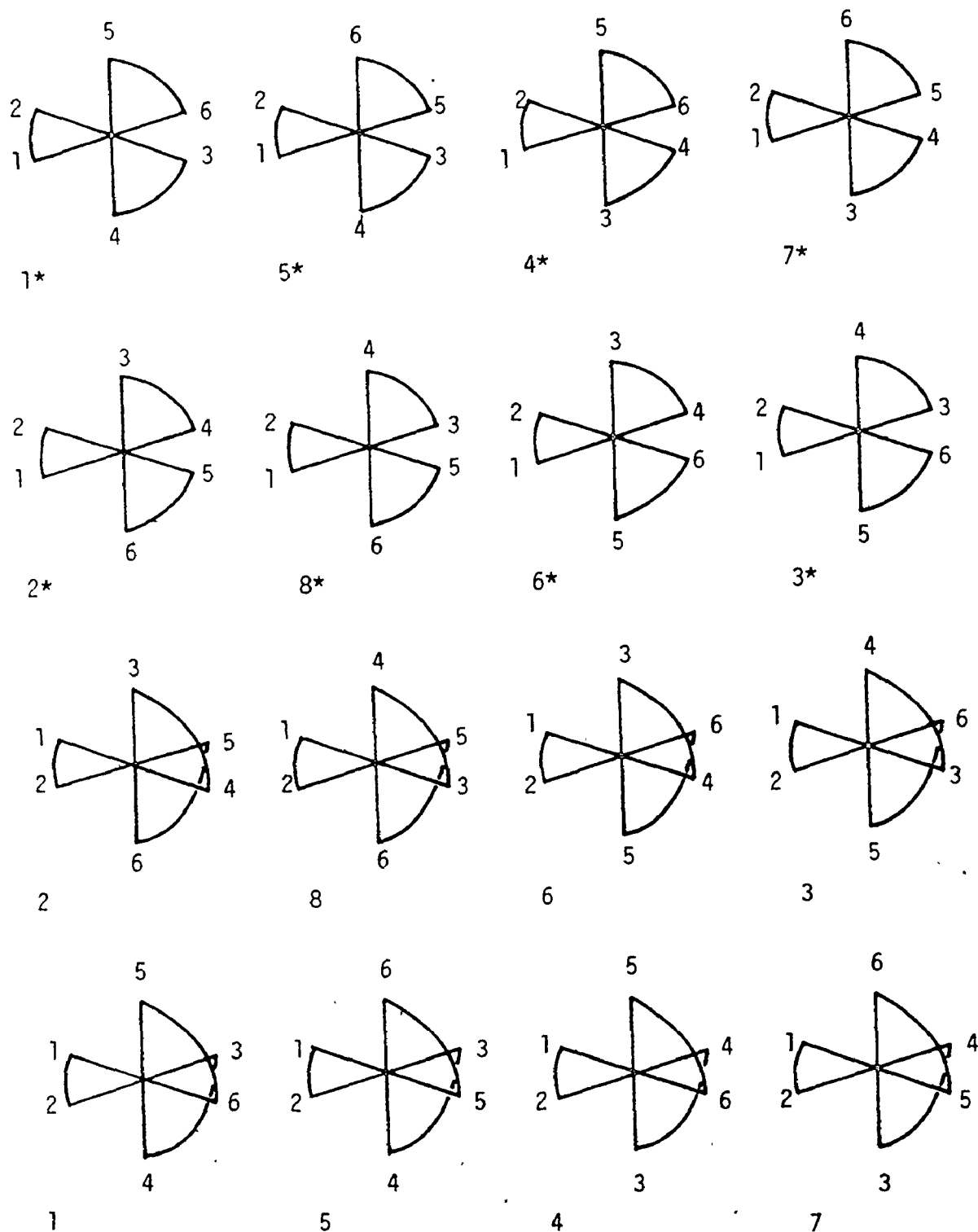


Figure 6-11 16 possible permutational isomers of a tris chelate complex (isomers numbered as in reference 138)



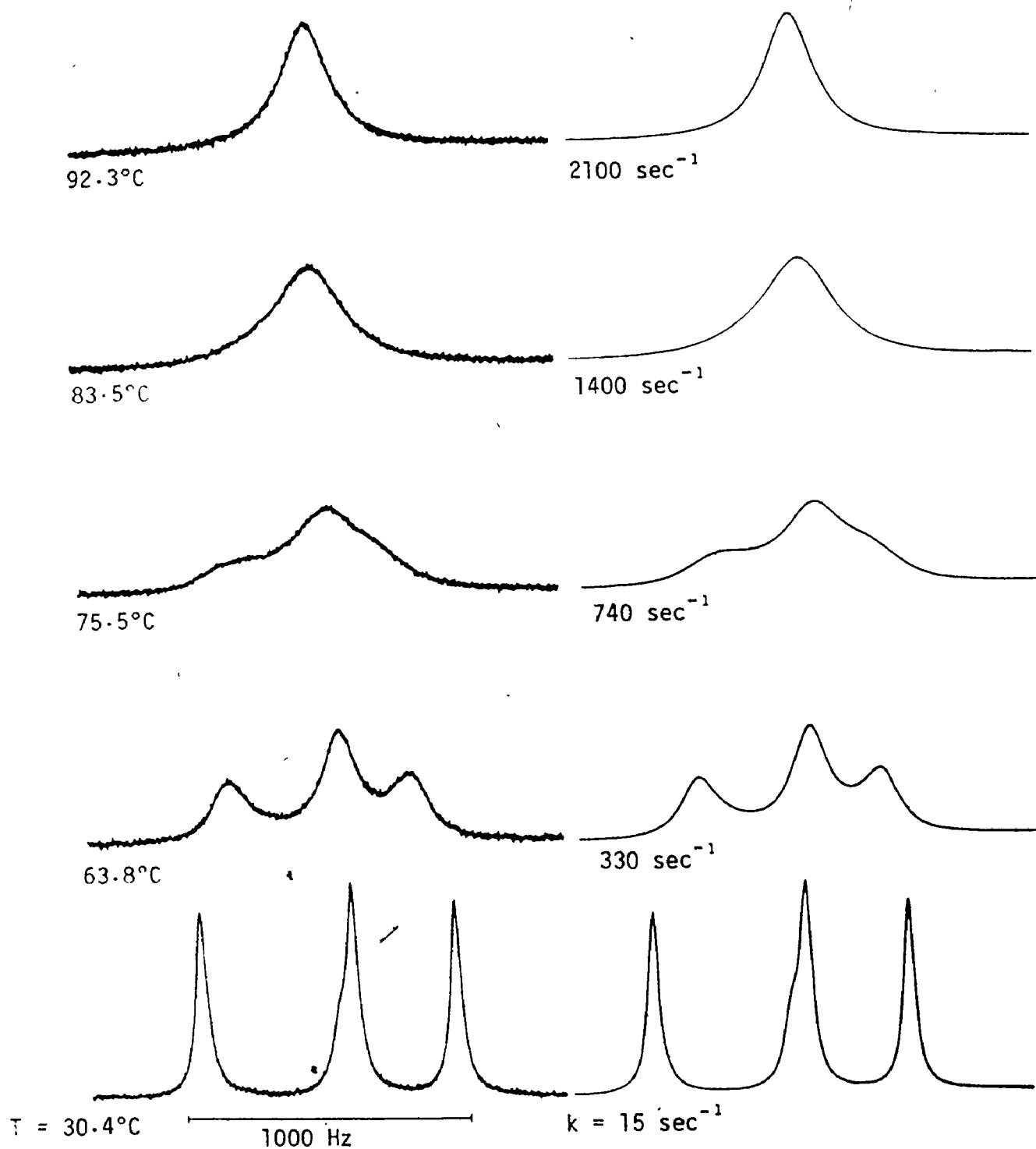


Figure 6-12. Comparison of experimental and simulated NMR spectra of  $V(tfac)_3$  at various temperatures.  $^{19}\text{F}$  at 58.3 MHz. in chlorobenzene. (equal lifetimes at all sites).

	1	2	3	4
1	—	.164	.418	.418
2	.333	—	.333	.333
3	.418	.164	—	.418
4	.418	.164	.418	—

The agreement between the experimental and simulated spectra is rather good, and it seems quite unlikely that the matrix elements determined by a fitting procedure would be substantially different from those already given.

Using this result, it is now worthwhile to consider a permutational analysis of the  $M(\mu\text{-chelate})$  system to determine which 'averaging set' and hence which mechanism(s) are compatible with the above result. The set of permutations and permutation inversions for an  $M(\mu\text{-chelate})$  system is given in table 6-3.

It is evident that processes which involve inversion cannot be distinguished from those involving retention in the case of  $V(\text{tfac})_3$ , as the sets of net site interchanges are identical for both permutation and permutation-inversion operations. The trivial cases of the identity and identity-inversion operations averaging sets  $A_1$  and  $A_5$ , can be dismissed immediately as neither results in any site interchange. Sets  $A_2$  and  $A_6$  can also be dismissed, as both give rise to a site interchange which involves only  $y$  and  $z$  of the trans complex, and do not

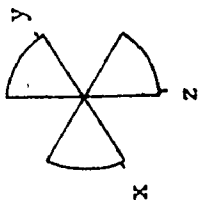
Table 6-3 Permutational Analysis of  $M(AB)_3$  and  $M(AA)_2(AB)$  complexes.  
 (Reproduced in part from reference 138)

Operation	Isomer	Permutation	Averaging Set
E	1	[135-462]	A <sub>1</sub> A <sub>2</sub>
(12)(34)(56)	2	[153-642]	
(12)	3	[164-532]	A <sub>3</sub>
(34)	4	[145-362]	
(56)	5	[136-452]	A <sub>4</sub>
(12)(34)	6	[163-542]	
(34)(56)	7	[146-352]	A <sub>5</sub> A <sub>6</sub>
(12)(56)	8	[154-632]	
E*	9	[153-264]	A <sub>7</sub>
(12)(34)(56)*	10	[135-246]	
(12)*	11	[146-235]	A <sub>8</sub>
(34)*	12	[154-263]	
(56)*	13	[163-254]	
(12)(34)*	14	[136-245]	
(34)(56)*	15	[164-253]	
(12)(56)*	16	[145-236]	

Averaging Set	Configurational change $V(tfac)_3$	Site interchange $V(tfac)_3$
A <sub>1</sub>	None	none
A <sub>2</sub>	None	(y z)
A <sub>3</sub>	cis → trans; trans → $\frac{1}{3}$ cis $\frac{2}{3}$ trans	(x y)(x z)
A <sub>4</sub>	cis → trans; trans → $\frac{1}{3}$ cis $\frac{2}{3}$ trans	(x y z)(x z y)
A <sub>5</sub>	$\Delta \neq \Lambda$	none
A <sub>6</sub>	$\Delta \neq \Lambda$	(y z)
A <sub>7</sub>	cis → trans; trans → $\frac{1}{3}$ cis $\frac{2}{3}$ trans; $\Delta \neq \Lambda$	(x y)(x z)
A <sub>8</sub>	cis → trans; trans → $\frac{1}{3}$ cis $\frac{2}{3}$ trans; $\Delta \neq \Lambda$	(x y z)(x z y)

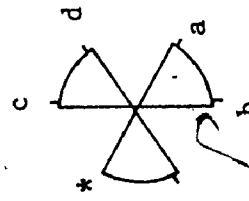
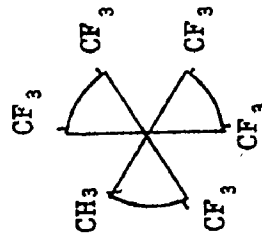
Table 6-3 continued



xyz environments as denoted in this diagram

Site interchange for  $V(\text{tfac})(\text{hfac})_2$

$A_1$	none
$A_2$	(ac)(bd)
$A_3$	(ad)(bc), (cd), (ab)
$A_4$	(adbc), (ab)(cd) (acbd)
$A_5$	none
$A_6$	(ac)(bd)
$A_7$	(ad)(bc), (cd), (ab)
$A_8$	(adbc), (ab)(cd), (acbd)



abcd environments as denoted in diagram

interconvert the cis and trans complex.

Sets  $A_3$  and  $A_7$  are rather more difficult to eliminate completely, as both provide for interconversion of cis and trans isomers and the exchange of all three trans sites. However, it is apparent that the lifetimes of the x, y and z sites of the trans complex cannot be equal, as there is no direct transfer of nuclei at site x to site z and vice versa.  $A_3$  and  $A_7$  each consist of a set of three permutations, but there is no guarantee that each of the three permutations occur with equal frequency. For the trans complex, one permutation results in the conversion of the trans complex to the cis complex. The probability of transfer of a nucleus from an x, y or z trans site to a cis site must be equal. The remaining two permutations cause the trans complex to be transformed into the trans complex with, in one case, the exchange of the x and y nuclei, and in the other, the x and z nuclei. At one extreme, if only one permutation is permitted to occur, then one resonance, either the z or the y will collapse more slowly than the others, as the nuclei will be in exchange only with the cis site. At the other extreme, if both permutations occur with the same frequency, then the x site will appear to have almost half the lifetime of the y and z sites. This condition would be met if there were no exchange with the cis site. This is probably not far from the case, as the cis resonance has approximately half the intensity of each of the trans resonances and furthermore, the cis site is in exchange with three trans resonances. Considering only the cis-trans reaction, the lifetime at the trans site would be approximately six times the lifetime at a

cis site. Thus, if the rate of transfer of nuclei from a trans site to a cis site were large, compared to transfer of nuclei from a trans site to another trans site, the collapse of the cis resonance would be very rapid compared to the collapse of the trans resonance. Although the cis resonance cannot be observed alone as in most cases, the cis resonance appears as a shoulder on the central trans resonance. It does not seem likely that the lifetime of the cis resonance could be very much different from the lifetime of the trans resonances without affecting the lineshape significantly. The exchange lifetimes of the upfield and downfield resonances of the trans complex are, within experimental error, equal. It is not possible to be as sure of the relative lifetime of the central trans resonance, because of the overlap with the cis resonance.

Unfortunately, we cannot be certain of the assignment of the x, y and z environments to the three trans resonances. There are, therefore, three possibilities to be considered:

$$\frac{1}{\tau_x} = \frac{1}{\tau_y} \quad (1) \quad , \quad \frac{1}{\tau_x} = \frac{1}{\tau_z} \quad (2) \quad \text{and} \quad \frac{1}{\tau_y} = \frac{1}{\tau_z} \quad (3)$$

where  $\tau$  represents the exchange lifetime of the site. If we label the probabilities of transfer of a nucleus from site x to site y, a; site x to z, b; and site x, y and z to cis as c; then, we have

$$\frac{1}{\tau_x} = (a + b + c)r$$

$$\frac{1}{\tau_y} = (a + c)r$$

$$\frac{1}{\tau_z} = (b + c)r$$

where  $r$  is the overall rate constant. For condition (1) to be met,  $b$  must = 0 and similarly for condition (2),  $a = 0$ ; for condition (3),  $a = b$ . This reduces to two possibilities: cases (1) and (2) correspond to the upfield and downfield resonances being in direct exchange with each other, and not with the central resonance, while case (3) corresponds to both the upfield and downfield resonances being in exchange with the central resonance. Simulated spectra representing these two possibilities are reproduced in Fig. 6-13, compared with simulated spectra assuming equal lifetimes at all sites, and experimental spectra. All the simulated spectra have been calculated assuming the same chemical shift and linewidth data.

Averaging sets  $A_3$  and  $A_7$  do not appear to agree with the experimental data. Thus, only sets  $A_4$  and  $A_8$  remain. Both sets consist of 3 permutation operations. Applied to the cis isomer, all result in transformation of the cis isomer into the trans isomer. Applied to the trans isomer, one operation results in transformation of trans to cis and the other two retain the trans configuration, but result in the

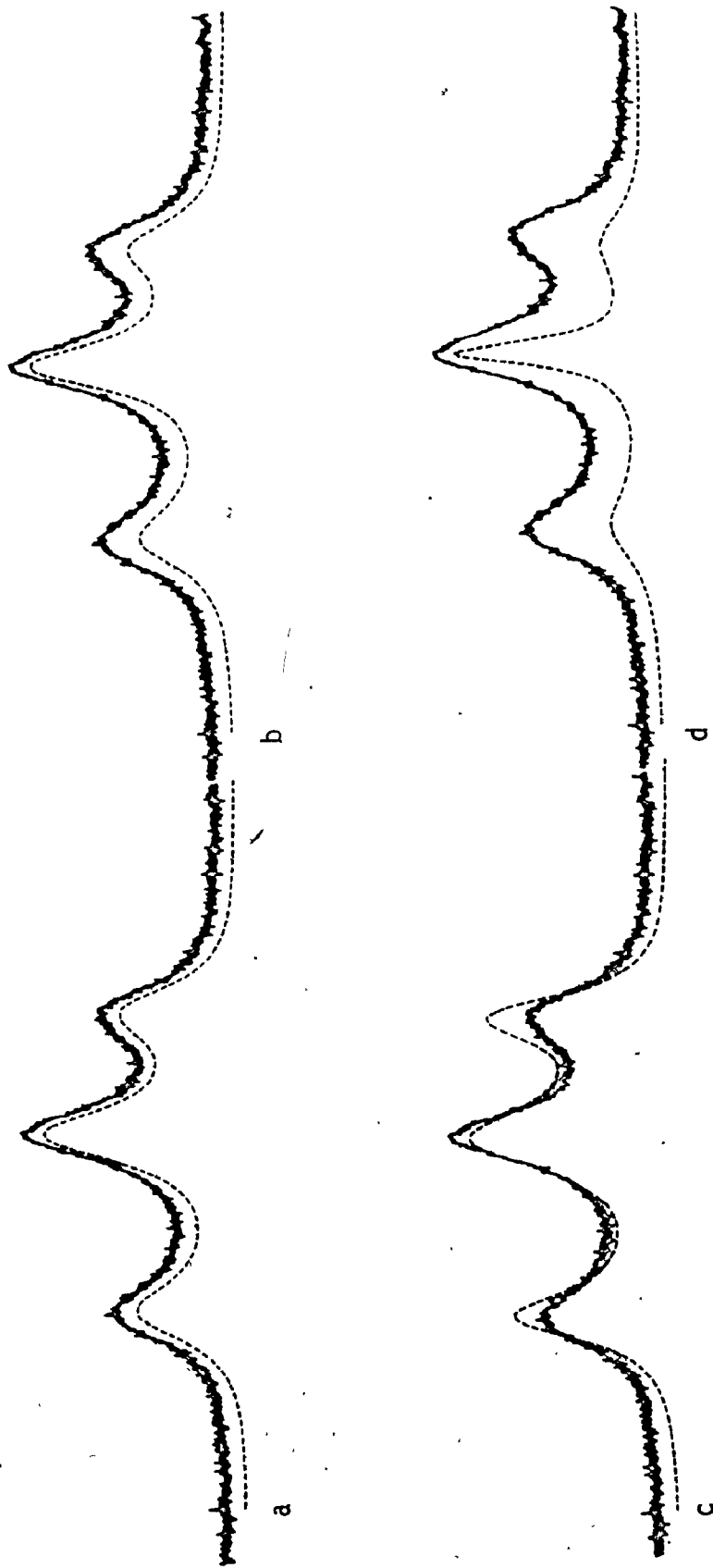
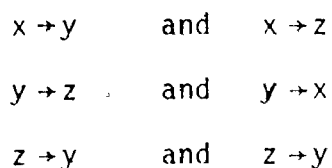


Figure 6-13. Comparison of experimental and simulated spectra of  $V(\text{tfac})_3$  at an intermediate rate of exchange. a, equal lifetimes at all sites,  $(RC_3(i))$  or SP primary and secondary or TBP with pseudorotation); b, SP primary assuming all bonds rupture and reform with equal probability; c and d, two cases for TBP mechanisms with lifetimes at downfield and upfield sites equal.



net site 'interchanges'



It should be noted that the one operation is the inverse of the other, and therefore, by the law of microscopic reversibility, one operation is as probable as the other. In the permutation group, however, each element is its own inverse. This apparent paradox arises, because in the permutation group, each site is given an arbitrary label which is invariant under a permutation operation, whereas the x, y and z labels refer to a specific environment in the complex which may change as the sites are permuted. The transfer of a nucleus at any site in the trans complex to the other two sites is therefore equally probable. Averaging sets  $A_4$  and  $A_8$  seem to best fit the data for the  $V(\text{tfac})_3$  complex.

On the basis of this argument, some mechanisms can be ruled out as the sole reaction pathway. The following correspondences between the various physical mechanisms discussed previously and the averaging sets can be made<sup>138</sup>.

$A_6$	-	$pC_3$ or $rC_3$ twist
$A_8$	-	$iC_3$ twists
$A_7$	-	TBP axial
$A_3$	-	TBP equatorial
$A_3 + 3A_6 + A_8$	-	SP apical

The  $pC_3$  or  $rC_3$  twists and both equatorial and axial trigonal bipyramidal intermediates can be excluded as the sole reaction pathways. The  $iC_3$  twists which correspond to the  $A_2$  averaging set are compatible with experimental results.

Of the commonly suggested mechanisms, only those involving SP apical intermediates remain. Holm has pointed out that rearrangement via this state is complicated by the possibility of two microscopically reversible pathways which have been designated as primary and secondary, (Fig. 6-3 a,b). Holm has argued that rearrangements involving SP apical states will most likely involve the primary process alone or a 1:1 mixture of primary and secondary processes<sup>110</sup>. If only the primary process is considered, there are a total of 24 individual pathways which may be considered. There are 6 bonds which may be broken leading to the SP apical state followed by attack of the free end of dangling ligand at any of the four basal corners of the SP. Table 6-4 shows the permutations resulting from each of the 24 operations. Of those, six correspond to the identity operation and therefore, contribute no observable effect. It is evident from the table that breaking of either bond of the same ligand leads to identical permutations. There is no guarantee, however, that all of these permutations occur with equal probability, or indeed that the relative probabilities will remain constant with changing temperature. In the lineshape analysis of  $Al(pmhd)_3$  and  $Ga(pmhd)_3$ , Hutcherson et al.<sup>140</sup> have made use of the

Table 6-4

Permutations of octahedral tris chelate complex obtained via a SP primary mechanism.

Bond Broken	Permutations			
1	1	7*	3	2*
2	1	7*	3	2*
3	1	8*	4	2*
4	1	8*	4	2*
5	1	6*	5	2*
6	1	6*	5	2*

assumption that all non-equivalent bonds in the cis and trans complex rupture with equal probability, and that each of the four corners of the basal plane are attacked by the dangling ligand with equal probability. If these assumptions are valid, the relative probability of transfer of a nucleus at each of the trans sites to any of the other trans sites can be expressed by the following matrix

$$\begin{array}{ccc} & x & y & z \\ x & - & 1 & 1 \\ y & 1 & - & 2 \\ z & 1 & 2 & - \end{array}$$

Thus, the y and z environments would have equal lifetimes, and the resonances would be expected to collapse slightly faster than the x resonance. The assumptions may not be correct, and it is therefore not possible to exclude this mechanism.

Inspection of table VII of reference 140 will show that if the same assumptions are made for the SP primary-secondary mechanism as for the SP primary mechanism, then the relative probabilities of transfer from any trans environment to either of the other trans environments are equal. This mechanism could, therefore, be compatible with the experimental results.

Another mechanism which has received little attention in the

literature is the pseudorotation of the TBP intermediates. Only the so-called 'Berry' pseudorotations will be considered here (Fig. 6-4). The TBP axial intermediate may rearrange in two ways to form a TBP equatorial intermediate. In the TBP intermediate with five monodentate ligands, the TBP structure may rearrange in three ways, i.e., any pair of three equatorial ligands may become axial. However, in a TBP axial intermediate, one pair of equatorial positions is spanned by a chelate group. The molecule cannot rearrange to have these positions exchanged with the axial positions, as the chelate cannot span the two axial sites. For the TBP equatorial intermediate, there is no such restriction and pseudorotations around all the pseudo  $C_2$  axes are possible. Fig. 6-14 illustrates the sixteen possible isomers of a TBP structure which can be obtained by rupture of a particular bond in the octahedral complex. Fig. 6-15 illustrates the correlation diagram obtained by consideration of all the Berry pseudorotations for these intermediates. It is evident from the diagram that any TBP isomer can be obtained from any other in a maximum number of five operations. Table 6-5 shows the correlation between the TBP isomers and the octahedral isomers formed by allowing the TBP intermediates to form products in the normal fashion. If it is assumed that a) the TBP intermediate is sufficiently long-lived for complete equilibration of all the isomers; b) each isomer is equally stable; c) all the isomers proceed to both possible products at the same frequency, then all of the octahedral isomers occur with equal frequency. In other words, each of the sixteen possible permutations is equally probable. Since the labelling of the isomers is arbitrary, this result is true for rupture of any of the six bonds of

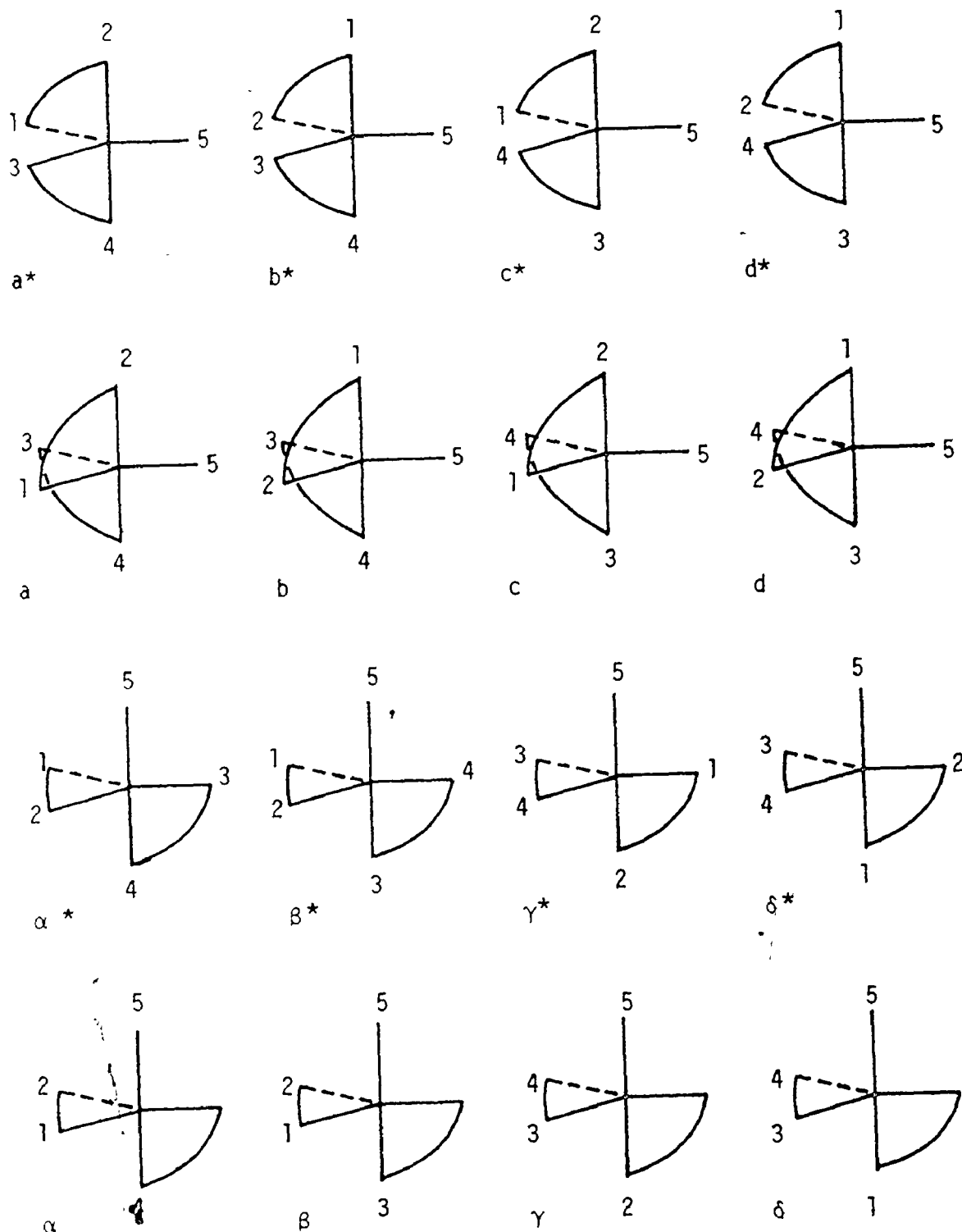


Figure 6-14 16 possible isomers of a TBP structure derived from a tris-chelate by rupture of bond 6.

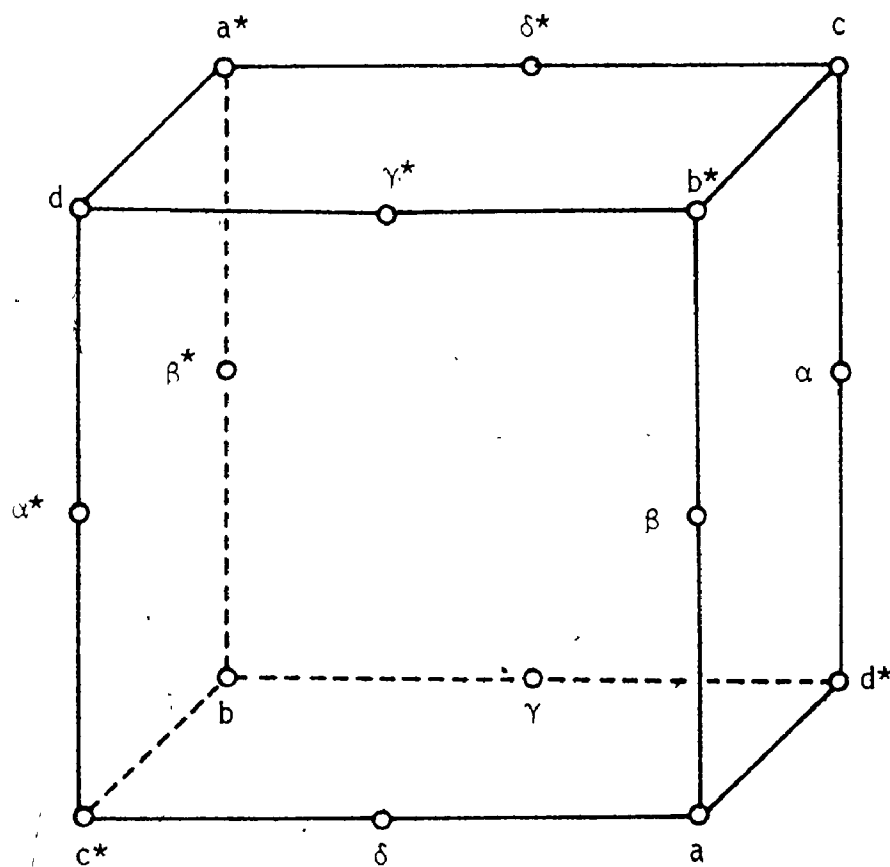


Figure 6-15. Correlation diagram connecting 16 isomers of Figure 6-14 by a Berry pseudorotation mechanism

Table 6-5

Correlation of octahedral isomers and TBP intermediates

## Equatorial intermediates

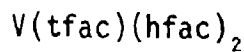
1	-	c	-	5		1*	-	c*	-	5*
2	-	b	-	6		2*	-	b*	-	6*
3	-	d	-	8		3*	-	d*	-	8*
4	-	a	-	7		4*	-	a*	-	7*

## Axial Intermediates

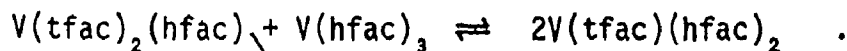
1	-	$\alpha$	-	3*
2	-	$\gamma$	-	8*
3	-	$\alpha^*$	-	1*
4	-	$\beta$	-	6*
5	-	$\delta^*$	-	7*
6	-	$\beta^*$	-	4*
7	-	$\delta$	-	5*
8	-	$\gamma^*$	-	2*



the octahedral chelate. Inspection of table 6-3 shows that if every permutation is equally possible, the probabilities of exchange of nuclei at any trans site to any other trans site are equal. Rearrangement via pseudorotation of the TBP intermediates can be considered a viable mechanism. A point worth mentioning is that pseudorotation of a TBP intermediate causes it to pass through a SP state. The interconversion of an axial and equatorial TBP state occurs via a SP basal state, while the interconversion of a TBP equatorial state with another TBP equatorial state occurs via a SP apical state. The Berry pseudorotation mechanism does not exchange TBP axial states directly. It is interesting to note that the products obtained by allowing the two TBP equatorial states derived directly from the SP apical state to go to products in the normal way, are the same as the products obtained by the SP primary mechanism, and that the products obtained by allowing the TBP equatorial states to pseudorotate to the next four axial TBP states, and then to proceed to products normally, gives the same isomers as the SP apical primary-secondary mechanism.



The complex  $V(\text{tfac})(\text{hfac})_2$  has no elements of symmetry. Consequently, one might expect to see five trifluoromethyl resonances. The complex is in equilibrium according to the equation



The resonances belonging to these complexes have been previously assigned by  $\text{---}$  and Chua<sup>6</sup>. In fact, only four separate resonances for  $V(\text{tfac})(\text{hfac})_2$

are observed, as the upfield pair are coincident. The presence of additional lines in the spectrum of  $V(\text{tfac})(\text{hfac})_2$  due to the equilibrium between  $V(\text{tfac})(\text{hfac})_2$ ,  $V(\text{hfac})_3$  and  $V(\text{tfac})_2(\text{hfac})$ , makes a precise fitting of the lineshape virtually impossible. The complex  $V(\text{tfac})_2(\text{hfac})$  has three isomers which give rise to a total of eight  $\text{CF}_3$  resonances. The increase in the number of parameters needed to include  $V(\text{tfac})_2(\text{hfac})$  in the lineshape calculation would have made the process much more time consuming, without necessarily making it much more accurate. It was, therefore, decided to use samples in which the concentrations of  $V(\text{tfac})_3$  and  $V(\text{hfac})_3$  were adjusted so that the equilibrium would tend towards  $V(\text{hfac})_3$ , and minimize the concentration of  $V(\text{tfac})_2(\text{hfac})$ . The single  $\text{CF}_3$  resonance due to  $V(\text{hfac})_3$  is readily included in the calculation, while the resonances due to  $V(\text{tfac})(\text{hfac})_2$  are simply ignored. The result obtained should therefore be regarded as qualitative rather than strictly quantitative.

For the purpose of the calculation, the elements of the site interchange matrix were assumed to be equal and sum to a total of unity for any row. A comparison of the simulated spectra and the calculated spectra for  $V(\text{tfac})(\text{hfac})_2$  in  $\text{CDCl}_3$  is illustrated in Fig. 6-16 :

One of the resonances attributed to  $V(\text{tfac})(\text{hfac})_2$  does not exchange with the others. This is due to the  $\text{CF}_3$  group attached to the trifluoroacetylacetonate ligand which preserves its uniqueness through any isomerization process. This resonance was incorrectly assigned by

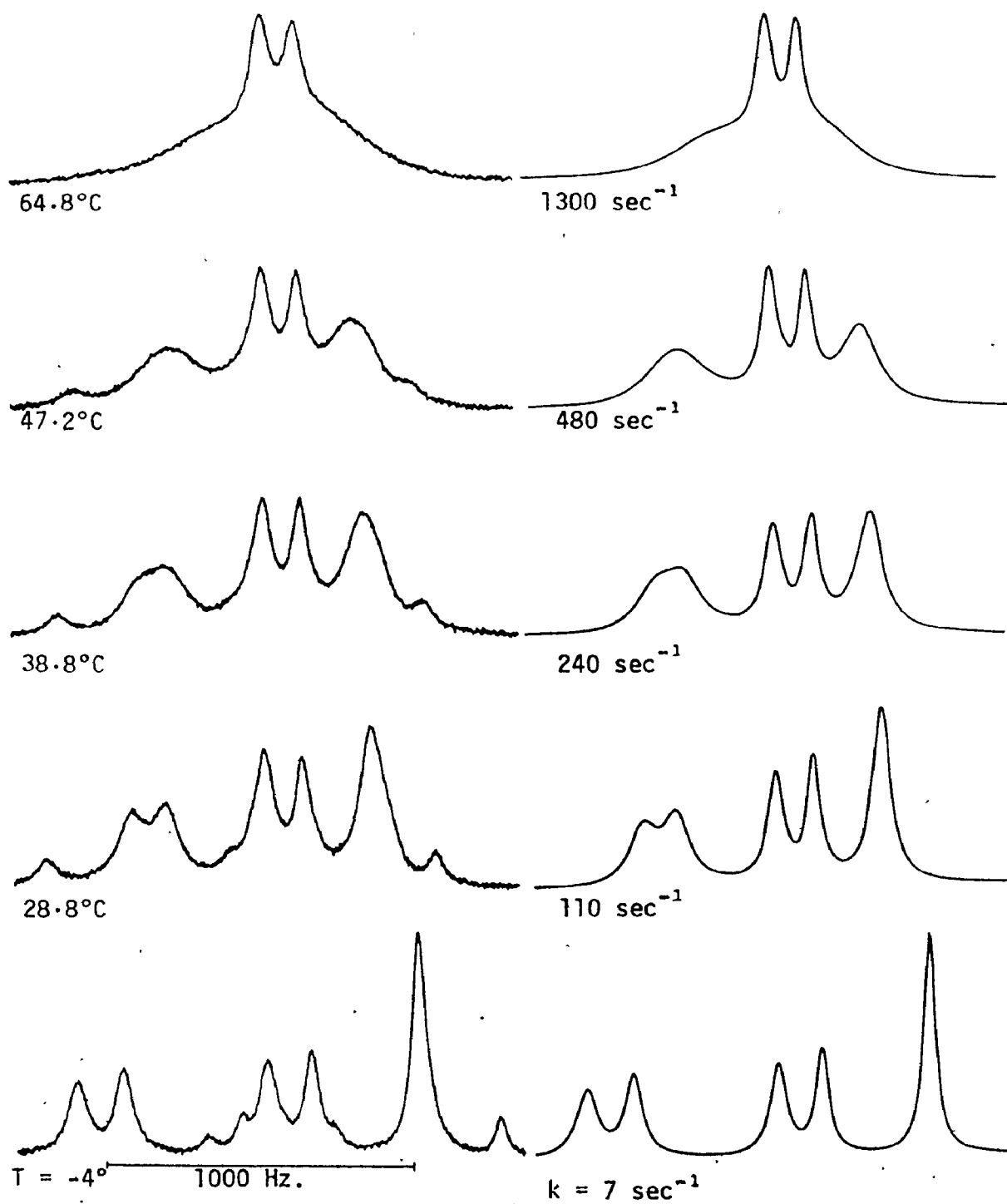


Figure 6-16. Comparison of experimental and simulated NMR spectra of  $V(hfac)_2(tfac)$  at various temperatures.  $^{19}F$  58.3 MHz. in  $CDCl_3$  (equal lifetimes at all sites).

Eaton and Chua<sup>6</sup> as one of the upfield pair of lines. At least one other resonance in the spectrum of  $V(\text{tfac})(\text{hfac})_2$  must have been incorrectly assigned.

Unfortunately, the spectra of  $V(\text{tfac})(\text{hfac})_2$  are able to provide less information on the mechanisms which are compatible with experimental results than  $V(\text{tfac})_3$ . The correspondence between the averaging sets and the site interchanges for  $V(\text{tfac})(\text{hfac})_2$  is given in table 6-3. As for  $V(\text{tfac})_3$ , the trivial cases of averaging sets  $A_1$  and  $A_5$  which do not result in site interchange, can also be excluded for  $V(\text{tfac})(\text{hfac})_2$ .

Averaging sets  $A_2$  and  $A_6$  predict that the four resonances which are capable of exchange will collapse to a pair of resonances. Unfortunately, it is possible that the two pairs may be chosen in such a way that the average chemical shift of each pair is very similar and the four resonances appear to collapse to a single resonance.

Provided each permutation which contributes to the averaging sets  $A_3$  and  $A_7$  is equally probable, each site will exchange with two others, e.g., site a exchanges directly with sites b and d, but not with c. This case would be very difficult to distinguish by lineshape analysis from the case where any site is in exchange with any other site. Only if there were a considerable difference in the relative probabilities of one of the permutations contributing to the averaging set, would a

significant difference in the lineshape of the rearranging complex be expected. This is a situation in which the SST technique could have been used to advantage, since the case where a single site is in direct exchange with two other sites, rather than three other sites, would have been readily distinguishable.

Sets  $A_4$  and  $A_8$  predict each site to be in exchange with each of the other three sites, provided the relative probabilities of each of the permutations are equal. If only permutation 7 occurs, the case would be indistinguishable from averaging sets  $A_2$  and  $A_6$ . Permutation 8 is clearly the inverse of permutation 6, and therefore, if one occurs, the other must occur with equal frequency.

Since none of the non-trivial averaging sets can be rigorously dismissed, it follows that none of the corresponding mechanisms can be excluded. Nor can the mechanisms, such as those which involve SP apical states, which correspond to a combination of averaging sets be excluded either. Thus, it is concluded that the experimental results from lineshape analysis do not favour any particular mechanism of rearrangement.

#### $V(acac)_2(hfac)$ and $V(hfac)_2(acac)$

The complexes  $V(acac)_2(hfac)$  and  $V(hfac)_2(acac)$  are similar in that  $V(acac)_2(hfac)$  has two pairs of magnetically non-equivalent  $CH_3$  groups and  $V(hfac)_2(acac)$  has two pairs of magnetically non-

equivalent  $CF_3$  groups. Both are observed to exchange on the NMR time scale. The mechanistic information provided, however, is minimal, since every non-trivial permutation except one of  $A_5$  results in site exchange.

#### Activation Parameters for Rearrangement of Vanadium $\beta$ -diketonates

Values of a number of activation parameters for various  $\beta$ -diketonate vanadium complexes are presented in table 6-2. The values of  $\Delta H^\ddagger$  and  $\Delta S^\ddagger$  are calculated from  $A$  and  $E_a$  using the relationships  $\Delta H^\ddagger = E_a - RT$  and  $\Delta S^\ddagger = (\ln A - \ln \frac{kT}{h} - 1)R$ . The values obtained for  $V(\text{tfac})_3$  are probably the most accurate, since the chemical shifts involved are large, and there is an absence of spurious resonances. The shifts of  $V(\text{tfac})(\text{hfac})_2$  are large, but a comparison of simulated and experimental spectra is hindered by the presence of the resonances of  $V(\text{tfac})_2(\text{hfac})$ . It is difficult to say how much difference this might make to the accuracy; however, the precision according to a least squares treatment of the Arrhenius plot is satisfactory. (Table 6-2). The activation parameters estimated for the symmetric chelate complexes  $V(\text{hfac})_2(\text{acac})$  and  $V(\text{dibm})_3$  are almost certainly the least accurate, as the estimated activation energies are highly sensitive to a choice of linewidth. The accuracy of the  $V(\text{acac})_2(\text{hfac})$  activation parameters is rendered highly suspect by the presence of a  $\gamma C-H$  resonance of the complex which is almost coincident with one of the  $CH_3$  resonances and are therefore not quoted.

Unfortunately, a comparison of activation parameters for the

different complexes does not allow us to distinguish between bond breaking and twisting modes of rearrangement, as theory suggest that replacement of  $\text{CH}_3$  groups by  $\text{CF}_3$  groups will lead to a decrease in activation energy in both cases. The electron withdrawing tendency of the  $\text{CF}_3$  groups would be expected to lead to a decrease in the strength of the M-O bond, and therefore, lead to a reduced activation energy for bond rupture. However, the electron withdrawing effect of the  $\text{CF}_3$  groups would also be expected to reduce the negative charge on the oxygen atoms, and thus reduce the non-bonded ligand interactions in the trigonal or rhombic twist mechanisms. It might be argued that a bond rupture mechanism might be more sensitive to the relative displacement of  $\text{CF}_3$  groups than a twist mechanism. Since the experimental results do not indicate preferential rupture of any bonds, it is difficult to pursue this line of reasoning.

The twist mechanism was originally proposed by Ray and Dutt<sup>113</sup> to account for the very small pre-exponential factor they observed for the racemization of tris(biguanidine)Co(III). However, Bickley and Serpone<sup>141</sup> have pointed out that  $\Delta S^\ddagger$  values for rearrangements which are thought to occur via a bond rupture process fall in the range -24 to +2 eu, whereas  $\Delta S^\ddagger$  values for rearrangements thought to occur via a twist mechanism fall within -23 to +10 eu.

The isokinetic relationship<sup>142</sup> has been taken by many chemists to imply a constant mechanism of reaction for a series of related compounds for which the relationship exists. A plot of  $\Delta H^\ddagger$  versus  $\Delta S^\ddagger$

for the rates of rearrangement of some vanadium  $\beta$ -diketonate complexes, measured in the present work, is presented in Fig. 6-17, suggesting an isokinetic relationship. There is evidently a strong correlation between  $\Delta H^\ddagger$  and  $\Delta S^\ddagger$ . This, however, cannot be taken as good evidence of an isokinetic relationship, as the temperature defined by the slope of the line is  $87^\circ\text{C}$ , which is not much different from the mean experimental temperature. The reason for this is that the errors in  $\Delta H^\ddagger$  and  $\Delta S^\ddagger$  are highly correlated and lie within an ellipse whose major axis is inclined to the  $\Delta S^\ddagger$  axis at a slope equal to the mean experimental temperature. Unless the values of  $\Delta H^\ddagger$  and  $\Delta S^\ddagger$  differ by more than experimental error, the existence of an isokinetic relationship is not established.

The  $\sigma$  values estimated from least squares treatment of the Arrhenius plots suggest the differences in  $\Delta H^\ddagger$  and  $\Delta S^\ddagger$  are indeed significant. It is rather more difficult to exclude systematic errors in  $\Delta H^\ddagger$  and  $\Delta S^\ddagger$ . Although one of the major errors in this type of work is the measurement of temperature, it is unlikely that this source of error will cause discrepancies between different estimations of  $\Delta H^\ddagger$  and  $\Delta S^\ddagger$  in the present work, as all temperatures were measured with the same apparatus in exactly the same fashion. The principal source of systematic error in this case is likely to be the choice of linewidth parameters for the two site exchange cases  $\text{V}(\text{dibm})_3$  and  $\text{V}(\text{hfac})_2(\text{acac})$ , particularly  $\text{V}(\text{hfac})_2(\text{acac})$ , where the ratio of linewidth to line separation is largest.



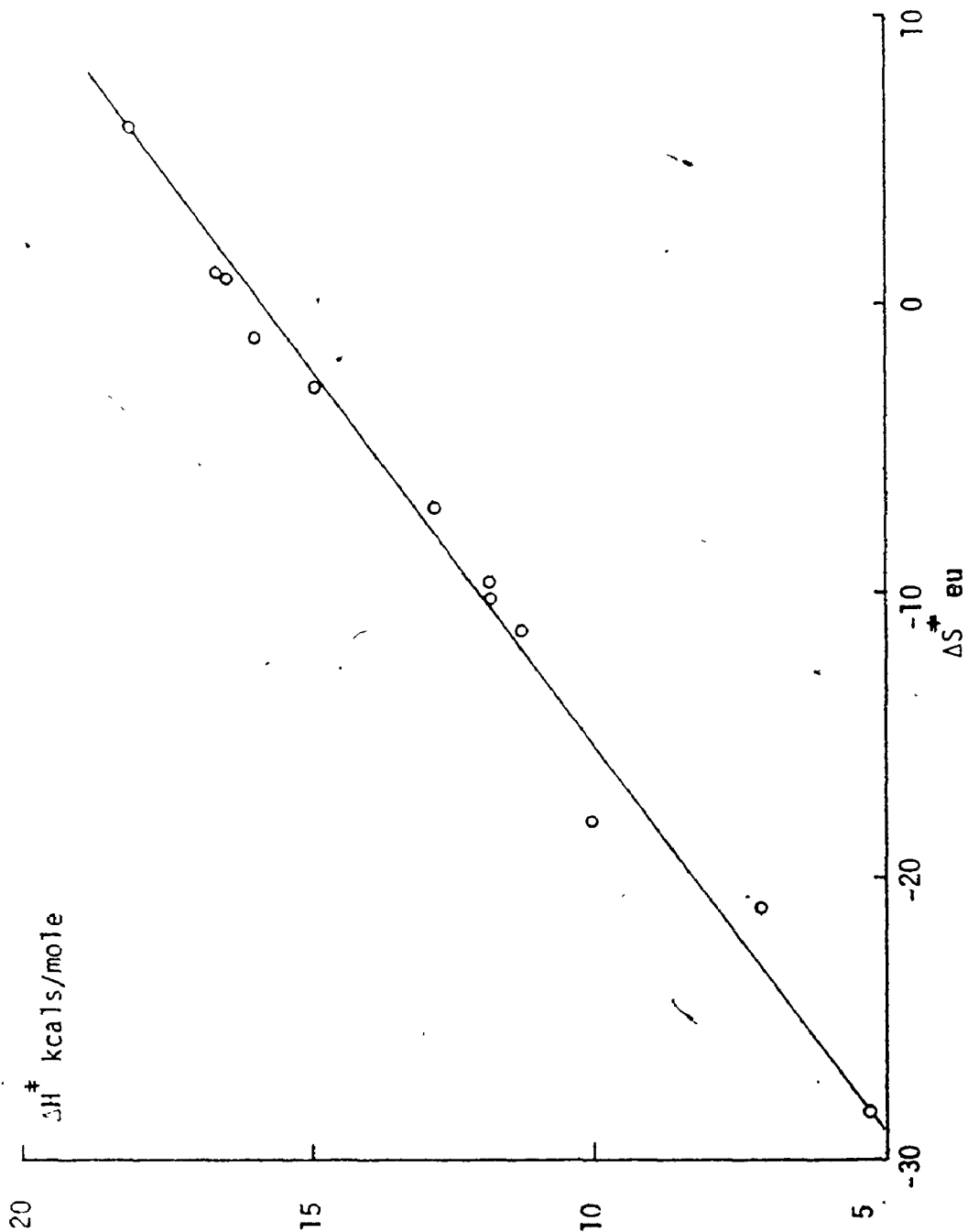


Figure 6-17 Linear relationship between  $\Delta H^\ddagger$  and  $\Delta S^\ddagger$  for rearrangement of vanadium  $\beta$ -diketonate complexes.

If the isokinetic relationship can be regarded as having been established for the various vanadium  $\beta$ -diketonate complexes presented in this work, with the consequent inference that the mechanism of rearrangement is constant for all the complexes examined, then it follows that the observation of a highly negative activation entropy is a rather unreliable criterion on which to base a mechanistic conclusion.

### Solvent Effects

Temperature dependent measurements of rate for two of the vanadium  $\beta$ -diketonate complexes,  $V(\text{tfac})_3$  and  $V(\text{hfac})_2(\text{acac})$  were run in a variety of solvents to determine if there were any correlations between solvent and the activation parameters. Although comparisons of rate between different complexes may be suspect for reasons already given, comparison of rate for the same complex in different solvents should involve little error other than the normal limits imposed by the precision of the measurements.

The variation of activation energy for  $V(\text{tfac})_3$  in the various solvents is barely significant, and apart from acetone, the activation enthalpies do not parallel the dielectric constants of the solvents. For  $V(\text{hfac})_2(\text{acac})$  however, the rates of rearrangement in acetone and acetonitrile are an order of magnitude faster than for the other solvents at 25°C. Fig. 6-18 compares spectra of  $V(\text{hfac})_2(\text{acac})$  in various solvents. There is no doubt whatever of the very large difference

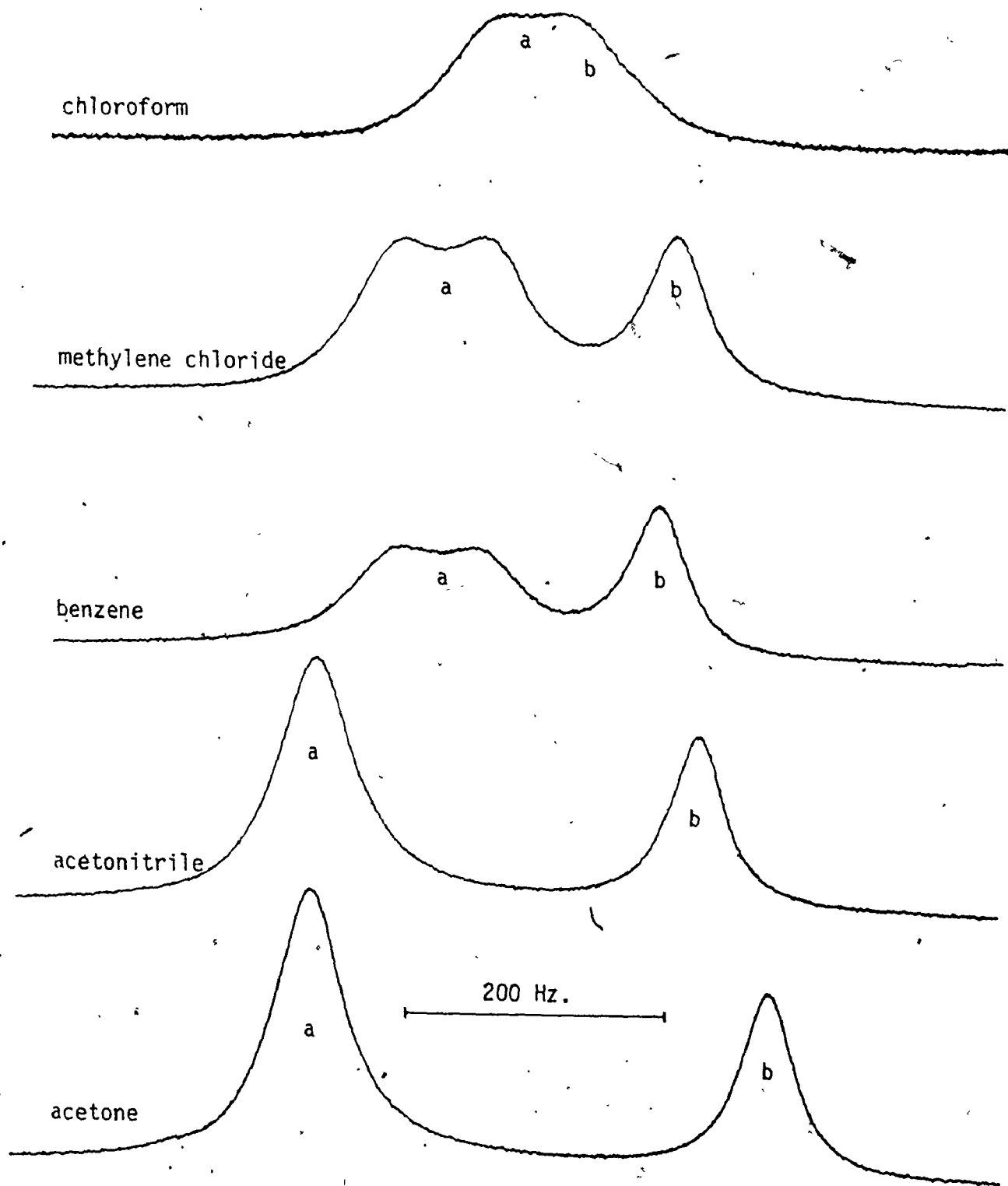


Figure 6-18.  $^{19}\text{F}$  NMR spectra of  $\text{V}(\text{hfac})_2(\text{acac})$  in various solvents at  $29^\circ\text{C}$ ; a,  $\text{V}(\text{hfac})_2(\text{acac})$ ; b,  $\text{V}(\text{acac})_2(\text{hfac})$ .

in rate at this temperature, as the spectrum of  $V(\text{hfac})_2(\text{acac})$  in acetone and acetonitrile is approaching the fast motion limit, while coalescence has not been reached in the other solvents.

The difference between the estimated activation enthalpy in acetone and in chloroform is approximately 4.4 kcal. Using the Kirkwood equation:

$$E = \frac{-\mu^2}{r^3} \frac{\epsilon-1}{2\epsilon+1}$$

which represents the energy of interaction of a point dipole  $\mu$  inside a sphere of radius  $r$  surrounded by a continuous medium of dielectric constant  $\epsilon$ , it is possible to estimate very approximately the charge separation required in the transition state to bring about a reduction in activation energy of 4.4 kcal. on going from  $\text{CDCl}_3$  to acetone. The molecular volume of  $V(\text{acac})_3$  is  $433 \text{ \AA}^3$ <sup>136</sup>. Assuming the complex to be spherical,  $r = 4.7 \text{ \AA}$ . A value of one electronic charge separated by a distance of  $3.3 \text{ \AA}$  is required to bring about the reduction in activation energy. This value is almost certainly larger than it should be, as the model assumes a point dipole at the centre of a sphere. It might be expected that a dangling ligand would allow very much closer approach of the solvent than  $4.7 \text{ \AA}$ , and that approximation of the dipole to a point dipole is unlikely to be valid. Both of these factors will tend to reduce the calculated energy relative to the actual energy of interaction. Thus, the dipole moment required in the transition state, to cause a solvent effect of the observed magnitude, is not unreasonably large for a bond rupture mechanism.

Fay and Piper<sup>101</sup> showed that the free energy of rearrangement of  $\text{Al}(\text{tfac})_3$  decreased with increasing dielectric constant of the solvent, and argued that the effect was due to a greater charge separation and greater solvation in the transition state. They also pointed out that the expected dipole moment of the rhombic twist intermediates are less than that of the cis isomer and comparable to the trans isomer. Consequently, very little change in solvation would be expected for a twist mechanism. The magnitudes of the solvent effect observed by Fay and Piper for  $\text{Al}(\text{tfac})_3$  are quite similar to the magnitudes of the solvent effect observed for  $\text{V}(\text{tfac})_3$  in the present work. It is interesting to note that the highest free energy of activation in both cases is observed for chloroform. This would not be expected if only solvent interaction due to charge separation were taken into account. It is tempting to speculate that a specific solvent interaction is responsible. Irving<sup>143</sup> has measured the enthalpies of solvation of a number of  $\text{M}(\text{acac})_3$  complexes in acetone, benzene and chloroform. The enthalpies for the different complexes are remarkably constant for a single solvent and quite similar in benzene and acetone, there being less than 1 kcal.<sup>2</sup> difference. The average enthalpy of solvation in chloroform is ~6 kcal./mole greater than in benzene and ~7 kcal./mole greater than acetone.

Steinbach et al.<sup>144</sup> have isolated solid compounds  $\text{M}(\text{acac})_3(\text{CHCl}_3)_2$  ( $\text{M} = \text{Al}, \text{Cr}, \text{Fe}$ ) and from a preliminary X-ray analysis, suggested that the two chloroform molecules are aligned along the 3 fold axis of the complex with their hydrogen atoms directed at the chelating oxygens.

It is possible that the rather higher energy of activation in chloroform is due to the partial dissociation of a second sphere complex of this type.

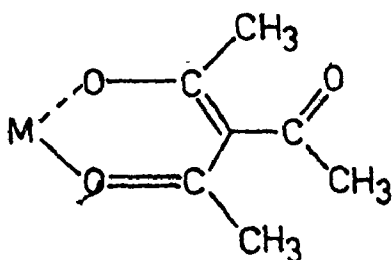
It is possible that the decrease in activation energy is due to an effect other than solvation of a charge separation. Not only do acetone and acetonitrile have the highest dielectric constants of solvents used, they are also the best ligands. A molecule of acetone or acetonitrile might be able to stabilize the transition state by coordinating to the site vacated by the dangling ligand. Although the molecule of solvent would have to be lost before rearrangement could take place, this process would allow the free end of the dangling ligand to become well-separated from the original site of attachment, and thus allow plenty of time for rearrangement of the five coordinate complex before coordination of the free end of the dangling ligand occurs.

The difference between the solvent effects for  $V(\text{tfac})_3$  and  $V(\text{hfac})_2(\text{acac})$  is rather large. It is not evident why there should be such a difference. If bond rupture of an M-O bond bearing a  $\text{CH}_3$  group occurred in  $V(\text{tfac})_3$ , and of a M-O bond bearing a  $\text{CF}_3$  group occurred in  $V(\text{hfac})_2(\text{acac})$ , the difference might be explicable due to the partial negative charge on the  $\text{CF}_3$  group, although it is difficult to see why the M-O bond bearing a  $\text{CH}_3$  group would rupture rather than that bearing a  $\text{CF}_3$  group. Although the precise nature of the solvent effect is not apparent, it seems to strongly support the hypothesis of a bond rupture

rather than a twist mechanism of rearrangement.

### Linkage Isomerization

The ligand triacetylacetonate has two of its three carbonyl groups bonded to a central metal ion in the fashion of a normal  $\beta$ -diketonate illustrated below.



The methyl groups on the carbonyl bonded to the metal and on the acetyl group, are magnetically non-equivalent. The exchange of these two kinds of groups can only occur if M-O bond rupture occurs, with subsequent rotation of the ligand, to allow the interchange of the carbonyl groups. This process is referred to as 'linkage isomerization'. The use of this ligand affords a means of detecting a bond rupture process.

### V(triac)<sub>2</sub>(acac)/V(triac)<sub>3</sub>

In an attempt to establish the existence of a bond rupture process for vanadium  $\beta$ -diketonates, the temperature dependence of the <sup>1</sup>H-NMR spectra of the complexes V(triac)<sub>2</sub>(acac) and V(triac)<sub>3</sub> was examined. Unfortunately, the complexes were not obtained pure, as under the conditions of the synthesis reaction, some of the triacetylacetonate ligand decomposed to yield acetylacetone. Although the reaction conditions were found which minimized this decomposition, it was not

possible to eliminate it altogether. Column chromatography failed to resolve the complexes because of their very rapid oxidation on the column. For the purposes of the present experiment, it was not essential to obtain the pure complexes, as the spectra of the complexes were sufficiently resolved. Fig. 6-19 illustrates the  $^1\text{H}$  NMR spectrum of a mixture of  $\text{V}(\text{triac})_2(\text{acac})$  and  $\text{V}(\text{triac})_3$ . The assignments of the methyl groups can be made on the basis of intensity.  $\text{V}(\text{triac})_3$  is expected to have two kinds of methyl groups in the ratio of 2:1, while  $\text{V}(\text{triac})_2(\text{acac})$  is expected to have four kinds of methyl groups in the ratio 1:1:1:1. Two of the signals are found in the diamagnetic region of the spectrum, and are presumably due to the acetyl groups of  $\text{V}(\text{triac})_2(\text{acac})$  and  $\text{V}(\text{triac})_3$  respectively. Although the potential exists for spin delocalization to the acetyl group, it apparently does not occur. This is probably because the acetyl group is not coplanar with the metal-ligand ring due to steric interactions. In their paper on spin distribution in N,N' substituted Ni(II) aminotroponeiminates, Eaton et al.<sup>145</sup> also found that there was no transmission of  $\pi$  spin density through the carbonyl group of a parabenzoylphenyl substituent. The assignments were confirmed by the addition of free ligand, both Hacac and Htriac, to a mixture of  $\text{V}(\text{triac})_2(\text{acac})$  and  $\text{V}(\text{triac})_3$  in solution and observing the changes in intensity of the NMR signals. A number of other signals are present in the paramagnetic region, owing to the presence of some  $\text{V}(\text{acac})_2(\text{triac})$  in equilibrium with the other complexes





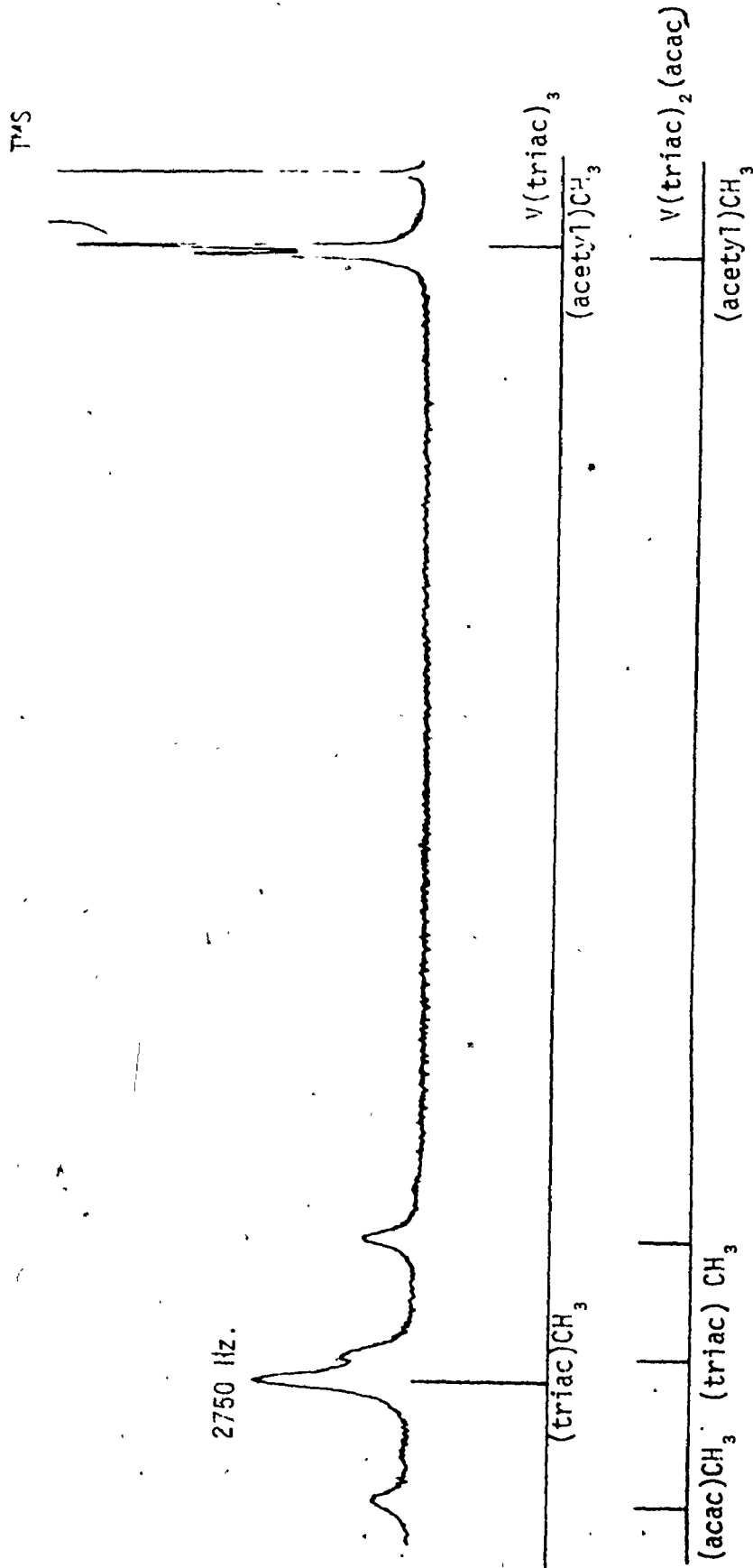


Figure 6-19. 58.3 MHz.  $^1\text{H}$  NMR spectrum of  $V(\text{triac})_3/V(\text{triac})_2(\text{acac})$  mixture  $30^\circ$  in  $\text{CDCl}_3$ .

There are also signals due to the methine proton of  $\text{acac}^-$  which occur in this region. The resonances due to the  $\gamma$ -acetyl groups occur in the diamagnetic region.

The experiment was carried out in two stages. The temperature dependence of the paramagnetic region of the spectrum was observed up to about  $100^\circ\text{C}$  in deuteriochloroform. Within this temperature range, the collapse of the upfield two paramagnetic signals was observed due to environmental averaging. The spectra thus obtained were used to estimate activation parameters for this process in the manner already described. The same reservations which applied to the case of  $\text{V}(\text{hfac})_2(\text{tfac})$  are also applicable in this case, as the signals of  $\text{V}(\text{acac})_2(\text{triac})$  were not assigned and the temperature dependence of the linewidth and chemical shift were not determined. The experimental spectra and simulated spectra are compared in Fig. 6-20. The linearity of the Arrhenius plot obtained from the  $k$  values for the simulated spectra suggests that the procedure is reasonable. The activation parameters for this process are reported in table 6-2. No evidence for exchange of the acetyl groups was obtained in deuteriochloroform.

In the second stage, the diamagnetic region of the spectrum of  $\text{V}(\text{triac})(\text{acac})/\text{V}(\text{triac})$  was examined up to approximately  $200^\circ\text{C}$  in *o*-dichlorobenzene. In this case, *o*-dichlorobenzene was used because of its high boiling point. The long liquid range of this solvent permits samples of normal concentration to be made up at ambient

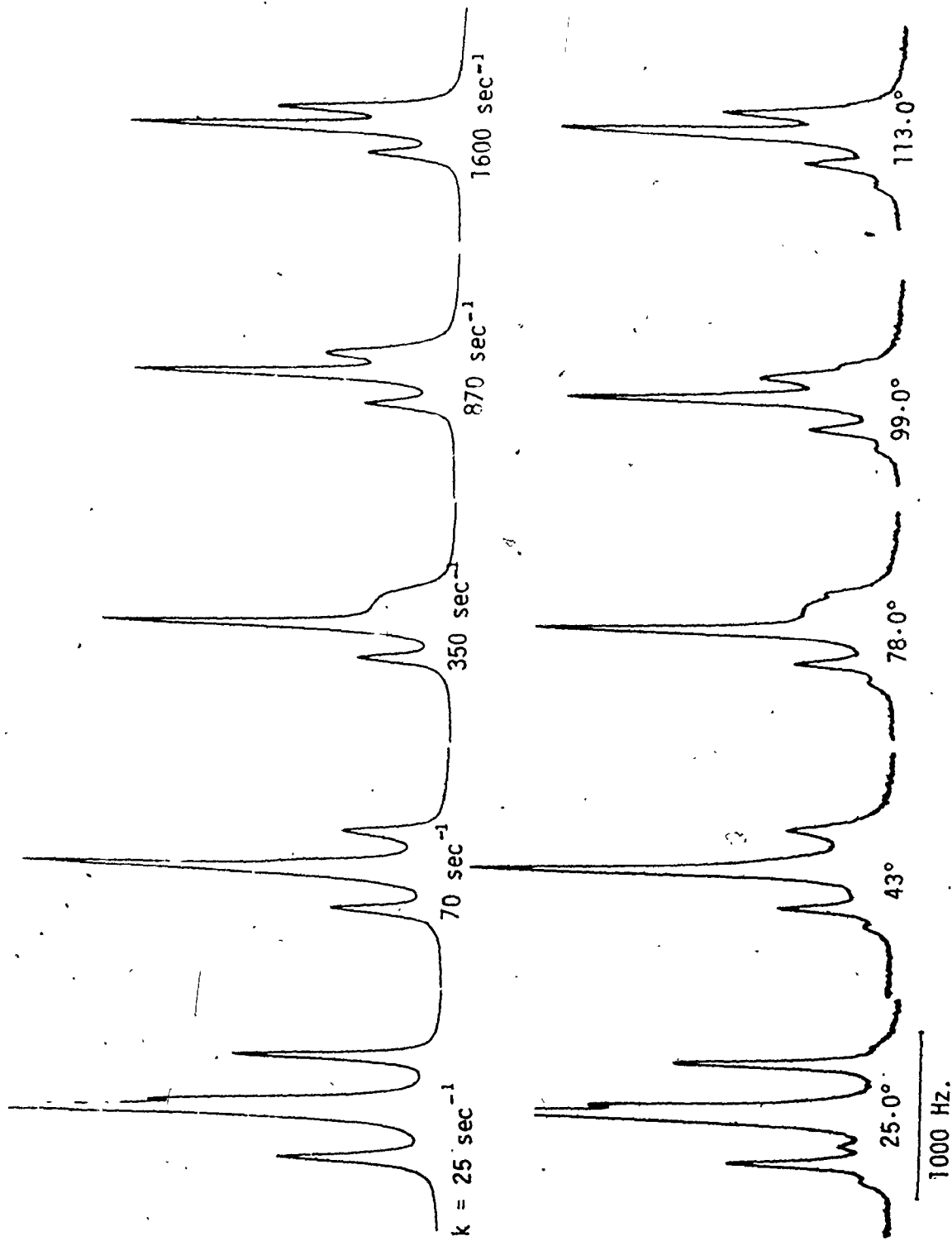


Figure 6-20. Experimental and simulated spectra of paramagnetic region of  $V(\text{triac})_3/V(\text{triac})_2(\text{acac})$  NMR spectra at various temperatures.  $^1\text{H}$ , 58.3 MHz.  $\text{CDCl}_3$

temperatures. The collapse of the triac  $\text{CH}_3$  signals was observed in this solvent as in chloroform; however, the rates for this process in o-dichlorobenzene were not established. There is no substantial difference between the spectra obtained in this solvent and those obtained in chloroform. The upper limit of the temperature range in this experiment is not known exactly, as temperatures were measured by inserting a thermocouple in place of the sample in the probe of the NMR spectrometer. The range of the thermocouple was limited to  $150^\circ\text{C}$ , and the temperature of the probe above  $150^\circ\text{C}$  was estimated by extrapolating the a plot of temperature measured on the thermocouple versus the temperature set on the dial of the temperature controller. The error in temperature is not expected to exceed  $\pm 5^\circ\text{C}$ . The sample contained only the complexes  $\text{V}(\text{triac})_2(\text{acac})$  and  $\text{V}(\text{triac})_3$  and solvent. There were no isolated narrow lines on which to fine tune the instrument and consequently, resolution may not have been as good as it might have been. A sample containing a low boiling solvent cannot be used for this purpose, because even if the NMR tube can withstand the pressure, the temperature difference between the top and bottom of the NMR tube causes the solvent to reflux, resulting in a loss of resolution. The maximum increase in linewidth can be limited to  $\sim 12$  Hz.

The activation enthalpies and entropies for the inversion of  $\text{Co}(\text{triac})_3$  are  $30.6$  kcal/mole and  $16$  eu. and for the linkage isomerization of  $\text{Co}(\text{triac})_3$  are  $38.9$  kcal/mole and  $28$  eu.<sup>102</sup> If it is assumed that both processes occur via a bond rupture process, then to a

first approximation, the difference in the activation parameters represents the activation parameters for the rotation of the ligand about the partial double bond, i.e., 8.3 kcal/mole and 12 eu. If it can be further assumed that these values are approximately independent of the metal bonded to the monodentate triac- ligand, it is possible to estimate the activation parameters for  $V(\text{triac})_2(\text{acac})$ , assuming that exchange of the triac methyl groups also occurs via a bond rupture process. The values thus obtained are 18.6 kcal/mole and 5.7 eu. At 200°C,  $\Delta G_{200}^* = 21.3$  kcal/mole;  $k$  can be estimated from the Eyring equation at  $1.4 \times 10^3 \text{ sec.}^{-1}$ . If linkage isomerization were occurring at this rate, exchange broadening of the acetylmethyl should be quite evident, as the acetyl resonances would have a linewidth of approximately 450 Hz. No such line broadening is apparent, the maximum line-broadening being approximately 12 Hz. as stated above. Two conclusions are possible: The assumptions made to estimate the activation parameters for the linkage isomerization of  $V(\text{triac})_2(\text{acac})$  are incorrect, or site exchange in  $V(\text{triac})_2(\text{acac})$  does not occur via a bond rupture process. Hutchison et al.<sup>140</sup> using a similar line of argument, have suggested that  $\text{Ga}(\text{pmhd})_3$  may rearrange via a twist mechanism.

#### The Enantiomerization of $V(\text{dibm})_3$

In the preceding discussion of the rearrangement of vanadium  $\beta$ -diketonates, no reference has been made to the experimental determination of enantiomerization. For the complexes which have been already discussed, the NMR spectra are not affected by changes in the

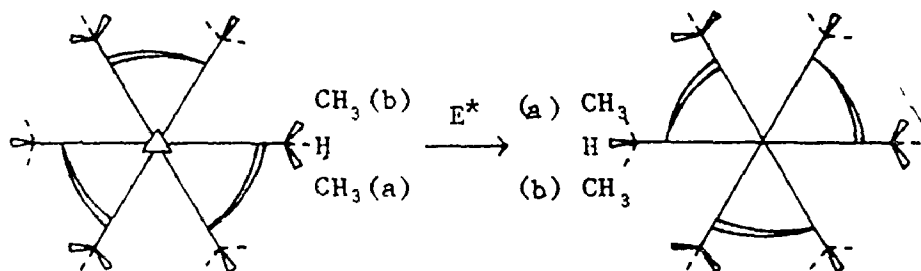
absolute configuration. In terms of the permutational analysis, it has not been possible to distinguish between permutation sets  $A_1$  to  $A_4$  and the corresponding sets  $A_5$  to  $A_8$ . Although only one of the proposed mechanisms, i.e., that proceeding through the TBP equatorial intermediate proceeds with exclusive retention of configuration, it is still of interest to determine whether in fact enantiomerization of the vanadium  $\beta$ -diketonates takes place.

The isopropyl group has been used by a number of workers as a probe to observe and determine the rate of enantiomerization for a variety of chelate complexes<sup>106,124,140,141,146</sup>.

The term 'diastereotopic' has been applied to such groups in this context. It is perhaps helpful to discuss briefly what is implied by this expression, as the term diastereotopic, as defined by Mislow and Raban<sup>147</sup>, has a somewhat broader application. Mislow and Raban have defined groups as being diastereotopic, if there is no symmetry operation of the point group to which the molecule belongs which will interchange the groups. Thus, for example, the B groups in an  $M(AA)(BB')_2$  tris chelate complex may be said to be diastereotopic, since there is no symmetry operation which will interchange the B groups on the same ligand. It is important to realize that environmental averaging of such groups does not necessarily imply enantiomerization, as exchange might take place via the TBP equatorial pathway.

The ligand employed in the present study is the anion of 2,6-dimethyl-3,5-heptanedione. The complex  $V(dibm)_3$  is illustrated

schematically below.



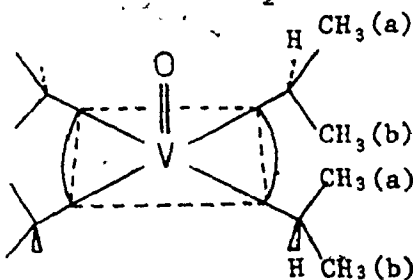
If rotamers of the isopropyl group are neglected, the complex has  $D_3$  symmetry, i.e., it has a principal  $C_3$  axis of rotation and three  $C_2$  axes of rotation perpendicular to the  $C_3$  axis. It should be evident from the diagram that neither a  $C_3$  nor a  $C_2$  rotation is capable of exchanging the methyl groups denoted a and b. The methyl groups are, therefore, diastereotopic. Rotation of the isopropyl group about the C-C bond between the isopropyl group and ring carbon does not interchange the a and b groups either, as the position of the proton is simultaneously altered. Complete inversion ( $E^*$ ) of the complex also does not result in the exchange of a and b groups, as all spatial relationships are preserved. However, inversion of the complex without inversion of the isopropyl group will result in interconversion of a and b environments of the methyl groups. Inversion of the i-propyl group alone would have an indistinguishable result; however, this process can be safely disregarded, as it would require an excessively high activation energy.

Some authors have denoted the environments of the diastereotopic methyl groups of the isopropyl groups as r and s. This seems to the present author an unfortunate choice of nomenclature. The use of Pro-R

and Pro-S designations is much to be preferred.

Since the methyl groups in this complex are diastereotopic, they are necessarily anisochronous. The term isochronous was originally coined by Abragam<sup>148</sup>, to describe the chemical shift equivalence of groups which are related by symmetry, i.e., groups which are equivalent or enantiotopic. The term anisochronous refers to chemical shift non-equivalence, even though the chemical shift might be negligibly small.

It should be remarked that, because the methyl groups in an isopropyl group are diastereotopic, the molecule or complex is not necessarily chiral in nature, e.g.,  $\text{VO}(\text{dibm})_2$  illustrated below



has  $C_{2v}$  symmetry, yet the methyl groups a and b are diastereotopic. This is merely to emphasize that care must be taken to ensure that exchange of diastereotopic groups is, in fact, due to enantiomerization and not some other process.

Jurado and Springer<sup>106</sup> have considered the possibility that the geminal methyls of the isopropyl groups are diastereotopic because of restricted rotation of the isopropyl group about the 2,3 C-C bond.



However, they have provided arguments to eliminate this possibility. Because of the structural similarity between aluminium and vanadium  $\beta$ -diketonates, the same arguments should be applicable in the present case.

### Results and Discussion

A  $^1\text{H}$  100 MHz. spectrum of  $\text{V}(\text{dibm})_3$  at  $39^\circ$  in  $\text{CDCl}_3$  is illustrated in Fig. 6-21. The expected resonances due to the methine proton, the isopropyl proton, and the methyl protons are evident with shifts of 39.2, 21.5, 2.38 and 1.99 ppm respectively. Assignments can be made readily on the basis of the intensities which are in the expected ratio of 1:2:12. A small splitting of the methyl groups is evident. At the ambient temperature of the probe, it is about 40 Hz. Since there is no comparable splitting of the isopropyl resonance, the source of the splitting of the methyl resonances must be the molecular dissymmetry centred at the vanadium. The coupling constant observed by Jurado and Springer<sup>106</sup>  $J_{\text{CH-CH}} = 6.4$  Hz. in the analogous aluminium complex, is unlikely to be much different from that in  $\text{V}(\text{dibm})_3$ . This coupling is not observed, presumably because of the rapid relaxation of the protons due to the paramagnetic vanadium.

Fig. 6-22 shows the temperature dependence of the chemical shift of the geminal methyl groups. The difference in temperature dependence is somewhat surprising, but may be in part due to changes in rotamer populations with temperature. From Fig. 6-22, it is evident that the

TMS

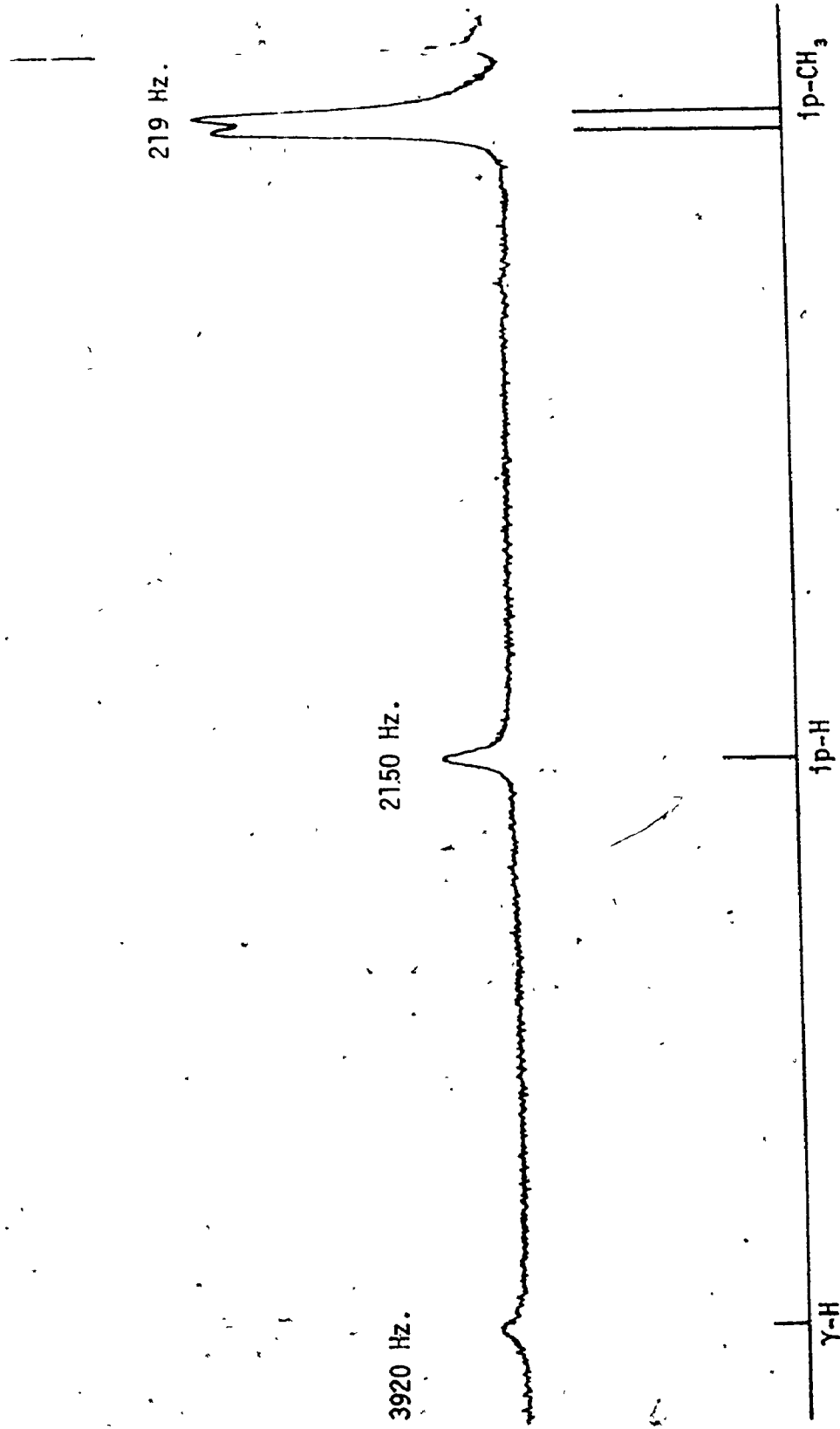


Figure 6-21. 100 MHz.  $^1\text{H}$  NMR spectrum of  $\text{V}(\text{dfbm})_3$  at  $37^\circ$  in  $\text{CDCl}_3$ .

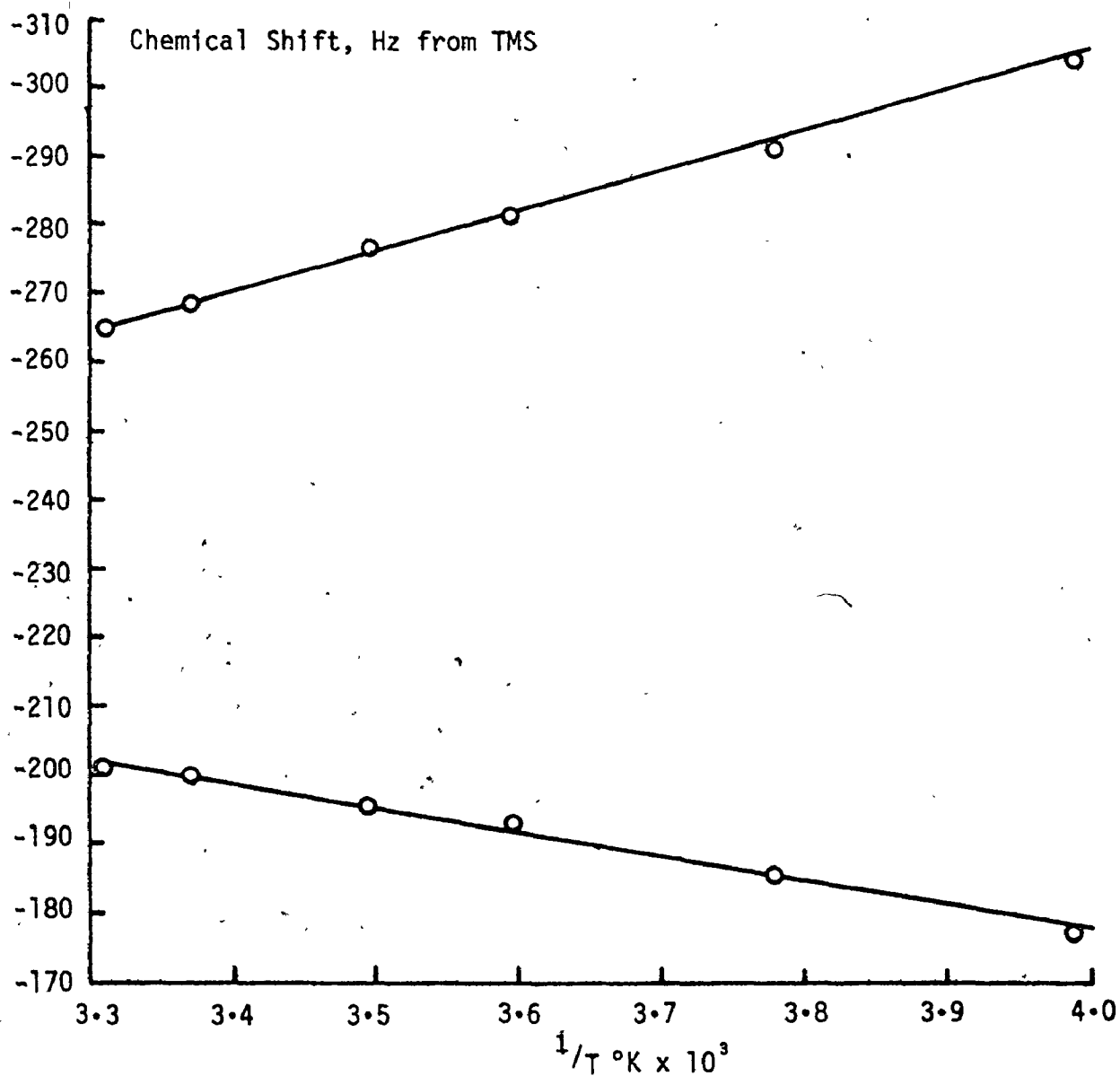


Figure 6-22 Chemical shift of methyl groups of  $V(\text{dibm})_3$  versus reciprocal temperature.  $^1\text{H}$ , 100 MHz. in  $\text{CDCl}_3$ .

shifts of the geminal methyl groups converge rapidly with temperature, and a simple calculation predicts that at 103°C, the methyl groups would have identical chemical shifts. Fortunately, rapid environmental averaging occurs well below this temperature. In figure 6-23 is illustrated the methyl region of the spectrum of  $V(dibm)_3$  at various temperatures, and simulated spectra using extrapolated chemical shift and linewidth parameters at different rates of exchange. There can be little doubt that enantiomerization of  $V(dibm)_3$  is occurring.

#### Activation Parameters of the Enantiomerization of $V(dibm)_3$

The linearity of an Arrhenius plot for the rearrangement of  $V(dibm)_3$  is reasonably good, indicating that the choice of linewidth parameters is reasonable. The activation parameters for the environmental averaging of the geminal methyl groups is reported in Table 6-2.

There appears to be nothing unusual about the activation parameters of this process, which are comparable to the activation parameters estimated for other  $\beta$ -diketonate complexes. It therefore seems probable that site exchange in  $V(dibm)_3$  occurs by the same mechanism as in the other  $\beta$ -diketonate complexes. The values of activation parameters may be compared with those determined by Springer for the analogous aluminium complex<sup>106</sup>,  $\ln A = 25.3$  and  $E_a = 19$  kcal.;  $k$  at the coalescence temperature of 120°C is approximately 2.7 sec.<sup>-1</sup>. The corresponding values for  $V(dibm)_3$  are  $\ln A = 29.1$  and  $E_a = 15.5$  kcal.;  $k$  at the coalescence temperature of approximately 43°C is estimated to

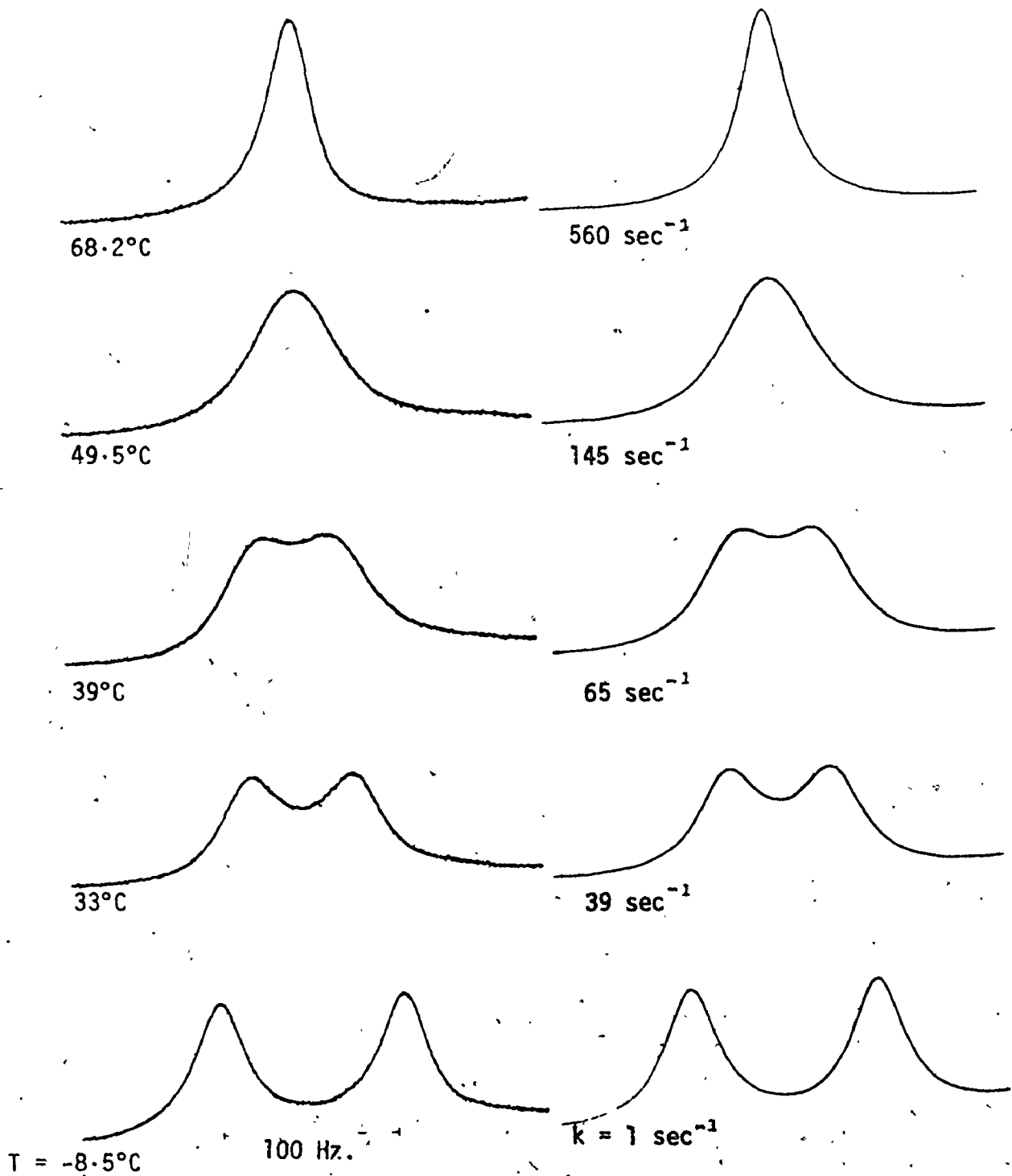


Figure 6-23. Comparison of experimental and simulated NMR spectra of methyl region of  $V(dibm)_3$  at various temperatures  $^1H$  100 MHz. in  $CDCl_3$ .

be about  $83 \text{ sec.}^{-1}$ . Typically, the vanadium complex is considerably more labile than its aluminium analogue.

The temperature dependent spectra of  $\text{V}(\text{dibm})_3$  do not provide any information about the mechanism of rearrangement beyond the fact that enantiomerization occurs. To determine if it would be possible to obtain further information from less symmetric complexes concerning the mechanism of isomerization, an attempt was made to observe the methyl region of the  $^1\text{H}$  NMR spectrum of  $\text{V}(\text{dibm})_2(\text{hfac})$ .

A sample of  $\text{V}(\text{dibm})_2(\text{hfac})$  was prepared by mixing  $\text{V}(\text{dibm})_3$  and  $\text{V}(\text{hfac})_3$  in stoichiometric amounts, i.e., a molar ratio of 2:1.

The methyl region of this mixture, which is expected to be primarily  $\text{V}(\text{dibm})_2(\text{hfac})$  with presumably small amounts of  $\text{V}(\text{hfac})_2(\text{dibm})$  and  $\text{V}(\text{dibm})_3$  also present, showed a broad band of unresolved resonances between 1.4 and 3.8 ppm which promised little hope for using this complex for kinetic studies. In view of the small shifts observed between the A and  $\text{A}^1$  groups of the other  $\text{V}(\text{AA}^1)_2(\text{BB})$  complexes examined in this study, this result is not surprising.

#### The Effect of Acid and Base on the Rate of Rearrangement

In chapter three, the possibility of rupture of the first M-O bond being assisted by protonation was discussed. If this were the case, not only ligand exchange, but also rearrangement of the complex would be acid catalysed, provided that rearrangement occurred via bond rupture.

In order to test this hypothesis, the  $^{19}\text{F}$  NMR spectra of  $\text{V}(\text{tfac})_3$  and  $\text{V}(\text{hfac})_2(\text{acac})$  were run at temperatures at which the rates of exchange were intermediate, both in the presence and absence of acid. At an intermediate rate of exchange, the spectra should be most sensitive to any significant change in rate.

Even at a concentration 0.1M of  $\text{CF}_3\text{COOH}$ , there was no significant change in the spectra of either  $\text{V}(\text{tfac})_3$  or  $\text{V}(\text{hfac})_2(\text{acac})$  which could be attributed to a change of rate. From the comparison of the simulated spectra with experimental spectra, it is estimated that a change of rate of 20% at an intermediate rate of exchange would be readily detectible. If there is any acceleration of rearrangement by acid, then it must be less than 20%. Compared to the catalytic effect of acid on ligand exchange, this is insignificant.

Two conclusions are possible from this result: 1) the rearrangement of these chelates does not occur via a bond rupture process, and therefore could not be assisted by acid catalysis. 2) if rearrangement does take place via a bond rupture mechanism to yield an intermediate with a dangling ligand, then in the ligand exchange process, rupture of the second M-O bond, rather than the first is assisted by protonation.

In view of the sensitivity of the rate of rearrangement of  $\text{V}(\text{hfac})_2(\text{acac})$  to the solvent, a bond rupture process is considered much more likely than a twist process.

The discrepancy between the present results and those obtained by Gordon et al.<sup>7</sup> remain somewhat puzzling. The possibility of catalysis by an impurity was considered. The similarity of reaction rates of  $V(\text{tfac})_3$  in different solvents and the reproducibility of the spectra with both different samples of  $V(\text{tfac})_3$  and solvent argues against this. Since acid was considered to be the most likely candidate for a catalyst, the effect of base, triethylamine, on the spectra at an intermediate rate of exchange was examined. Again, as expected, the results were negative. No change in the spectra was observed.

### Conclusion

A careful study of the environmental averaging of the trifluoromethyl groups of  $V(\text{tfac})_3$  leads to the conclusion that not all of the proposed mechanisms can account for rearrangement. The probability of transfer of a nucleus from any site to any other site appears within experimental error to be equal. This result rules out the trigonal twist ( $pC_3$ ) and TBP axial and equatorial pathways. The SP primary mechanism under certain conditions could account for the results. However, the mechanisms which best fit are either the rhombic ( $iC_3$ ) twist or a bond rupture mechanism involving SP states, either as intermediates being formed and forming products by both primary and secondary processes, or as transition states in the rearrangement of TBP intermediates.

It is difficult to answer the question of whether a bond rupture



or a twist mechanism is favoured by the experimental evidence which appears to be somewhat contradictory. On the one hand, the very large solvent dependences of the rate of environmental averaging would seem to indicate a bond rupture mechanism while the failure to observe linkage isomerization in  $V(\text{triac})_3$ , or  $V(\text{triac})_2(\text{acac})$ , would suggest that perhaps a twist mechanism is responsible for environmental averaging. It should be borne in mind that the estimation of the activation parameters for rotation of the monodentate  $\text{triac}^-$  ligand are based only on a single pair of results, those for  $\text{Co}(\text{triac})_3$ . With only one set of data available, it is difficult to ascertain the validity of generalization of these values to other complexes containing the monodentate  $\text{triac}^-$  ligand.

The similarity of the rates of rearrangement of the vanadium  $\beta$ -diketonate complexes studied and the probable existence of a linear free energy relationship, suggest that whatever the mechanism of rearrangement, it is common to all the complexes observed.

The site exchange patterns provide little insight into the relationship between mechanisms of rearrangement and substituent effects in the complexes. The statistical nature of the averaging patterns precludes the identification of a favoured axis of rotation or bond most likely to rupture.

Environmental averaging of the diastereotopic methyl groups of  $V(\text{dibm})_3$  confirms that enantiomerization of the complex occurs at a

rate which is comparable to environmental averaging in other vanadium  $\beta$ -diketonate complexes. Other than to exclude the TBP axial mode of rearrangement as the sole mechanism of rearrangement, this result provides little mechanistic information, as all the other proposed mechanisms of rearrangement involve enantiomerization. Only a precise measurement of the ratio of the rate of environmental averaging to the rate of enantiomerization would be able to distinguish between, say, a rhombic twist mechanism and a bond rupture mechanism involving SP states.

The only metals for which measurements of the rates of rearrangement of tris  $\beta$ -diketonate complexes have been carried out are those of aluminium and cobalt and to a lesser extent gallium. No conclusive evidence has been presented in any case. On the basis of a full lineshape analysis, Hutchison et al.<sup>141</sup> have concluded that the most probable mechanisms of rearrangement for Al and Ga(pmhd)<sub>3</sub> are certain twist processes, and bond rupture to form SP states. Their study of Ga(triac)<sub>3</sub> led them to suggest that Ga(triac)<sub>3</sub> might rearrange via a twist mechanism. In a study of tris(5-methylhexane-2,4-dionato)Co(III), (Co(mhd)<sub>3</sub>), Gordon and Holm<sup>110</sup> were led to the conclusion that the mechanism consistent with the observed kinetics was a bond rupture type leading to the formation of TBP axial states with a small amount of either TBP equatorial (~10%) or SP axial (~20%).

Piper and Fay<sup>101</sup> concluded, on the basis of solvent effects,

that  $\text{Al}(\text{tfac})_3$  probably rearranges via a bond rupture mechanism. Only the trigonal twist could be conclusively ruled out for the group III compounds and for  $\text{cis Cr}(\text{bzac})_3$ .

A recent report by Kotal and Sievers<sup>149</sup> suggests that  $\text{Cr}(\text{tfac})_3$  isomerizes via a twist mechanism in the gas phase. This conclusion was based on the observation that the activation energy of cis-trans isomerization is substantially lower than the Cr-O bond energy in  $\text{Cr}(\text{tfac})_3$ . The argument presupposes that the strength of the remaining bonds is unaffected by rupture of one of the bonds. This is rather unlikely, particularly with respect to the remaining M-O bond of the dangling ligand. Rupture of one of the bonds of the ligand is most likely to be accompanied by migration of the negative charge to the bound end of the ligand, thereby increasing the strength of the remaining bond. Bickley and Serpone<sup>141</sup> have also criticized this conclusion.

Bickley and Serpone<sup>141</sup> have carried out permutational and mechanistic analyses of some  $\text{R}_2\text{Sn}(\text{acac})_2$  and  $\text{RClSn}(\text{acac})_2$  complexes, and have concluded that rearrangement probably occurs via twist mechanism. However, they were unable to unambiguously exclude bond rupture pathways. Thus, although it has been possible to come to some conclusions about the rearrangement of  $\beta$ -diketonate complexes, in very few cases has it been possible to unambiguously answer the fundamental question of whether rearrangement proceeds via bond rupture or a twist mechanism.

It is of interest to compare the relative rates of rearrangement

of complexes containing identical ligands and differing only in the central metal ion. For complexes containing the  $M-O_6$  core, only for those having trifluoroacetylacetonate and tropolonate as ligands, have an extensive number of measurements been made. Eaton et al.<sup>146</sup> have pointed out that the rates of rearrangement in the two series of complexes parallel each other with the exception of the placement of vanadium and cobalt. The position of vanadium in the trifluoroacetylacetonate series has been based on erroneous information. From the present work, it can be seen that, in fact, the rate of rearrangement of  $V(\text{tfac})_3$  is substantially faster than that of  $Al(\text{tfac})_3$  and comparable to that of  $Ga(\text{tfac})_3$  and  $Mn(\text{tfac})_3$ . Thus, only cobalt appear to be anomalous in its position in the two series.

The rates of rearrangement of a variety of  $\beta$ -diketonate complexes are compared in table 6-6. The rate of rearrangement of the vanadium complex is consistently faster than its aluminium analogue. For either a bond rupture or a twist mechanism, this might be expected, due to the larger size of the vanadium  $3^+$  ion.

Table 6-6 Comparison of rates and activation energies of rearrangement of some tris  $\beta$ -diketonate complexes.

Metal	Ligand (tfac) <sub>3</sub>	k(sec <sup>-1</sup> )	°C	Ea kcal/mole	Reference
Fe		36	-57°	< 14	7
In		10 <sup>3</sup>	70°	—	101
Mn		330	64°	18.7	7
V		38	62°	21	—
Ga		34	103°	24	101
Al		5 x 10 <sup>-8</sup>	25°	31	101
Co		2 x 10 <sup>-12</sup>	25°	33	7
Rn		10 <sup>-8</sup>	163°	> 42	101
Rh					
V	(dibm) <sub>3</sub>	76	42°	15.5	
Al		2.5	120°	19	106
Ga	(acac) <sub>2</sub> (hfac)	8 x 10 <sup>2</sup>	25°	15	154
Al		80	25°	18	154
V		42	25°	—	
V	(hfac) <sub>2</sub> (acac)	82.5	25°	12.5	
Al		.86	25°	21.3	154

A central theme in the discussion of the preceding three chapters is the possible existence of the dangling ligand intermediate and its relevance to the ligand exchange and rearrangement reactions. In fact, the evidence for an intermediate of this kind in reactions of tris  $\beta$ -diketonate complexes in ligand exchange and in rearrangement processes is scant. In similar work on other  $\beta$ -diketonate systems, other workers have also explained experimental results in terms of a dangling ligand intermediate without any direct evidence. A brief review of the results to examine the importance of this intermediate in the present work is therefore desirable.

In chapter three, we attempted to find evidence for the protonated dangling ligand suggested by Saito and Masuda<sup>2</sup> to account for acid catalysis in the exchange of Hacac with  $\text{Al}(\text{acac})_3$ . The experimental results did not support the existence of such a species. The expected downfield shifts of the methyl and methine resonances of  $\text{Al}(\text{acac})_3$  in the presence of strong acid were not observed, indicating the concentration of protonated dangling ligand intermediate was small if existent. On the other hand, definite evidence was obtained for protonation of the  $\gamma$ -carbon. This result is not surprising in view of the fact that the majority of metal derivatives of neutral  $\beta$ -diketones have the ligand bonded in the keto form through both oxygen atoms. This result does not rule out the possibility of the protonated dangling ligand

intermediate. However, it does demonstrate that it is not necessary to invoke this species to explain acid catalysis of ligand exchange between  $\beta$ -diketonate complexes and free ligand.

In chapter four, the kinetics of ligand exchange were discussed in terms of the dangling ligand mechanism of Adams and Larsen<sup>81</sup>. It was found that a pathway of ligand exchange existed for  $V(acac)_3$  with  $Hhfac$  which was first order in the concentration of  $Hhfac$ . In the scheme of Adams and Larsen, this corresponds to either the coordination of a neutral molecule of ligand to the site on the complex vacated by the free end of the dangling ligand or the transfer of a proton from one of the dangling ligands to the other being the rate determining step. There are, however, other mechanisms which could give rise to a first order dependence on ligand concentration.

The formation of a second sphere complex followed by ligand interchange could result in such a dependence. If this were the case, one might expect this to be true of all tris-  $\beta$ -diketonate complexes as the exterior aspects of the complex should be rather similar in most cases. This is not the case. A number of instances of ligand exchange mechanisms with a zero order dependence on ligand concentration have been reported<sup>2, 97</sup>. In contrast to this, it is possible to consider that the complex is in rapid equilibrium with a dissociated form of the complex. A reaction between the dissociated form of the complex and a neutral ligand as a rate determining step would again result in a first order dependence on ligand concentration. The calculations of Fay and Piper<sup>101</sup> suggest

that the dissociation energy of  $\text{Al}(\text{acac})_3$  may be as high as 250 kcal/mole, indicating that this is not an energetically favourable process. The dissociation energies of other  $\beta$ -diketonate complexes of trivalent ions are likely to be comparable. A simple associative reaction cannot be considered likely for complexes of trivalent ions of the first transition because of their relatively small size.

Finally, in chapter six, the conclusions from lineshape analysis of  $\text{V}(\text{tfac})_3$  and  $\text{V}(\text{hfac})_2(\text{tfac})$  were discussed. It was concluded that the results could equally well be caused by a set of rhombic twists around the  $iC_3$  axes, or a bond rupture mechanism involving either a SP dangling ligand intermediate in a primary-secondary rearrangement or a TBP intermediate in a pseudo-rotation rearrangement. A bond rupture mechanism was supported only by the solvent dependence of the rearrangement of  $\text{V}(\text{hfac})_2(\text{acac})$ .  $\text{V}(\text{tfac})_3$ , on the other hand, did not exhibit such a dependence.

Holm et al.<sup>140</sup> were similarly unable to distinguish unequivocally between bond rupture mechanisms forming SP axial states and certain twist mechanisms for  $\text{Al}(\text{pmhd})_3$ , and  $\text{Ga}(\text{pmhd})_3$ . On the other hand, Gordon and Holm<sup>110</sup> were able to exclude a twist mechanism for the rearrangement of  $\text{Co}(\text{mhd})_3$ , implying that the rearrangement of this complex must proceed through a dangling ligand intermediate.

Although the existence of the dangling ligand intermediate has been inferred from studies on ligand exchange and rearrangement of tris



$\beta$ -diketonates, there are a number of cases where considerably more direct evidence exists to support existence of the dangling ligand.

Unequivocal evidence has been obtained from electronic and NMR spectra for the anion of acetylacetonate bonded to mercury in the open-ended form by Hammond et al.<sup>150</sup>. There is an interesting compound reported by Howe et al.<sup>151</sup>. The compound, 2-trimethylsiloxy-2-penten-4-one, exists in a cis-trans equilibrium. The trans form is apparently stereochemically rigid. However, the cis form undergoes a rapid intramolecular rearrangement at room temperature. A suggested mechanism has the non-equivalent methyl group environments of the acetylacetonate ligand averaged by passing through a five coordinated complex with the ligand bonded as the oxygen chelate. It is curious that in this compound, the normal relationship of the complex with the chelated ligand and dangling ligand as the ground state and intermediate is apparently reversed.

A crystal structure of a copper complex containing a monodentate hexafluoroacetylacetonate ligand has been reported by Bush and Fenton<sup>152</sup>. Whether or not the hexafluoroacetylacetonate anion can really be considered a ligand is questionable. The authors cite a number of other crystal structures of similar compounds containing such ions as nitrate and perchlorate in which the copper-oxygen distances are significantly shorter.

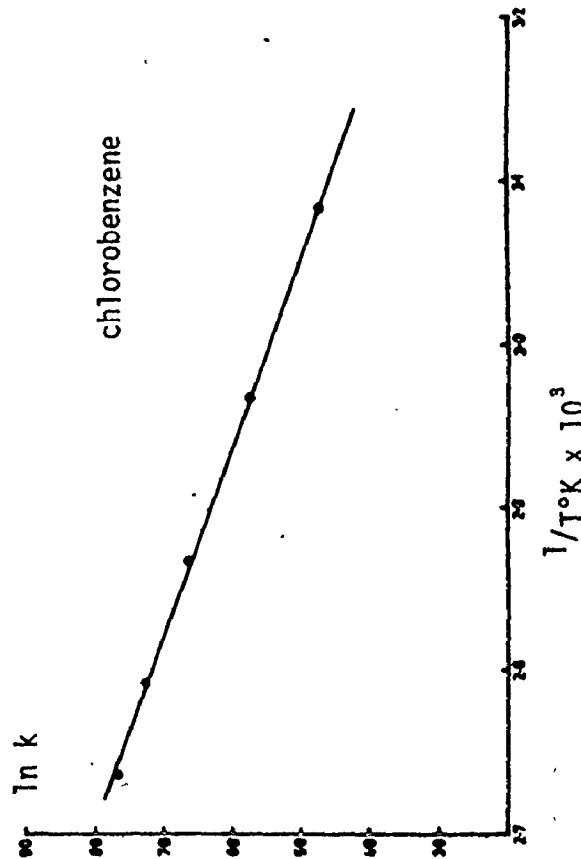
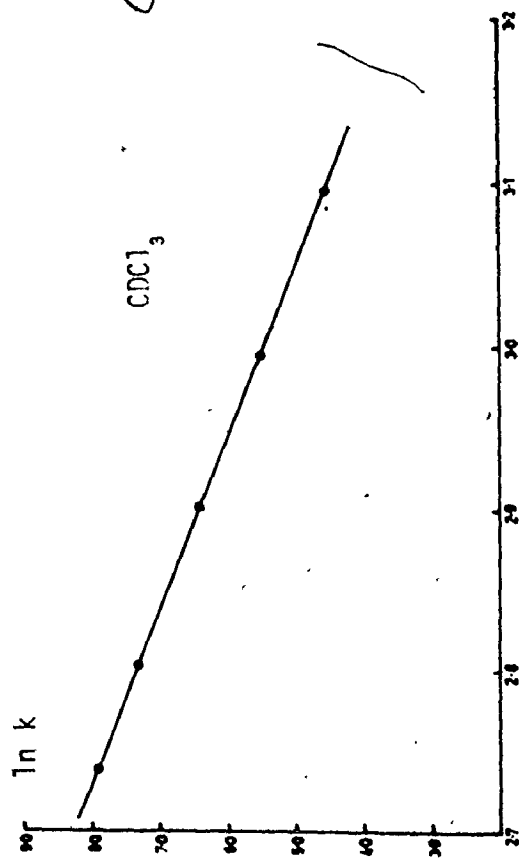
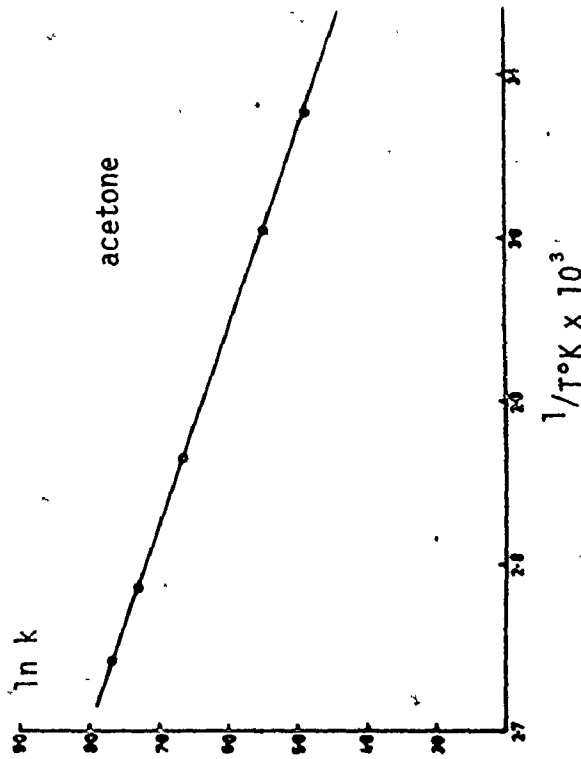
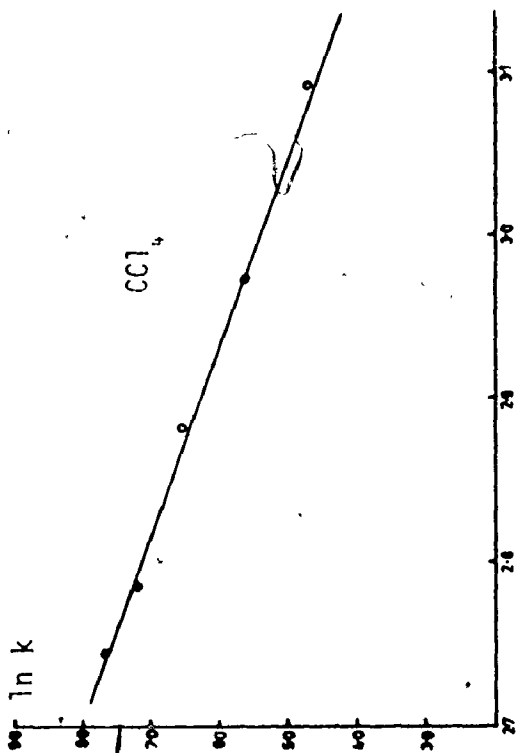
Although the monodentate dangling ligand is by no means common, which is to be expected, it has been observed. There does not appear to be any good reason why this type of species should not be considered

as a reasonable intermediate in ligand exchange and rearrangement reactions of  $\beta$ -diketonates. It would be desirable to find support for the dangling ligand intermediate from other types of experiment. One type of experiment which could, potentially, provide evidence for a dangling ligand intermediate would be the observation of the collapse of hyperfine structure caused by coupling between the central metal ion and a ligand nucleus. It would, of course, be necessary to demonstrate that the process which caused the collapse of the fine structure was the rearrangement by determining rates at different temperatures if possible. Furthermore, it would be necessary to demonstrate that the rearrangement process was intramolecular. Unfortunately, it does not seem likely that such an experiment can readily be carried out for  $\beta$ -diketonate complexes. Those which are paramagnetic are immediately ruled out, as unpaired electronic spin density causes rapid nuclear relaxation which makes the observation of inter-nuclear coupling impossible. Observation of coupling is likely to be difficult for nuclei with spins greater than  $1/2$ , particularly those with large electric quadrupole moments. The  $\beta$ -diketonate complexes are not spherically symmetric; therefore, the electric quadrupole moment can couple with the electric field gradient at the nucleus to produce rapid nuclear relaxation. All of the diamagnetic tris  $\beta$ -diketonates which are known to rearrange at a suitable rate on the NMR time scale, i.e., those of Al, Ga and In have central metal ions with large electric quadrupole moments.

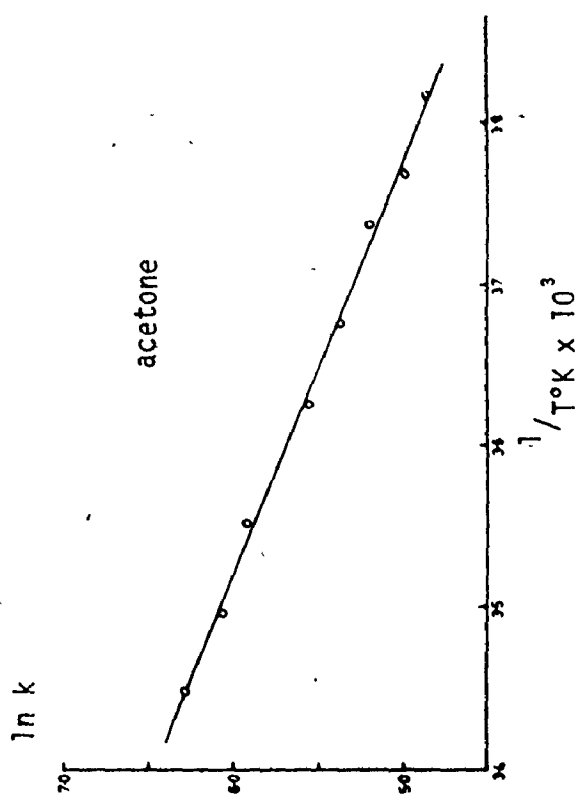
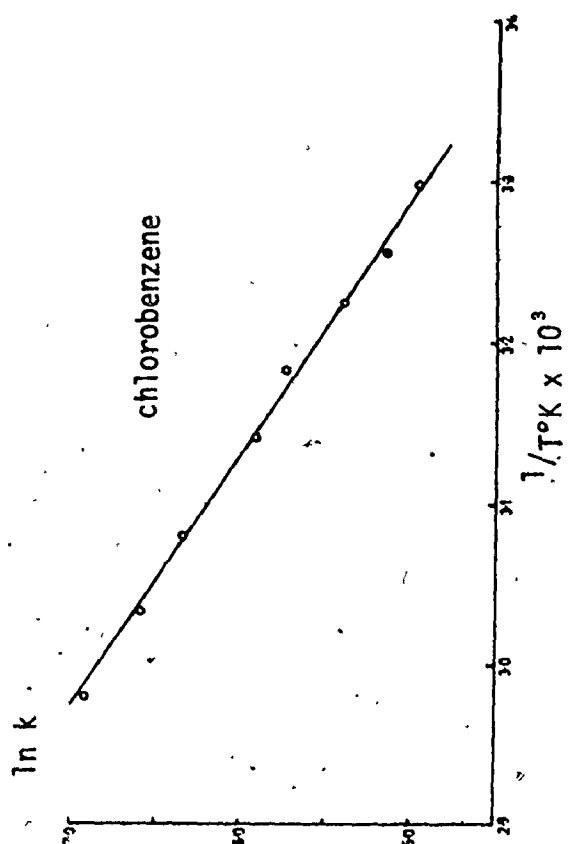
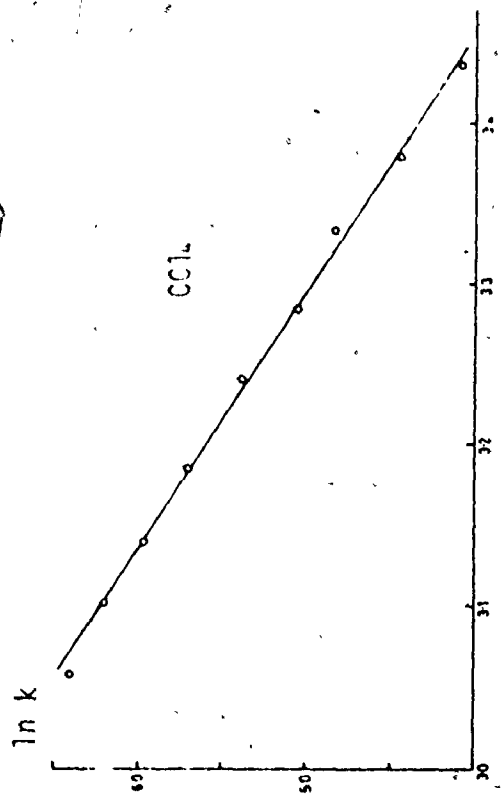
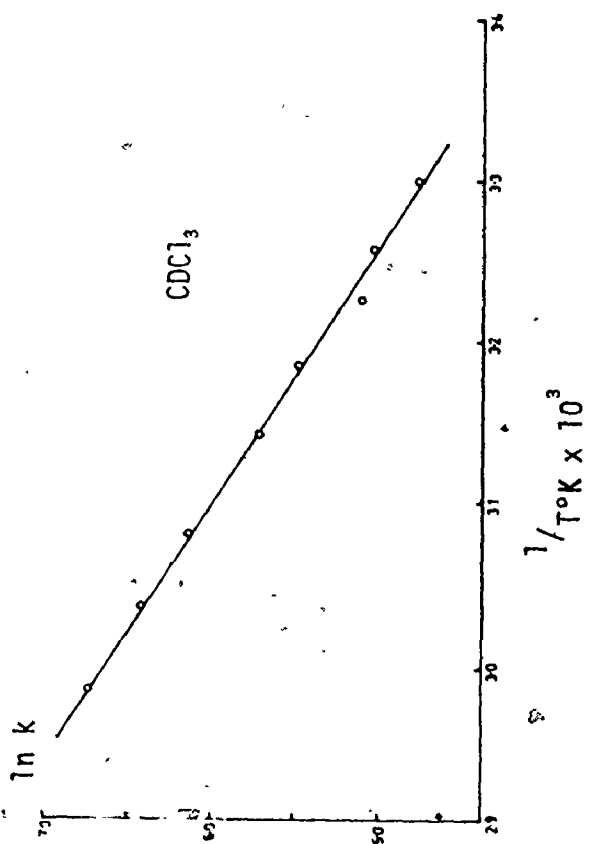
Tuck<sup>97</sup> has approached the problem in a different way. By attaching a suitable chromophore to the carbonyl groups of an In(III)

trifluoro- $\beta$ -diketonate complex, he hoped to be able to detect very low concentrations of the dangling ligand. Although he was not successful in this case, it is possible that this approach may yet prove useful.

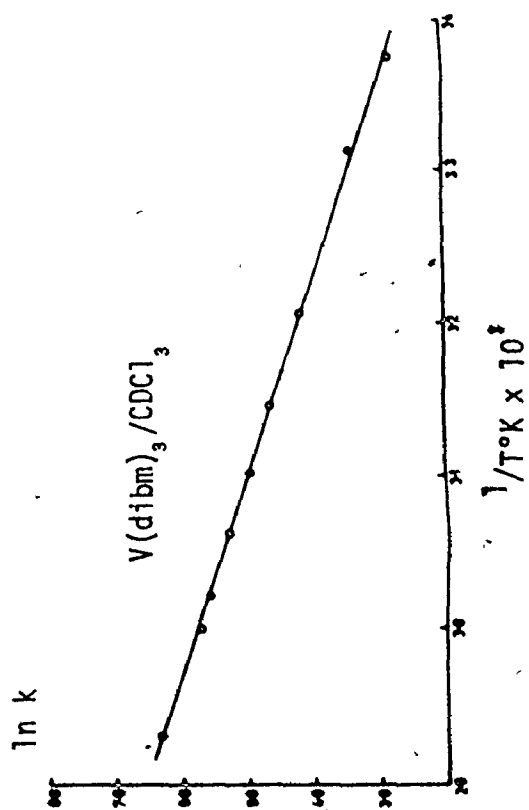
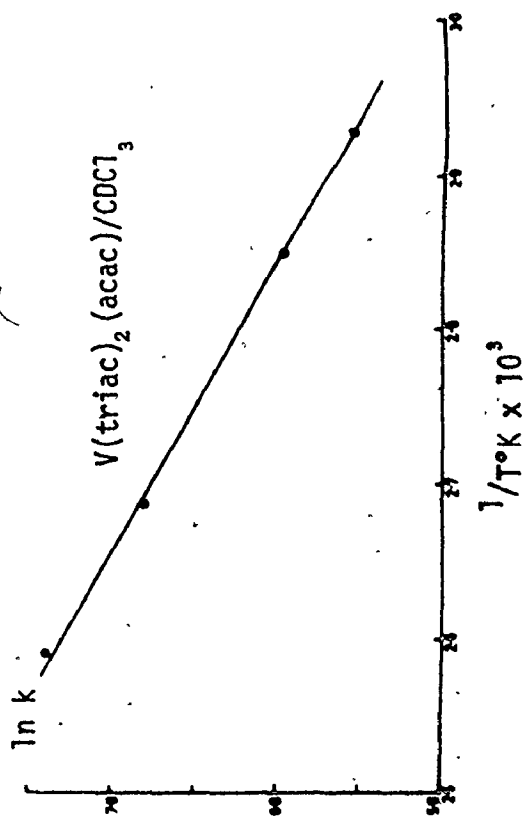
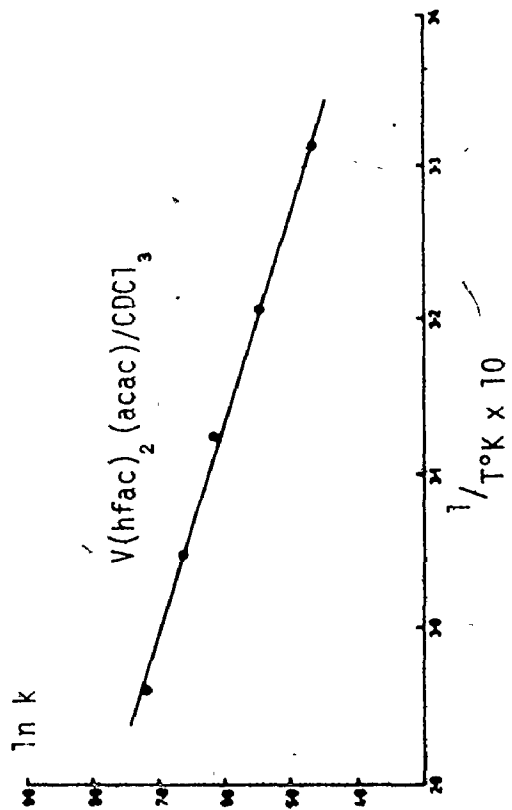
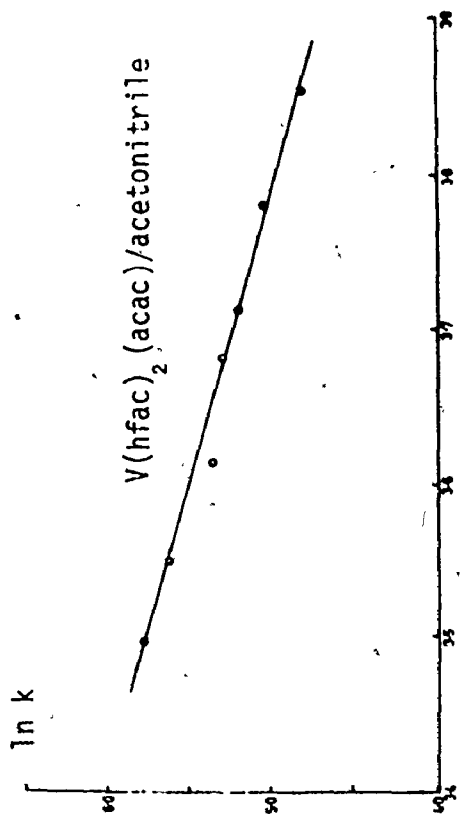
It is almost invariably the case in the study of the reactions of inorganic compounds that the intermediates are not directly observed, and that their presence must be inferred from kinetic data. The criteria for distinguishing between various mechanisms has been discussed in detail by Wilkins<sup>104</sup> as well as by Langford and Gray<sup>153</sup>. Thus, for example, the evidence for a five coordinate intermediate in the anation reactions of  $\text{Co}(\text{CN})_5\text{OH}^-$  which Langford and Gray describe as the 'best documented' case of a dissociative substitution reaction (on an octahedral centre) is solely kinetic. In the same sense, the dangling ligand hypothesis referred to in the present work is supported by kinetic evidence rather than by direct observation. The evidence for such an intermediate is not definitive, since many of the results taken individually can be accounted for in other ways. Nevertheless, the hypothesis serves well to correlate much of the kinetic data presented here.



Arrhenius plots of rearrangement rates of  $\text{V}(\text{tfac})_3$  in various solvents.



Arrhenius plots of rearrangement rates of  $\text{V}(\text{hfac})_2(\text{acac})$  in various solvents



Arrhenius plots of rearrangement rates of various vanadium  $\beta$ -diketonates.

## REFERENCES

1. A. Combes, *Compt. Rend.*, 105, 871 (1887)
2. K. Saito and K. Masuda, *Bull. Chem. Soc. Jap.*, 43, 119 (1970)
3. K. Saito and M. Takahashi, *Bull. Chem. Soc. Jap.*, 42, 3462, (1969)
4. R.G. Pearson and D.A. Johnson, *J. Amer. Chem. Soc.*, 86, 3983 (1964)
5. D.R. Eaton and K.L. Chua, *Can. J. Chem.*, 49, 56 (1971)
6. D.R. Eaton and K.L. Chua, *Can. J. Chem.*, 51 2260 (1973)
7. J.G. Gordon II, M.J. O'Connor and R.H. Holm, *Inorganica Chimica Acta*, 5, 381 (1971)
8. G.T. Morgan and H.W. Moss, *J. Chem. Soc.*, 105, 189 (1914)
9. J.P. Fackler Jr., *Progr. Inorg. Chem.*, 7, 361 (1967)
10. D.W. Thompson, *Structure and Bonding*, 9, 27 (1971)
11. R.W. Moshier and R.E. Sievers, *Gas Chromatography of Metal Chelates*, Pergamon (1965)
12. J.P. Collman, *Reactions of Coordinated Ligands*, Amer. Chem. Soc., Washington, D.C. (1963)
13. J. Selbin, *Chem. Rev.*, 65, 153 (1965)
14. A. Lempicki, H. Samelsen, and C. Brecher, *Appl. Opt. Suppl. on Chem. Lasers*, Suppl. 2, 205, (1965)
15. J.J. Fortman and R.E. Sievers, *Coord. Chem. Rev.*, 6, 331 (1971)
16. E.C. Lingafelter and R.L. Braun, *J. Amer. Chem. Soc.*, 88, 2951 (1966)
17. A. Avdeef and J.P. Fackler, Jr. *Inorg. Chem.*, 14, 2002 (1975)
18. G.J. Bullen, R. Mason and P. Pauling, *Inorg. Chem.*, 4, 456 (1965)
19. F.A. Cotton and R.C. Elder, *J. Amer. Chem. Soc.*, 86, 229 (1964)
20. M.J. Bennett, F.A. Cotton, R. Eiss and R.C. Elder, *Nature*, 213, 174 (1967)

21. J.J. Fortman and R.E. Sievers, *Inorg. Chem.*, 6, 2022 (1967)
22. A.L. Allred and D.W. Thompson, *Inorg. Chem.*, 7, 1196 (1968)
23. M. Calvin and K.W. Wilson, *J. Amer. Chem. Soc.*, 67, 2003 (1945)
24. D.W. Barnum, *J. Inorg. Nucl. Chem.*, 21, 221 (1961)
25. D.W. Barnum, *J. Inorg. Nucl. Chem.*, 22, 183 (1961)
26. R.L. Belford, A.E. Martell and M. Calvin, *J. Inorg. Nucl. Chem.*, 2, 11 (1956)
27. R.H. Holm and F.A. Cotton, *J. Amer. Chem. Soc.*, 80, 5658 (1958)
28. C.K. Jorgensen, *Act. Chem. Scand.*, 16, 2406 (1962)
29. F.A. Cotton, J. Lewis and R. Wilkins, eds., *Modern Coordination Chemistry*, Interscience, New York, 1960, p. 379
30. K. Nakamoto, *Infrared Spectra of Inorganic and Coordination Compounds*, Wiley, New York, 1963, p. 379
31. M. Mikami, I. Nakagawa and T. Shimanouchi, *Spectrochim. Acta.*, Part A, 23, 1037 (1967)
32. K. Nakamoto, C. Udovitch and J. Takemoto, *J. Amer. Chem. Soc.*, 92, 3973 (1970)
33. K. Nakamoto, Y. Morimoto and A.E. Martell, *J. Phys. Chem.*, 66, 346 (1962)
34. R.E. Hester, *Chem. Ind. (London)* 1397 (1963)
35. J.O. Hill, and R.J. Irving, *J. Chem. Soc. (A)*, 3116 (1968)
36. R.C. Fay and N. Serpone, *J. Amer. Chem. Soc.*, 90, 5701 (1968)
37. R.G. Link, and R.E. Sievers, *Inorg. Chem.*, 5, 806 (1966)
38. A. Forman, J.N. Murrell and L.E. Orgel, *J. Chem. Phys.*, 31, 1129 (1959)
39. W.C. Fernelius and B.E. Bryant, *Inorg. Synth.*, 5, 105 (1957)



40. A.E. Martell and M. Calvin, Chemistry of the Metal Chelate Compounds, Prentice Hall, New York, (1952)
41. E.M. Purcell, H.C. Torrey and R.V. Pound, Phys. Rev., 69, 37 (1946)
42. F. Bloch, W.W. Hansen, and M.E. Packard, Phys. Rev., 69, 127 (1946)
43. J.T. Arnold, S.S. Dharmatti and M.E. Packard, J. Chem. Phys., 19, 507 (1951)
44. S.I. Weissman, J. Townsend, D.E. Paul and G.E. Pake, J. Chem. Phys., 21, 2227 (1953)
45. S.I. Weissman, J. Chem. Phys., 22, 1135 (1954)
46. H.S. Jarrett, G.R. Sloan, J. Chem. Phys., 22, 1783 (1954)
47. H.M. McConnell, J. Chem. Phys., 24, 764 (1956)
48. H.M. McConnell and D.B. Chesnut, J. Chem. Phys., 28, 107 (1958)
49. H.M. McConnell, and R.E. Robertson, J. Chem. Phys., 29, 1361 (1958)
50. H.M. McConnell and C.H. Holm, J. Chem. Phys., 27, 314 (1957)
51. H.M. McConnell and C.H. Holm, J. Chem. Phys., 28, 749 (1958)
52. W.D. Phillips and R.E. Benson, J. Chem. Phys., 33, 607 (1960)
53. R.E. Benson, D.R. Eaton, A.D. Josey and W.D. Phillips, J. Amer. Chem. Soc., 83, 3714 (1961)
54. D.R. Eaton, A.D. Josey and W.D. Phillips, J. Amer. Chem. Soc., 84, 4100 (1962)
55. D.R. Eaton, A.D. Josey, W.D. Phillips, and R.E. Benson, Discussions, Faraday Soc., 34, 77 (1962)
56. D.R. Eaton, A.D. Josey, W.D. Phillips, and R.E. Benson, J. Chem. Phys., 37, 347 (1962)
57. D.R. Eaton, A.D. Josey, W.D. Phillips and R.E. Benson, Mol. Phys., 5, 407 (1962)

58. D.R. Eaton, W.D. Phillips and D.J. Caldwell, *J. Amer. Chem. Soc.*, 85, 397 (1963)
59. D.R. Eaton and W.D. Phillips, *J. Chem. Phys.*, 43, 392 (1965)
60. E. Fermi, *Z. Phys.*, 60, 320 (1930)
61. R.J. Kurland and B.R. McGarvey, *J. Mag. Res.*, 2, 286 (1970)
62. J.P. Jesson in *NMR of Paramagnetic Molecules, Principles and Applications*, Ed. G.N. LaMar, W. DeW. Horrocks, J.R. and R.H. Holm, Academic Press, New York, 1973
63. T.J. Swift, *ibid.*
64. H.S. Gutowsky, D.W. McCall and C.P. Slichter, *J. Chem. Phys.*, 21, 279 (1953)
65. H.M. McConnell, *J. Chem. Phys.*, 28, 430 (1958)
66. M. Saunders, *Tetrahedron Lett.*, 1699 (1963)
67. R.A. Sack, *Mol. Phys.*, 1, 163 (1958)
68. M.L. Morris, R.W. Moshier and R.E. Sievers, *Inorg. Synth.*, IX, 28 (1967)
69. D. Grdenic and B. Kopljar-Colig, *Inorg. Chem.*, 3, 1328 (1964)
70. H.D. Young, *Statistical Treatment of Experimental Data*, McGraw-Hill, 1962, pp. 121, 122
71. *Lange's Handbook of Chemistry*, 11th Ed., Ed: John A. Dean, McGraw-Hill Book Co.
72. R.O.C. Norman, M. Poustie, *J. Chem. Soc. (C)*, 196 (1969)
73. W.G. Movius and N.A. Matwiyoff, *J. Amer. Chem. Soc.*, 90, 5452 (1968)
74. P.W.N.M. van Leeuwen and A.P. Praat, *Inorganica Chimica Acta*, 4, 101 (1970)
75. R.E. Cramer, *Inorg. Chem.*, 12, 1193 (1973)

76. M.I. Larsen and F.W. Moore, *Inorg. Chem.* 5, 801 (1966)
77. P.W.N.M. van Leeuwen, *Recl. Trav. Chim. Pays. Bas.*, 87, 396 (1968)
78. Y. Nakamura and S. Kawaguchi, *Chem. Commun.*, 716 (1968)
79. S. Koda, S. Ooi, H. Kuroya, K. Isobe, Y. Nakamura, and S. Kawaguchi, *Chem. Commun.*, 1321 (1971)
80. Y. Nakamura, K. Isobe, H. Morita, S. Yamakazu and S. Kawaguchi, *Inorg. Chem.*, 11, 1573 (1972)
81. A.C. Adams and E.M. Larsen, *Inorg. Chem.*, 5, 814 (1966)
82. R.P. Bell, E. Gelles and E. Moller, *Proc. Roy. Soc. (Lond.)*, (A) 198, 308 (1949)
83. R.G. Pearson and O.P. Anderson, *Inorg. Chem.*, 9, 39 (1970)
84. D.M. Brouwer, *Recl. Trav. Chim. Pays. Bas.*, 87, 225 (1968)
85. S. Koda, S. Ooi, H. Kuroya, Y. Nakamura and S. Kawaguchi, *Chem. Commun.*, 280 (1971)
86. M.C. Fredette and C.J.L. Lock, *Can. J. Chem.*, 51, 1116 (1973)
87. J.C. Barrick, M. Fredette and C.J.L. Lock, *Can. J. Chem.*, 51, 317 (1973)
88. T.J. Pinnavaia and R.C. Fay, *Inorg. Chem.*, 5, 233 (1966)
89. S. Kida, *Bull. Chem. Soc. Jap.*, 34, 962 (1961)
90. Y. Marcus and I. Eliezer, *J. Phys. Chem.*, 66, 1661 (1962)
91. J.R. van Wazer, *Ann. N.Y. Ac. of Sc.*, 159, 5 (1969)
92. A.G. Sykes, *Kinetics of Inorganic Reactions*, Pergamon, 1966
93. B.G. Shultz, and F.M. Larsen, *J. Amer. Chem. Soc.*, 71, 3250 (1949)
94. L.G. Van Uitert, W.C. Frenelius and B.E. Douglas, *J. Amer. Chem. Soc.*, 75, 457 (1953)
95. A. Barabas, *Inorg. Nucl. Chem. Lett.*, 6, 744 (1970)
96. G.E. Glass, R.S. Tobias and J. Organometal., *Chem.* 15, 481 (1968)

97. G.M. Tanner, D.G. Tuck and E.G. Wells, *Can. J. Chem.*, 50, 3950 (1972)
98. N. Serpone and R. Ishayek, *Inorg. Chem.*, 13, 52 (1974)
99. R.W. Kluber, *J. Amer. Chem. Soc.*, 82, 4839 (1960)
100. A. Werner, *Ber.*, 45, 3061 (1912)
101. R.C. Ray and T.S. Piper, *Inorg. Chem.*, 3, 348 (1964)
102. N. Serpone and D.G. Bickley, *Progr. Inorg. Chem.*, 17, 391 (1972)
103. F. Basolo and R.G. Pearson, *Mechanisms of Inorganic Reactions*, Wiley, 1958
104. R.G. Wilkins, *The Study of Kinetics and Mechanism of Reactions of Transition Metal Complexes*, Allyn and Bacon, 1974.
105. Tentative Proposals of the Commission on the Nomenclature of Absolute Configuration of Complexes Based on the Octahedron, *Inorg. Chem.*, 9, 1 (1970)
106. B. Jurado, and C.S. Springer, Jr. *Chem. Commun.*, 85 (1971)
107. W. Thomas, *J. Chem. Soc.*, 119, 1140 (1921)
108. R.G. Wilkins, and M.J.G. Williams, *J. Chem. Soc.*, 1763 (1957)
109. J.A. Broomhead, and F.P. Dwyer, *Aust. J. Chem.* 16, 51 (1963)
110. J.G. Gordon II, and R.H. Holm, *J. Amer. Chem. Soc.*, 92, 5319 (1970)
111. L.H. Pignolet, R.A. Lewis and R.H. Holm, *J. Amer. Chem. Soc.*, 93, 360 (1971)
112. E.L. Muetterties, *Acc. Chem. Res.*, 3, 266 (1970)
113. P.C. Ray and N.K. Dutt, *J. Indian Chem. Soc.*, 20, 81 (1943)
114. J.C. Bailar Jr., *J. Inorg. Nucl. Chem.*, 8, 165 (1958)
115. W.G. Gehman, Ph.D. Diss. Penn State U., State College, Pa. (1954)
116. L. Seiden, Ph.D. Diss., N.W.U., Evanston, Ill., (1957)

117. C.S. Springer Jr., and R.E. Sievers, *Inorg. Chem.*, 6, 852 (1967)
118. N. Serpone and R.C. Fay, *Inorg. Chem.*, 6, 1835 (1967)
119. E.I. Stiefel and G.F. Brown, *Inorg. Chem.*, 11, 434 (1972)
120. E.L. Muetterties, *J. Amer. Chem. Soc.*, 90, 5097 (1968)
121. T.S. Piper, and R.L. Carlin, *J. Chem. Phys.*, 36, 3330 (1962)
122. R. Hutgren, *Phys. Rev.*, 40, 891 (1932)
123. F. Basolo, J.G. Hayes and H.M. Neumann, *J. Amer. Chem. Soc.*, 76, 3807 (1954)
124. S.S. Eaton, J.R. Hutchison, R.H. Holm and E.L. Muetterties, *J. Amer. Chem. Soc.*, 94, 6411 (1972)
125. E.L. Muetterties and L.J. Guggenberger, *J. Amer. Chem. Soc.*, 94, 8046 (1972)
126. A. Allerhand, H.S. Gutowsky, J. Jonas, and R.A. Meinzer, *J. Amer. Chem. Soc.*, 88, 3185 (1966)
127. R. Rohrscheid, R.E. Ernst and R.H. Holm, *Inorg. Chem.*, 6, 1315 (1967)
128. G.W. Everett Jr., and A. Johnson, *J. Amer. Chem. Soc.*, 94, 6397 (1972)
129. D.R. Eaton, *J. Amer. Chem. Soc.*, 87, 3097 (1965)
130. Y.T. Chen and G.W. Everett Jr., *J. Amer. Chem. Soc.*, 90, 6660 (1968)
131. G.W. Everett Jr., and Y.T. Chen., *J. Amer. Chem. Soc.*, 92, 508 (1970)
132. W.D. Perry and R.S. Drago, *J. Amer. Chem. Soc.*, 93, 2183 (1971)
133. B.N. Figgis, J. Lewis, and F. Mabbs, *J. Chem. Soc.*, 2480 (1960)
134. D.R. Eaton and K. Zaw, *Inorg. Chim. Act.*, 16, 61 (1976)
135. G.N. LaMar, *J. Amer. Chem. Soc.*, 87, 3568 (1965)
136. B. Morosin and H. Montgomery, *Acta Cryst.*, 25 (B), 1354 (1969)
137. S.O. Chan, and D.R. Eaton, *Can. J. Chem.*, 15, 1332 (1976)
138. S.S. Eaton and G.R. Eaton, *J. Amer. Chem. Soc.*, 95, 1825 (1973)

139. H.C. Longuet-Higgins, Mol. Phys., 6, 445 (1963)
140. J.R. Hutchinson, J.G. Gordon II, and R.H. Holm, J. Amer. Chem. Soc., 10, 1004 (1971)
141. D.G. Bickley and N. Serpone, Inorg. Chem., 13, 2908 (1974)
142. J.E. Leffler, and E. Grunwald, Rates and Equilibria of Organic Reactions, Wiley, 1963
143. R.J. Irving, and R.A. Schulz, J. Chem. Soc., Dalton, 2414 (1973)
144. J.F. Steinbach, and J.H. Burns, J. Amer. Chem. Soc., 80, 1839 (1958)
145. D.R. Eaton, A.D. Josey and R.E. Benson, J. Amer. Chem. Soc., 89, 4040 (1967)
146. S.S. Eaton, G.R. Eaton and R.H. Holm, J. Amer. Chem. Soc., 95, 1116 (1973)
147. K. Mislow and M. Raban, Top. in Stereochem., 1, 1 (1967)
148. A. Abragam, The Principles of Nuclear Magnetism, Oxford (1961)
149. C. Kutzl and R.E. Sievers, Inorg. Chem., 13, 897 (1974)
150. G.S. Hammond, D.C. Nonhebel and C.S. Wu, Inorg. Chem., 2, 73 (1963)
151. J.J. Howe and T.J. Pinnavaia, J. Amer. Chem. Soc., 91, 5378 (1969)
152. M.A. Bush and D.E. Fenton, J. Chem. Soc. (A), 2446 (1971)
153. C.H. Langford and H.B. Gray, Ligand Substitution Processes, Benjamin, 1966, p. 87.
154. D.A. Case and T.J. Pinnavaia, Inorg. Chem., 10, 482 (1971)